# Wind Tunnel and Field Test of Three 2D Sonic Anemometers

***Wiel Wauben***

***R&D Information and Observation Technology, KNMI***

**September 17, 2007**

# Table of Contents

# 1. Introduction

The Royal Netherlands Meteorological Institute (KNMI) uses conventional cup anemometers and wind vanes to measure wind speed and direction. Although the KNMI cup and vane meet WMO and ICAO requirements concerning the accuracy of wind measurements, the sensors require a large amount of maintenance and occasionally some anemometer freeze during calm winter situations. Therefore, the use of alternative wind sensors is considered. Sonic anemometers, in this report referred to as sonics, have no moving part, which makes them robust and almost maintenance free. In addition, the sonics have virtually no detection limit and detect changes almost instantly, whereas cup and vane have a threshold speed and need some time to adjust to the prevailing conditions. Furthermore sonic anemometers can easily be equipped with a heater in order to prevent malfunctioning due to icing. Sonic anemometers have been available for several years. These sensors are generally used for scientific research particularly because the 3-D sonics also measure the small vertical wind component very accurately and with a high temporal resolution so that turbulence can be measured. Furthermore, sonics are used on wind turbines and on buildings - e.g. for operating sun blinds - since they require little maintenance. The first sonic sensors already measured wind speed and direction accurately, but the sensors did not perform well during precipitation. Using more advanced measurement techniques and especially improvements in the processing of the raw data makes the new sonic anemometers reliable under all conditions. Several tests of sonic anemometers in various environments have been performed (cf. e.g. Gregoire and Oualid, 1997; Gouveia and Lockhart, 1998; Wastrack et al, 2001; Gilhousen and Hervey, 2001; Tammelin et al, 2003; Borstnik and Knez, 2003; Lewis and Dover, 2004; Larre et al, 2005). The results of the sonic anemometers show that they can be considered for operational use. Therefore KNMI considered it a good moment to perform a test of sonic anemometers in order to find out whether they are suitable for use in the operational meteorological network. The test is restricted to commercially available 2D sonic anemometers since the more expensive 3D sensors are not required in the climatological, synoptical and aeronautical meteorological network.

# 2. Wind sensors

A brief description of the wind sensors considered in this investigation is given in this section. First the operational KNMI cup anemometer and the wind vane are discussed. Next some details are given of the three 2D sonic anemometers considered in this test. Lastly the main differences are addressed.

## *2.1. KNMI cup anemometer and wind vane*

KNMI use a cup anemometer and wind vane that have been developed indoors. A picture of the cup and vane is given in
Figure 1. The design of the KNMI cup anemometer and wind vane stems from around 1990 and is based on older versions of the instruments used for research and testing various designs in the period 1960-1980. The KNMI vane type 01.00.524 employs an 8-bit optical shaft encoder to determine the direction; hence the resolution is 1.4º. The vane has a length of 710mm and the aluminum fin with a height of 400mm has an area of $0.05m^2$. The KNMI cup anemometer type 01.00.029 consists of 3 nylon cups with a diameter of 100mm connected to a cylindrical shaft with 32 slits. The distance between the center of axis and the center of the cups is 100mm. A photodiode in combination with opto-interrupter is used to determine the wind speed, where one revolution or 32 pulses according to the calibration factor corresponds to 1.98±0.02m. The KNMI wind sensors remained unchanged since 1990, although some changes were made to the electronics and the encoder that did not affect its characteristics. An overview of the sensor characteristics is given in Table 1. Further details can be found in Monna and Driedonks (1979) and in the KNMI technical documentation (van den Berg, 1996a and 1996b).

The cup anemometer and the wind vane are both connected to a SIAM sensor interface that reads the instruments on a 4Hz-sampling rate. The sensor interface calculates running averages for wind speed (scalar) and direction (unit vector), computes the wind gust (highest 3-second averaged speed) and takes care of marked discontinuity according to WMO and ICAO regulations (WMO 1996; ICAO, 2004). Optionally the sensor interface can also perform vortex compensation (van der Meulen, 1998) and does check whether the wind mast is lowered. The sensor interface outputs a measurement string every 12 seconds that includes the sample values, 1-minute averages and 10-minute averages, standard deviations and extremes. The output string also contains status information. Bijma (1998) gives details of the sensor interface for the KNMI cup and vane.

Details of the processing steps performed within the sensor interface are given below. Note that the underlined parts of the processing are disputable.

- Wind speed is a scalar averaging. Vector averaging was considered by KNMI, but up to now this has not been implemented.
- Wind direction is a unit vector averaging.
- The cup anemometer and wind vane are read with 4Hz. All calculations are also performed with a 4Hz frequency (thus 48 samples in a 12” interval, 2400 in a 10’ interval).

- Running 3-second averages are calculated for speed and direction, which serve as the basic input for all further calculations.
- Vortex compensation can be performed in case the sensor is operated along a runway at an airport (which was not the case during this test). A vortex is detected when the the 3-second averaged wind speed WS3>WSa+4*WSd+0.5m/s, but only in situations when WS3<15m/s, the 10-minute averaged wind speed WSa≥0.5m/s, the 10-minute standard deviation WSd≥0.5m/s and the percentage of measurements missed during these 10 minutes ≤10%. The 10-minute values are taken from the previous reporting interval of the sensor interface. In case a vortex is detected, all running 3-second averaged wind speed data in that 12-second interval (including any WS3≥15m/s) are limited to the acceptable value of WS3=WSa+2*WSd+0.5m/s.
- The sample value for wind speed is the highest 3-second running average of the previous 12 seconds.
- The sample value for wind direction is the running 12-second average calculated from 48 3-second running averages of the previous 12 seconds. Note that in the new sensor interface DW0 the reported sample wind direction is the 3-second running averaged wind direction corresponding with the reported wind speed.
- The running 1-minute averages are calculated from 240 3-second running averages of the previous minute.
- Temporary running 2-minute averages are calculated.
- Marked discontinuity detection is performed on the averaged wind speed and direction of the previous 2 minutes (0-2 minutes ago) and the 2-minute average between 2 and 4 minutes ago (not the previous 8 minutes as stated by ICAO, 2006). A marked discontinuity is detected when (i) a change in wind direction of the last and preceding 2-minute intervals of 30° or more occurs and both 1 minute averaged wind speeds of the last and preceding 2-minute interval (not the averaged values) are 10kts or more, or (ii) a change in wind speed of 10kts or more lasting at least 2 minutes occurs. The sensor interface (in contradiction to ICAO specifications) requires that all 4 1-minute averaged wind speeds should exceed 10kts in order to report a marked discontinuity.
- The 10-minute interval for the determination of averaged and extreme values is adjusted (set to 2 min at occurrence of a marked discontinuity, and otherwise the measurement period is increased with the update period up to a maximum of 10-minutes).
- The running 10-minute variables and percentage of measurements missed over the 10-minute averaging interval are calculated.
- The extremes are the highest/lowest running 3-second averages in the averaging interval. The extremes of the 10-minute wind direction are determined w.r.t. to the oldest 3-second averaged wind direction and differences of more than 180° are assumed to be negative. In fact the sensor interface initialises the computation of the extremes at an arbitrary 3-second sample value (not the 10-minute averaged wind direction).

  The individual steps in the computation of the wind direction extremes with running 3-second averaged sample WR3(i), and WR3(i+1) the previous sample are:
  - ΔWR=WR3(i)-WR3(i+1)
  - Δveered=WR3(i)-WRveered

  - Δbacked=WRbacked-WR3(i)
  - swath= WRveered-WRbacked
  - All variables are mapped into [0,360> interval, hence if (WR<0) WR=WR+360, instead of the range <0,360] since the North direction is usually reported as 360.
  - If (ΔWR<180 and Δveered<180 and swath<360-Δbacked) WRveered=WR3(i)
  - If (ΔWR≥180 and Δbacked<180 and swath<360-Δveered) WRbacked=WR3(i)
- The 10-minute standard deviation of the wind direction is calculated using the approximation $\sigma \approx \sqrt{2\frac{n}{n-1}(1-E)}$ (in radians) with $E = \sqrt{\bar{x}^2 + \bar{y}^2}$ the vector averaged wind speed of *n* samples (van der Hoeven, 1981). There is no documented exact equation for the computation of the standard deviation of the wind direction using unit or vector averaging.
- In addition to the 'delay' resulting from the 12-second refresh rate of the SIAM output string an additional delay of 11 seconds is generated by the fact that the interface reports the previous result before initiating a new calculation cycle.

Figure 1: Picture of the KNMI cup anemometer and the wind vane as well as the standard measurement setup using a 10m mast at the test site in De Bilt.

The KNMI wind sensors are generally installed on a 10-meter mast, an open structure with a diameter of about 45cm. The top of the mast is a 2 armed holder that places the cups of the anemometer at a height of 10m whereas the vane is located about 45cm below separated horizontally by about 75cm (cf. Figure 1). The cup and vane are connected via a 9-pole plug through which not only the power supply and signal are transmitted, but the plug also takes care of the alignment of the wind vane. The connector is aligned to true North by using a camera mounted on the plug and using known positions of reference points, whereas the plug is aligned to the sensor and camera in the KNMI calibration facilities. The advantage of this connection is that a sensor can easily be replaced without the necessity for a new alignment on site.

## 2.2. Sonic anemometers

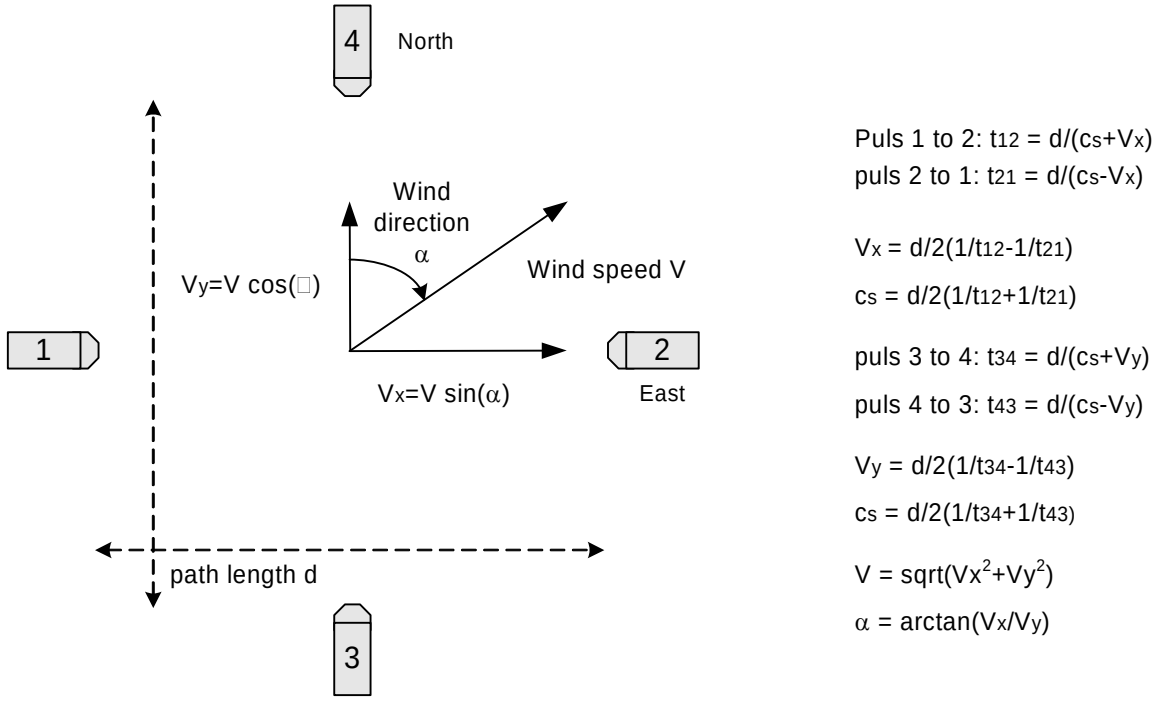


Figure 2: Sketch of the basic principle of measurement of wind speed and direction by a sonic anemometer. The travel time $t_{ij}$ of a pulse from transducer i to j depends on the distance d between the transducers, the speed of sound in air $c_s$ and the component of the wind speed V along the path.

Sonic anemometers determine wind speed and direction from the travel time of sound pulses. The travel time over a fixed distance between the transducers depends on the speed of sound in air, which is a function of the temperature and to a lesser degree the humidity, and the wind speed along the path. Modern sonics use transducers that act in turn as transmitter and receiver. With these transducers the travel time from transducer 1 to 2 as well as from 2 to 1 is measured from which the speed of sound in air can be eliminated. This process is schematically shows in Figure 2. With one transducer pair the wind speed along their path can be determined. With 2 such pairs in different horizontal orientations the wind speed in 2 directions can be determined from which the horizontal 2D wind can be reconstructed. For scientific purposes 3D sonic anemometers with 3 transducer pairs are used that also give the vertical wind component. Since these 3D sonic anemometers are more expensive than the 2D sonics and since there is no operational need for 3D winds for synoptic meteorology these 3D sensors are not considered here.

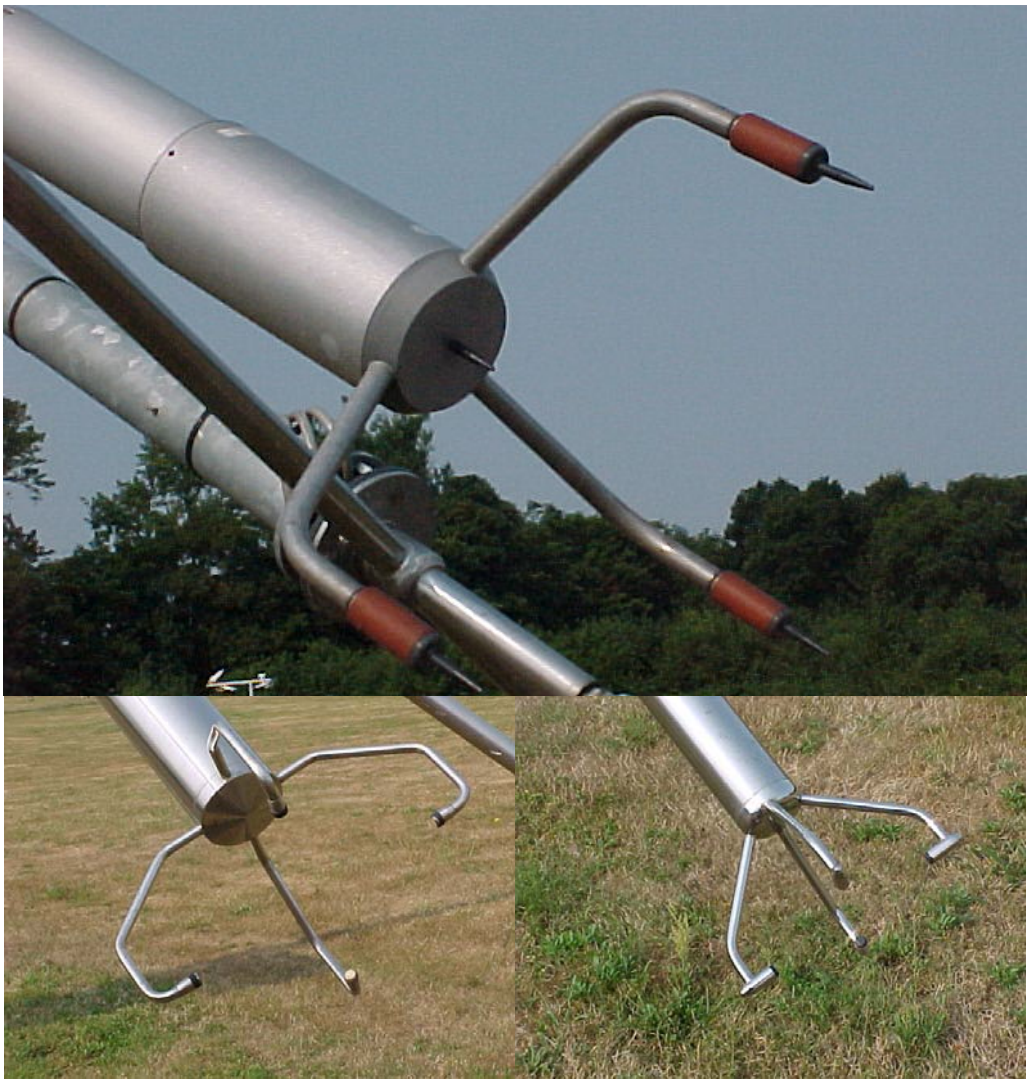

Figure 3: The Thies (lower left), Gill (lower right) and Vaisala (upper panel) sonic anemometers.

Three 2D sonic anemometers have been selected for the test. The specifications of these sensors meet the requirements (cf. Table 1) and the sensors are already extensively used, albeit not operationally by the meteorological community, although some tests have been performed. The selected sonics are the Thies 2D ultrasonic anemometer, the Gill Solent WindObserver II ultrasonic wind sensor and the Vaisala WAS425 ultrasonic wind sensor. The Thies and Gill sensors have 4 arms equipped with transducers resulting in 2 perpendicularly oriented transducer pairs. The Vaisala sensor has 3 arms, but since the signal transmitted by one transducer is received by the 2 other transducers, this sensor has in fact 3 transducer pairs oriented at 60º angles. Details of these three sensors are given in Table 1 whereas pictures of the sensors are shown in Figure 3. Details for the sensors can be found in the documentation of the manufacturers (Thies Clima, 2001; Gill Instruments, 2000; Vaisala, 2000). All sensors support vector and scalar averaging, polling mode, and have a digital RS422 output (Vaisala at the time the test started only supported RS232, but their latest version supports RS422 as well).

The sonics eliminate the sound speed dependency as mentioned above, but the measurements are also affected by the disturbance of the wind field caused by the arms and by precipitation. Although the sound speed dependency is eliminated, this speed can still be derived. The speed of sound $c_s$ in m/s is given by (cf. e.g. Handbook of Geophysics, 1960):

$$c_s = \sqrt{\frac{\gamma R^*}{M} T},$$

where $\gamma$=1.4 is the ratio of specific heats of air at constant pressure and constant volume, $R^*$=8314.39JK$^{-1}$kg$^{-1}$ is the universal gas constant, M is the molecular weight of air, which for dry air is $M_{da}$=28.966, and T is the temperature in Kelvin. Since the pressure is proportional to the number density, the molecular weight of most air can be calculated from:

$$M = \frac{eM_{wv} + (P-e)M_{da}}{P},$$

with $e$ the vapor pressure of water in air and $P$ the total atmospheric pressure in hPa and $M_{wv}$=18.01534 the molecular weight of water vapor. Substitution of the expression for $M$ in the equation for the speed of sound and making a Taylor expansion for small $e$ gives:

$$c_s^{\,2} \approx \frac{\gamma R^*}{M_{da}} \times T \times \left[1 + \left(\frac{M_{wv}}{M_{da}} - 1\right)\frac{e}{P}\right] = 402 \times T \times \left(1 + 0.38\frac{e}{P}\right). \quad (1)$$

This is almost exactly the expression commonly used for the speed of sound as a function of the temperature and water vapor content reported by Kaimal and Gaynor (1991). Note that in the above derivation the acoustic virtual temperature is set to the meteorological virtual temperature by assuming dry air $\gamma = \gamma_{wv} = \gamma_{da}$. The relation between the virtual temperature $T_v$ and the real kinetic temperature is now given by:

$$T_v = T \times \left(1 + 0.38\frac{e}{P}\right).$$

The virtual temperature is reported by the Thies and Gill sonic anemometers and can serve as a parameter for quality checking purposes of the sonic anemometer as well as a measure for the temperature. A correction for the water vapor content can be performed off-line using the available relative humidity data. It should however be noted that whereas the sonics measure at 10m the relative humidity and ambient temperature are measured at 1.5m inside a radiation screen. For the purpose of the above mentioned correction the relation between the vapor pressure of water in air $e$ and relative humidity $U$:

$$U = 100\frac{e}{e_s}, \quad (2)$$

is used, which involves the saturation vapor pressure $e_s$ (WMO, 1996):

$$e_s(t) = \left(1.0016 + 3.15 \times 10^6 P - 0.074/P\right) \times 6.112 \exp\left(\frac{17.62t}{243.12 + t}\right), \quad (3)$$

with *t* the air temperature in ºC. In order to compute the temperature from the measured sound speed, relative humidity and pressure the relations (1) to (3) have to be solved by iteration.

Table 1: An overview of the general characteristics of the wind sensors considered in this test and the WMO requirements.

| **General sensor characteristics** | | | | | |
|---|---|---|---|---|---|
| *Parameter* | *KNMI cup* | *KNMI vane* | *Thies* | *Vaisala* | *Gill* |
| *Name* | KNMI cup anemometer | KNMI wind vane | Ultrasonic Anemometer 2D | Ultrasonic wind sensor | Solent |
| *Type* | 01.00.029 | 01.00.524 | 4.3800.00.140 | WAS 425 AH | WindObserver II |
| *Sensor nr.* | 115 | 003 | 0601050 | 00360 | 000274 |
| *Software version* | 4.0 | 4.0 | 1.90 | 6.04 | 2.01 |
| *Operating Frequency* | N.A. | N.A. | 250kHz | 100kHz | ± 180kHz |
| *Environment* | –20 to 50°C IP55 | –20 to 40°C IP55 | –40 to 70°C | –40 to 50°C –55 to 55°C if heated up to 130m/s | –55 to 70°C 5 to 100% RH up to 85m/s up to 300mm/u |
| *Output rate* | 1/12Hz | 1/12Hz | 10Hz | 1Hz | 1, 4 or 10Hz |
| *Weight* | 1.6kg | 2.4kg | 2.5kg | 1.3kg | 1.5kg |
| *Size* | Ø310x250mm | 710x705x69mm | Ø275x422mm | Ø279x533mm | Ø213x381mm |
| *Status information* | Sensor interface | Sensor interface | virtual temperature and # meas. in averaging | NMEA message | self diagnostics |
| *Internal checks* | - | - | checks for heating, converter, electronics | Power-on self test RAM and ROM | self diagnostics & reporting |
| *Voltage sensor* | 24VDC 35mA | 24VDC 100mA | 12-24VAC/DC (–10% to 20%) 3VA | 10-15VDC 12mA | 9-30VDC 40mA@12VDC |
| *Voltage heater* | N.A. | N.A. | 24VAC/DC, 70VA | 36VDC±10% 0.7A | 24VAC/DC 3A |
| *MTBF* | ? | ? | 15yrs calculated | 26yrs | 10yrs |

An error that occurs with sonic anemometers is the transducer shadowing effect (Wyngaard and Zhang, 1985; Mortensen and Højstrup, 1995), i.e. the underestimation of the wind component measured along the acoustic path due to the wakes generated by the transducers. The disturbance by the transducers can be minimized by the design of the sensor (cf. e.g. Wieser et al, 2001), and/or by applying corrections derived form wind tunnel measurements and/or, as is the case for the Vaisala, by using 3 transducer pairs where only those 2 pair are considered that are least affected by the disturbance. The disturbance caused by precipitation in the path of a transducer pair is handled either by performing measurements with a high repetition frequency and filtering out spurious

events or, as again is the case for the Vaisala, the transducer is specifically made larger so that a good measurement is still possible in the presence of a hydrometeor in the path.

Table 1: Continued.

| **Wind direction** | | | | | |
|---|---|---|---|---|---|
| *Parameter* | *WMO* | *KNMI* | *Thies* | *Vaisala* | *Gill* |
| *Range* | 360° | 0 to 359.9° | 1 to 360° | 0 to 359° | 0 to 359° or 1 to 360° |
| *Resolution* | 3° | 1° | 1° | 1° | 1° |
| *Accuracy* | ±5° | ±3° | ±1.5° | ±2° | ±2° |
| *Sample rate* | 4Hz | 4Hz | 400Hz | 20Hz | 40Hz |
| *Running average* | 3sec | 3sec | 0, 1, 10sec or 2min (3sec in SW upgrade end 2000) | 1 to 9sec (RS232) | 0 or 1 to 3600sec |
| *Detection limit* | 0.5m/s | 0.4m/s | 0.01m/s | virtually zero | below 0.5m/s no direction reported, but u,v in 0.01m/s |
| *Damped wavelength* | < 10m | 3.8m | N.A. | N.A. | N.A. |
| *Damping ratio* | 0.3 to 0.7 | 0.36 | N.A. | N.A. | N.A. |
| *Time constant* | 1sec | - | meas. time 0.0025sec, response time 0.1sec | meas. time 0.2sec response time 0.35sec | < 0.1sec |

| **Wind speed** | | | | | |
|---|---|---|---|---|---|
| *Parameter* | *WMO* | *KNMI* | *Thies* | *Vaisala* | *Gill* |
| *Range* | 0.5 to 75m/s | 0.5 to 75m/s | 0 to 60m/s (above value) | 0 to 65m/s | 0 to 65m/s (above value or error) |
| *Resolution* | 0.5m/s | 0.01m/s | 0.1m/s | 0.1m/s | 0.01m/s |
| *Accuracy* | Max of ±0.5m/s and ±10% | ±0.5 m/s | Max of ±0.1m/s and ±2% | Max of ±0.135 m/s and ±3% | ±2% |
| *Sample rate* | 4Hz | 4 Hz | 400Hz | 20Hz | 40Hz |
| *Running average* | 3sec (gust) | 3 sec | 0, 1, 10sec or 2min (3sec in SW upgrade end 2000) | 1 to 9sec (RS232) | 0 or 1 to 3600sec |
| *Threshold speed* | 0.5m/s | <0.5m/s typically 0.3m/s | 0.001m/s | virtually zero | 0.01m/s |
| *Response length* | 2 to 5m | 2.9m | 0.20m | 0.40m | 0.15m |
| *Time constant* | 1sec | - | meas. time 0.0025sec, response time 0.1sec | meas. time 0.2sec, response time 0.35sec | < 0.15sec |

## 2.3. Data acquisition

The basic quantity, which is needed for the measurement of wind gust in particular, are running 3-seconds averages with an update frequency of 4Hz as recommended by WMO (1991). Not all three sonics facilitate running 3 seconds averages in their output message, nor do all three sensors give 4Hz updates. For the purpose of this test all three sensors are polled identically with 1Hz at which the 1-second averaged wind is obtained. Examples of the output strings of the sensors are given in Table 2.

The KNMI cup anemometer and wind vane are operated in combination with a sensor interface. This interface outputs a string every 12 seconds although the internal update frequency is 4Hz. The output string of the sensor interface is acquired by a data-acquisition PC and time stamped. The output string contains the data for the wind direction (WR) in 0.1º and the wind speed (WS) in 0.01m/s. For each parameter the status of the measurement (0=good, a-z is warning, A-Z is error), the instrument number (0), and the sample, 1-minute average, 10-minute maximum, 10-minute minimum, 10-minute average, 10-minute standard deviation and the percentage of samples missed in the past 10-minute interval (00-99%) are reported. In case of a sensor errors during the entire averaging period, the corresponding values are replaced by slashes ("////").

The sonic anemometers are polled by the data-acquisistion PC every second and time stamped. The settings of the sonic anemometers are an averaging interval 1 second, data rate 9600 baud, 8 data bits, no parity and 1 stop bit. The RS422 interface is used when available, the Vaisala which supported at the time only a RS232 interface was converted to RS422 using a separate RS232/RS422 converter. Wind speed is reported in m/s and no north correction or threshold is applied. The heater is switched on. A sample of a sonic is considered missing is no reply from the sensor was received within 0.5sec.

The so-called VDT telegram string of the Thies is requested, which reports the 1-second averaged wind speed in 0.1m/s, the 1-second averaged wind direction in º, the virtual temperature in 0.1ºC, the unit indicator M for m/s, 2 status bytes, the check sum marker *, and 2 byte HEX check sum. In case the Thies sensor could not perform a valid measurement the wind speed, direction and temperature are reported as FFF.F, FFF and FF.F, respectively. The so-called Handar RS232 message is requested from the Vaisala that reports the averaging interval (W1), status indicator (P/F), the wind direction in º, the wind speed in 0.1m/s, the unit indicator T for m/s and a check sum. In case of a Vaisala sensor error the values 999 and 999.9 are reported for direction and speed, respectively. The ASCII message format is used for the Gill consisting of a comma seperated list with the sensor identification A, the wind direction in º, the wind speed in 0.01m/s, the unit indicator M for m/s, the speed of sound in dry air in 0.01 m/s, the virtual temperature in 0.01ºC and a status field (60 indicates that heating is operational). Unfortunately the format of the output string changed unnoticed after a software upgrade before the field test so that the virtual temperature and status of the Gill is missing from the dataset. In case of a sensor error the values 999, 999.99 and 999.99 are reported by the Gill sensor for wind direction and speed and sound speed, respectively.

Table 2: Examples of the data strings obtained for the wind sensors are given below in bold face. The strikethrough part of the Gill data string was not stored during the field test.

| Sensor | **Sample output string**<br>Explanation of fields |
|---|---|
| KNMI | **WR 0 0 0633 0626 1083 0098 0528 0151 00  WS 0 0 0544 0561 0899 0214 0486 0111 00**<br>WR wind direction indicator<br>0 instrument number<br>0 sensor status<br>//// sample value wind direction in 0.1°<br>//// 1-minute averaged wind direction in 0.1°<br>//// 10-minute minimum wind direction in 0.1°<br>//// 10-minute maximum wind direction in 0.1°<br>//// 10-minute averaged wind direction …<br>//// 10-minute standard deviation …<br>99 % missed samples in 10'<br>WS wind speed indicator<br>Wind speed in 0.01m/s uses same fields as wind direction |
| Thies | **005.5 052 +01.3 M 08*6B**<br>FFF.F wind speed in m/s<br>FFF wind direction in °<br>FF.F virtual temperature in ºC<br>M unit indicator for m/s<br>BB status bytes<br>* checksum indicator<br>XX checksum |
| Vaisala | **W1P0460005.4TED**<br>W1 indicator for 1 second average<br>F status indicator (Pass/Fail)<br>999 wind direction in °<br>999.9 wind speed in m/s<br>T unit indicator for m/s<br>XX checksum |
| Gill | **A,049,005.50,M,+335.33,+~~25.40,60~~**<br>A sensor indicator<br>999 wind direction in °<br>999.99 wind speed in m/s<br>M unit indicator for m/s<br>999.99 speed of sound in m/s<br>99.99 virtual temperature in ºC<br>II status indicator |

A Testpoint application was written to acquire the data from the KNMI cup anemometer and wind vane every 12 seconds when new data was reported. The application also polled the three sonic anemometers at 1Hz and stored the data received from the sensors with a time stamp in daily files.

# 3. Test setup

In this section a description is given of the setup and devices used during the tests. This includes the sensor coupling device, the alignment of the sensors, the KNMI rotation device, the KNMI wind tunnel that was used at several stages during the test, the LST wind tunnel that was used as the reference for the wind speed and direction calibration check over the full wind speed range, the setup during the field test, and the location of the field test.

## *3.1. Coupling device*

The three sonic anemometers have different mounting mechanism, power and signal connectors, dimensions and alignment methods. In order to facilitate the installation of each of these sensors a coupling device was developed that allows the mounting of the sensor to the standard 9-pole plug of the KNMI cup anemometer and wind vane. The same pins of the plug are used as far as possible as for the KNMI sensor for providing the power supply and to transmit the signal. The sonic anemometer can be aligned with respect to the connector of the coupling device so that the North direction alignment of the sensor can be transferred to the connector and via the connector to the alignment of the plug. The coupling device also compensates for the different heights of the sonics. However, since the height of KNMI cup anemometer is less than the height of the sonics, a height difference between the sonics and the KNMI sensors exists. During the tunnel tests this height difference was adjusted manually. During the field test this height difference is compensated by the cross arm that is used to mount the three sonic anemometers to the mast. The sensor coupling devices and the cross arm containing the three sonic anemometers can be seen in Figure 4.

Figure 4: The cross arm on top of the 10m mast with the 3 sonic anemometers during the field test.

## 3.2. Sensor alignment

The alignment of the KNMI wind vane to the connector is determined electronically and mechanically using an alignment device. For that purpose the connector is fixed with a reference pin in the device and the axis of the wind vane is turned to North, by finding the middle between the 2 neighboring positions of the optical angle encoder. Next the orientation of the wind vane is checked against a reference line. The position is set within ±0.15mm of the reference line, which corresponds to an accuracy of ±0.3º.

The alignment of each of the sonics to its connector was performed using the alignment setup of the KNMI wind vane, but the North orientation of the sonic anemometer as specified by the manufacturer was set as good as possible in alignment with the device manually. For the purpose of this test no special equipment was developed in order to facilitate the alignment and to make it reproducible. For a cross check of the alignment the KNMI wind tunnel in combination with a rotation device was used. The alignment of the sonics agreed within ±1º. The absolute alignment of the plug in the tunnel tests was not considered during this test. However, it should be noted that the camera that is used in the field to align the plug to North can be used for aligning the plug to the axis of the wind tunnel.

## 3.3. KNMI rotation device

During the test in the KNMI wind tunnel a rotation device of the Oceanographic Research Department of KNMI was used. This device is developed at KNMI as an instrument that can be used during the calibration of 3D sonic anemometers in wind tunnels. A sensor can be mounted to this device and the sensor can be rotated around 360º in azimuth and the sensor can also be tilted between –40º and +40º. The accuracy of the rotation and tilt angles is better than 0.1º. A pipe with the standard 9-pole plug has been connected to the rotation device of the KNMI to which the sonic anemometers can easily be mounted. Using this setup the wind direction measurements of the sonics could be tested in the KNMI wind tunnel.

A Testpoint application has been developped that performes the measurements for such a calibration check and stores all relevant information. The application controlled the rotation device, performing 360º azimuth scans with a configurable step. After reaching a new position a brief delay is introduced in order to allow the wind flow and 1-second sensor average to become stable. Next, the sonic anemometer is polled and the reference of the tunnel speed is read several times. All information, i.e. azimuth, tunnel speed, sensor speed and direction is stored with a time stamp.

## 3.4. KNMI wind tunnel

The KNMI wind tunnel is of the so-called Eiffel type with a closed measurement section. The space available for calibration in this measurement section has a length of 0.4m and a diameter of 0.4m. The wind speed range is 0.2m/s to about 27m/s. The variation in wind speed across the measurement volume is maximally 3% and turbulence is below 1%. Further details of the KNMI wind tunnel can be found in Monna (1983). A Lambrecht 1405 vane anemometer is used as the reference for measuring the tunnel wind speed in the KNMI wind tunnel. This anemometer is regularly calibrated outdoors together with a

KNMI cup anemometer. The absolute calibration of both sensors is determined and from that the calibration factor to be used for the cup anemometer in the KNMI wind tunnel is determined. The accuracy of the wind speed calibration of the KNMI cup anemometers in the KNMI wind tunnel over the wind speed range is estimated to be ±2%±0.1m/s (Monna, 1987).

The KNMI wind tunnel has been used to test the sonic anemometers before and after the field test. It was found that the Vaisala sonic anemometer showed a error in the wind speed as a result of the disturbance of the transducers. This was caused by the usage of incorrect transducer pairs at the particular settings used by KNMI. Furthermore, the Thies sonic anemometer showed signs of a history exceding the 1-second averaging. Both problems were solved by a software upgrade of the Vaisala and Thies anemometers prior to the field test.

## *3.5. DNW-LST wind tunnel*

The Low Speed Tunnel (LST) of the Dutch National Aerospace Laboratory (NLR) is operated by DNW (German-Dutch Wind Tunnels). The LST is an atmospheric, closed-circuit wind tunnel with a contraction ratio of 1:9 for improving the flow quality. The test section has a width of 3.0m and a height of 2.25m. The wind speed range is 1.5m/s to 80m/s. The variation in wind speed across the test section is less than 0.2% and turbulence is below 0.03%. The horizontal and vertical flow angularities are within 0.1°. The second test section of the LST tunnel with a length of 3.0m is used for the anemometer test. The sensors are mounted on a monopod with a height of 1.1m that is equipped with a standard 9-pole plug and brings the sensor near the middle of the test section. The monopod is fixed to the center of the turntable in the floor of the test section that can be rotated over 360° with accuracy well below 0.1° (cf. Figure 5). Further details of the LST wind tunnel can be found in de Vries (1992).

The tunnel reference pressure difference is used for the determination of the velocity in the central part of the test section. The reference pressure difference is obtained from the average of 4 pressure differences over the contraction of the tunnel, measured with Rosemount transducers. The standard calibration of the test section consists of measuring the relation between the reference pressure difference over the contraction of the tunnel and the dynamic pressure in the test section, which is measured with a standard pitot-static tube. The measured pressure differences are converted to the corresponding velocities by assuming an ideal gas and using the observed air temperature and water vapor pressure in the determination of the air density. Furthermore, a so-called blockage correction of the form $(1+\varepsilon)^2$ is applied to the tunnel speed in order to account for the reduction of wind speed in the test section caused by the presence of the sensor and its support. The blocking is proportional to the area and the applied corrections as determined by DNW were 2.1% for the KNMI cup anemometer; 2.5% for the Gill and Thies sonic anemometers and 2.7% for the Vaisala sonic anemometer (Willemsen and Goedegebuure, 2003). The accuracy of the blocking correction is better than 10%, hence the uncertainty in the tunnel wind speed due to blocking is below 0.3%. The accuracy of the tunnel wind speed calibration is ±0.11m/s at 2.0m/s, decreases to ±0.05m/s at 5.0m/s, remains ±0.05m/s up to 10.0m/s and increase to ±0.15m/s at higher wind speeds

(Willemsen, 1994 and 1996). The flow temperature is the average of 8 temperature sensors along the corners of the contraction.

Figure 5: The Thies sonic anemometer situated on the monopod in the LST wind tunnel. Note the arc of the turntable in the floor.

## *3.6. TNO wind tunnel*

The TNO wind tunnel is an outdoor tunnel, which means that the tunnel is in connection with the outside air. Therefore the actual wind speed in the tunnel is influenced by the conditions outside. The situation on April 20, 2001 was rather calm, with wind speeds of about 2m/s. At low tunnel speeds of 1m/s a variation in the tunnel wind speed has been observed. In order to account for the variations in the wind speed of the tunnel, and also

to serve as a reference sensor, the measurements of the sonic anemometers were performed with a KNMI cup anemometer running parallel to the sonic sensors. Also a Schiltknecht propeller anemometer (operated by the Oceanographic Research Department of KNMI) was used as a reference giving readings every second. The tunnel wind speed can be varied between 0 to about 17 m/s.

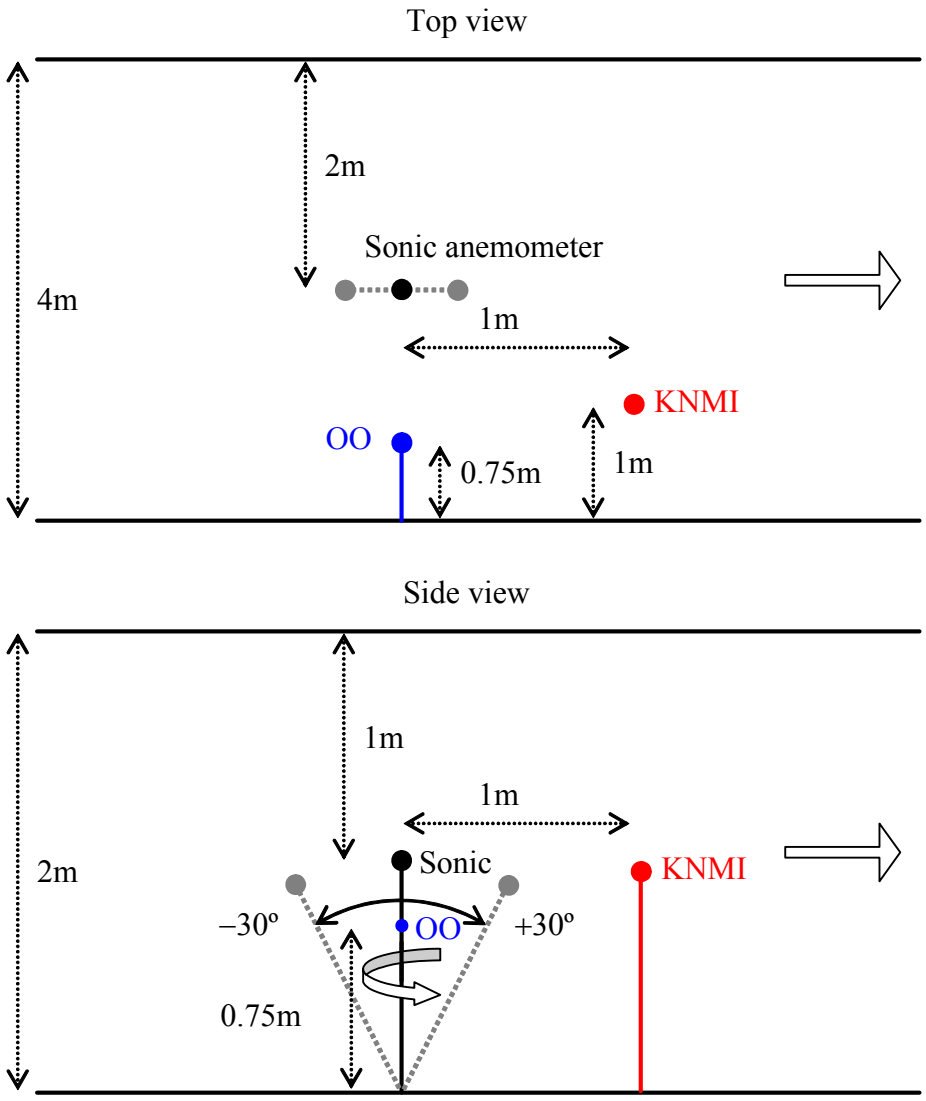


Figure 6: Sketch of the setup of the anemometers in the TNO wind tunnel test.

A brief overview of the tunnel dimensions and the position of the instruments are given in Figure 6. The TNO wind tunnel has a width of 4m and height of 2m. The instrument to be calibrated was located in the middle of the tunnel mounted on a pole that is controlled by the KNMI rotation/inclination device that is sunk into the floor of the tunnel. The KNMI cup anemometer was located 1m downwind and towards the wall on a fixed

vertical pole. The small Schiltknecht was located at the same position as the instrument to be calibrated, but 75cm from the wall using a fixed vertical rod.

The calibration was performed with the sonic anemometer in an upright position (inclination angle of 0º) and varying the azimuth angle from 0 to 360º in step of 5º. The measurement at each orientation consisted of (i) setting the desired orientation, (ii) reading the position of the rotation/inclination device, (iii) waiting 3 seconds, (iv) performing 5 1-second averaged wind speed measurements at 1 second intervals. The tunnel speeds considered are 1, 2, 5, 10 and 17m/s. The azimuth scans at 5m/s were also performed using smaller steps (1º and 2º) in order to resolve the fine structure. In all cases the average of the 5 1-second measurements is used. The effect of an inclination of the sonic anemometers was also investigated at a tunnel speed of 5m/s. For that purpose the inclination was varied between –30º and 30º with steps of 5º for the azimuth angles 0 to 90º with steps of 15º, i.e. a total of 31×7=217 orientations. A negative inclination indicates that the sensor is inclined towards the tunnel flow, i.e. the sensor is exposed from above. The Schiltknecht served as the reference during the inclination tests.

## 3.7. KNMI climate chamber

The three sonic anemometers were also subjected to a temperature test in the climate chamber at the calibration facilities of KNMI. The climate chamber is a CTS C-25/600 from Clima Temperatur Systeme. The absolute accuracy and stability of the temperature and the relative humidity are below ±0.1°C and ±1%, respectively. All three sonics were placed individually in the climate chamber and subjected to temperatures down to –20°C. During these tests it was found that the heater of the Gill sonic anemometer did not work. This was solved by a software upgrade prior to the field test.

## 3.8. Field test setup

During the field test the 3 sonics were mounted on a 10-meter mast on the KNMI test site in De Bilt in the vicinity of the 10-meter mast of the De Bilt test station (261). All three sonic anemometers were mounted in the same mast on a cross arm that separates the sonics by 1m and positions the sensors with the coupling device at a height of 10m. While the Bilt test was equipped with a standard 10m mast, the sonics were mounted on a tilt mast (see Figure 7). Both mast types have an identical maximum horizontal deviation at 10m of 13cm and a rotation of less than 1.3° for wind speeds up to 35m/s.

Wind measurements are affected by obstacles since they reduce the wind speed and increase the variability of wind speed and direction. This disturbance is occurs mainly downstream of the wind. The disturbance caused by obstacles depends on their size and structure. Generally, KNMI applies the rule that a suitable location for wind measurements should have a distance to obstacles like trees and buildings of at least 10 times the height of these obstacles, although a factor of 20 is preferred. The disturbance of one wind mast on another mast depends on the diameter of the mast. If the separation of the masts is 20 times their diameter, then the turbulence is below 10%. Using these rules a suitable location for the sonic test on the De Bilt test field was determined 20m SouthWest of the 261 wind mast. It should, however be noted that the location of the test field is far from optimal for wind measurements. In fact, the operational station De Bilt

(260) is situated next to the test field, but the operational wind measurements for De Bilt are performed by a 20m mast located about 200m to the SouthEast. A sketch of the layout at the De Bilt test site is given in Figure 8.

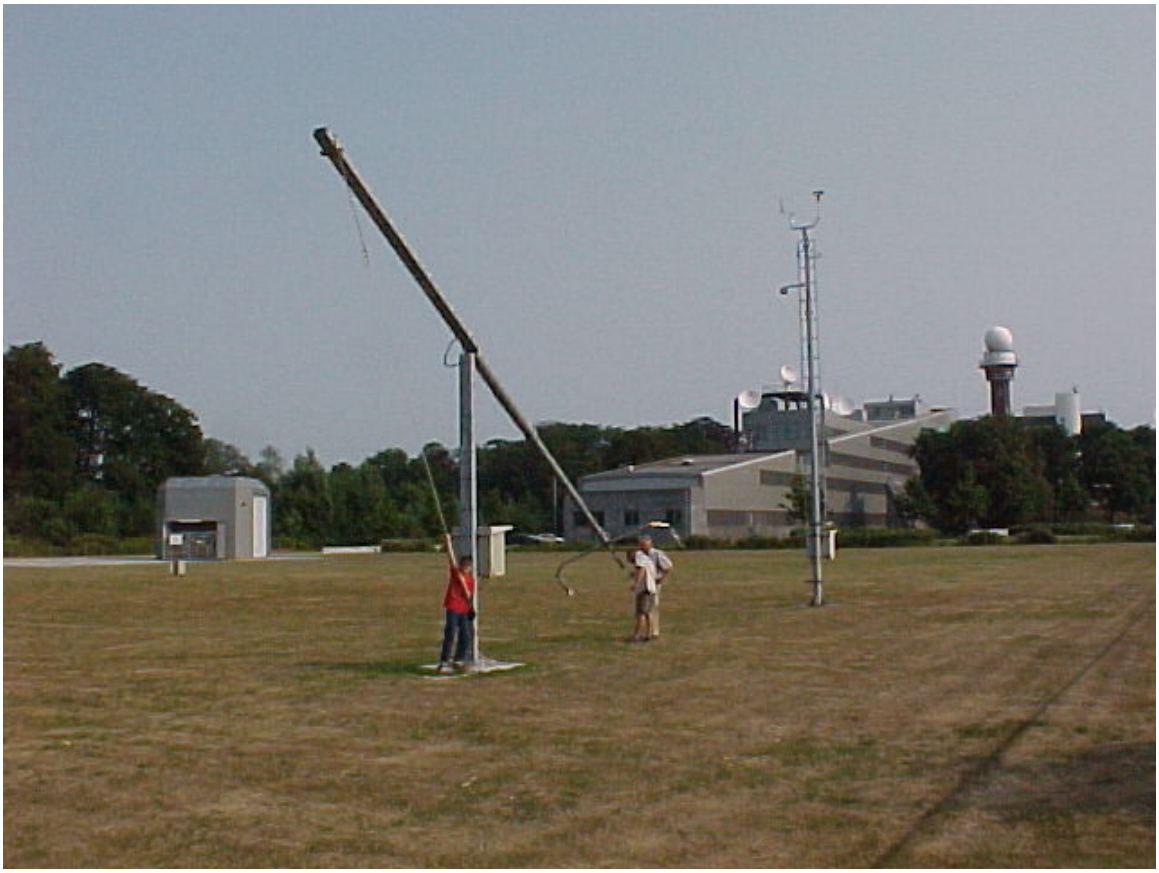

Figure 7: An overview of test field at De Bilt facing North with the 10m mast containing the KNMI cup anemometer and wind vane and the tilt mast with the 3 sonic anemometers.

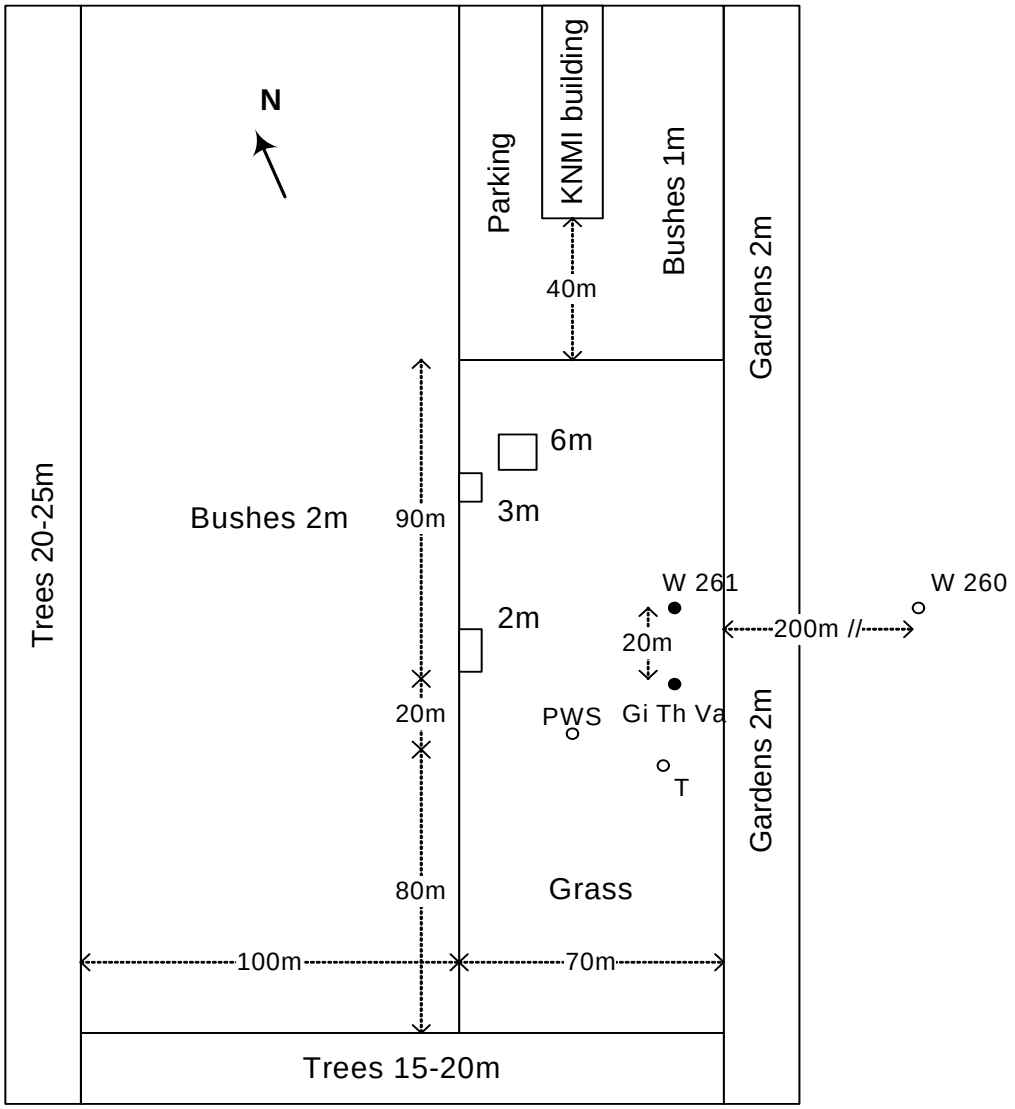


Figure 8: Sketch of the layout of the test site at De Bilt. The bullets denoted by W261 and Gi Thi Va indicate the location of the KNMI cup anemometer and wind vane and the three sonics, respectively. T denotes the location of the ambient temperature and relative humidity sensors and PWS denotes the FD12P present weather sensor. The atmospheric pressure is measured at W261.

# 4. Wind tunnel test

In these section results of the wind tunnel tests are presented and discussed. The wind tunnel measurements follow as far as possible the requirements, procedures and data-analysis described by ISO16622 (2002) and Sturgeon (1999, 2005).

## *4.1. DNW-LST wind tunnel test*

### 4.1.1 Test setup and procedure

The test of the sonic anemometers and the KNMI cup anemometer at the DNW-LST wind tunnel were performed on 23-25 September 2003. The corresponding DNW-LST project reference number is 2710.3621.

The acquisition of the data of the sonic anemometers and the cup anemometers during the DNW-LST wind tunnel test was performed using the power supply, converters, PC and Testpoint software of KNMI. The 1-second averaged wind speed and direction of the sonic anemometers was obtained every second and the data string of the SIAM sensor interface of the cup-anemometers containing the sample value of the wind speed was available every 12-seconds. This information was provided via a RS232 string to the acquisition system of the DNW-LST wind tunnel in a fixed format and included the date and time of the PC, the sensor identification, and the wind speed and direction reported by the sensor. The acquired raw data was continuously time stamped and stored on disk during the test. The acquisition setup is described in Wauben (2003).

During the LST tunnel tests the standard data acquisition system of the DNW-LST wind tunnel was used. The RS232 signal provided by KNMI was decoded by the LST data acquisition system. Any faulty wind sensor data (containing “F”, “9” or “/”) was set to zero. The test of the cup anemometers were performed for a fixed orientation. Tests were performed for tunnel reference wind speeds of 2, 3, 5, 10, 20, 50, 60, 65, 75, 70, 30, 15, 5 and 5m/s. The tunnel wind speed was changed to the requested value, although no action was taken to get the value exactly right. Each time a delay was introduced so that the tunnel and sensor wind speed could adjusted and tunnel measurements were only taken when tunnel and sensor showed stable readings. The tunnel measurements for a fixed orientation were taken with a 1Hz frequency for a duration of 1 to 2 minutes. The sonic anemometers were tested for a fixed tunnel wind speed while the turntable rotated over 360° with a constant angular speed of about 0.5°/s. The turntable was moved alternating from −180° to 180° and backwards to avoid twisting of the cables. The angle of the turntable is defined such that an increasing angle turns the sensor anticlockwise so that the experienced wind direction increases also. Only during the tunnel measurements the sensor information is stored by the LST data acquisition system together with the run number, polar number, wind tunnel speed, the Reynolds number, flow temperature and orientation of the turntable. The temporal resolution is 0.5sec for the sonic anemometers and 1sec for the cup anemometers (cf. Willemsen and Goedegebuure, 2003). The typical number of samples taken for each tunnel measurement is about 1500 and 100 for sonic anemometers and cup anemometers, respectively. A 360° measurements for a sonic

anemometer required about 15 minutes, whereas a cup anemometer test took about 4 minutes for each tunnel reference speed.

During the first day there were some problems with the data acquisition of the sensor information of the LST system. This resulted in the loss of sensor information in the LST data acquisition system so that old sensor information was repeated. The problems were solved at the end of the first day when the collection mode was modified from character to buffer mode and the baud rate of the RS232 signal was reduced to 1200bps. Because of the large amount of missing data the test of the Gill anemometer was repeated on the last day. However, the sensor information could be substituted by the next raw sensor information stored on the PC whenever it was repeated more than 3 or 13 times for the sonic anemometers and cup anemometers, respectively. The results of the first Gill tunnel tests are denoted Gill$^+$.

### 4.1.2 Data processing and analysis

The tunnel measurement data, specified uniquely by a run and polar number, required some processing.

- Any missing or faulty sensor information indicated in the data set by zero sensor wind speed and direction are ignored.
- The data is scanned for repeated sensor information which were replaced by the appropriate values obtained from the raw data file, as described above.
- The virtual temperature measured by the Thies and Gill sonic anemometers is also extracted from the raw data file for the time interval corresponding with the tunnel measurements.
- The averaged wind tunnel speed $<V_t>$ and temperature $<T_t>$ are calculated for each tunnel measurement (see Appendix A1). The standard deviation of the wind tunnel speed is typically 0.001m/s.
- The turntable reference direction is corrected for the 1-second averaging period of the sonic anemometers. Since the output rate is 2Hz, the previous instantaneous turntable value is used as the reference direction.
- The averaged offset $<D_{off}>$ between the reference direction and the sensor wind direction is determined (see Appendix A1). In this calculation all differences are mapped into the −180° to 180° range by addition/subtraction of ±360° if necessary. Next the offset $<D_{off}>$ is averaged over all available wind speeds in order to obtain a overall direction offset $<X_{off}>$ for each sonic anemometer. $<X_{off}>$ is 61.38° for the Gill$^+$; 61.91° for the Thies; 62.22° for the Vaisala; 61.59° for the Gill sonic anemometer.
- The turntable was started and stopped manually during each tunnel measurement. Hence, the start and end of a tunnel measurement do not coincide with the start and end of the rotation of the turntable so that multiple tunnel measurements occur at the turntable orientations of −180° and 180°. Furthermore the raw measurements can show some fluctuations (cf. Figure 9 to Figure 11). To overcome these issues the results are averaged over bins of 2° of the turntable. While averaging the sensor wind direction the overall direction offset is accounted for and all differences between the sensor direction and the overall direction offset as well as between the sensor and the

reference direction are mapped into the −180° to 180°. The tunnel reference direction, wind speed and temperature and the sensor wind speed and virtual temperature are also averaged in bins. Furthermore the standard deviation for each parameter in each bin is calculated.

- Finally the differences between the direction $\Delta D$, speed $\Delta V$, and temperature $\Delta T$ are determined for each bin (see Appendix A2) and the corresponding averages $<\Delta D>$, $<\Delta V>$ and $<\Delta T>$ and standard deviations over all bins are determined (see Appendix A1).
- The differences between the tunnel reference and the cup anemometer wind speed measurements are determined for the entire period of the tunnel measurement. From these values the averaged differences $<\Delta V>$ and the standard deviation is determined (see Appendix A1).

### 4.1.3 Results

In Figure 9 to Figure 11 examples are given of the raw data obtained for the Gill, Thies and Vaisala, respectively. The raw results of all 3 sonic anemometers show a band of about 1° that is the result of the resolution of the reported wind direction. All differences for all sensors shows some fluctuations so that the results are averaged in direction bins in order to improve the readability of the results as mentioned above. The binned results at all wind tunnel reference speeds are given in Appendix A2.

#### Gill

During installation, without a reference wind speed, the Gill reported a wind speed below 0.1m/s always in combination with a wind direction. Even when the reported speed is 0.00m/s a direction is indicated. During the tests a tunnel reference of 70m/s was also tried, but in that case the sensor often reports invalid data. Therefore a polar scan at 70m/s was not performed. However, it should be noted that during these tests sensor wind speed reports above 70m/s did occur. In fact single events with reports of 74.82, 75.36 and 81.62m/s occurred. In these situations a virtual temperature is reported, but this shows unrealistic values (e.g. +68.28°C was reported at 81.62m/s which differed more than 20°C from the surrounding 1 second values).

The results for the Gill are rather smooth and consistent, even the raw measurements at the lowest reference speed of 2m/s. The error curves show a good reproducibility over each 90° symmetry angle. The disturbance of the wind field caused by the transducer is clearly visible in the graphs. The disturbance mainly occurs when the wind flow is parallel to a transducer pair. Since the sensor wind direction is corrected for the overall offset with the tunnel reference of about 62°, the sensor North corresponds with a tunnel reference direction of −62°, East corresponds with 28°, etc. Hence the disturbances occur, as expected, around North, East, South and West directions. The disturbance is smallest around 10m/s and increases for lower and particularly for higher wind speed values. This can be explained by the fact that each Gill sensor is calibrated 12m/s, but a generic table, based on the measurements of obtained of many Gill sonic anemometers at several wind tunnels and wind speeds, is used to apply a correction at other wind speed values (Gill, 2005a). This generic correction seems not to work so well at higher wind speed values, whereas overcompensation can be observed at other wind speed values. At low wind

speed the correction introduces an overestimation of the measured wind speed when the flow is parallel to a transducer pair, whereas an underestimation of the wind speed occurs for other directions. At wind speeds of 30m/s and higher the disturbance caused by the transducers of the Gill is very pronounced and spread over a wide angular range. The deviations in the reported direction show an 8-fold symmetry. This is probably caused by the superposition of the 4-fold sensor symmetry and the applied correction. At 60m/s the reported wind direction exceeds the WMO at some orientations.

A so-called custom calibration at 12 and 40m/s was performed by Gill after completion of the tests at KNMI (Gill, 2005b). The unit was tested in their wind tunnel prior to the custom calibration and the results of the DNW measurements could roughly by reproduced, i.e. the underestimation of the wind speed was about 2% at 5m/s, and errors up to about 5% occurred in a broad region around the transducers at 46m/s. After the custom calibration their results showed that the underestimation at 2m/s was reduced to about 1% while the errors at 46m/s reduced to about 2-3%. At 5m/s the disturbance caused by the transducers is however still visible with excursions to –3% (–4% prior to the custom calibration) and the results at 50m/s have no smooth direction dependence but show scatter of about ±1%.

## Thies

Without a reference wind speed the Thies reported 0.0m/s. In these situations the reported wind direction is mostly 000, although sometimes a direction is reported. The North direction is always indicated by the Thies as 360 in case a wind speed >0.0m/s is reported. A test at 60m/s showed that the sensor reported mostly invalid results. The highest reported wind speed by the Thies is 62.0m/s. After an invalid measurement the sensor often reports a faulty wind speed results, e.g. during the test at 60m/s invalid data was seen to be followed by single events of 18.4 m/s and 35.4m/s and once a correct speed was directly reported. In these cases the reported temperature was reduced by about 5 and 3°C compared to the following 1 second results. A polar scan at 60m/s was not considered in this test.

The results of the Thies clearly show that the sensor compensates for the disturbance caused by the transducer arms, although a small effect can still be observed at wind speeds below 15m/s. The Thies results for all wind speeds up to 30m/s are close to the reference. The gap in the data around –45° at 2m/s is caused by 15 seconds of missing wind tunnel data. The Thies experienced problems at 50m/s. During the polar scan at 50m/s 5 periods with faulty data occurred. Once this was directly followed by correct data, twice it was followed by a single report of 25 and 35m/s, the long interruption around 45° was followed by 2 reports of 10m/s and between 2 invalid readings 12 faulty report of 20m/s were observed.

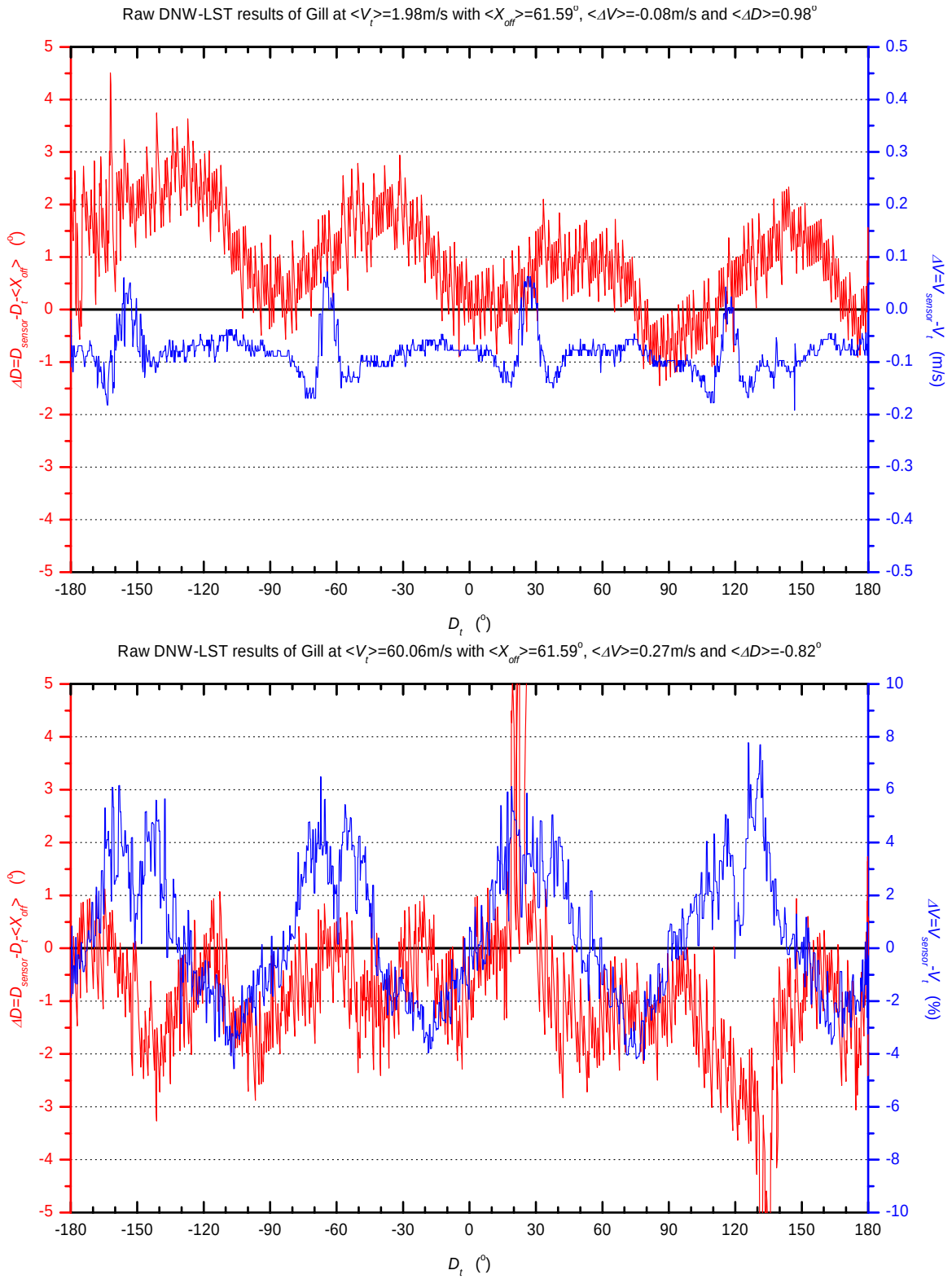


Figure 9: The raw DNW-LST results of the Gill sonic anemometer at wind tunnel reference speeds of 2 and 60m/s.

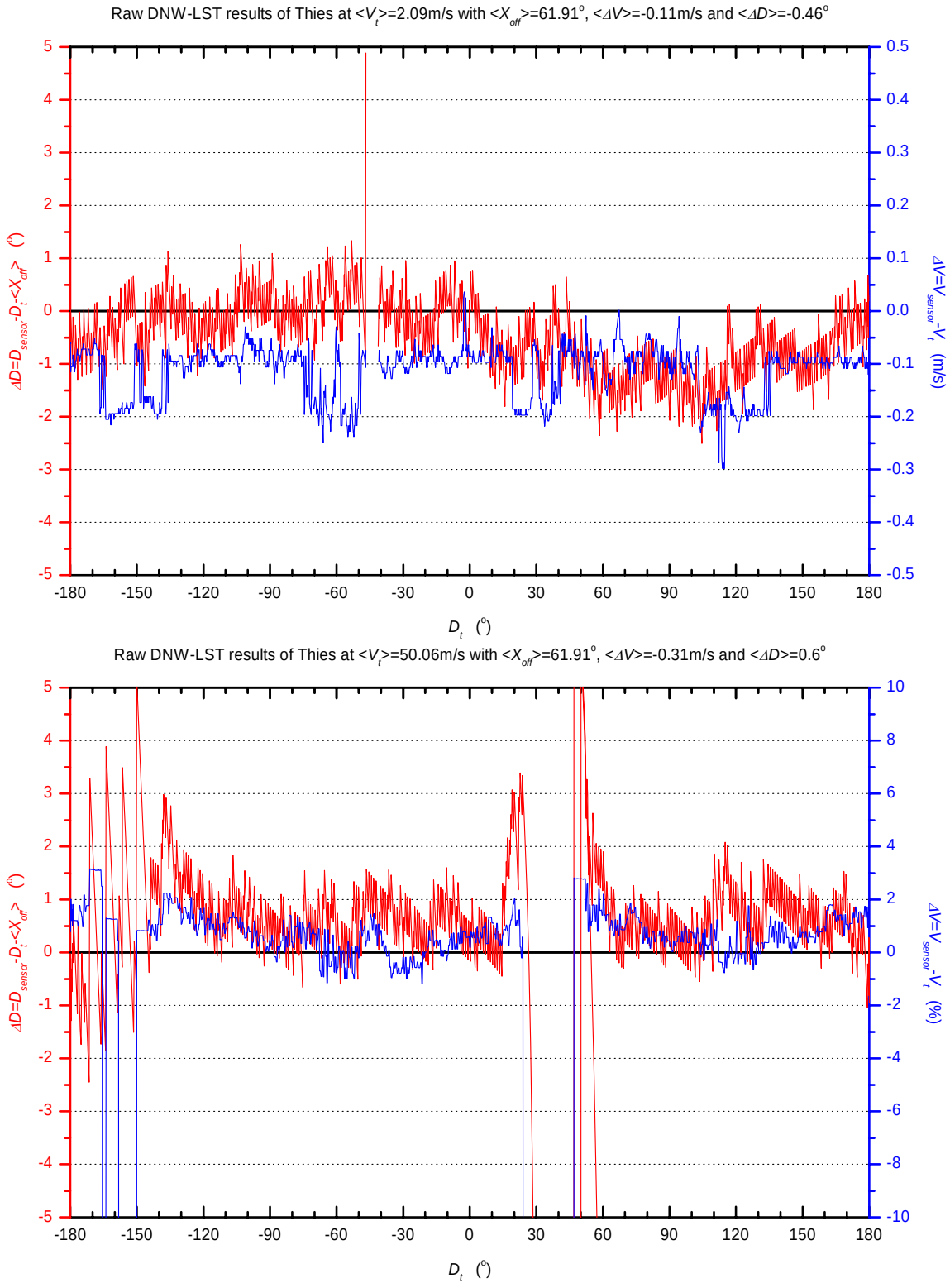


Figure 10: The raw DNW-LST results of the Thies sonic anemometer at wind tunnel reference speeds of 2 and 50m/s.

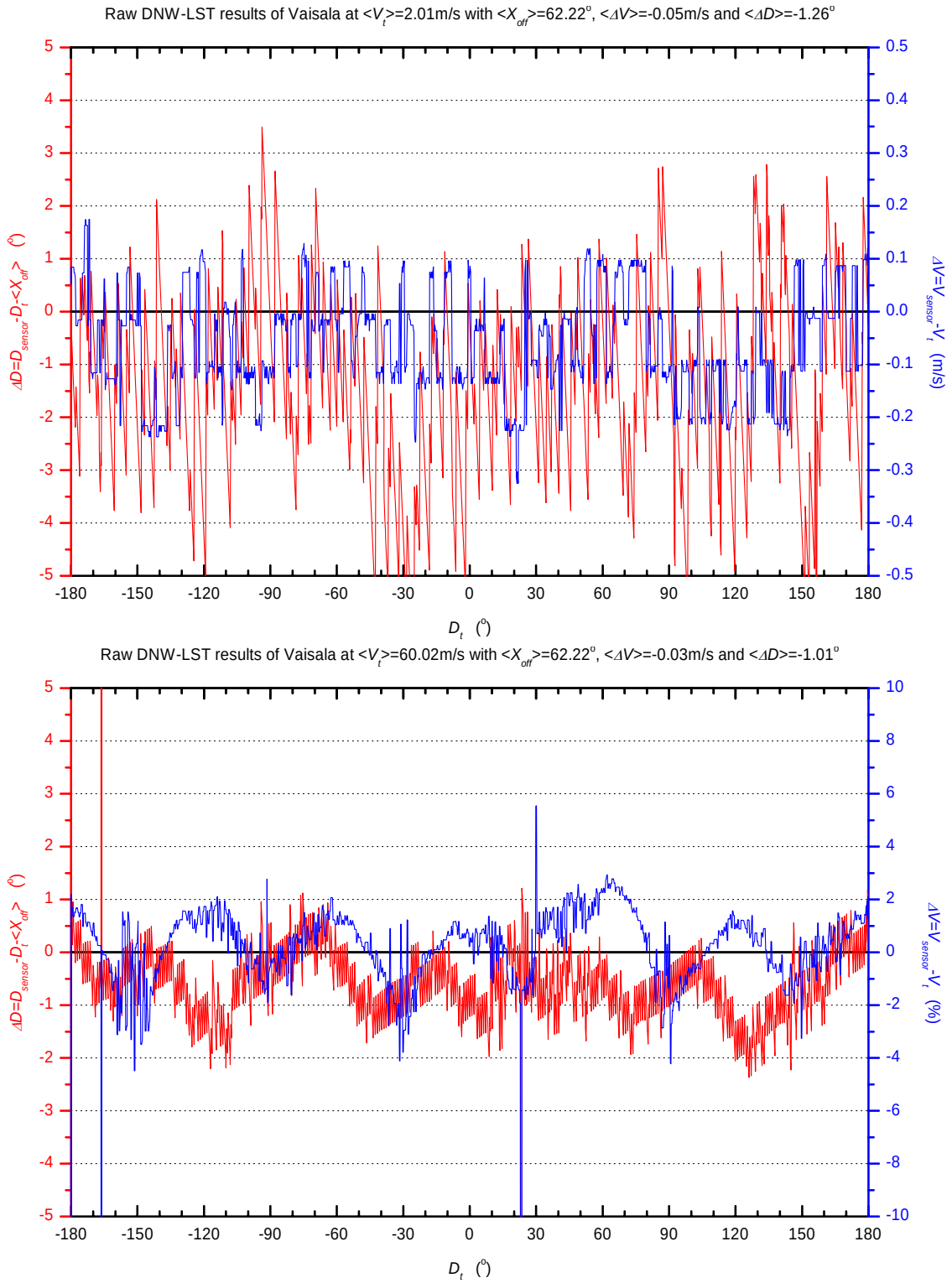


Figure 11: The raw DNW-LST results of the Vaisala sonic anemometer at wind tunnel reference speeds of 2 and 60m/s.

After the test at KNMI the sensor was returned to Thies for inspection. They reported that humidity entered the transducer housing as a result of the bird-inflicted damage during the field test, which deteriorated the transducer electro-acoustic characteristics and probably caused the problems at wind speeds of 50m/s and higher (Thies, 2004). The sensor was repaired by Thies and equipped with anti-bird wires. Recently, Thies launched a new 2Da DSP version of the sonic anemometer in which the rubber caps around the transducers have been replaced by Stainless steel caps in order to prevent any bird-inflicted damage.

## Vaisala

During installation, without a reference wind speed, the Vaisala reported a wind speed of 0.0m/s always in combination with a wind direction of 000. The Vaisala frequently reported invalid measurements during the polar run at 70m/s. The invalid data do not show up in the binned results because they occur mainly as isolated events. The highest wind speed reported by the Vaisala at 70m/s was 77.8m/s.

The results of the Vaisala sonic anemometer are noisy at low wind speeds (<5m/s). In the raw data this can over lead to differences in the wind direction exceeding the WMO limit of ±5°, but binned results are within the WMO limits. The results of the Vaisala improve at higher wind speeds and show little angular dependence with a 6-fold symmetry (3 transducers each paired with the 2 others). For wind speeds of 50m/s and more a small disturbance caused by the transducer arms can be observed. The Vaisala sonic anemometer sometimes gives an incorrectly formatted response in which the “1” denoting the 1-second averaging is substituted by a <CR><LF>. This format error is corrected in the acquisition and processing software. During the wind tunnel tests 4 of these format errors occurred and all during the 60m/s scan. The wind speed and direction reported during these format errors was incorrect.

The results of all polar scans were used to calculate the azimuthally averaged differences in the measured wind speed. The percentage deviations of these averaged wind speeds from the tunnel wind speed are shown in Figure 11 as a function of the tunnel wind speed. The numerical values of the azimuthally averaged results and the standard deviation are also listed in Appendix A1. The two KNMI cup anemometers are also included in this figure. Figure 12 shows that the azimuthally averaged wind speeds of all sensors agree with the tunnel reference speed within the accuracy of ±10% required by WMO. All sensors give lower averaged wind speed values at low tunnel speeds. The cup anemometers measurements are close to the tunnel values in the middle wind speed range of 5 to 30m/s, but underestimate the wind speed at low and high wind values. The underestimation at low wind speeds is probably the result of friction, whereas at high wind speeds turbulence might cause the deviation from the assumed linearity between revolution frequency of the cups and wind speed. Please note that the usage of a percentage difference partly explains the increasing deviation for lower wind speeds. The results of both cup anemometers are consistent. The reason for the 1.5% difference for the results of cup anemometer 115 at 5m/s is unclear. The sonic anemometers generally show the largest relative differences at low wind speed values and the differences decrease for higher wind speed values. The Vaisala and Thies show the same behavior,

but the results of the Thies are generally about 2% lower than for the Vaisala. The Vaisala slightly overestimates the wind speed above 5m/s whereas the Thies always reports wind speeds slightly too low. The 0.5% difference in the results obtained for the Vaisala at 5m/s might be caused by temperature dependence since the temperature differed 11°C. The Gill generally differs more from the tunnel reference compared to the other 2 sonic anemometers and also shows larger fluctuations between the differences at neighboring wind speed values. Note that the successive wind speed values were measured alternatively in the upward and downward sweep through the full wind speed range and that the temperature changed between 8 and 32°C. The results of the Gill indicate a temperature dependence of about –2% for a 20°C increase in temperature. The results of the Gill$^+$ were obtained for temperatures between 18 and 27°C indicate a temperature dependence of about –1% for a 10°C. However, the results at 2m/s show hardly any temperature dependence, at 3m/s an increase of 10°C leads to a 1% increase of the wind speed and at 5m/s the results of 28 and 23°C coincide while the results of 19°C are 1% higher. The wind speed reported by the Thies anemometer is generally closest to the results of the cup anemometer, but without the increased underestimation of the wind speed by the cup anemometers at wind speeds exceeding 20m/s.

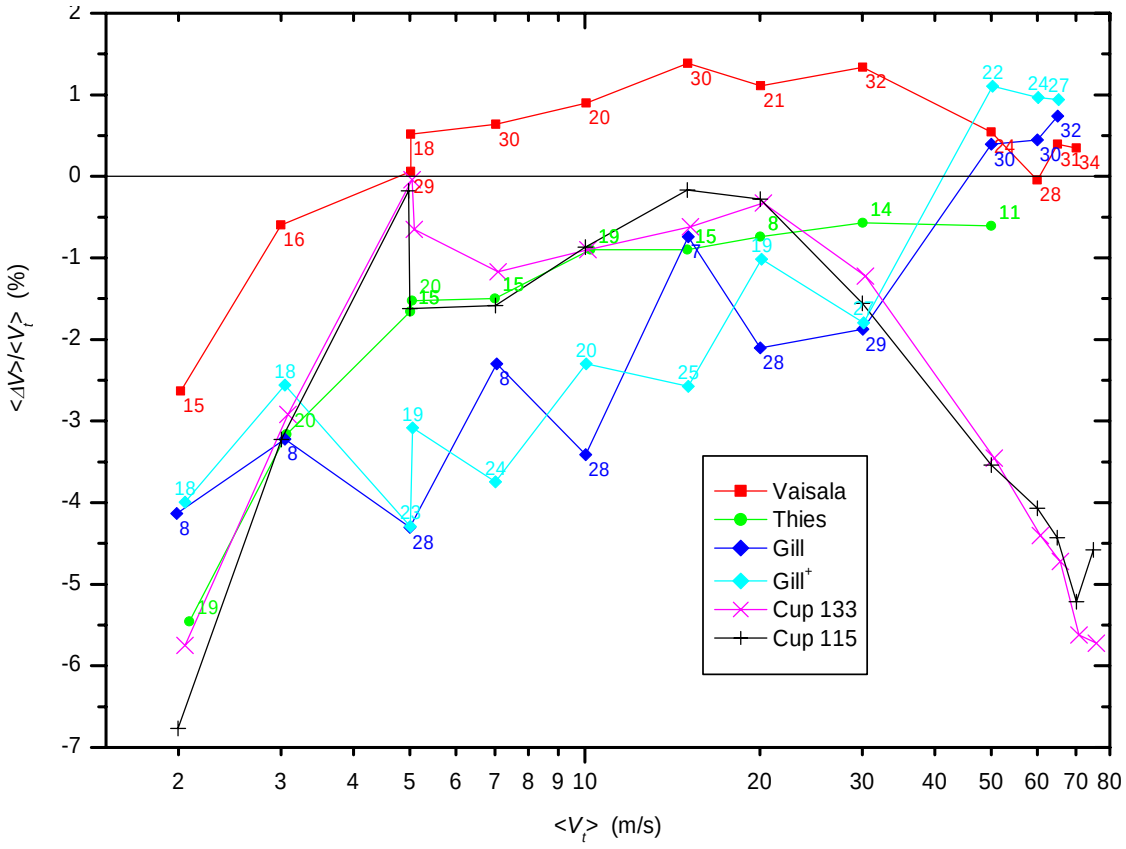


Figure 12: Relative differences between the DNW-LST tunnel reference speed and the wind speed reported by the sensor averaged over all angles as a function of the tunnel speed. The numbers indicates the temperature in the wind tunnel during the respective measurement.

## *4.2. KNMI wind tunnel test*

### 4.2.1 Test setup and results

The results of the tests of the sonic anemometers and the KNMI cup anemometers in the KNMI wind tunnel have been obtained after the field test in December 1-4, 2003. Tests have also been performed prior to the field test, but these results are not considered here since they were obtained with older software versions of the sensors. It should be noted that the measurement section of the KNMI wind tunnel is rather small. The disturbance of the wind flow caused by the anemometer itself will therefore be quite large. Hence the tests results obtained in KNMI wind tunnel are not considered as checks of the calibration of the sonic anemometers. The purpose of the tests was to perform a functional check of the sonic anemometers. The results can, however, also be used to determine up to what accuracy the calibration can be verified in the KNMI wind tunnel. In addition, consistency checks between sonic anemometers and a check of the alignment of the sensor to the coupling device can be performed in the KNMI wind tunnel. The latter is evident from the small differences observed in the offset in wind direction between sensor and rotation device at various wind speeds for each sensor.

The tests in the KNMI wind tunnel have been obtained at several tunnel wind speeds raging from 1 up to 20m/s. For each tunnel speed the sonic anemometer was rotated over 360° in azimuth in steps of 5°. After each azimuth step a 3 second delay was introduced followed by 5 measurements at 1 second intervals. The results have been averaged for each azimuth angle and are reported in Appendix B for each sensor and tunnel wind speed as a function of the azimuth angle of the KNMI rotation device. The results obtained in the KNMI and DNW wind tunnel show a similar behavior, but some differences can also be observed. The Gill shows a good reproducibility and a good symmetry over 90° azimuth angles. The disturbance by the transducers is clearly visible in the wind speed results up to 5 m/s and decreases for higher wind speeds. Contrary to the results obtained at DNW tunnel there is hardly any offset between the sensor and tunnel wind speed. The wind direction shows less scatter than in the DNW tunnel, probably as a result of the fixed azimuth angle at which the measurements are performed. As a consequence the 90° azimuth symmetry in the differences is more clearly visible. The Thies also shows good agreement with the tunnel wind speed, without an underestimation. A small overcorrection for the disturbance caused by the transducers can be observed around wind speeds of 7m/s. The Vaisala again shows much scatter at low wind speeds, particularly for the wind direction measurements. Near the azimuth angle of −80° (sensor wind direction of about 280°) the Vaisala shows faulty readings probably as a result of an internal reflection. In these situations the Vaisala reports either invalid readings, or wind speeds that are nearly twice the tunnel value, or measurements that are obviously wrong. At tunnel speeds of 15m/s or more this disturbance was not observed, nor at a zero tunnel speed reference run. The wind speed reported by the Vaisala is generally higher than the KNMI wind tunnel speed.

### 4.2.2 Detailed results

The results of all azimuth scans were used to calculate the azimuthally averaged differences in the measured wind speed. The percentage differences of the azimuthally averaged sensor wind speeds and tunnel speed are shown in Figure 13 as a function of the tunnel speed. The Vaisala shows a nearly constant 3 to 4% overestimation of the wind speed, but at 1 and 2m/s the deviation is +5 and –3%, respectively. The Thies gradually moves from a 2% underestimation at 1m/s to a small overestimation at 20m/s. The relative difference of the Gill wind speed varies between –1.5 and +2.5%. Finally, the 2 cup anemometers show good agreement within ±1% of the tunnel speed, but at 1m/s both overestimate the wind speed by about 3%, whereas an underestimation could be expected as a result of friction.

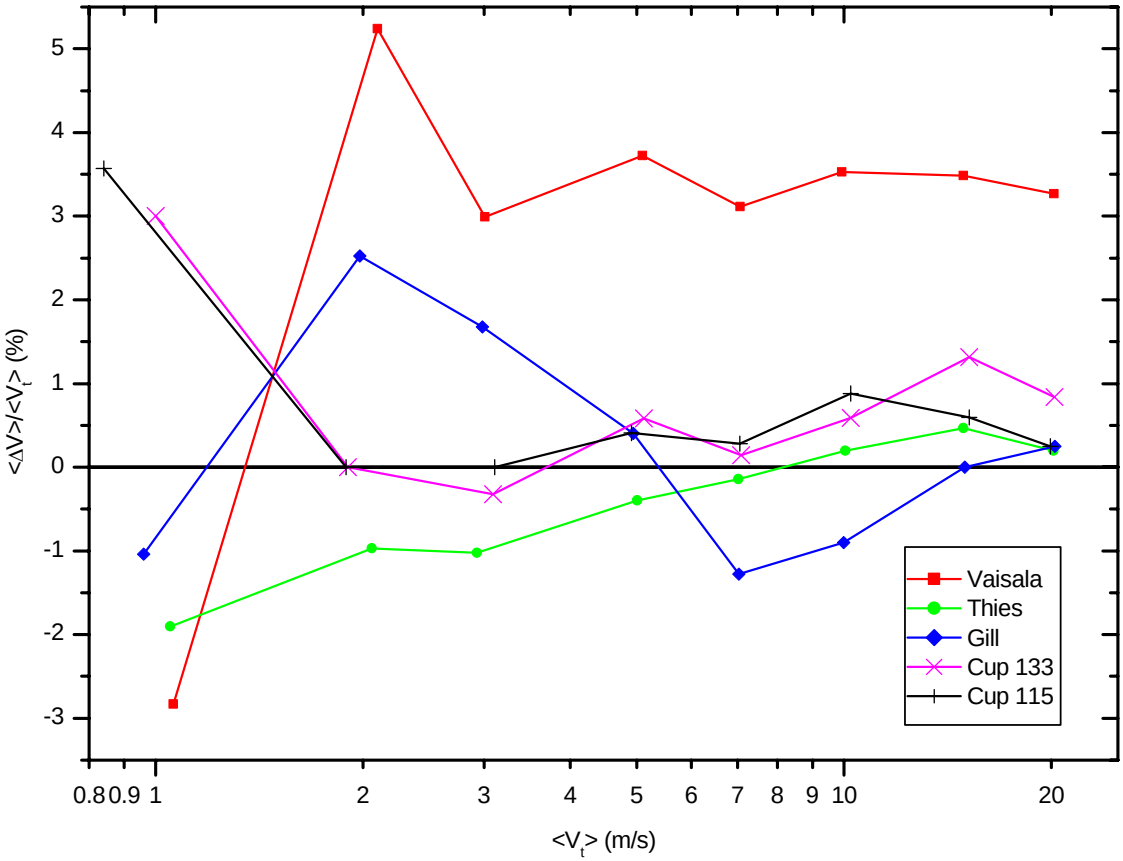


Figure 13: Relative differences between the KNMI tunnel speed and the wind speed reported by the sensor averaged over all azimuth angles as a function of the tunnel speed.

The azimuth averaged results obtained in the KNMI wind tunnel are compared to the corresponding results obtained at the DNW wind tunnel in order to check the validity of the results obtained with the KNMI wind tunnel. The absolute differences obtained at KNMI and DNW are given in Figure 14. For that purpose the double results obtained in the DNW tunnel at 5m/s and for the Gill are averaged. The differences for all sensors are about 0.1 to 0.2m/s, but the differences increase to about 0.4m/s at 20m/s for the Vaisala and Gill. The results obtained in the KNMI wind tunnel generally show an overestimation compared to the results obtained at DNW. This overestimation can be described by

0.1m/s+1%, or more precisely 0.1m/s+1.5% for the Vaisala and Gill and 0.1m/s+0.5% for the Thies. It should be noted that this correction should be applied in addition to the correction that is currently used in the KNMI wind tunnel and that has been derived for the KNMI cup anemometer. In fact, the KNMI cup anemometers overestimate the wind speed by about 0.1m/s in the KNMI wind tunnel and one of the cup anemometers shows a small increase with tunnel speed. Clearly, the KNMI wind tunnel is suitable to check the absolute calibration of the sonic anemometers in the 2 to 20m/s wind speed range within the required accuracy limits of ±0.5m/s or ±10%.

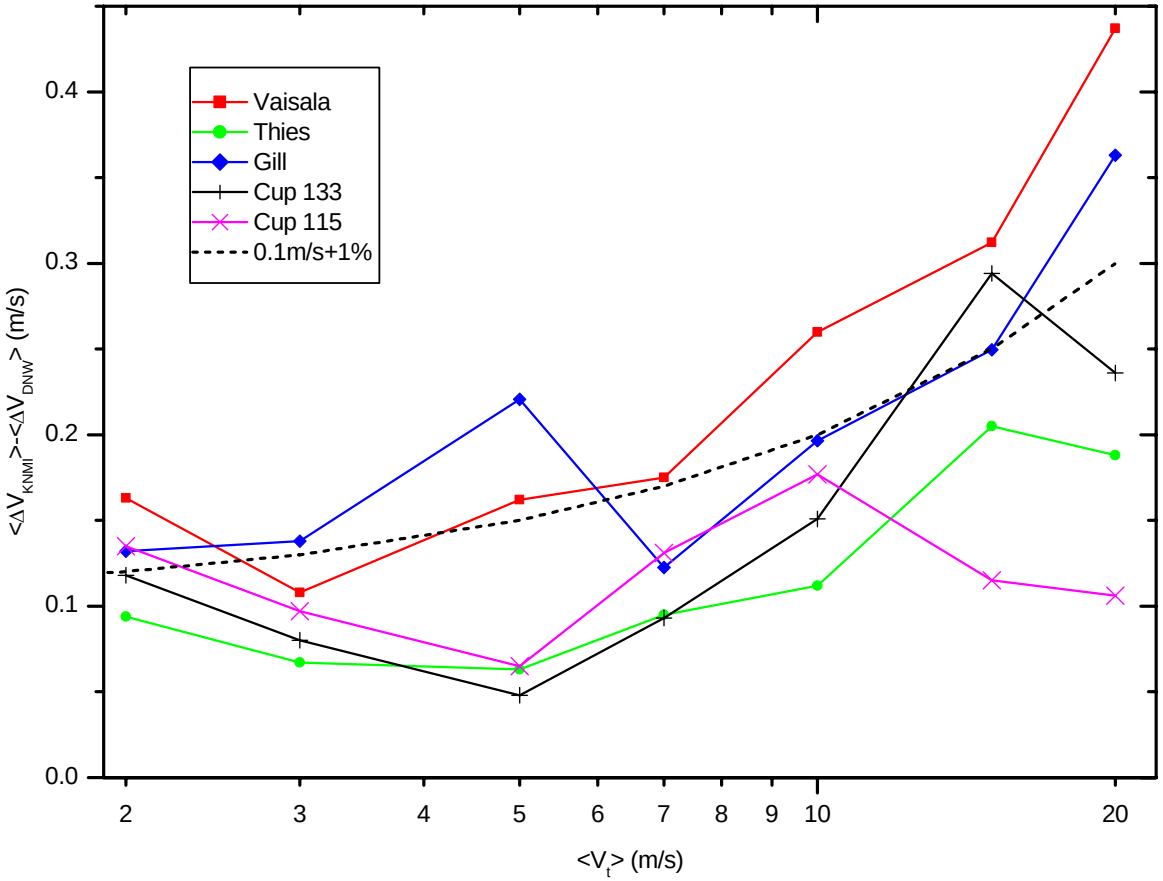


Figure 14: Absolute differences between the azimuth averaged wind speed reported by the sensors in the KNMI and the DNW wind tunnel and a function of the tunnel speed.

Finally the results obtained for the sonic anemometers in the KNMI wind tunnel at 5m/s, but with a step in azimuth of 2° are discussed. The results for the Gill, Thies and Vaisala are given in Figure 15 to Figure 17, respectively. The Gill and Thies again show the good reproducibility. The steps in the curves are the results of the output resolution of the sensor. Particularly, for the wind speeds reported by the Thies the disturbances are restricted to a narrow angular range. A small step in azimuth is required to resolve this fine structure and to determine the maximum differences. The results for wind speed and direction of the Vaisala show much variability. Although the wind speed reported by the Vaisala is generally identical for all 5 individual measurements at a particular azimuth angle, the differences often vary by ±0.1m/s and sometimes more from one azimuth orientation to the next.

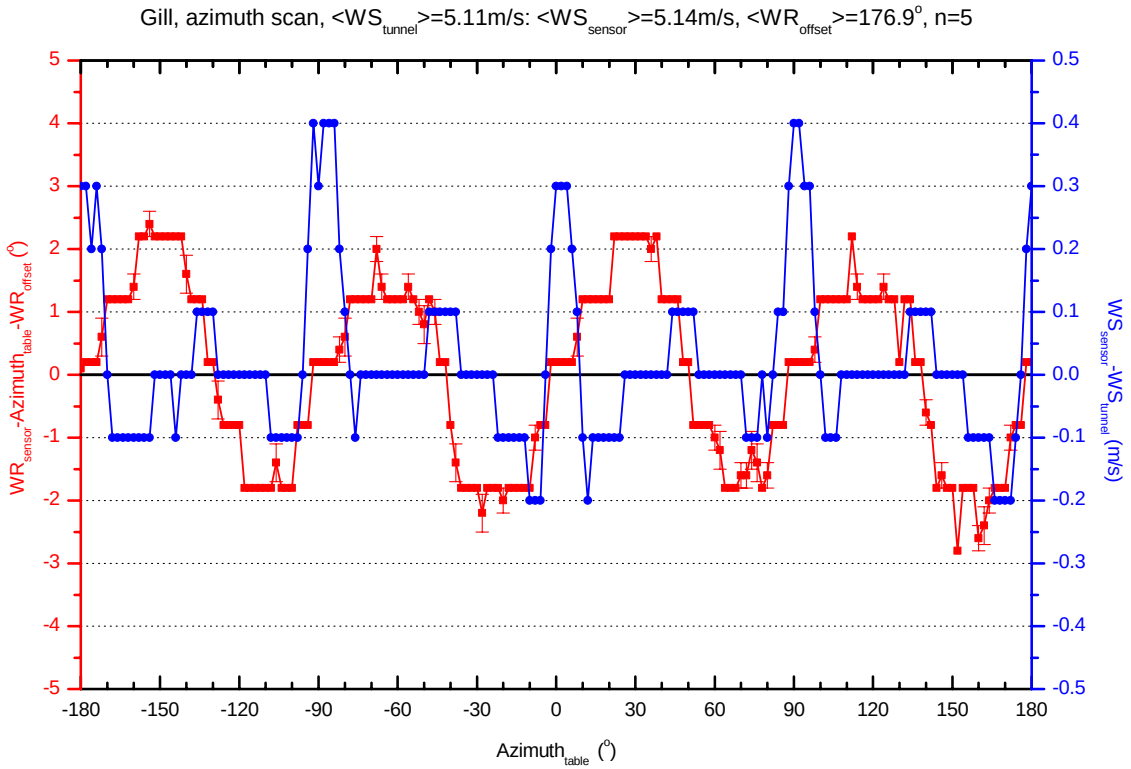


Figure 15: The KNMI wind tunnel results of the Gill sonic anemometer for a tunnel speed of 5m/s and a step in azimuth of 2°.

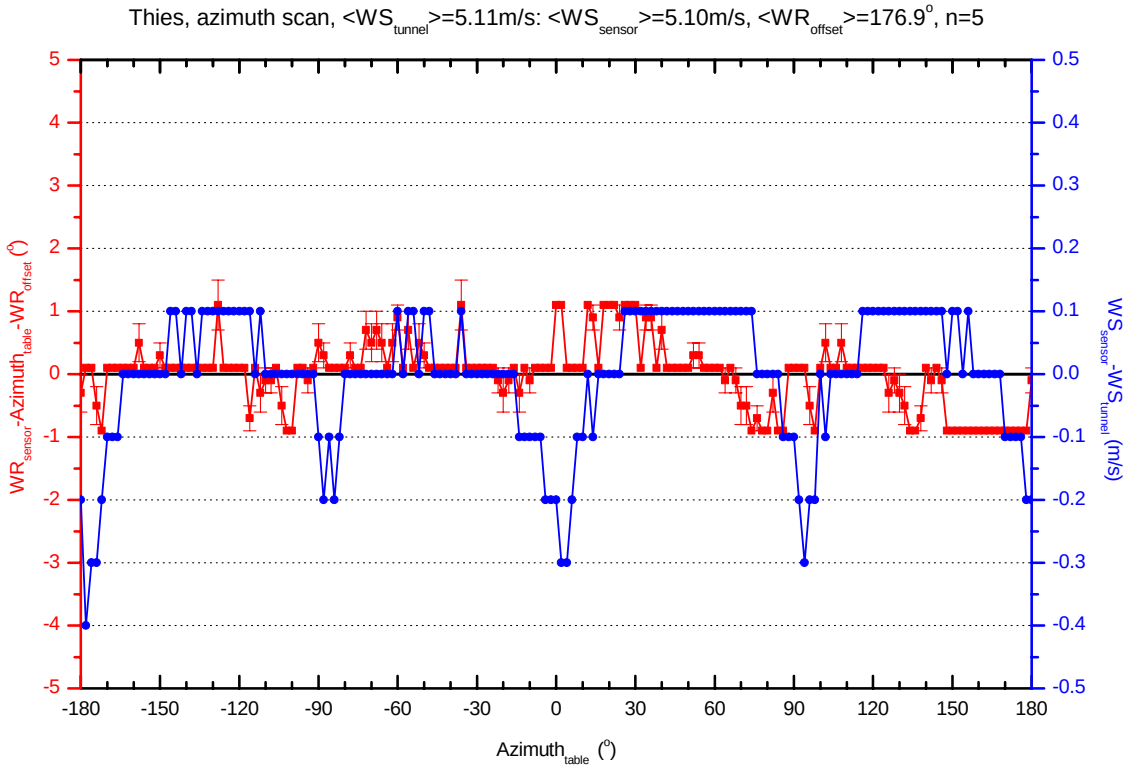


Figure 16: The KNMI wind tunnel results of the Thies sonic anemometer for a tunnel speed of 5m/s and a step in azimuth of 2°.

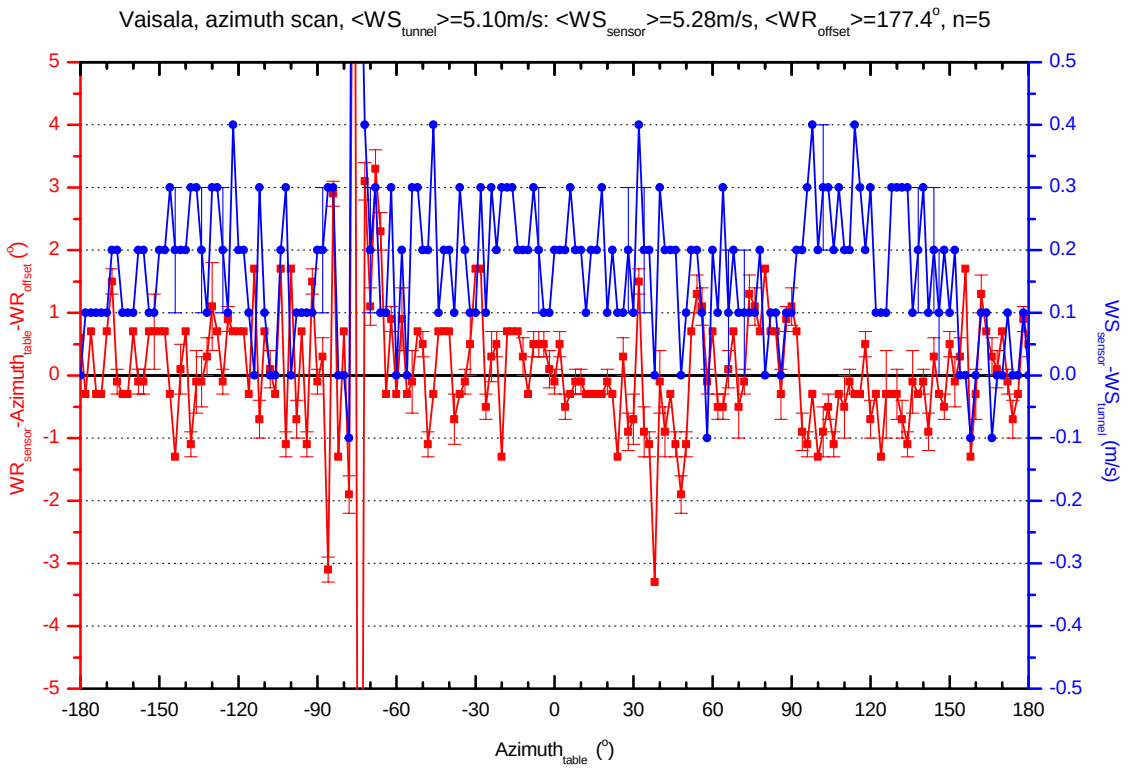


Figure 17: The KNMI wind tunnel results of the Vaisala sonic anemometer for a tunnel speed of 5m/s and a step in azimuth of 2°.

## 4.3. TNO wind tunnel test

A calibration of the sonic anemometers has been performed at the TNO wind tunnel in Apeldoorn on April 20, 2001. This calibration was performed prior to the field test. Since each of the sonic anemometers was upgraded afterwards, the results of the TNO are not considered for a verification of the calibration. The reason to present results of the TNO wind tunnel test is that the inclination dependency of the anemometers has been investigated in this tunnel only. The inclination was varied between −30 and +30º with steps of 5º and performed for the azimuth angles 0 to 90º with steps of 15º for a tunnel speed of 5m/s. The results are given in Appendix C and show the relative difference of the sensor results form the expected cosine behaviour. The results for the inclination of 0º show similar results as for the azimuth scan at 5m/s, but the contour graph has less detail due the coarse azimuth step of 15º. In general, all three sonics show the expected cosine behaviour.

The azimuth scan of the Gill clearly shows the disturbance caused by the arms. The measurements of the Gill show a good reproducibility over 90º intervals and the wind speed show a general underestimation. The Thies shows almost no influence of a disturbance of the arms, but some variability in the results can be observed. The step change in the differences of wind direction between the −180º to 0º and 0º to180º azimuth interval is related to the history exceeding 1 second averaging period mentioned in section 3.4. The inclination behaviour of the Gill and Thies anemometers is very similar.

The disturbance by the transducers introduces increasing errors in the wind speed when the inclination deviation from zero. Furthermore, the deviation is not symmetric for both sensors. The largest deviation from the expected cosine behaviour occurs for an inclination of +30º when the wind is parallel to a transducer pair. In this situation the wind speed is underestimated up to about 10% for the Thies and 20% for the Gill. For an inclination of −30º the deviation is only small and the disturbance by the transducers is not so pronounced. At an inclination around −10º the disturbance by the transducers shows a local extreme with enhanced negative values of about −10% for the Thies, whereas the Gill reports a local maximum with differences of about +1%. The latter might be affected by the 15º resolution in azimuth which did not resolve the narrow positive disturbance caused by the transducers for an inclination of 0º. The large deviation for positive inclination angles is probably induced when the disturbance generated by the sensor housing reaches the transducers. The errors in the reported wind direction show little dependency with inclination angle. The differences for Gill anemometer are always within about 1º. The Thies gives slightly higher differences for inclination angles outside the –25º to 20º range.

The azimuth scan of the Vaisala shows no effect of a disturbance by the arms in the wind direction, but it shows up in the wind speed. As mentioned above (section 3.4), it turned out that for this particular setting (m/s) the sensor used the wrong transducer pair for deriving the wind speed. The wind speed results of the Vaisala show almost perfect cosine behaviour at all azimuth angles and inclinations. Only for the azimuth angle of 45º with an inclination angle exceeding +25º the deviation increases to almost 10%. At this azimuth angle the disturbance of the arms is most pronounced (about 6% in the sensor in the vertical position). For a small inclination the differences first decrease slightly, but around 20º they start increasing again. At this inclination angle the disturbance caused by the bent in the arms is probably sensed. The wind direction results also show very little dependency on inclination angle. Note however, that the output resolution of 1º of the Vaisala conceals any smaller details.

Clearly the selection of the undisturbed transducer pairs by the Vaisala gives good results for inclined wind flow attack angles. The Gill and Thies use a correction algorithm that has been determined for horizontal flow conditions which performs less well for inclined situations, particularly when wind speed is considered. It should however be noted that the vertical component of the wind is generally an order of a magnitude less than the horizontal component. Hence the resulting error resulting from the vertical component will be reduced accordingly.

The inclination test was also performed with the KNMI cup anemometer fixed to the pole of the rotation/inclination device in the central position. The results of the sensor wind speed readings as a function of inclination angle are presented in Figure 18. The cup anemometer shows no clear cosine response. Between inclinations of −15 and 15º the cup anemometer reports lower values for increasing inclination, but at more extreme inclinations the sensor reports higher values again. The cup anemometer follows the cosine response within ±5% between inclinations of –20 and 20º while at higher inclination angles an overestimation is reported. The results at inclination angles

exceeding ±20º are much better by assuming that the cup anemometer experiences no cosine effect at all.

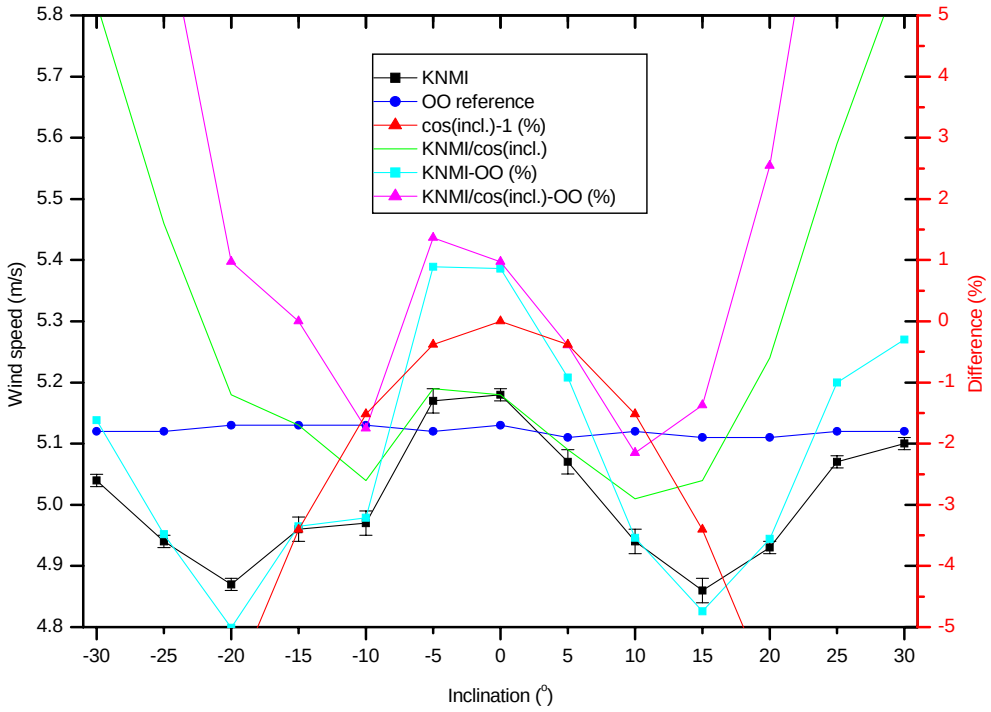


Figure 18: Dependency of the KNMI cup anemometer on inclination measured at a tunnel reference speed of 5.12m/s.

# 5. Field test

## *5.1. Data acquisition, processing and availability*

The field test was conducted at the test site in De Bilt between June 15, 2002 and July 2003. The 3 sonic anemometers were mounted on a 10m mast using a head that separated the central axis of the sonics by 1m. The mast was located 20m to the south-southwest of the 10m mast containing the KNMI cup and vane. The 3 sonic anemometers Gill, Thies and Vaisala were oriented ENE to WSW. See section 3.8 for details. During the period of the field test 12-second data of the KNMI wind sensor set and 1sec values of the sonic anemometers were archived. The sonic 1Hz data was processed off-line into running 3-second averages from which the 10-minute averaged values and extremes were derived following the processing in the KNMI sensor interface (cf. section 2.1). The analysis given below is based on 10-minute data.

First the availability of sensor data is considered. For each 10-minute interval any 10-minute measurement with more than 0% missing data, i.e. with 3 or more 1 second values of the sonics missing, are counted. Situations when data of all 3 sonics is not available are not considered since this is caused by gaps in the data acquisition. Furthermore, all 10-minute intervals with sonic measurements during which lightning was reported, i.e. when the lightning detection system reported lightning events within a 15km radius around De Bilt, are considered. The number of occurrences per sensor is reported in Figure 19. The total number of cases is 469. In 318 10-minute intervals lightning is detected, in 110 cases no lightning is detected and in 41 cases the lightning information is not available. There are in total 152 cases during which at least one of the sensors experienced missing data. In only 2 occasions the missing data events correspond with lightning detections, both cases are missing data reported by the Vaisala sonic anemometer. Furthermore only 4 of the 152 missing cases correspond with situation when precipitation is reported (2 for Vaisala and 2 for Gill). The total number of cases with missing data is 92, 65, 58 and 28 for the Vaisala, Thies, Gill, and KNMI sensor, respectively. The 32 cases where all three sonics show (identical) missing values are situations when the data acquisition was temporarily interrupted, in 15 of these cases the KNMI sensor information is also missing. In 10 cases 2 sonics experience missing data simultaneously, although the actual percentage differs. Note that there are situations that a significant fraction of the measurements is missing. The number of 10-minute interval with significant amounts of missing data (missed$\geq$10%) not related to problems with data acquisition is 9, 17, 6 and 11 for Vaisala, Thies, Gill, and KNMI sensor, respectively. The missing cases for the KNMI sensor are related to maintenance (9), during which the sensor is disabled, a communication error with the wind vane (4), and a reset of the sensor interface (1). The problems with the sonics seem not related to lightning or precipitation as was noted in previous studies (cf. e.g. Siebert and Teichmann, 2000; Gilhausen and Hervey, 2001). The invalid measurements encountered during this field test could be caused by the presence of birds in the sampling area between the transducers. This has not been confirmed by visual reports, but the damage observed on the Thies after the field test confirms the presence of birds. The highest observed missing rates not associated to

problem in data acquisition are 66%, 98% and 84% for Vaisala, Thies, and Gill, respectively.

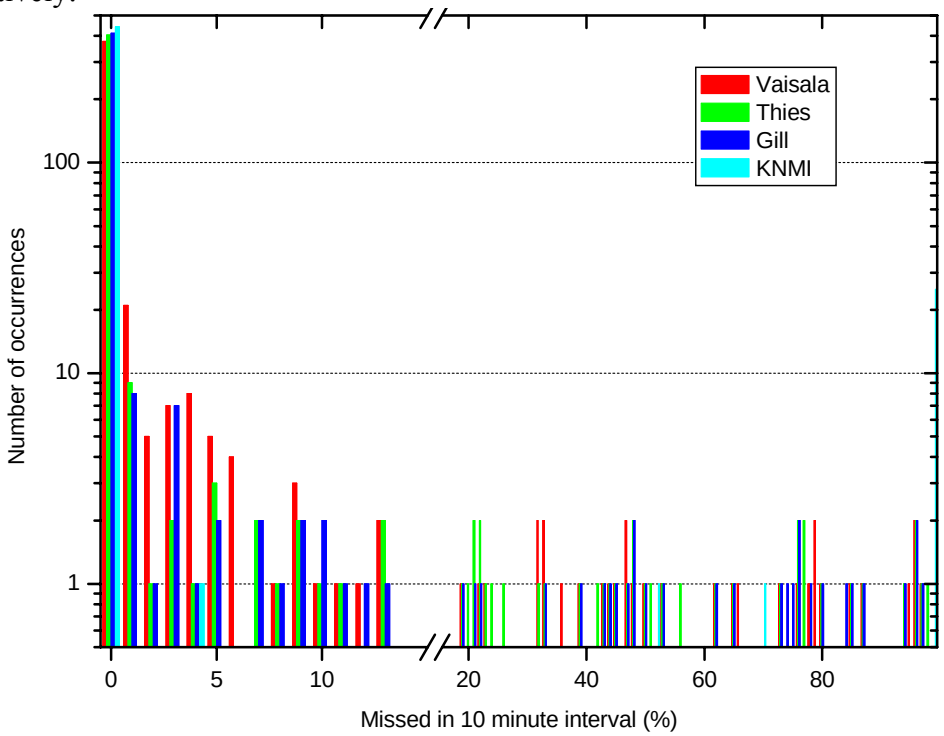


Figure 19: Histogram showing the frequency distribution of missing data for the three sonics and KNMI anemometer and wind vane in 1% bins. Only 10-minute intervals with missing data or lightning reports are considered.

## 5.2. Overview of results

A histogram of the 10-minute averaged wind speed data shows that the cup anemometer reports more cases with a wind speed below 0.5m/s than the sonic anemometers and generally also reports more cases with wind speeds above 3m/s (cf. Figure 20). The first is related to the detection threshold of the cup anemometers and the latter is probably related to the so-called overspeeding (cf. e.g. Busch and Kristensen, 1976). Speeding was clearly observed during a storm on October 27, 2002 (cf. Figure 21) when the cup anemometer and sonics showed good agreement for wind gusts up to 28m/s, whereas for the 10-minute averaged wind speed up to 12m/s the cup anemometer systematically reported higher values by about 1m/s. The differences in the number of occurrences per wind direction bin show large fluctuations (cf. Figure 20). The KNMI cup anemometer and Gill e.g. shows more occurrences at 250° and 140°, respectively, whereas Thies and Vaisala show lower values at 60° and 250°, respectively. Note that the differences can partly be caused by the binning of the results, even when the actual differences are within 10°.

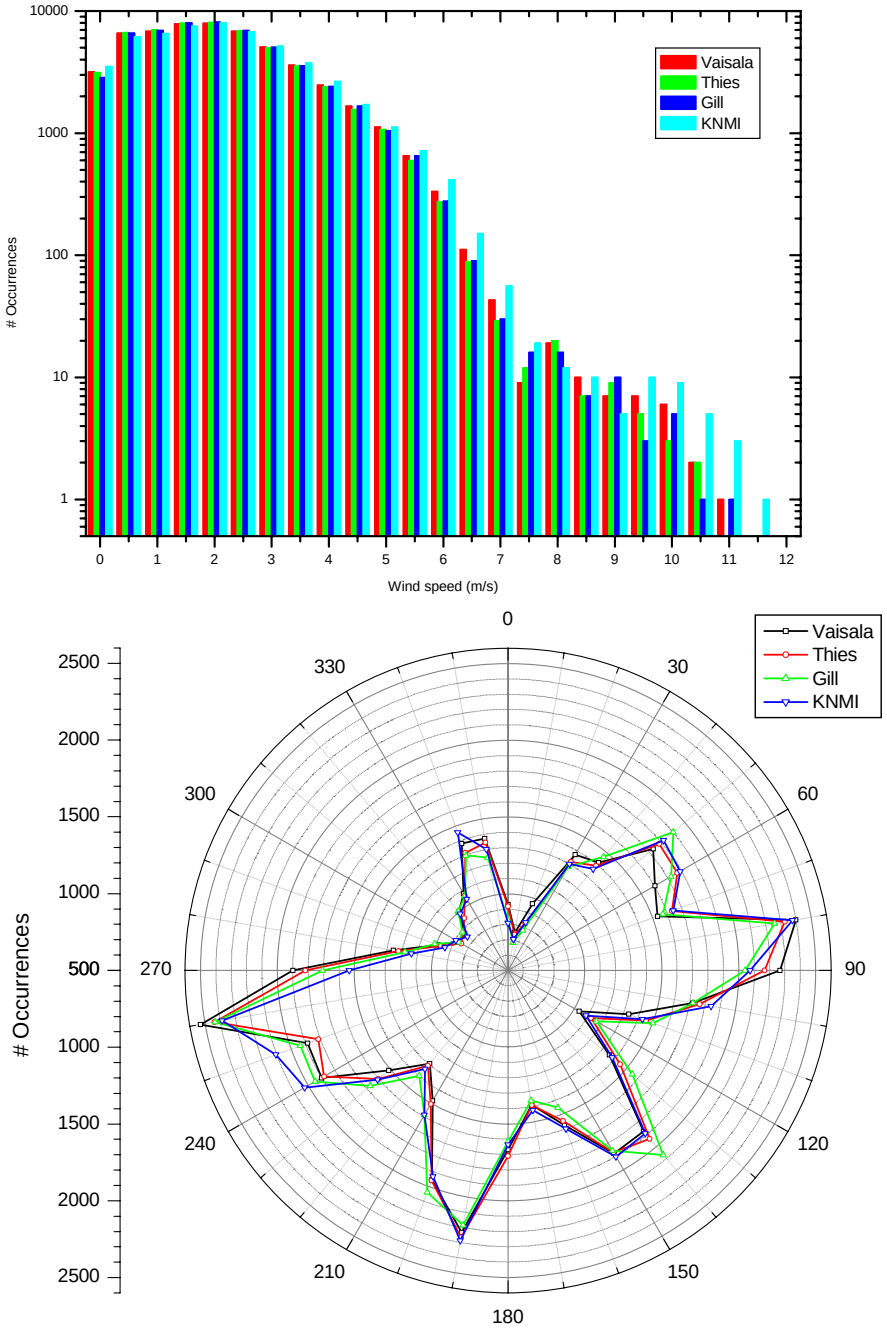


Figure 20: Histogram showing the frequency distribution of the 10-minute averaged wind speed in 0.5ms/ bins (top) and wind direction in 10° bins (bottom).

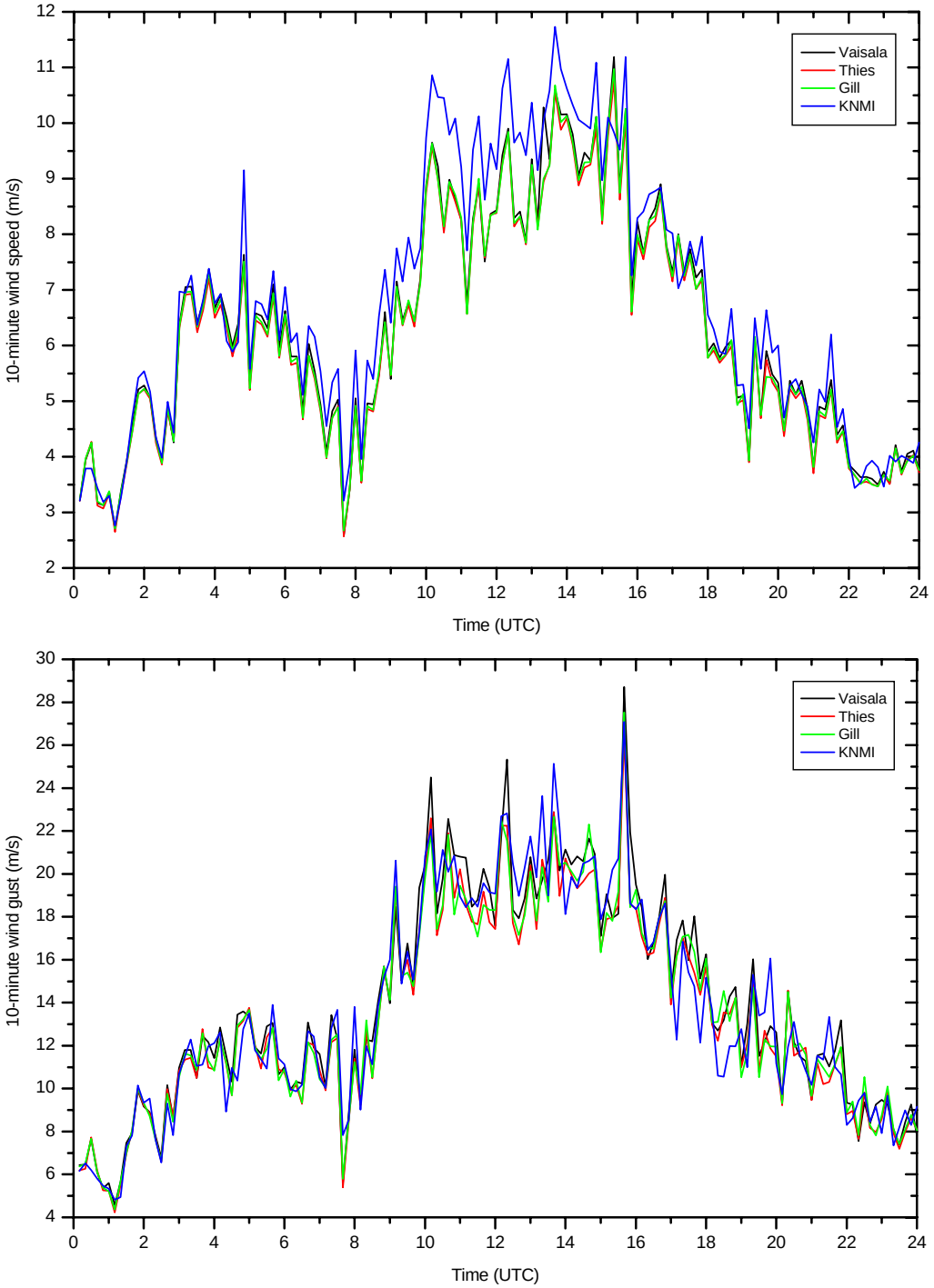


Figure 21: The 10-minute averaged wind speed (top) and wind gust (bottom) observed in De Bilt on October 27, 2002.

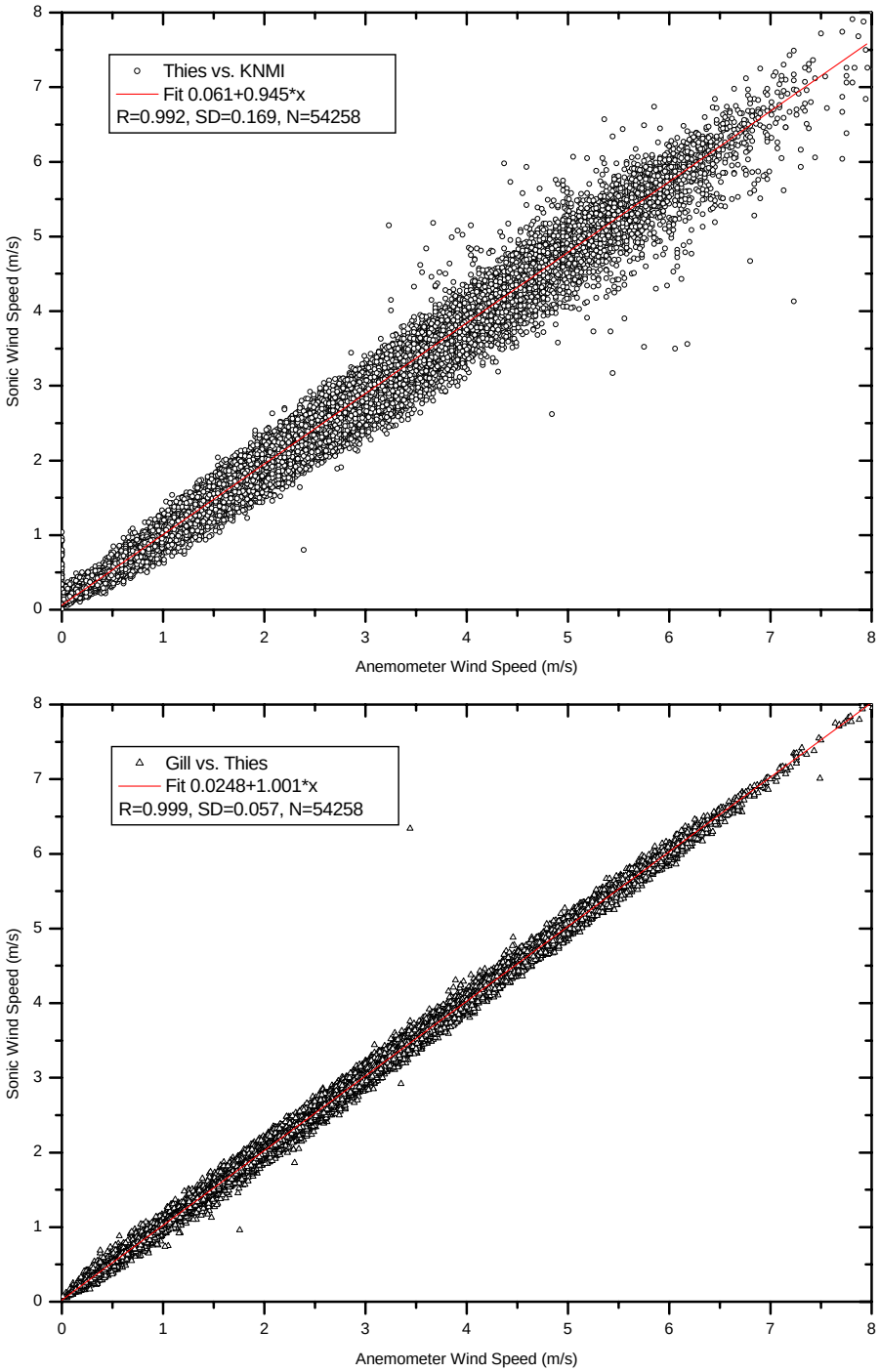


Figure 22: Scatter plot of the 10-minute averaged wind speeds showing Thies versus KNMI (top) and Gill versus Thies (bottom).

A scatter plot of all 10-minute wind speed data of the cup anemometer versus a sonic is given in Figure 22. The correlation is 0.992, the slope of a linear fit is about 0.95 (0.97 for Vaisala versus cup anemometer) and the standard deviation of the fit is 0.17m/s for all three sonics. Although the overall agreement is quite good some cases with large differences that exceed WMO requirements do occur. Most striking are the cases where

all 3 sonics reported wind speeds between 0.5 and 2m/s while the cup anemometer was probably frozen and reported 0m/s. All these cases occurred on December 18, 2002 (cf. Figure 23) during which the ambient temperature observed at 1.5m was below -3°C. In all other 99 situations when the cup anemometer reports 0m/s, the sonics report a wind speed below 0.32m/s and hence is close to the allowed starting threshold of 0.3m/s. The slope of the linear fit below unity indicates the overestimation of the 10-minute averaged wind by the cup anemometer compared to the sonic wind. Comparison between the 3 sonics shows much better agreement with a correlation of 0.999, slope of the linear fit of 0.98 (1.00 between Thies and Gill) and a standard deviation of 0.06m/s.

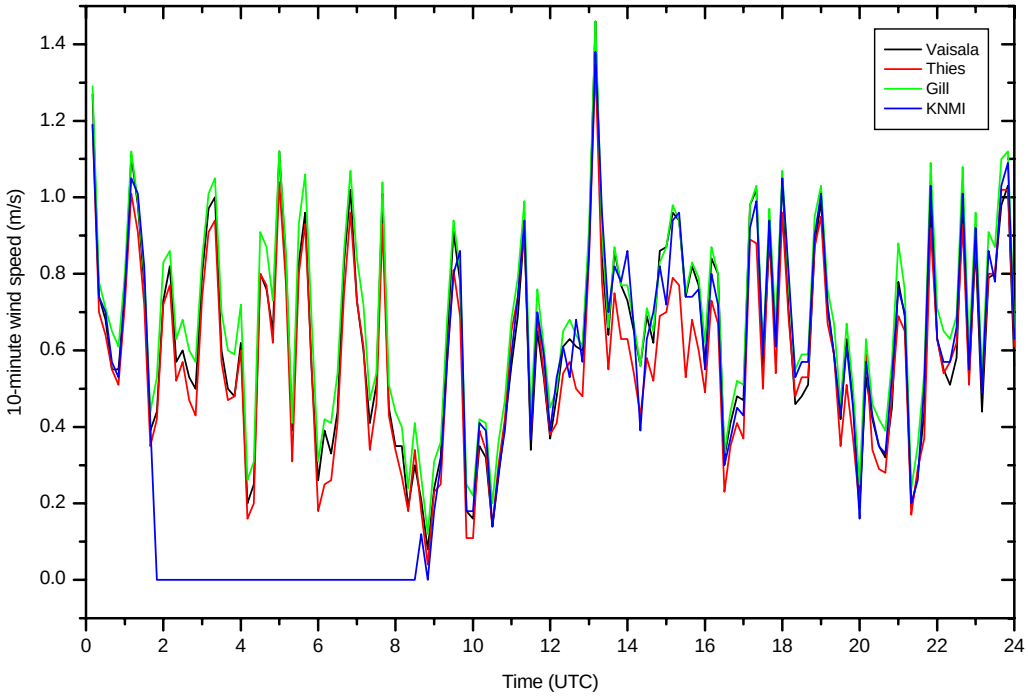


Figure 23: The 10-minute averaged wind speed observed in De Bilt on December 18, 2002.

When the 10-minute wind gust is considered (cf. Figure 24), the overestimation by the cup anemometer compared to the sonics is even larger. This is contrary to the effect one could expect when comparing the extremes of running 3-second averages on a 4Hz update rate with a 1 Hz rate. Furthermore the smaller gust values reported by the cup anemometer is not in agreement with the expect effect due to speeding. The offset of the linear fit is typically 0.26m/s (0.28 for Gill), the slope is 0.92 (0.95 for Vaisala), the correlation coefficient is 0.975 and the standard deviation of the fit is 0.55m/s (0.48 for Thies) when the wind gust reported by a sonic is compared to that of the KNMI cup anemometer. The sonics between themselves typically have a correlation coefficient of 0.99 (0.98 between Gill and Vaisala), a slope of the linear fit of 0.955 (0.998 between Gill and Thies) and a standard deviation of 0.3m/s (0.4m/s between Gill and Vasiala).

The 10-minute averaged wind direction of the vane and a sonic have typically a correlation coefficient of 0.994, a slope of the linear fit of 1.00 and a standard deviation of 11° (cf. Figure 25). Again cases occur when the differences exceed the WMO

requirements and some even reach 180°, but that is during low wind speeds. Note that when comparing wind direction differences exceeding ±180° are mapped within the ±180° range by adding or subtracting 360°. The agreement between the 3 sonics is again much better with typical values of 0.999 for the correlation coefficient, 0.99 for the slope and 4° for the standard deviation.

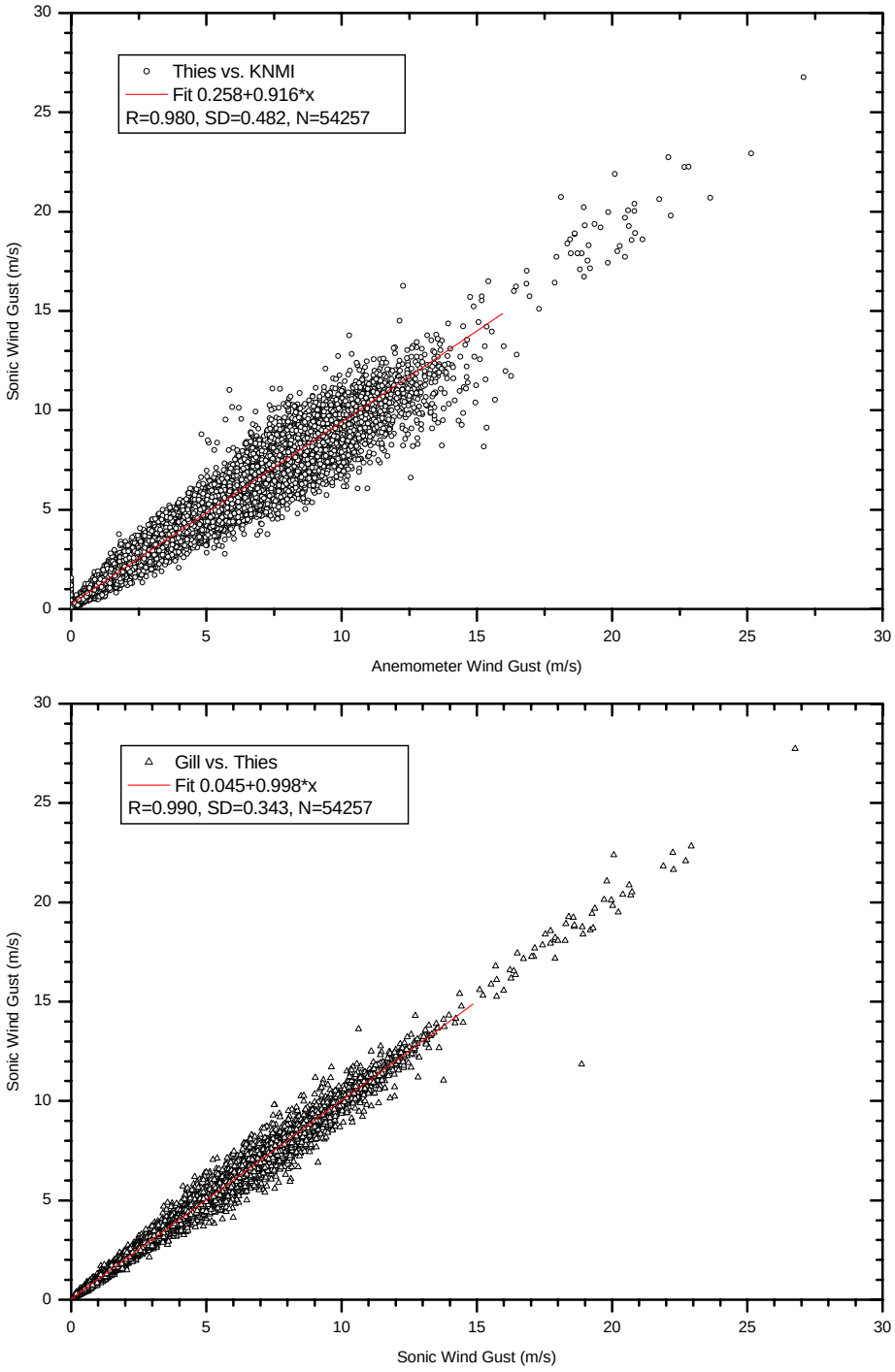


Figure 24: Scatter plot of the 10-minute wind gust showing Thies versus KNMI (top) and Gill versus Thies (bottom).

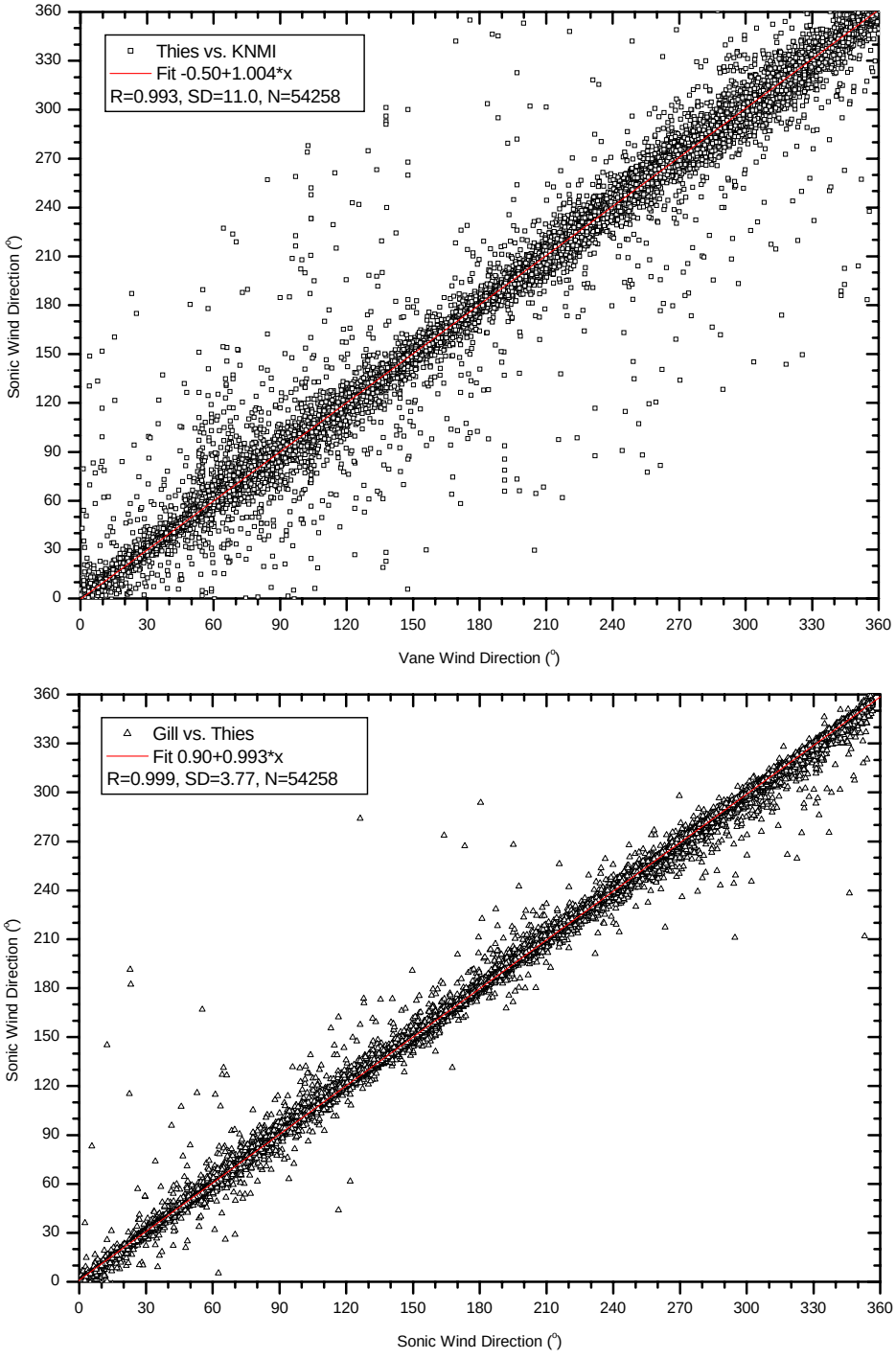


Figure 25: Scatter plot of the 10-minute averaged wind direction showing Thies versus KNMI (top) and Gill versus Thies (bottom).

## *5.3. Detailed analysis*

Next the differences between the 10-minute averaged wind speed, direction and gust reported by the sensors are studied in more detail. In Appendix D1 to D4 the differences are reported as a function of wind direction, wind speed, precipitation intensity and type, and as a function of ambient temperature, respectively. In this section the results will be briefly discussed. For more details the reader is referred to the figures in Appendix D.

### 5.3.1 Results as a function of wind direction

There are in total 54258 cases with valid wind speed and direction. The differences in wind direction between sonics and KNMI wind vane are in 87% of the cases (89% for Gill) within the WMO limit of ±5°. The fraction of the cases within the WMO limits deteriorates in the wind sector 250-340° reaching values down to 65%. The differences between the sonics are smaller (around 95%) and show no dependency on wind direction. When only wind speeds above 2m/s are considered (30212 cases) the results for the wind direction improve. The fraction of the sonic wind direction results within the WMO limits of the vane is typically 96% and the feature in wind sector 250-340° reaches values down to 75%. The sonics now show in more than 99% good agreement. The averaged differences in wind direction are nearly zero since the offset in wind direction has been taken into account, but the averaged differences per wind sector shows typical differences of about ±2°. The Vaisala wind direction shows a systematic underestimation in the 10-60° sector and an overestimation in the 240-280° sector. The averaged differences for sonic versus vane are of the same order as for sonic versus sonic. The overall averaged absolute differences are about 3° for sonic versus vane and about 1.5° for sonic versus sonic. When the wind speed is restricted to values larger than 2m/s the averaged differences show a slight improvement. Furthermore, the differences as a function of wind direction are smoother. The differences involving the Gill show evidence of the disturbance caused by the transducers around 30, 110 and 200°, but not around 300°. The vane shows a distinct difference from all 3 sonics at 260°. The averaged absolute differences for sonic versus vane exceed 5° in the 280-330° sector. The standard deviation of the differences in wind direction is almost identical to the averaged absolute differences. For wind speeds above 2m/s the averaged absolute differences and the standard deviation reduce by about a factor of 2.

The differences in wind speed between sonics and KNMI cup anemometer are in 98% of the cases within the WMO limit of ±0.5m/s or ±10%. A large reduction up to about 91% (87% for Thies) can be observed near 240°. The fraction within the WMO limits has reduced values of about 98% in the sector 210-10°, which is the roughly in the direction of a line of 20-25m trees at a distance of about 150m, but also coincides with the direction of the highest wind speeds. Furthermore, small features around 90, 180 and 340° can be observed. The wind speed of the sonics show almost perfect agreement with each other, without any wind direction dependence. The averaged differences in wind speed are small (typically ±0.05m/s) and show little dependency on direction except for the disturbance in the 200-280° sector, where the cup anemometer overestimates the wind speed by bout 0.2m/s. The averaged absolute differences are typically 0.13m/s for sonic versus cup and 0.05m/s for sonic versus sonic. The dependency of the averaged absolute

differences on wind direction shows the same behavior as the fraction of cases within the WMO limits. The standard deviation resembles the averaged absolute differences, although the dependency on wind direction is slightly different and the maximum deviation at 240° is smaller. When the analysis is restricted to cases with a wind speed larger than 2m/s, the results show a small deterioration.

The differences in wind gust between sonics and KNMI cup anemometer are in 83% of the cases within the WMO limit of ±0.5m/s and ±10%. A large reduction up to about 70% can be observed in the 230-300° sector. The agreement between sonics and cup anemometer is much less for the wind gust than for the averaged wind speed. The sonics between themselves also show larger differences (typically 97%) and the agreement is worse in the 210-30° sector than in the other sector. The averaged (absolute) differences in wind gust show larger absolute deviations than for the averaged wind speed. In relative numbers the differences for wind gust and averaged wind speed are small since the absolute differences of about a factor of 2 are compensated by the gust values which are typically a factor 2 larger the averaged wind speed. A difference between the behavior for wind speed and wind gust can be observed for the Vaisala sensor. The Vaisala sonic anemometer generally reports lower wind gust values than the Thies and Gill and shows larger differences with any of the other 2 sonics then the other 2 sonics between themselves. Again the results deteriorate slightly when the analysis is restricted to cases with a wind speed larger than 2m/s.

### 5.3.2 Results as a function of wind speed

The differences as a function of wind speed are discussed below. It should be noted that the results for wind speeds above 6.5m/s need to be treated with care because of poor statistics. The results are shown in Appendix D2.

At low wind speeds the fraction of cases where the wind direction reported by the sonics is outside the WMO limits of the wind vane is rather large, but the agreement gets gradually better at higher wind speeds. The agreement is best around 4m/s and deteriorates again at higher wind speeds. When only situations with wind speeds larger than 2m/s are considered the sonics and wind vane are typically 96% of the time within the WMO requirement of ±5°. The Gill shows slightly better agreement with the vane than the other 2 sonics. The wind direction of sonics is 99.5% of the time within the WMO limits. The averaged differences in wind direction generally show good agreement, especially when the results at low and high wind speeds are not taken into account. Around 5m/s there is no offset between any of the sensors. The dependency of the averaged differences in wind direction with wind speed is nearly identical for all 3 sonics, only the Vaisala shows a sudden negative offset in the lowest wind speed bin. At wind speeds of 9m/s and higher the differences between the 3 sonics increases to about 1°, but statistics is poor. The averaged absolute differences in wind direction are nearly identical to the standard deviations. The averaged absolute differences show little dependency with wind speed, except the sharp increase at wind speed values below 2m/s. The averaged absolute differences in wind direction between sonics and vane show a gradual increase from 1.5° at 4m/s to 2.5° at 8m/s, and decrease again at higher wind

speeds. The averaged absolute differences in wind direction between the sonics are typically 0.5° for the Thies and 1° when either the Gill or Vaisala is involved.

The fraction of cases where the wind speed reported by sonics and cup anemometer agrees within the WMO limits shows a gradual deterioration with increasing wind speed. The agreement is better than 99% up to 2.5m/s and decreases to about 80% at 6.5m/s. At 8 and 8.5m/s the results of all sonics show better agreement with the cup anemometer, but the number of cases involved is small. The Vaisala sonic shows the best agreement with the cup anemometer and Thies the worst. The agreement is best between the Gill and Thies sonic anemometer. The averaged differences in wind speed show a similar behavior, i.e. at 0.5m/s the sonics report slightly higher averaged wind speeds (0.07m/s), but at higher wind speeds the sonic report increasingly lower speeds (-0.4m/s at 6.5m/s). The wind speed reported by the Vaisala sonic is closest to the cup anemometer, whereas the Gill and Thies show the smallest differences. The Vaisala underestimates the wind speed compared to the other 2 sonics by about 0.12m/s at 6.5m/s. The averaged absolute differences in wind speed are nearly identical to the standard deviations. Again a gradual increase with wind speed can be observed with reduced values at 8 and 8.5m/s.

The fraction of cases where the wind gust reported by sonics and cup anemometer agrees within the WMO limits deteriorates with increasing wind speed up to 2m/s and remains nearly constant at 77% up to 6.5m/s. The sonics between themselves show a similar behavior reaching values of about 95%. The averaged differences in wind gust increase gradually with wind speed. All three sonics show a feature at 7 and 7.5m/s. Above 10m/s the results of Gill and Thies show a sudden improvement, whereas the Vaisala results show an overshoot. The averaged absolute differences in wind speed and the standard deviations show an almost linear increase with wind. The Vaisala sensor is closest to the cup anemometer, but deviates from the other 2 sonics.

### 5.3.3 Results as a function of precipitation class

In this section the differences are studied as a function of the precipitation class, considering both precipitation intensity and precipitation type as measured by a FD12P present weather sensor. The 10-minute averaged precipitation intensity and the ‘maximum’ precipitation type observed in the 10-minute interval are used for that purpose. The precipitation classes considered are, respectively, no precipitation (NP), traces (TR with 10-minute averaged intensity below 0.05mm/h) and intensity classes rounded to mm/h in the range 0-10 where the last bin also contains all cases with higher intensity values. Next all cases with precipitation are summed (AP) and a distinction is made between the precipitation types liquid (LP), solid (SP) and unknown precipitation (UP). Finally the results are given regardless of precipitation (All). In all classes the number of cases is above 100, except for the classes for intensity larger than 4mm/h. The results are shown in Appendix D3.

The fraction of cases where the wind direction reported by sonics and vane agrees within the WMO limits shows a small dependency with precipitation intensity and better agreement during situations with solid precipitation. The small dependency on precipitation intensity disappears when only situation with wind speed above 2m/s are

considered, although the reduced agreement for situation with intensities higher than 5mm/h, with poor statistics, remains. The averaged (absolute) differences and the standard deviation of the differences in wind direction also show a dependency on precipitation intensity, particularly when low wind speeds are not considered. The differences increase from about 1.5° to 4°. The sonics show no dependency on precipitation intensity when compared to each other. The differences between the three sonics and the KNMI wind vane are smaller during solid precipitation events. The same behavior can be observed when the sonics are compared to each other.

The differences in wind speed reported by the sonics and the cup anemometer show a clear dependency on precipitation class. The differences between sonics and cup generally increase with increasing precipitation intensity and are higher during liquid precipitation events, and solid precipitation seems to have less effect on the differences that liquid precipitation. The differences in wind speed between the sonic themselves show little dependency with precipitation class, although the averaged absolute differences and the standard deviation increase slightly up to precipitation intensities of 5mm/h and these differences are generally higher during precipitation. The same behavior again holds for the fraction of cases the sonics are within WMO limits from the cup anemometer which is about 97%, but decreases to about 85-90% at high intensity values. The results indicate that the Thies is slightly more affected by precipitation than the other 2 sonics when compared to the KNMI cup anemometer. When the sonics are compared to each other the wind speed of the Thies and Gill agree almost in 100% of the cases within the WMO limits, whereas the Vaisala shows a slightly reduced agreement of about 98% at mid and high intensity levels.

The differences in wind gust between sonics and cup anemometer show a dependency on precipitation class. A similar dependency can also be observed for the differences between the sonics, except for the averaged differences. The averaged absolute differences and the standard deviation show some outliers caused by the Gill (at UP) and the Vaisala at (NI=8 and 9).

It should be noted that the observed differences between the sonics and the conventional cup anemometer and wind vane during precipitation need not be the result of degradation in the performance of the sonics. The precipitation will adhere to the conventional sensors and hence also affect their dynamical properties. Since the differences between each of the sonics and the conventional sensors show a similar behavior, it is most likely that the observed differences between sonics and the conventional wind sensor are caused by changes in dynamical properties of the latter.

### 5.3.4 Results as a function of ambient temperature

The results as a function of the ambient temperature are shown in Appendix D4. The differences in wind direction reported by the sonics and vane show a strong dependency on the ambient temperature. Similar, but smaller, differences can be observed for the differences between the sonics themselves. The differences between sonics and vane for temperature above 10°C is very pronounced for cases with wind speeds exceeding 2m/s. The averaged differences show a temperature dependency of the wind direction reported

by the Vaisala. The difference increase from -1.8° to about 0.5° between -15 and 20°C. The averaged absolute differences gradually increase with temperature, but this effect is masked by the variability at low wind speeds which also introduces enhanced values around 12.5°C. The standard deviation is nearly independent of temperature, except for Vaisala versus vane.

The differences in wind speed and wind gust also show a temperature dependency. This can also be observed in the averaged differences in wind speed and gust between the sonics themselves. The Vasiala sonic anemometer shows the smallest temperature dependence compared to the cup anemometer; Gill the largest. A temperature dependence in the measurements of a 3D Solent Gill sonic anemometer), which is related to small variations in the properties of the transducers, was reported by Mortensen and Højstrup (1995) and resulted in errors of about ±2% in wind speed and ±5K in temperature.

The temperature dependence mentioned above need not necessarily be differences in the sensor output resulting directly from changes the ambient temperature, since the meteorological conditions also change with temperature.

## *5.4. Surface roughness*

Wind speed measurements are affected by the surface roughness of the terrain surrounding the measurement area (Wieringa and Rijkoort, 1983; Handboek waarnemingen, 2001). The surface roughness generally depends on the wind direction and may vary with season due to changes in the foliage. Below, the surface roughness is estimated from the wind data obtained for the 4 sensors during the field test. The data for each of the sensors has been grouped into wind direction bins of 10° centered around 10°, 20°, …, 360°. The frequency distribution of the number of case in each bin is given in Figure 26 for each wind sensor. Only cases where the 10-minute averaged wind speed reported by the KNMI cup anemometer exceeds 5m/s are considered. The distribution is generally the same, but it can be noted that the KNMI wind vane reports less cases in the 90, 180, 270 and 360° wind sectors compared to the sonics and shows larger values in the adjoining sector. This is probably caused by inaccuracies in the gray code disk of the vane. Note, furthermore, that the number of cases is small, particularly around 10° and between 280 and 330°. The total number of cases involved is 2534.

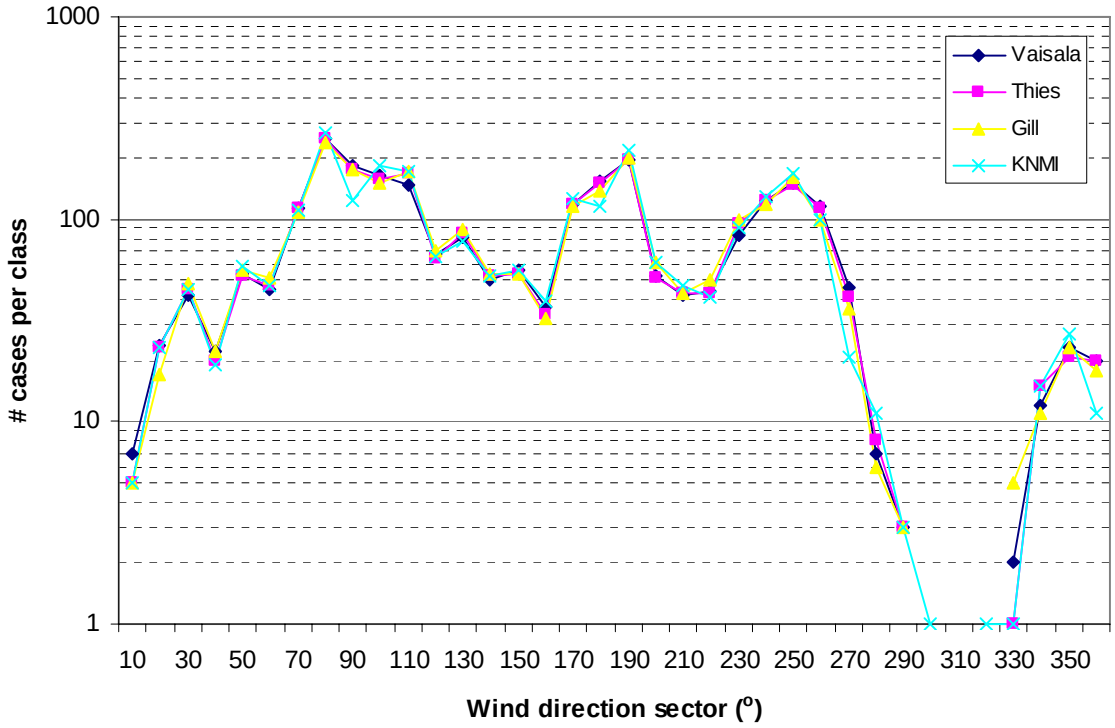


Figure 26: Histogram showing the frequency distribution off wind direction reports in bins of 10° for each of the 4 wind sensors involved in the field test.

The surface roughness can be taken into account by using 2 methods (Benschop and van der Meulen, 2005). The first method to estimate the roughness is by using the gustiness of the wind. The so-called gust factor <*G*>, i.e. the median of the wind gust to 10-minute averaged wind speed ratio $U_x/U$ for each wind direction sector, is determined first. The gust factor is related to the surface roughness $z_0$ according to $z_0 = 10 \times \exp\left(2.12/[1 - < G >]\right)$. The surface roughness derived from the gust factor is given in Figure 27. The surface roughness derived from the turbulence of the wind $\sigma_u/U$ using $\sigma_u / U = 1/\ln(10/z_0)$ is given in Figure 28. In addition, the shelter factor $BF = [1 + 1.79/(2.3 - \ln(z_0))]/1.308$, i.e. the factor that transform the observed averaged wind into to potential wind at 10m with a surface roughness of 0.03, and the exposure correction factor $F = 0.764 \times (1 + 1.791 \times \sigma_u / U)$ are computed and shown in Figure 27 and Figure 28, respectively. The surface roughness derived using the wind gust and the standard deviation show large differences. The results for the standard deviation also show an offset between the surface roughness obtained for the cup anemometer and the sonics. The differences are smaller between the shelter and exposure correction factor. All curves show a sine like behavior with maximum values near 310. Although these curves cannot explain the details of the observed differences in the wind speed as a function of wind direction, they clearly show that the largest disturbances are to be expected in the 230-340° sector.

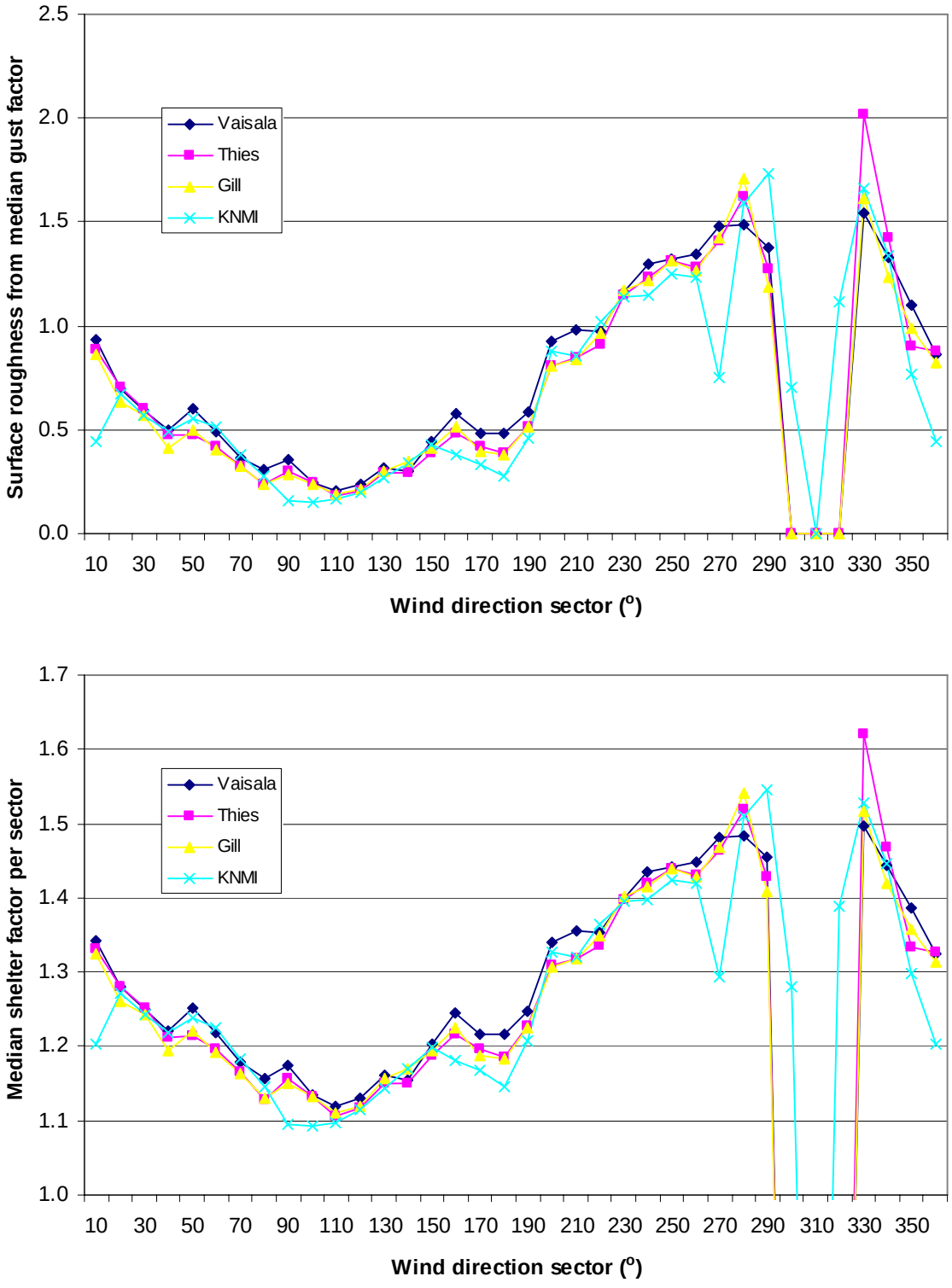


Figure 27: Surface roughness derived from the measured median wind gust factor and the associated shelter factor.

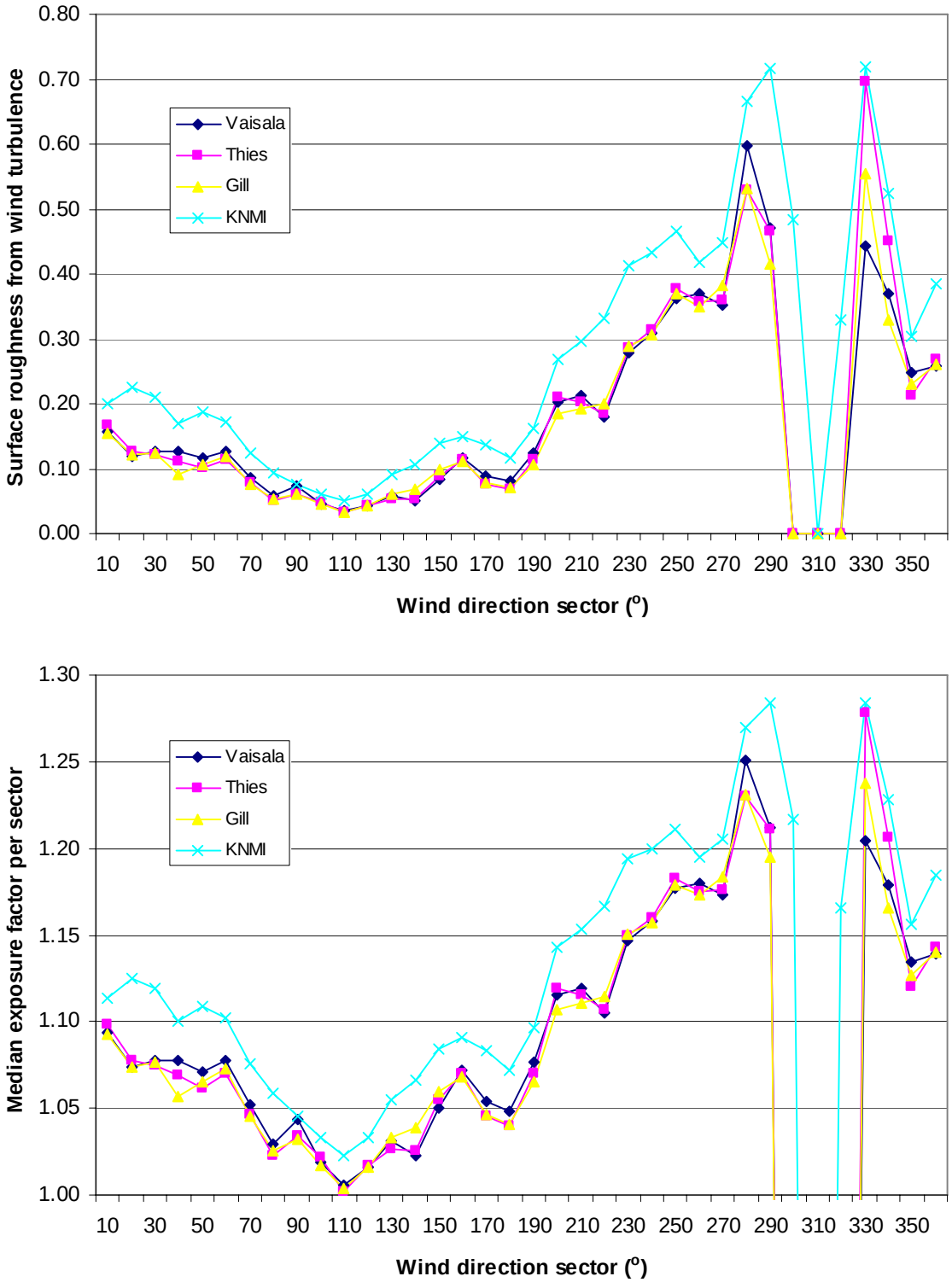


Figure 28: Surface roughness derived from the measured wind speed turbulence and the associated exposure correction factor.

The relatively large differences in the results for the surface roughness derived from the wind turbulence of the KNMI cup anemometer and the sonics is the result of differences in the 10-minute standard deviation of the wind speed. A scatter plot of the standard deviation of the wind speed is given in Figure 29 for Thies versus KNMI anemometer and Gill versus Thies. Evidently the standard deviation of sonic and cup anemometer shows much less agreement than for 2 sonic anemometers. The standard deviation between any 2 sonics shows very good agreement with typical values for the offset of 0.005m/s, slope 0.97m/s, correlation coefficient 0.99, and residual of linear fit 0.05, whereas typical values between cup and sonic anemometer are 0.06m/s for the offset, slope 0.85m/s, correlation coefficient 0.96, residual of linear fit 0.09. Note that the low standard deviation values of the cup anemometer are not reproduced by the sonic anemometer. The standard deviation reported by the cup anemometer is on average 0.66m/s, and is larger than the corresponding value of the sonic anemometers (0.64m/s for Vaisala and 0.62m/s for Thies and Gill). The variability of the standard deviation of the cup anemometer is also higher than for the sonic anemometers, 0.41 versus 0.36m/s, respectively. The standard deviation of the wind direction (cf. Figure 30) also shows less agreement between sonic and vane (typical values for offset 1.6° (2.2° for Vaisala), slope 0.85, correlation coefficient 0.83 and residual of the fit 6°) than between the sonics themselves (typical values for offset 0.2°, slope 0.98, correlation coefficient 0.98 and residual of the fit 2°). Again, situation with low standard deviation of the vane are not reproduced by the sonic anemometers. The averaged standard deviation is 20° for the vane and 19° for the sonics and the corresponding variability is 10.3 and 10.7° for vane and sonics, respectively.

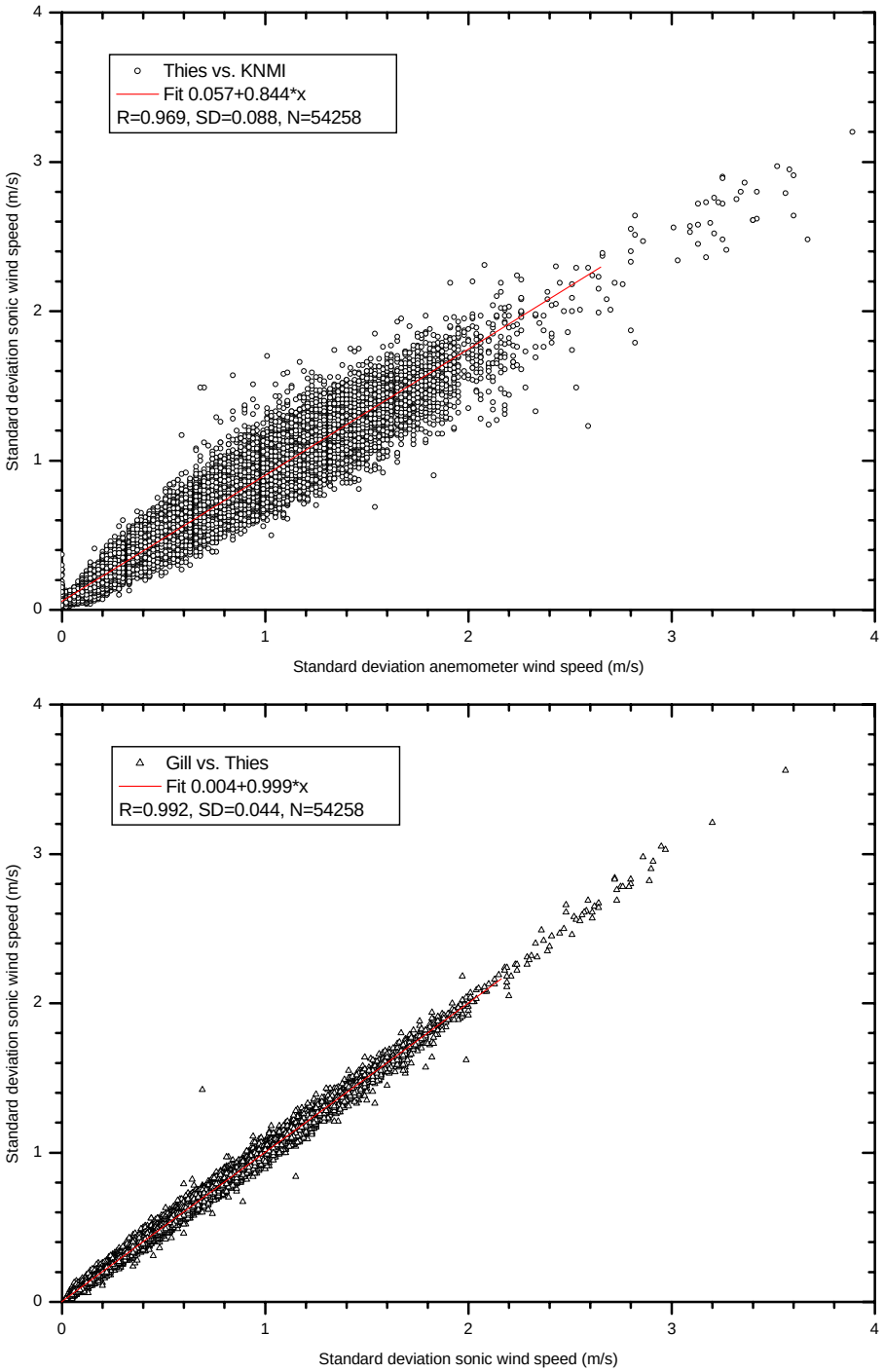


Figure 29: Scatter plot of the standard deviation of the 10-minute averaged wind speed showing Thies versus KNMI (top) and Gill versus Thies (bottom).

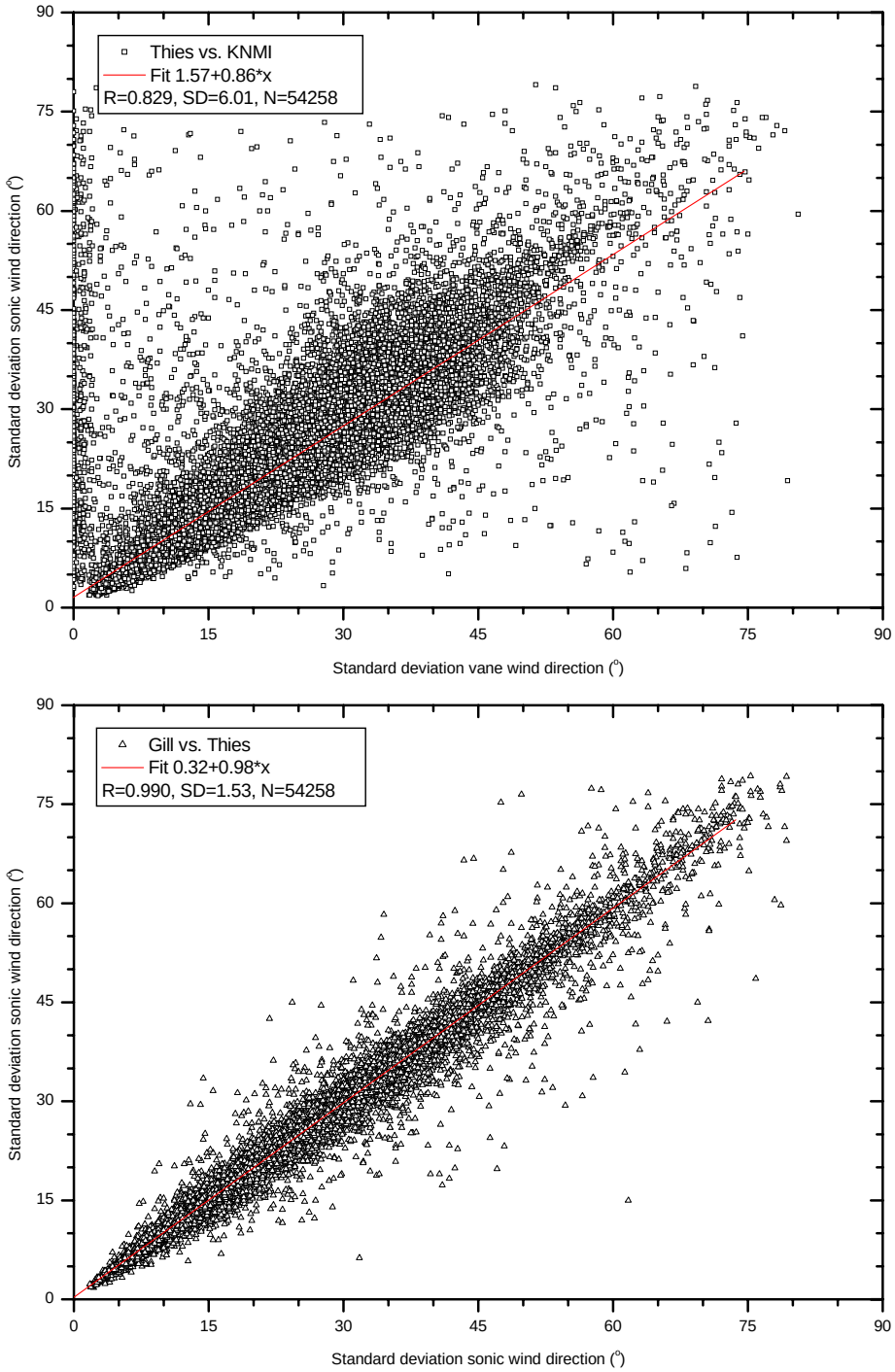


Figure 30: Scatter plot of the standard deviation of the 10-minute averaged wind direction showing Thies versus KNMI (top) and Gill versus Thies (bottom).

## 5.5. Normalized wind

A useful parameter to investigate is the so-called normalized wind speed $u_n = (u_{12} - U)/\sigma_u$ where $u_{12}$ is the 12-second wind gust and $U$ and $\sigma_u$ are the 10-minute

averaged wind speed and its standard deviation (cf. van der Meulen, 1998 and 2000). The normalized wind speed is evaluated at 12-second intervals using the derived 12-second wind gust, which is reported as the sample value by the SIAM sensor interface, and the 12-second running average and the corresponding standard deviation of the wind speed. The advantage of this quantity is that it is nearly independent of the averaged wind speed. This is illustrated in Figure 31, which shows the 12-second wind gust and the normalized wind on October 27, 2002 (cf. also Figure 21). The normalized wind clearly shows the variability of the observed wind, but not the changes of the averaged wind.

The agreement between the normalized wind obtained by the KNMI cup anemometer and the three sonics can be investigated in a scatter plot (cf. Figure 32). The normalized wind speed is reported for each 12-second interval with valid measurements for all 4 wind sensors and a 10-minute standard deviation exceeding 0.1m/s. The normalized wind of Thies versus KNMI shows much scatter. The scatter plot contains about 2.6 million points; hence the agreement between the sensors cannot easily be seen because many points overlap. A linear fit to the data gives a slope of 0.60 and the regression coefficient is 0.59. This poor agreement can be expected because of the fluctuations that occur in the normalized wind. Hence the scatter plot not only shows scatter due to differences in sensor characteristics, but also due to timing and the spatial difference between the sensors. Since the SIAM introduces almost a delay of 12 seconds (cf. section 2.1) it is better to compare the normalized wind speed of the cup anemometer to the sonic normalized wind of the next 12-second interval. In that case a linear fit to the normalized wind speed gives $u_n$(Thies)=0.28+0.67 $u_n$(KNMI), the regression coefficient is 0.65 and the standard deviation of the fit is 0.92. The agreement between Thies and KNMI improve when taking the time delay into account, but the overall agreement is still poor. The scatter plot of the normalized wind of Thies versus Vaisala shows a much better agreement (slope 0.95 and regression coefficient 0.96). This can partly be ascribed to a better agreement of the sensor characteristics, but the differences in distance (20m between KNMI and sonic and 1m between sonics) also affect the results.

The effects of timing and distance are eliminated by comparing the frequency distributions of the observed normalized wind speed for each of the sensors. The distributions are given in Figure 33. The frequency distributions of all sensors show good agreement. The KNMI cup anemometer gives slightly smaller values (median normalized wind speed is 0.56, averaged normalized wind speed is 0.62) and a narrower distribution (standard deviation of normalized wind speed is 1.18). Thies and Gill show very good agreement with each other and the Vaisala give the largest values (median normalized wind speed is 0.68, averaged normalized wind speed is 0.74) and a broadest distribution (standard deviation of normalized wind speed is 1.22). The differences between median and averaged normalized wind speed (respectively 0.63 and 0.69 for both Thies and Gill) result from deviations from a normal distribution. Fluctuations can be observed in the frequency distributions of all 4 sensors, even around the peak of the distribution where the number of occurrence is high. This is probably the result of the 0.01m/s resolution of the raw sensor data and the subsequent calculation and binning into narrow classes of 0.1.

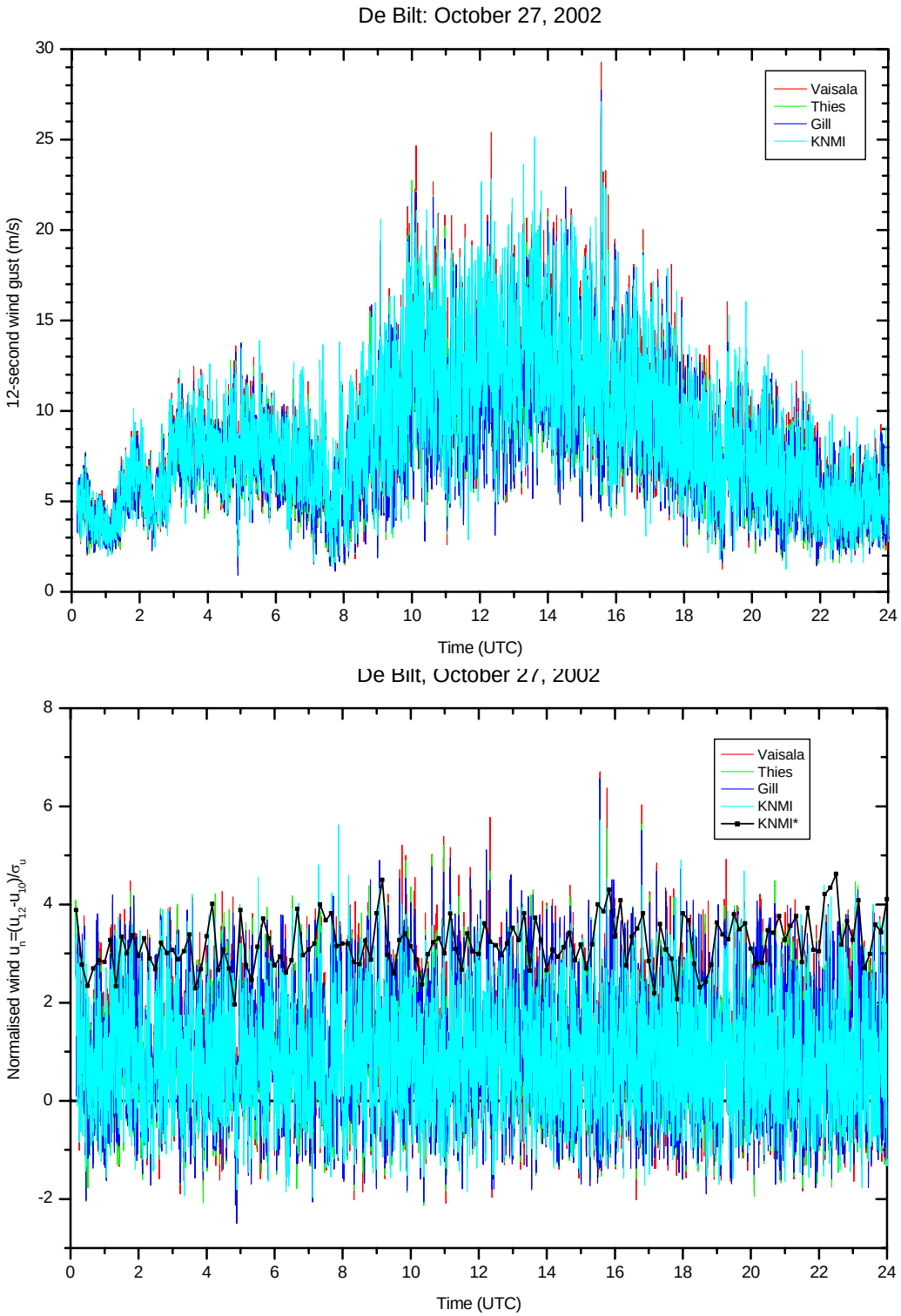


Figure 31: The 12-second wind gust (top) and normalized wind (bottom) observed in De Bilt on October 27, 2002. The curve denoted KNMI* in lower panel is the normalized gust of the KNMI sensor derived from 10-minute data.

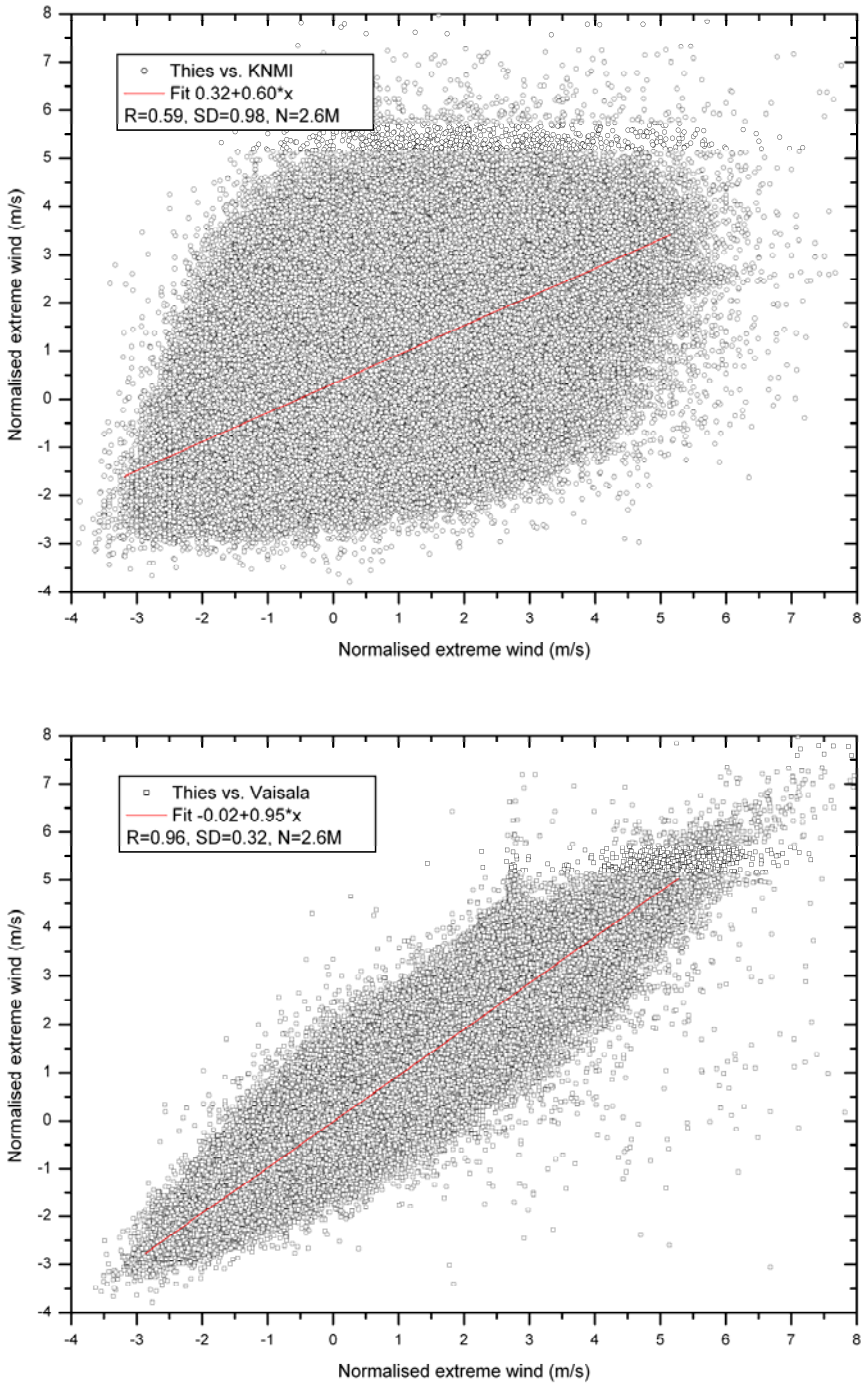


Figure 32: Scatter plot of the normalized wind speed showing Thies versus KNMI (top) and Thies versus Vaisala (bottom).

A Gaussian fit to the frequency distribution of the KNMI cup anemometer illustrates the non-normal behavior of the frequency distribution of the normalized wind. The Gaussian distribution is given by $y = y_0 + \frac{A}{w\sqrt{\pi/2}} \exp\left[\frac{-2(u_n - u_{nc})^2}{w^2}\right]$, where $y_0$ is the vertical

offset and $A$ is the area of the distribution which were set to fixed values. The horizontal offset $u_{nc}$ and the width $w$ of the distribution were obtained by the fit. It should be noted that the frequency distribution is given in a logarithmic scale, hence the differences at low occurrences have little impact on the fit. Note that the width $w$ is related to the full width at half maximum by $FWHM = w\sqrt{\ln(4)}$. A log normal fit of the form $y = y_0 + \frac{A}{wu_n\sqrt{2\pi}}\exp\left[\frac{-[\ln(u_n/u_{nc})]^2}{2w^2}\right]$ gives a better description of the behavior of the frequency distribution, particularly for the small number of event at extreme values of the normalized wind speed. Note that the log normal distribution is only valid for positive $u_n$, hence a translation of $u_n \rightarrow u_n + 10$ was applied to the data before and after the fit.

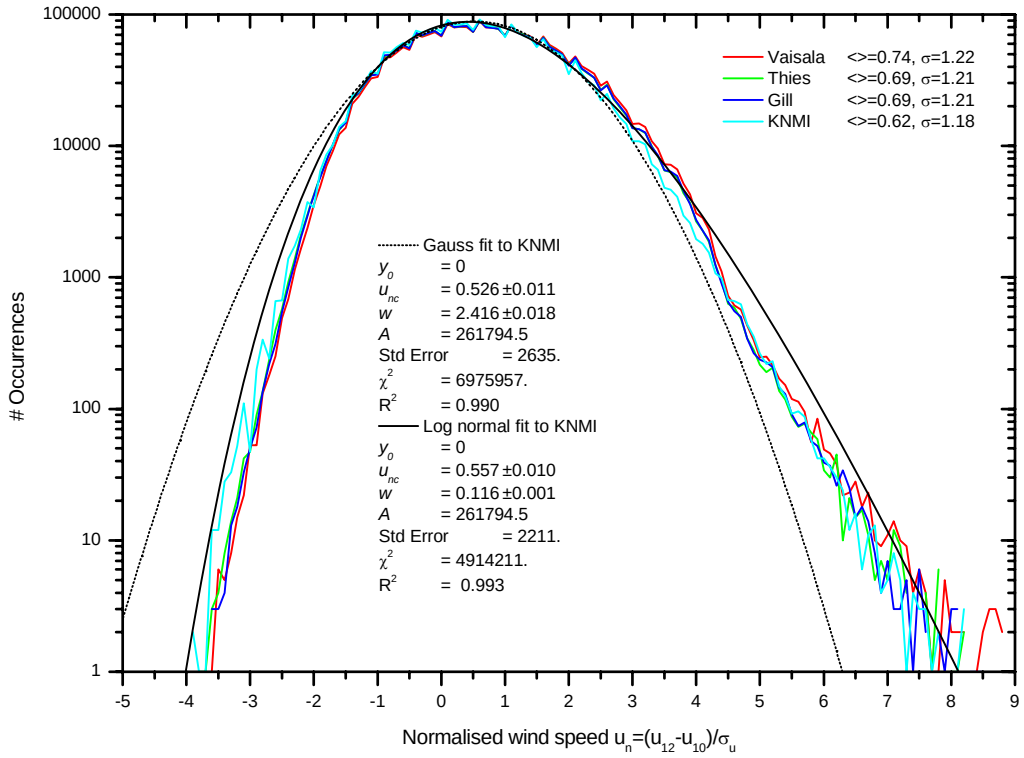


Figure 33: Frequency distribution of the normalized wind speed for each sensor in bins of 0.1 and a Gaussian and log normal fit to the frequency distribution of the KNMI sensor.

The normalized wind speed can also be shown as a cumulative frequency distribution (cf. Figure 34). Figure 34 is given using a probability scale. In such a plot normal distributions show up as straight lines. Again the plots show that the normalized wind speeds of all 4 sensors follow each other rather nicely and that the behavior at the extreme ends of the distribution can be described by a log normal. A distribution that is often used to describe the cumulative amount (cf. e.g. Wieringa and Rijkoort, 1983) is the so-called Weibull distribution $y = y_0 - (y_0 - y_\infty)\exp\left[-[(u_n/a)]^k\right]$. However, the Weibull distribution does not follow the observed behavior. The central part of the cumulative distribution of the normalized wind speed which contains 90% of the cases behaves, however, like a normal distribution.

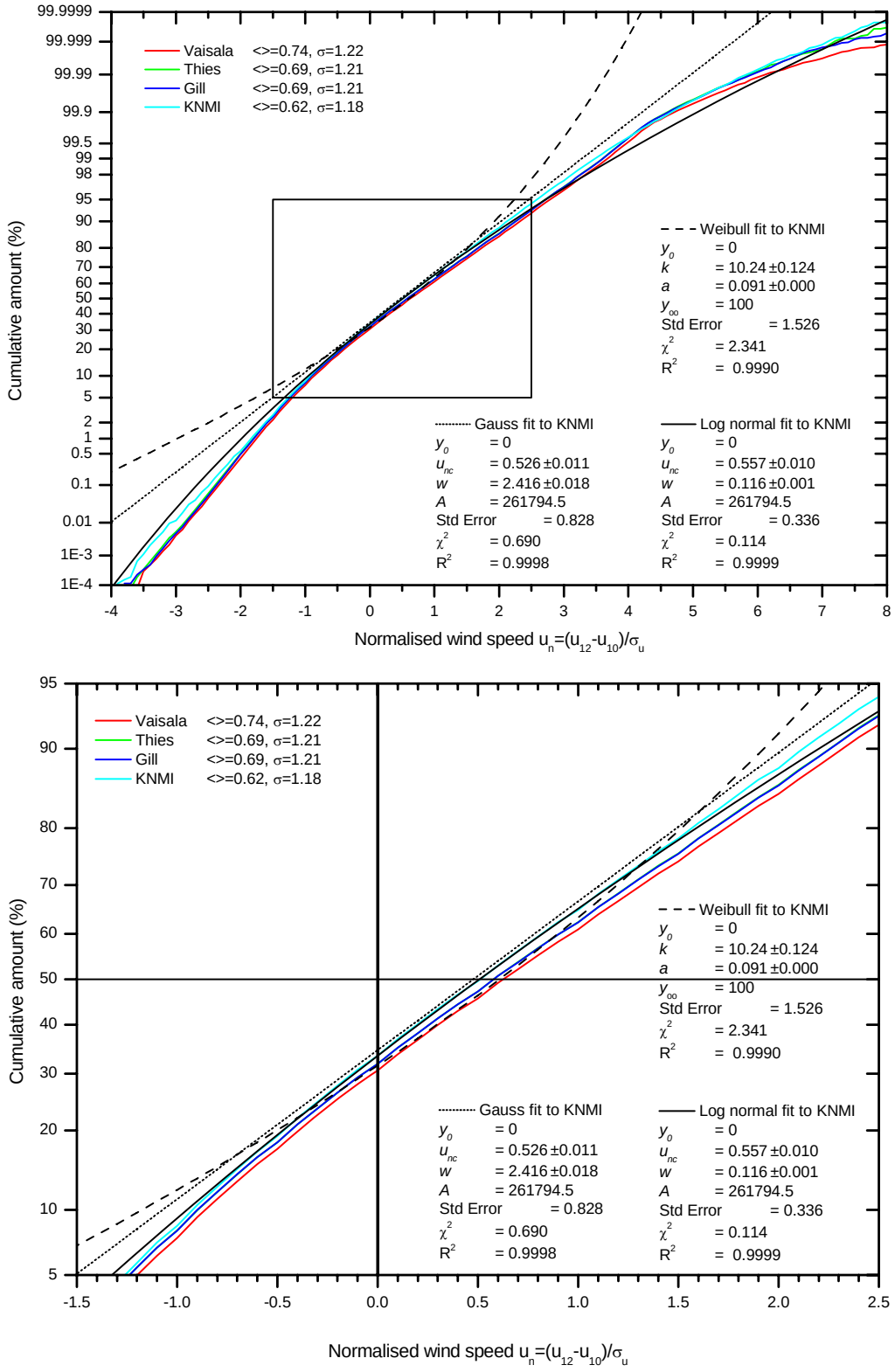


Figure 34: Cumulative frequency distribution of the normalized wind speed for each wind sensor and the Gaussian and log normal fit to the frequency distribution of the KNMI cup anemometer and the Weibull fit to the cumulative distribution. The lower panel shows the central part op the top panel containing 90% of the cases.

The above analysis of the frequency distribution of the normalized wind uses the information of each 12-second SIAM output string. Normally only daily climatological data or hourly synoptic data are available for such studies (and similarly for the determination of the surface roughness discussed in section 5.4). Therefore daily or hourly averages and extremes of the wind speed are used. The last couple of years 10-minute data is archived on a non-operational basis. The equivalent of the normalized wind using 10-minute data is the so-called normalized wind gust $g_n = (u_x - U)/\sigma_u$. Figure 31 shows that the normalized gust also eliminates the smooth variations during the day. As could be expected, the 10-minute normalized gust follows the maxima of the 12-second normalized wind speed.

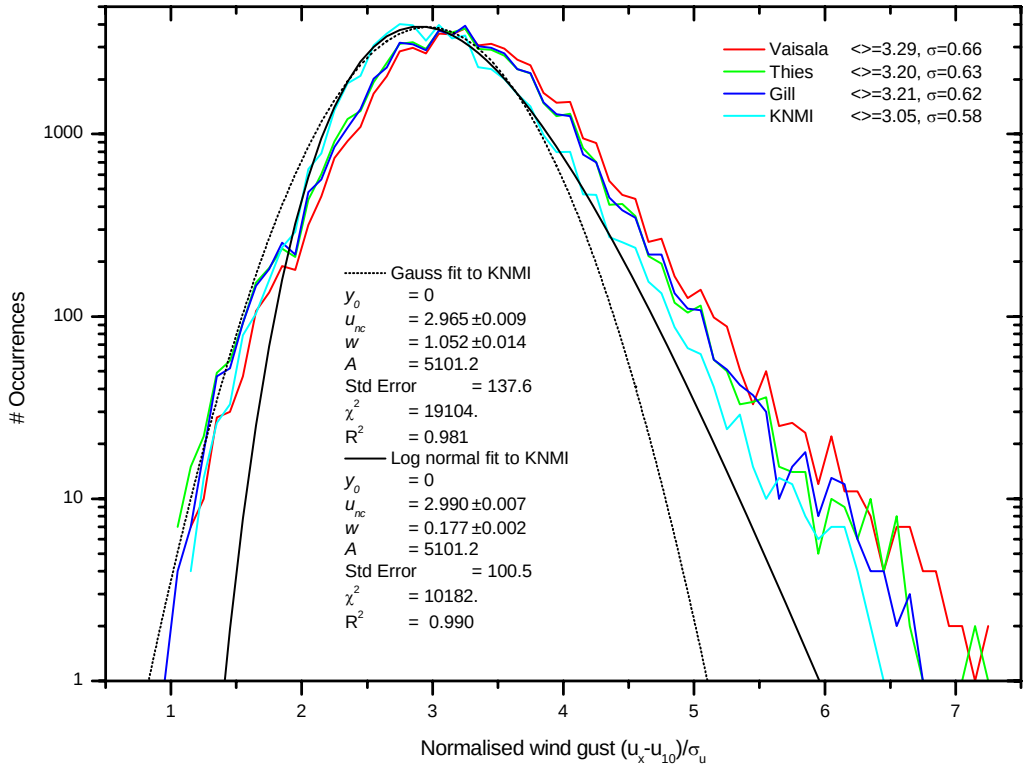


Figure 35: Frequency distribution of the normalized wind gust for each of the 4 sensor derived by using 10-minute data.

The frequency distribution and cumulative frequency distribution of the normalized wind gust are given in Figure 35 and Figure 36, respectively. The distributions for the 4 wind sensors are again similar. The KNMI sensor clearly given lower normalized wind gust values than the sonics, even near the maximum of the distribution. The agreement between the observed distributions and the theoretical distributions is less for the 10-minute normalized wind gust than for the 12-second normalized wind.

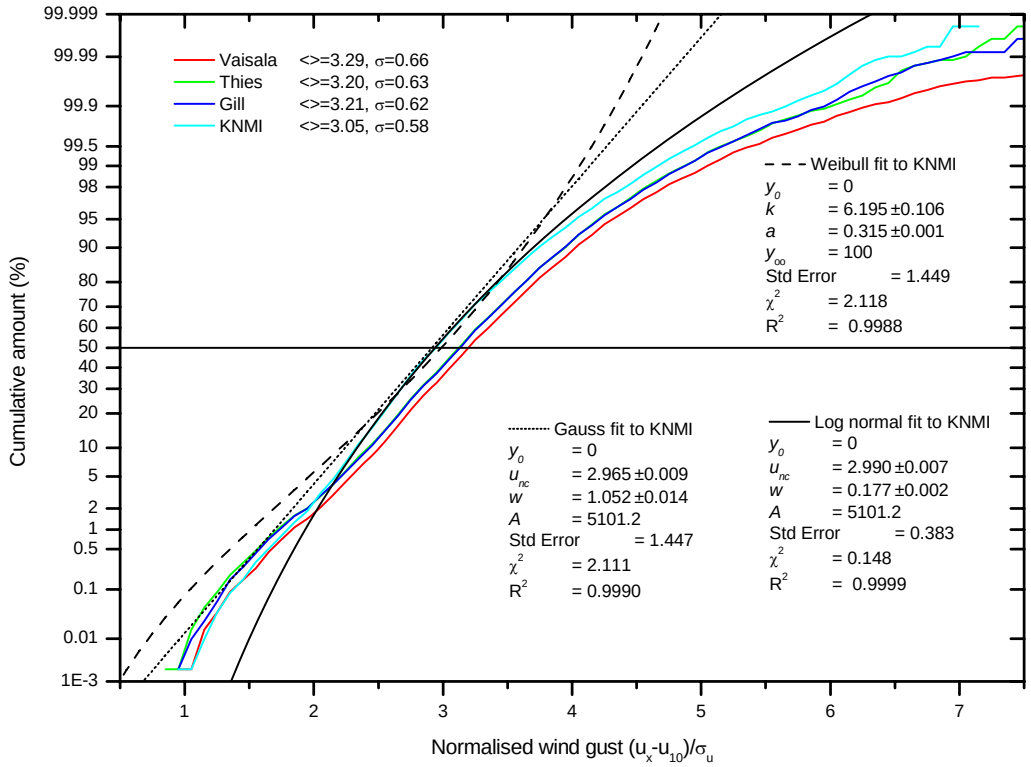


Figure 36: Cumulative frequency distribution of the normalized wind gust for each wind sensor and a Gaussian, log normal and Weibull fit to the frequency distribution of the KNMI cup anemometer.

## 5.6. Temperature

The sonic anemometers not only measure the wind speed, but also the speed of sound. The speed of sound in air depends on the temperature, and to a lesser degree on humidity and atmospheric pressure. Hence the so-called virtual temperature can be obtained from the sonics. Only Gill and Thies report this temperature. Laboratory evaluations of the accuracy of the temperatures reported by sonic anemometers have been performed by e.g. Mortensen and Højstrup (1995) and Lanzinger and Langmack (2005). In this section the temperature derived by the sonics at 10m is compared to the ambient temperature measured at 1.5m.

The correlation between the ambient temperature and the sonic temperatures is good. This is illustrated in Figure 37, which gives the 10-minute temperatures as a function of time during a fortnight. The ambient temperature and the Thies sonic temperature show good agreement. The curves follow each other very well, although the Thies underestimates some extreme values. Fast changes in ambient temperature are generally reproduced by the Thies. The Gill sonic temperature also reproduces the changes in ambient temperature, but the reported temperature is generally 1-2°C too high.

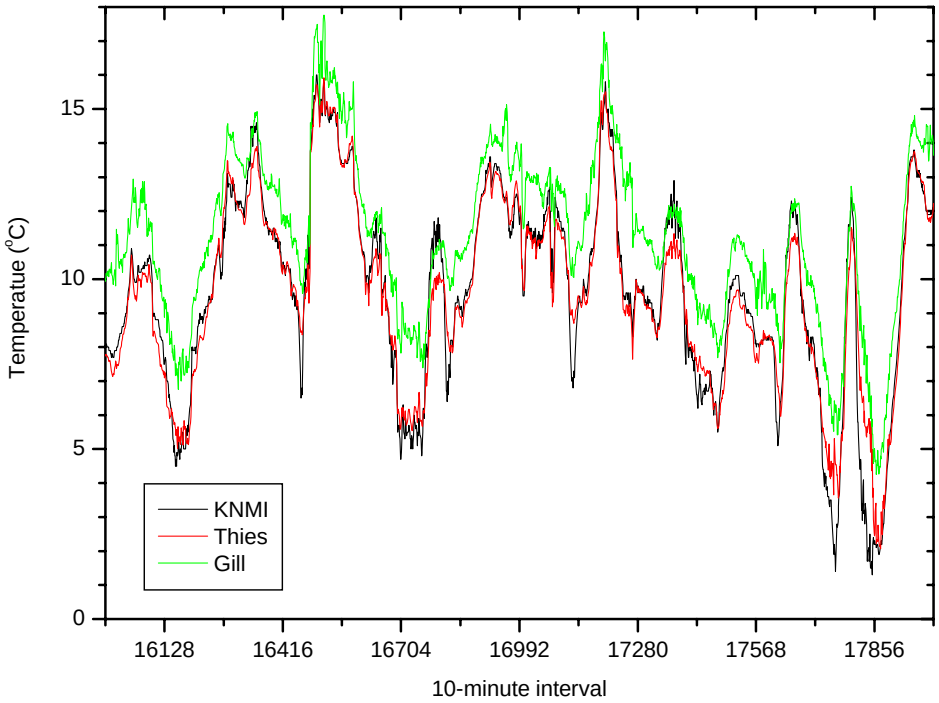


Figure 37: The 10-minute temperatures observed during a 14-day period of the field test.

Scatter plots of the sonics versus the ambient temperature are given in Figure 38. The Thies virtual temperature shows a good correlation with the ambient temperature (0.987) and the linear fit through all points has a small offset (0.70°C) and a slope of nearly 1 (0.95). The standard deviation of the linear fit is 1.18°C. The red curve shows the averaged difference in temperature per 10°C temperature bin and the standard deviation. The Thies slightly overestimates the temperature for temperatures below freezing, and underestimates temperatures above 20°C. The temperature reported by the Gill shows a clear temperature dependency. Furthermore, the response is not linear, but shows a bend near 15°C. This bend can also be observed if the field test data of the first and second half are plotted separately. Hence the bend is not the result of a degradation of the sensor during the test. The virtual temperature of the Gill is derived from the speed of sound by using the mean relative humidity of 80% and the standard surface pressure of 1013hPa. When the measured relative humidity and surface pressure is used, the parameter of the linear fit improve only slightly (offset 4.32 into 4.15°C, slope 0.72 becomes 0.73 and the standard deviation changes from 1.36 to 1.21°C), and the bend remains.

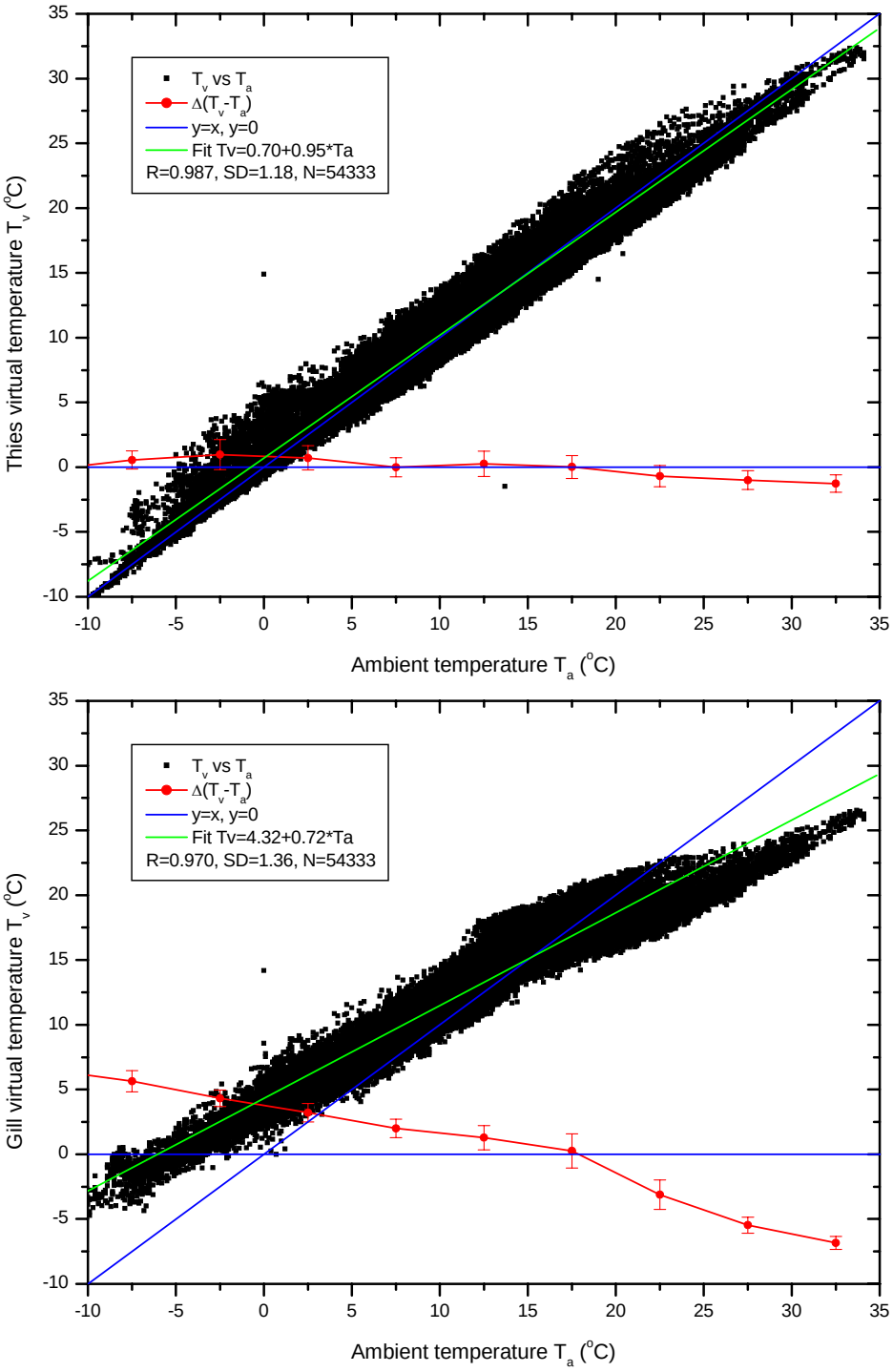


Figure 38: Scatter plots of the virtual sonic temperature versus the ambient temperature measured during the field test in De Bilt for the Thies (top) and Gill (bottom). The linear fit (green line) and averaged differences and standard deviation for 10°C bins (red curve) is also shown.

# 6. Summary of results

Three 2D sonic anemometers, the Thies 2D, the Gill WindObserver II and the Vaisala WAS425, have been selected and tested against the conventional KNMI cup anemometer and wind vane. Although not at the time of the test, all three sensors are currently available with a RS422 interface and can report a 3-second running averaged wind speed and direction. The Gill and Thies sonic anemometer have a high internal measurement rate and an output rate which meet the measurement frequency of 4Hz recommended by WMO. The Vaisala measures with a 20Hz rate, but only during a 200msec interval of each second and the output rate is only 1Hz. This seems to have only a small effect on the measurements, but it could explain the higher variability of the Vaisala results during the tunnel tests at low wind speeds. A coupling device has been made for each sonic anemometer, so that the sensor could be easily exchanged and aligned. The alignment was performed manually, but tests revealed that an accuracy of ±1° could be obtained. All sensors were connected according to the specifications. For the heating of the Vaisala a 36VDC power supply was specifically purchased. Probably a power supply of 24V suffices in practice to prevent icing in Dutch conditions. The weight of the sonic anemometer ranges between 1.3 and 2.5kg and the MTBF between 10 and 26years. Only the Gill sonic anemometer is available as an intrinsically safe version.

The three sonic anemometers are tested in a wind tunnel up to wind speeds of 75m/s. Generally the results of all three sonic anemometers agree within the WMO accuracy limits (±5° en ±10%) with the tunnel reference.

- The Vaisala shows good agreement over the entire angle en wind speed range. The disturbances caused by the transducers are avoided by using the transducer pairs that are not affected. The measurements at low wind speeds (<5m/s), show relatively large fluctuations, but the differences are generally within the WMO limits. Only at some angles the reported wind direction differs more than 5° from the tunnel reference. At high wind speeds (≥50m/s) the disturbance by the transducers can be observed in 60° intervals with a magnitude of about 2% in speed and 1° in direction.
- The Gill measurements are very consistent. The curves as a function of the direction of the tunnel reference are very reproducible, smooth and symmetric over 90° intervals. The disturbance caused by the transducers is clearly visibly and causes errors exceeding the WMO limits when the wind is parallel to a transducer pair at high wind speeds (>60m/s). Generally, the Gill reports lower wind speeds compared to the tunnel reference and the results exhibit a temperature dependence. After completion of the test Gill performed a new calibration. The transducers were bend when the sensor arrived at Gill. This occurred probably during transport since the tunnel measurements at the end of the field test showed no indication of problems and the results showed good symmetry between 90° sectors. Gill not only performed a standard calibration at 12m/s, but also a “custom” calibration at 40m/s. The results provided by Gill showed that after the calibration the underestimation by the Gill is reduced to about 1% and the disturbance by the transducers is reduced by about a factor of 2. The disturbance, although within the WMO limits at all wind speeds (up to 46m/s) is, however, still noticeable.

- The Thies shows good agreement over the full direction and wind speed range. This sensor compensates for the disturbance caused by the transducers. Only a small signature of the disturbance is visible in the results. Measurements for wind speeds above 50m/s were not possible due to the damage inflicted by birds during the field test. At the time of the test Thies had no experiences of damage caused by birds. Optionally the sensor could be equipped with anti-bird wires. Recently a new Thies 2DA version became available with metal instead of the rubber fastening of the transducers. The Thies generally underestimates the wind speed and is closest to the results of the cup anemometer, but without the increased underestimation of the cup anemometers at higher wind speeds.

Table 3: Qualitative overview of the main results of the sonic anemometer tests.

| Item | Vaisala | Thies | Gill |
|---|---|---|---|
| *Wind speed range* | –/+ | –/+ | –/+ |
| *Accuracy* | + | ++ | –/+ |
| *Sample frequency / Output rate* | –/+ | + | + |
| *Reproducibility / variability* | –/+ | + | + |
| *Low wind speed* | –/+ | + | + |
| *Temperature* | – | + | –/+ |
| *Icing* | + | ++ | + |
| *Robustness / maintenance* | + | – | + |
| *Communication* | –/+ | + | + |
| *Weight* | + | –/+ | + |
| *Costs* | –/+ | + | + |
| *Pros* | Highest MTBF<br>No transducer correction required | Good accuracy<br>Temperature | Reproducibility<br>IS version |
| *Cons* | No temperature<br>Variability low wind speed<br>Sample frequency<br>Missing/corrupt data strings<br>36VDC heating | Robustness | Disturbance transducers<br>Temperature effect |

The three sonic anemometers have also been compared with the KNMI cup anemometer and wind vane during a field test of about 1 year. None of the 3 sonic anemometers showed any problems during the field test. After the test the Thies sensor showed clear signs of damage inflicted by birds, although this was not observed during the test. The Vaisala sensor sometimes failed to give a data string or reported a corrupt string, but this has hardly any effect on the 10-minute averaged values. The results of all three sonics generally agree within the WMO limit with the speed and direction reported by the KNMI cup anemometer and wind vane, respectively. The results of the 3 sonics show

good agreement when compared toe ach other. The differences between the sonics and the cup anemometer and wind vane are much larger than the differences between the sonics. These differences mainly occur at low wind speeds, where the sonic anemometer is much more sensitive than the cup and vane, the 10-minute averaged wind speed, where the cup anemometer overestimates the wind speed due to speeding, and the reaction of the sensors to the gustiness of the wind. The latter shows up as increased differences in wind direction, speed and gust in the sector where a line of trees disturbs the wind field. "Speeding" of the cup anemometer was also observed during the tunnel tests when the tunnel reference speed was changed from a higher to a lower value. The sonics anemometers perform well during lightning and precipitation. The differences that have been observed during (heavy) precipitation can probably be ascribed to changes in the behavior of the cup anemometer under these conditions. A quantitative overview of the results of the three sonic anemometers is given in Table 3.

# 7. Conclusions and recommendations

## *7.1 Conclusions*

The sonics anemometers are suitable for operational use at KNMI. The measurements meet the WMO and KNMI specifications and maintenance requirements. It should be noted, however, that none of the tested sonic anemometers met the 75m/s wind speed range of the current KNMI cup anemometer. Sonic anemometers are more suitable to measure at low wind speeds and in highly variable conditions than conventional cup anemometers and wind vanes. Furthermore, the measurements show less dependency on wind speed. The field test of one year is insufficient to give definite conclusions regarding maintenance and related costs. However, the introduction of sonic anemometers in the operational network of meteorological institutes in other countries, e.g. USA, Germany, Austria and Norway, seems promising.

The Vaisala sonic anemometer performed well during the tests. The sensor gives results that meet the WMO accuracy limits, but the results at low wind speeds show some variability and the reproducibility at low wind speeds is questionable. The internal sampling rate is not continuous and the output rate of the sensor is low. Furthermore the sensor does not report the sonic temperature. There seem to be no new developments regarding this sensor. The Gill anemometer also performed well during the tests. Particularly the reproducibility of the measurements is good. However, the measurements clearly show the disturbance induced by the transducers. A so-called custom calibration seems to improve the results, although some disturbance by the transducers remains. Gill currently works on a version of the sonic anemometer with an increased wind speed range of 90m/s which should come on the market in 2007. The Thies sonic anemometer shows only a small disturbance induced by the transducers. The results of the measurements are generally good, but unfortunately the sensor was damaged during the field test by birds. This can probably be prevented by using anti-bird wires. Thies recently introduced a new 2Da version of the sonic anemometer with an increases sampling and output frequency and a stainless steel protection cap of the transducers. The sensor is calibrated up to wind speeds of 65m/s, but it can report wind speeds of more than 75m/s, although the accuracy might be reduced.

Different types of users (aviation, general meteorology, climatology, scientific, modelers) were consulted in order to pinpoint the relative importance of the performance of the sonic anemometers regarding various aspects. Preliminary conclusions of the test were provided to these users. As could be expected, the feedback did not give a consistent view. Generally, the users react positively to the introduction of new and better sonic anemometers even if differences with the KNMI cup anemometer and wind vane can be expected. However, these differences need to be characterized by parallel tests at various locations. The reduction in the wind speed range is unacceptable for some users. A reduction in the sensor specification in this regard is undesirable, particularly in view of expected consequences due to climate change. The 75m/s wind speed range is therefore a must. The reproducibility between sensors is important in operational as well as in research applications. Any wind direction dependent error such as the disturbance caused

by the transducers is undesirable. The improved results at low wind speeds and the virtual temperature are nice to have.

Based on the results of the tests the "conservative" choice would be the Vaisala WAS425 sonic anemometer. The sensor does not meet the 75m/s wind speed range and the results at low wind speeds are rather poor. The Thies sonic anemometer is to be preferred due to the good performance over the full wind speed range, the good compensation for the disturbance by the transducers and the sonic temperature. Unfortunately the robustness of the sensor was unsatisfactory due to the damage inflicted by bird. The new 2Da version of this sensor with the protection cap and a range up to 75m/s looks very promising since it seems to overcome the 2 drawbacks of this sensor. The Gill sonic anemometer also performed well and a new version will soon be available with an extended range up to 90m/s. However, there is no indication that the disturbance caused by the transducers and the observed temperature dependency can be overcome shortly. In view of the above the new Thies 2Da sonic anemometer is preferred.

## *7.2 Recommendations*

Assuming that KNMI wants to proceed with the introduction of sonic anemometers in the operational network the following steps have to be followed:

Make a definite choice for the sonic anemometer to be considered for operational use in the KNMI network by taking as far as possible maintenance and commercial aspects into account. Also consider any new sensor developments and changes to specifications (e.g. usage maritime usage by the Dutch Royal Navy and at Voluntary Observing Ships and usage of 3D sonic anemometers onboard ships, for turbulence and possibly aircraft induced vortex observations).

Once the sensor is selected purchase several units (about 10) with an option for more. In order to keep the period of introduction within limits subject all sensors to an indoor test in the KNMI wind tunnel. The KNMI wind tunnel tests are suitable for acceptance testing and for testing the reproducibility of the sensors. At least 3 sonic anemometers should undergo an extended test over the full wind speed range in the DNW wind tunnel. It should be possible to perform these tests shortly after reception of the units using the operational settings as far as possible. Care should be taken of the sensor coupling device and the sensor alignment.

Next the sensor should be subjected to a parallel test in the field. A SIAM sensor interface is required and the test sites should cover all operational conditions. During the parallel test of at least 1 year the various user communities should evaluate the results (or at least participate in the evaluation of the results) and the so-called transfer functions should be constructed. Attention should also be given to regular checks in order to determine any degradation and to determine maintenance intervals.

The implementation project should also pay attention to:

1. Optimize the coupling device between sonic anemometer and KNMI plug. Once the sonic anemometer is selected there is no need to handle different sizes of sonic anemometers. Furthermore, future changes to the cross arm holding the wind sensors should be taken into account.

2. The alignment of the sensor to the plug should be facilitated be a mechanical setup in order to guarantee reproducibility. The alignment could be tested in the KNMI wind tunnel.
3. Make a mould in order to verify or measure the position of the transducers within the allowed tolerances.
4. Make a new cross arm to facilitate usage of cup, vane and sonic during parallel test and a version for sonic only after replacement of cup and vane by a sonic.
5. A SIAM sensor interface should be developed for the new sonic anemometer.
6. At least 3 sonic anemometers should undergo an extended test over the full wind speed range in the DNW wind tunnel. The test is required to verify the correct operation of the new sensor design / software and the reproducibility of the results of identical sensors. The test should be performed using (as far as possible) operational settings (e.g. sensor settings, sampling and output rate).
7. The KNMI wind tunnel should be used for acceptance test for each sonic anemometer. The absolute value of the wind speed can be determined by comparison of the results of identical sensors in the KNMI and DWN wind tunnel, from which a correction function for the blockage of the sensor in the KNMI wind tunnel can be derived. Furthermore, the wind direction, angular dependence, reproducibility and the sensor alignment can be verified. In addition a zero-measurement can be performed.
8. During the introduction of sonic anemometers transfer functions have to be made in order relate the results of the cup anemometer and wind vane to the results of the sonic anemometer. For that purpose parallel measurements of about 1 year have to be performed. Make clear arrangements with the users regarding the number of locations and the duration of the parallel tests. Furthermore, the responsibility regarding data analysis and reporting should be made clear.
9. The sonic anemometer should be evaluated with parallel tests at test sites covering all operational conditions. The test sites include e.g. airports (1 sensor at 2 airports), North Sea platform (2 sensors at 1 platform), 220m research mast at Cabauw (1 sensor at 3 levels), coastal station (1 sensor at Vlissingen), disturbed site with large variations in surface roughness per sector (1 sensor at De Bilt), perfect site (1 sensor at Cabauw).
10. Special attention should be given to the anti-vortex algorithm in the SIAM sensor interface since this algorithm might be sensitive to changes in the sensor properties. In order to perform a good evaluation and optimization raw sensor data might be required for locations with aircraft induced vortices as well as naturally disturbed sites in order to discriminate aircraft induced from natural variability of the wind.

11. The properties of the current KNMI cup anemometer en wind vane need to be determined. The properties like reporting threshold, distance constant, damping constant were determined in the 1970, but changes have been made to the sensors since then. Furthermore, the constants for acceleration en deceleration must be determined separately and as a function of the change in wind speed or direction. Recently these characteristics were determined for the current operational version of the KNMI cup anemometer (De Roosz, 2007) and confirmed the earlier results (Monna, 1978). Once these properties are known, it might be possible to understand the changes observed during a field test.
12. The accuracy of the sonic temperature measurements need to be analyzed in more detail over the full operational range. Measurements can be performed in the climate chamber at the KNMI calibration facilities under various temperature and humidity conditions as well as via comparison with the operational 1.5m ambient temperature measurements during the field test. The suitability of the sonic for temperature profile measurements, which are useful for boundary layer processes such as fog, can be investigated at Cabauw.
13. Hourly and 10-minute wind data are commonly considered by users. However, wind data at a higher time resolution contain much more information. The 12-second wind data should be used in the analysis of the upcoming parallel test of the KNMI cup anemometer and wind vane versus a selected sonic anemometer. The higher time resolution allows a more detailed comparison of the characteristics of the sensors.
14. Storage and usage of meteorological data at a higher temporal resolution should be implemented by KNMI. Currently all SIAM data is acquired by the Metnet systems, but only a small amount is used in the cyclic 7-day database and hardly any 12-second data is stored. A higher time resolution has advantages for cases studies, validation, and allows reprocessing of data in case of changes to reporting practices and/or processing algorithms.
15. KNMI should revise and update the evaluation of the surface roughness for the wind measurement sites by using wind data with a higher temporal and angular resolution. Furthermore, the usage of exposure and/or sheltering factors should be reevaluated. The frequency distribution of the wind speed and gust should also be updated and the usage of normalized wind speed and gust should be considered.

## *7.3 Acknowledgements*

It is a pleasure to thank Hans Beekhuis for his support with the data-acquisition software and the wind tunnel tests. Discussions with and feedback from Jitze van der Meulen on a previous version of this report are also much appreciated.

# 8. References

Benschop, H. and Meulen, van der, J.P.: Quality and Representativity of Wind Measurements, WMO-TECO, IOM-82, TD-1265 Bucharest, Romania, 4-7 May 2005.

Berg, van den, B.: Digital Anemometer (in Dutch), TD-01-002, Instrumental Department, KNMI, De Bilt, 1996a.

Berg, van den, B.: Digital Wind Vane (in Dutch), TD-01-003, Instrumental Department, KNMI, De Bilt, 1996b.

Bijma, J.R.: XW0-SIAM Wind (in Dutch), Version 4.0, Instrumental Department, KNMI, De Bilt, 1998.

Borstnik, A. and Knez, J.: The Intercomparison of the Ultrasonic Anemometers in Real Conditions at the Ljubljana Airport, 3rd International Conference on Experiences with AWS, Torremolinos, Spain, 19-21 February 2003.

Busch, N.E. and Kristensen, L.: Cup Anemometer Overspeeding, J. Appl. Meteorology 15, 1328-1332, 1976.

Gilhousen, D.B. and Hervey, R.: An Evaluation of Gill Sonic Anemometers in the Marine Environment, AMS Annual Meeting, Albuquerque, USA, 14-18 January 2001.

Gill Instruments: WindObserver II Ultrasonic Anemometer, User Manual, 1390-PS-0001, Issue 1, Hampshire, England, 2000.

Gill Instruments: Test WindObserver II, February 23, 2005a.

Gill Instruments: WindObserver II SNo. F000274, Certificates of Calibration at 5, 10, 12, 20, 32 and 46m/s, April 2005b.

Gouveia, F. and Lockhart, T.: Comparison of In-Situ Data from the Handar Sonic Anemometer and the Met One Cup and Vane, AMS Annual Meeting, Phoenix, USA, 14-16 January 1998.

Gregoire, P. and Oualid, G.: WMO Wind Instrument Intercomparison, WMO, IOM-62, TD-859, 1997.

Handboek Waarnemingen, Chapter 5 – Wind (in Dutch), KNMI, De Bilt, Version March 2001.

Handbook of Geophysics, Revised edition, MacMillan Company, New York, USA, 1960.

Hoeven, van der, P.C.T.: Het behandelen van de wind als vector-gegeven (in Dutch), KNMI memorandum FM-81-36, december 1981.

ICAO: Annex 3 Meteorological Services for International Air Navigation, Edition 15, July 2004.

ICAO: Manual on Automatic Meteorological Observing Systems at Aerodromes, Doc 9837, AN/454, Edition 1, 2006.

ISO: Sonic anemometers/thermometer – Acceptance Test Methods for Mean Wind Measurements, ISO/FDIS 16622, Geneva, Switzerland, 2002.

Kaimal, J.C. and Gaynor, J.E.: Another look at Sonic Thermometry, Boundary-Layer Meteorology 56, 401-410, 1991.

Lanzinger, E. and Langmack, H.: Measuring Air Temperature by using an Ultrasonic Anemometer, WMO-TECO, IOM-82, TD-1265 Bucharest, Romania, 4-7 May 2005.

Larre, M.H. et al.: Testing of Windsensors and the Usefulness of Video Technology at Marine Stations, WMO-TECO, IOM-82, TD-1265 Bucharest, Romania, 4-7 May 2005.

Lewis, R. and Dover, J.M.: Field and Operational Tests of a Sonic Anemometer for the Automated Surface Observing System, AMS Annual Meeting, Seattle, USA, 11-15 January 2004.

Meulen, van der, J.P.: Wake Vortex Induced Wind Measurements at Airfields: A Simple Algorithm to Reduce the Vortex Impact, WMO-TECO, IOM-70, TD-877, Casablanca Morocco, 4-12 May 1998.

Meulen, van der, J.P.: Wind Measurements: Potential Wind Speed Derived from Wind Speed Fluctuations Measurements and the Representativety of Wind Stations, WMO-TECO, IOM-74, TD-1028, Beijing, China, 23-27 October 2000.

Monna, W.A.A.: Comparative Investigation of Dynamic Properties of Some Propeller Vanes, Scientific Rapport WR 78-11, KNMI, De Bilt, 1978.

Monna, W.A.A.: The KNMI Wind Tunnel (in Dutch), Technical Report 32, KNMI, De Bilt, 1983.

Monna, W.A.A.: Accuracy of the Anemometer Calibrations in the KNMI Wind Tunnel (in Dutch), Memorandum FM-87-19, Scientific Department, KNMI, De Bilt, 1987.

Monna, W.A.A., Driedonks, A.G.M.: Experimental Data on the Dynamic Properties of Several Propeller Vanes, Journal of Applied Meteorology 18, 699-702, 1979.

Mortensen, N.G. and Højstrup, J.: The Solent Sonic – Response and Associated Errors, AMS Annual Meeting, Charlotte, USA, 27-31 March 1995.

Press, W.H., Teukolsky, S.A., Vetterling, W.T. and Flannery, B.P.: Numerical Recipes in Fortran, Second Edition, Cambridge University Press, 1992.

Roosz, de, M.: Bepaling van de karakteristieken van de KNMI cup anemometer (in Dutch), KNMI, Stageverslag, 5 september 2007.

Siebert, H. and Teichmann, U.: Behaviour of an Ultrasonic Anemometer under Cloudy Conditions, Boundary-Layer Meteorology 94, 165-169, 2000.

Sturgeon, M.C.: A Wind Tunnel Acceptance Test Method for Sonic Anemometers, AMS Annual Meeting, Dallas, USA, 10-15 January 1999.

Sturgeon, M.C.: Wind Tunnel Tests of Some Low-Cost Sonic Anemometers, WMO-TECO, IOM-82, TD-1265 Bucharest, Romania, 4-7 May 2005.

Tammelin, B., Heimo, A., Leroy, M., Peltomaa, A. and Rast, J.: Ice-Free Wind Sensors, 3rd International Conference on Experiences with AWS, Torremolinos, Spain, 19-21 February 2003.

Thies Clima: Ultrasonic Anemometer 2D, Operating Instructions 4.3800.00.xxx, Adolf Thies GmbH, Göttingen, Germany, 2001.

Thies Clima: Ultrasonic Anemometer 2D SNo. 0601050, Failure Analysis, February 19, 2004.

Vaisala: Ultrasonic Wind Sensors WAS425, User's Guide, U428en-1.1, Helsinki, Finland, 2000.

Vries, de, O.: Calibration of Anemometers in the LST, Memorandum AX-92-003 U, NLR, Marknesse, 1992.

Wastrack, K.G., Pittman, D.E., Hatmaker, J.E. and Hamberger, L.W.: Wind Sensor Comparison – Ultrasonic versus Wind Vane/Anemometer, AMS Annual Meeting, Albuquerque, USA, 14-18 January 2001.

Wauben, W. M. F and H. Beekhuis: TNO Calibration of sonic wind sensors, KNMI internal memo, 14 June 2001.

Wauben, W. M. F: Measurements DNW wind tunnel 23-25 September 2003, KNM internal memo, 12 October 2003.

Wauben, W. M. F: Measurements KNMI wind tunnel 1-4 December 2003, KNM internal memo, 10 December 2003.

Wauben, W. M. F: Wind Tunnel and Field Test of Three 2-D Sonic Anemometers, WMO-TECO, IOM-82, TD-1265 Bucharest, Romania, 4-7 May 2005.

Wieringa, J. and Rijkoort, P.J.: Wind Climate of the Netherlands (in Dutch), KNMI, De Bilt 1983.

Wieser, A., Fiedler, F. and Corsmeier, U.: The Influence of the Sensor Design on Wind Measurements with Sonic Anemometer Systems, J. Atmos. Oceanic Technol. 18, 1585-1608, 2001.

Willemsen, E.: Onnauwkeurigheden bij Anemometer Kalibraties, Lage Snelheids-Optie, DNW-LST, notitie juni 1994.

Willemsen, E.: Uncertainties in the Reference Wind Speed during Anemometer Calibrations in the DNW-LST Wind Tunnel, DNW-LST, 26 April 1996.

Willemsen, E., and Goedegebuure, B.: KNMI Anemometers tested in the DNW-LST Wind Tunnel, LST-2003-09, Project number 2710.3621, DNW, Marknesse, 2003.

WMO: Guide to Meteorological Instruments and Methods of Observation, Sixth edition, WMO-No. 8, Geneva, Switzerland, 1996.

Wyngaard, J.C. and Zhang, S.F.: Transducer Shadow Effects on Turbulence Spectra Measured by Sonic Anemometers, J. Atmos. Oceanic Technol. 2, 548-558, 1985.

# Appendix A1: Overview DNW-LST wind tunnel results

The table below gives an overview of the azimuth-averaged results of the DNW-LST wind tunnel measurements. See section 4.1 for details.

| *Run* | *Polar* | *Date* | *Time* | *Sensor* | $V_{tunnel}$ | $\langle V_t \rangle$ | $\langle \Delta V \rangle$ | *Stdev* | $\langle D_{off} \rangle$ | $\langle \Delta D \rangle$ [1] | *Stdev* | $\langle T_t \rangle$ | $\langle \Delta T \rangle$ | *Stdev* | # |
|---|---|---|---|---|---|---|---|---|---|---|---|---|---|---|---|
| 02 | 01 | 030923 | 082553 | Cup-133 | 2 | 2.05 | -0.12 | 0.00 | - | - | - | 12.49 | - | - | 121 |
| | 02 | 030923 | 083106 | Cup-133 | 3 | 3.09 | -0.09 | 0.00 | - | - | - | 12.99 | - | - | 125 |
| | 03 | 030923 | 083554 | Cup-133 | 5 | 5.09 | -0.03 | 0.00 | - | - | - | 13.98 | - | - | 120 |
| | 04 | 030923 | 084130 | Cup-133 | 10 | 10.12 | -0.09 | 0.00 | - | - | - | 14.70 | - | - | 120 |
| | 05 | 030923 | 084606 | Cup-133 | 20 | 20.29 | -0.07 | 0.00 | - | - | - | 15.18 | - | - | 120 |
| | 06 | 030923 | 085042 | Cup-133 | 50 | 50.61 | -1.75 | 0.01 | - | - | - | 16.99 | - | - | 95 |
| | 07 | 030923 | 085418 | Cup-133 | 60 | 60.71 | -2.67 | 0.01 | - | - | - | 18.46 | - | - | 61 |
| | 08 | 030923 | 085706 | Cup-133 | 65 | 65.75 | -3.10 | 0.02 | - | - | - | 19.61 | - | - | 61 |
| | 09 | 030923 | 090006 | Cup-133 | 75 | 75.88 | -4.34 | 0.01 | - | - | - | 21.34 | - | - | 61 |
| | 10 | 030923 | 090254 | Cup-133 | 70 | 70.81 | -3.98 | 0.01 | - | - | - | 22.08 | - | - | 61 |
| | 11 | 030923 | 090706 | Cup-133 | 30 | 30.37 | -0.18 | 0.05 | - | - | - | 20.78 | - | - | 87 |
| | 12 | 030923 | 091042 | Cup-133 | 15 | 15.18 | -0.09 | 0.01 | - | - | - | 20.53 | - | - | 58 |
| | 13 | 030923 | 091418 | Cup-133 | 7 | 7.09 | -0.08 | 0.00 | - | - | - | 20.48 | - | - | 70 |
| | 14 | 030923 | 091718 | Cup-133 | 5 | 5.04 | 0.00 | 0.00 | - | - | - | 20.55 | - | - | 71 |
| 04 | 03 | 030923 | 101141 | Gill$^+$ | 2 | 2.05 | -0.08 | 0.00 | 59.51 | -1.85 | 0.06 | 18.37 | 2.06 | 0.01 | 1577 |
| | 04 | 030923 | 102844 | Gill$^+$ | 3 | 3.05 | -0.08 | 0.00 | 62.34 | 1.04 | 0.06 | 18.32 | 1.73 | 0.01 | 1401 |
| | 05 | 030923 | 104531 | Gill$^+$ | 5 | 5.06 | -0.16 | 0.01 | 61.13 | -0.26 | 0.04 | 19.49 | 1.30 | 0.02 | 1555 |
| | 06 | 030923 | 110032 | Gill$^+$ | 10 | 10.06 | -0.23 | 0.00 | 62.16 | 0.81 | 0.03 | 19.58 | 1.38 | 0.01 | 1428 |
| | 07 | 030923 | 111655 | Gill$^+$ | 20 | 20.15 | -0.21 | 0.01 | 60.81 | -0.58 | 0.03 | 19.48 | 1.68 | 0.02 | 1536 |
| | 08 | 030923 | 113216 | Gill$^+$ | 50 | 50.29 | 0.63 | 0.09 | 61.85 | 0.50 | 0.05 | 21.57 | -1.85 | 0.10 | 1296 |
| | 09 | 030923 | 114611 | Gill$^+$ | 60 | 60.25 | 0.65 | 0.09 | 60.44 | -0.99 | 0.09 | 24.45 | -4.54 | 0.15 | 1545 |
| | 10 | 030923 | 120112 | Gill$^+$ | 65 | 65.28 | 0.69 | 0.11 | 60.46 | -0.93 | 0.64 | 27.20 | -2.37 | 0.54 | 1407 |
| | 11 | 030923 | 121725 | Gill$^+$ | 30 | 30.18 | -0.52 | 0.04 | 60.81 | -0.59 | 0.04 | 26.72 | -1.14 | 0.03 | 1564 |
| | 12 | 030923 | 123246 | Gill$^+$ | 15 | 15.06 | -0.39 | 0.01 | 62.54 | 1.18 | 0.02 | 24.59 | -0.44 | 0.01 | 1421 |

[1] Note that $\langle \Delta D \rangle$ is determined w.r.t. the sensor averaged offset $\langle X_{off} \rangle$ which is 61.38° for the Gill$^+$; 61.91° for the Thies; 62.22° for the Vaisala; 61.59° for the Gill sonic anemometer.

| *Run* | *Polar* | *Date* | *Time* | *Sensor* | $V_{tunnel}$ | $<V_t>$ | $<\Delta V>$ | *Stdev* | $<D_{off}>$ | $<\Delta D>$ [1] | *Stdev* | $<T_t>$ | $<\Delta T>$ | *Stdev* | # |
|---|---|---|---|---|---|---|---|---|---|---|---|---|---|---|---|
| | 13 | 030923 | 124633 | Gill$^+$ | 7 | 7.02 | -0.27 | 0.00 | 61.34 | -0.09 | 0.03 | 23.59 | -0.68 | 0.01 | 1551 |
| | 14 | 030923 | 130104 | Gill$^+$ | 5 | 5.01 | -0.22 | 0.01 | 63.15 | 1.77 | 0.03 | 22.79 | -0.44 | 0.00 | 1577 |
| 5 | 01 | 030923 | 140006 | Thies | 2 | 2.09 | -0.12 | 0.00 | 61.45 | -0.49 | 0.05 | 18.66 | 1.71 | 0.01 | 1541 |
| | 02 | 030923 | 141536 | Thies | 3 | 3.07 | -0.10 | 0.00 | 62.10 | 0.19 | 0.03 | 19.68 | 0.71 | 0.01 | 1429 |
| | 03 | 030923 | 142952 | Thies | 5 | 5.05 | -0.08 | 0.00 | 61.73 | -0.21 | 0.02 | 20.40 | 0.74 | 0.00 | 1570 |
| 6 | 01 | 030923 | 150132 | Thies | 10 | 10.23 | -0.10 | 0.01 | 62.05 | 0.15 | 0.02 | 19.41 | 0.86 | 0.00 | 1264 |
| 8 | 01 | 030924 | 073330 | Thies | 20 | 20.04 | -0.15 | 0.01 | 61.30 | -0.65 | 0.02 | 7.98 | -0.15 | 0.00 | 1583 |
| | 02 | 030924 | 074905 | Thies | 50 | 50.06 | -0.58 | 0.39 | 62.51 | 0.67 | 0.13 | 11.08 | -4.29 | 0.10 | 1335 |
| | 03 | 030924 | 081010 | Thies | 30 | 30.04 | -0.17 | 0.01 | 61.42 | -0.54 | 0.02 | 13.70 | -1.01 | 0.02 | 1586 |
| 9 | 01 | 030924 | 083159 | Thies | 15 | 15.01 | -0.14 | 0.01 | 62.28 | 0.38 | 0.02 | 14.63 | 0.01 | 0.00 | 1429 |
| | 02 | 030924 | 084630 | Thies | 7 | 7.00 | -0.11 | 0.01 | 61.62 | -0.32 | 0.02 | 14.71 | 0.16 | 0.00 | 1566 |
| | 03 | 030924 | 090108 | Thies | 5 | 5.01 | -0.09 | 0.01 | 62.42 | 0.53 | 0.02 | 15.23 | 0.09 | 0.00 | 1416 |
| 10 | 01 | 030924 | 093538 | Vaisala | 2 | 2.02 | -0.06 | 0.01 | 60.95 | -1.35 | 0.11 | 15.06 | - | - | 1575 |
| | 02 | 030924 | 095059 | Vaisala | 3 | 3.00 | -0.02 | 0.01 | 62.18 | -0.03 | 0.07 | 16.45 | - | - | 1439 |
| | 03 | 030924 | 100537 | Vaisala | 5 | 5.02 | 0.02 | 0.01 | 61.94 | -0.36 | 0.05 | 17.61 | - | - | 1577 |
| | 04 | 030924 | 102133 | Vaisala | 10 | 10.06 | 0.09 | 0.01 | 62.69 | 0.46 | 0.04 | 19.65 | - | - | 1443 |
| | 05 | 030924 | 103514 | Vaisala | 20 | 20.07 | 0.22 | 0.01 | 61.54 | -0.74 | 0.03 | 21.07 | - | - | 1581 |
| | 06 | 030924 | 105013 | Vaisala | 50 | 50.03 | 0.24 | 0.04 | 62.88 | 0.66 | 0.03 | 24.17 | - | - | 1454 |
| 11 | 01 | 030924 | 111118 | Vaisala | 60 | 60.02 | 0.01 | 0.11 | 61.21 | -0.79 | 0.20 | 27.85 | - | - | 1578 |
| | 02 | 030924 | 112607 | Vaisala | 65 | 65.06 | 0.22 | 0.05 | 62.97 | 0.75 | 0.04 | 31.15 | - | - | 1445 |
| | 03 | 030924 | 114007 | Vaisala | 70 | 70.09 | 0.22 | 0.10 | 61.79 | -0.45 | 0.06 | 33.81 | - | - | 938 |
| | 04 | 030924 | 115332 | Vaisala | 30 | 30.05 | 0.40 | 0.02 | 61.82 | -0.51 | 0.02 | 31.76 | - | - | 1639 |
| | 05 | 030924 | 121046 | Vaisala | 15 | 15.03 | 0.21 | 0.01 | 62.81 | 0.59 | 0.03 | 30.48 | - | - | 1441 |
| | 06 | 030924 | 122514 | Vaisala | 7 | 7.03 | 0.05 | 0.01 | 62.44 | 0.18 | 0.04 | 29.75 | - | - | 1567 |
| | 07 | 030924 | 124107 | Vaisala | 5 | 5.01 | 0.01 | 0.01 | 63.59 | 1.33 | 0.05 | 28.98 | - | - | 1437 |
| 12 | 01 | 030924 | 130648 | Gill | 5 | 5.00 | -0.22 | 0.00 | 61.12 | -0.47 | 0.03 | 27.97 | -2.36 | 0.01 | 1584 |
| | 02 | 030924 | 132143 | Gill | 50 | 50.07 | 0.25 | 0.10 | 61.87 | 0.31 | 0.05 | 29.64 | -4.18 | 0.09 | 1438 |
| 13 | 01 | 030924 | 135305 | Gill | 10 | 10.03 | -0.35 | 0.00 | 61.22 | -0.40 | 0.02 | 27.82 | -2.05 | 0.01 | 1594 |
| | 02 | 030924 | 140729 | Gill | 20 | 20.04 | -0.42 | 0.01 | 61.88 | 0.32 | 0.02 | 27.52 | -1.68 | 0.02 | 1440 |
| | 03 | 030924 | 142051 | Gill | 60 | 60.06 | 0.33 | 0.11 | 60.77 | -0.86 | 0.11 | 29.82 | -5.53 | 0.15 | 1585 |
| | 04 | 030924 | 143459 | Gill | 65 | 65.08 | 0.53 | 0.13 | 60.38 | -1.27 | 0.63 | 31.68 | -3.10 | 0.52 | 1441 |

| *Run* | *Polar* | *Date* | *Time* | *Sensor* | $V_{tunnel}$ | $<V_t>$ | $<\Delta V>$ | *Stdev* | $<D_{off}>$ | $<\Delta D>$ [1] | *Stdev* | $<T_t>$ | $<\Delta T>$ | *Stdev* | # |
|---|---|---|---|---|---|---|---|---|---|---|---|---|---|---|---|
| 14 | 01 | 030924 | 145907 | Gill | 30 | 30.07 | -0.55 | 0.04 | 60.61 | -1.00 | 0.04 | 29.18 | -1.78 | 0.02 | 1594 |
| 15 | 02 | 030925 | 062211 | Gill | 15 | 15.05 | -0.11 | 0.01 | 62.51 | 0.95 | 0.03 | 7.44 | 4.42 | 0.02 | 1405 |
| | 03 | 030925 | 063617 | Gill | 7 | 7.05 | -0.16 | 0.00 | 61.09 | -0.55 | 0.03 | 7.90 | 3.38 | 0.03 | 1573 |
| | 04 | 030925 | 065231 | Gill | 3 | 3.05 | -0.10 | 0.00 | 63.46 | 1.93 | 0.04 | 7.77 | 2.27 | 0.03 | 1408 |
| | 05 | 030925 | 070738 | Gill | 2 | 1.98 | -0.08 | 0.00 | 62.57 | 0.98 | 0.06 | 7.84 | 1.92 | 0.04 | 1577 |
| 16 | 01 | 030925 | 074027 | Cup-115 | 2 | 2.00 | -0.14 | 0.00 | - | - | - | 8.33 | - | - | 93 |
| | 02 | 030925 | 074507 | Cup-115 | 3 | 3.01 | -0.10 | 0.00 | - | - | - | 8.59 | - | - | 93 |
| | 03 | 030925 | 075011 | Cup-115 | 5 | 5.00 | -0.08 | 0.01 | - | - | - | 9.09 | - | - | 83 |
| | 04 | 030925 | 075326 | Cup-115 | 10 | 10.02 | -0.09 | 0.00 | - | - | - | 9.42 | - | - | 69 |
| | 05 | 030925 | 075629 | Cup-115 | 20 | 20.03 | -0.06 | 0.00 | - | - | - | 9.83 | - | - | 70 |
| | 06 | 030925 | 075932 | Cup-115 | 50 | 50.01 | -1.77 | 0.01 | - | - | - | 11.27 | - | - | 67 |
| | 07 | 030925 | 080234 | Cup-115 | 60 | 60.00 | -2.44 | 0.01 | - | - | - | 12.63 | - | - | 71 |
| | 08 | 030925 | 080549 | Cup-115 | 65 | 65.01 | -2.88 | 0.01 | - | - | - | 13.94 | - | - | 77 |
| | 09 | 030925 | 080904 | Cup-115 | 75 | 75.00 | -3.43 | 0.01 | - | - | - | 16.13 | - | - | 133 |
| | 10 | 030925 | 081344 | Cup-115 | 70 | 70.02 | -3.65 | 0.01 | - | - | - | 17.28 | - | - | 75 |
| | 11 | 030925 | 081736 | Cup-115 | 30 | 30.02 | -0.47 | 0.01 | - | - | - | 15.87 | - | - | 72 |
| | 12 | 030925 | 082103 | Cup-115 | 15 | 15.00 | -0.03 | 0.00 | - | - | - | 15.50 | - | - | 73 |
| | 13 | 030925 | 082454 | Cup-115 | 7 | 7.02 | -0.11 | 0.00 | - | - | - | 15.51 | - | - | 71 |
| | 14 | 030925 | 082834 | Cup-115 | 5 | 4.97 | -0.01 | 0.00 | - | - | - | 15.55 | - | - | 71 |

# Appendix A2: DNW-LST wind tunnel measurements

In this appendix the averaged binned results of the 360° rotation test in the DNW-LST wind tunnel are presented for the Gill, Thies and Vaisala sonic anemometers with increasing reference speed. For that purpose the raw 1-second sensor measurements and tunnel readings at 2Hz are averaged over 2-degrees interval of the turntable and presented as a function of the reference angle $D_r$ of the turntable. The figures show for each sensor tunnel reference speed the angular dependence of the differerences between sensor wind speed and the tunnel reference value $\Delta V$ and the diffference between the sensor wind direction and the turntable reference value $\Delta D$ and compensated for the overall offset $<X_{off}>$ of the sonic anemometer. The full scale of the figures are fixed at the WMO accuracy requirements, i.e. ±5° for wind direction and ±0.5m/s or ±10% for wind speeds below and above 5m/s, respectively.

## *Gill sonic anemometer*

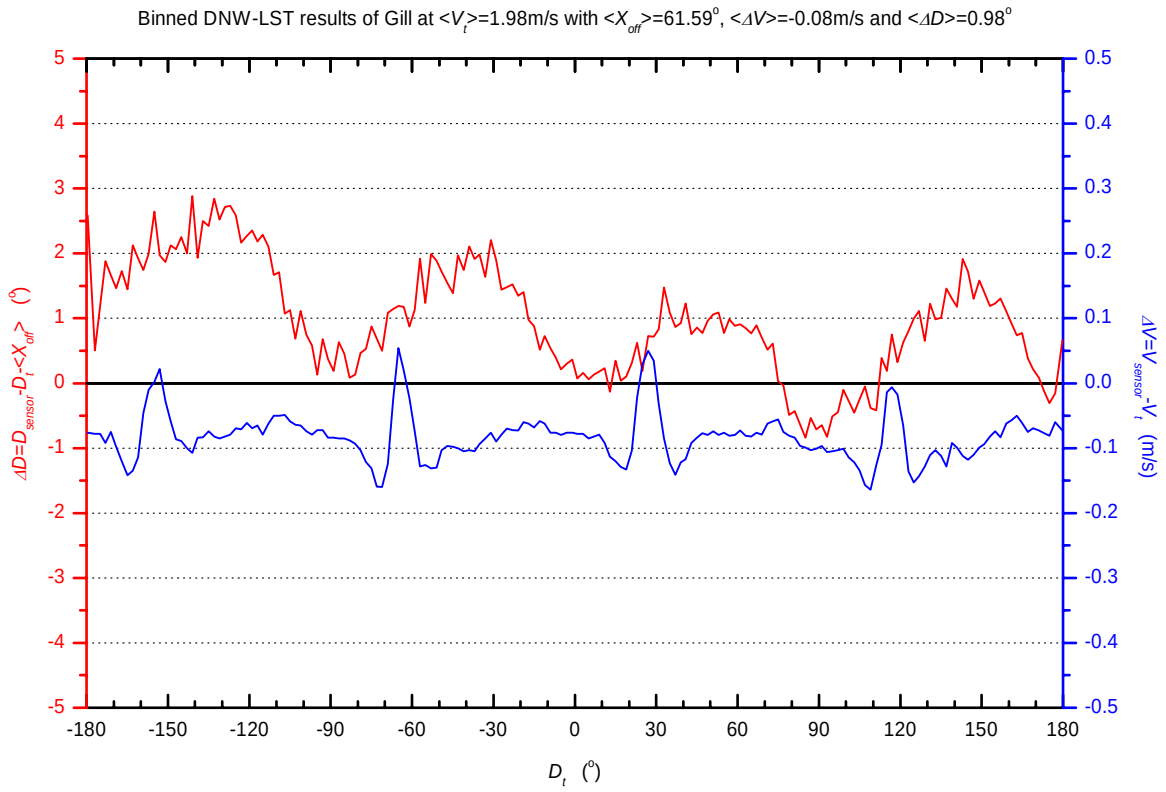

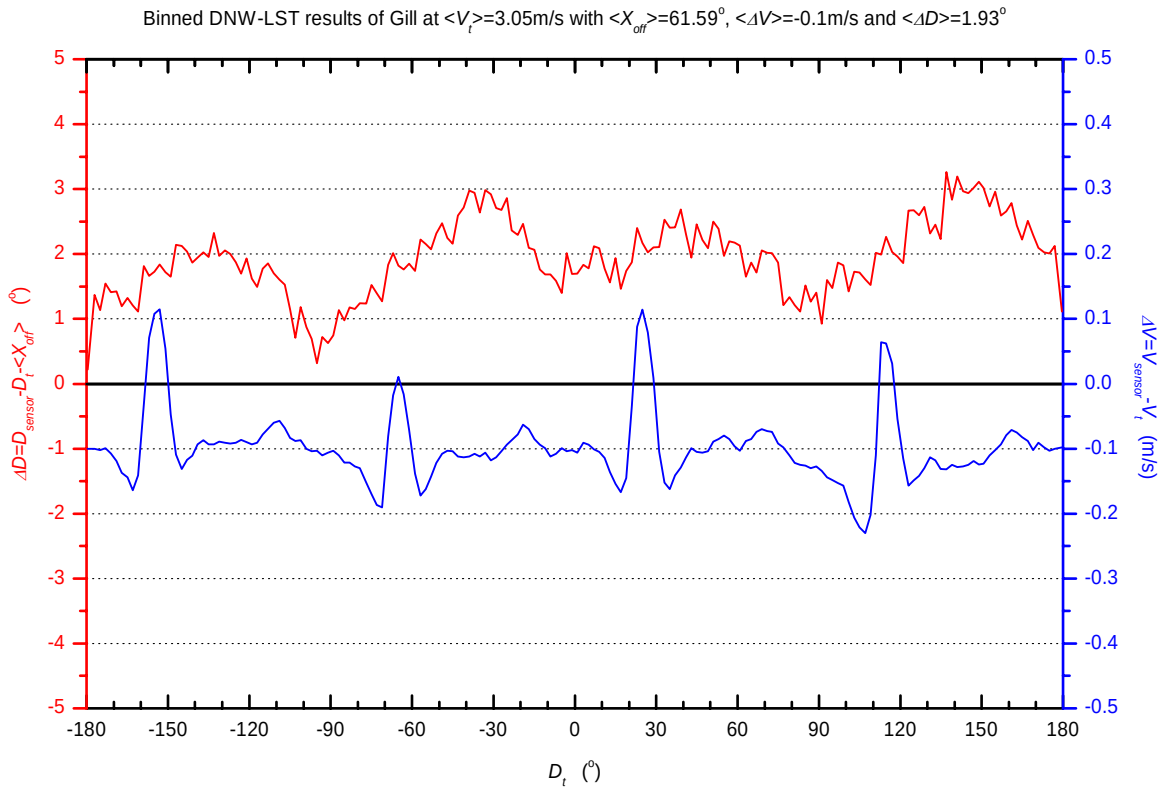
Binned DNW-LST results of Gill at <$V_t$>=3.05m/s with <$X_{off}$>=61.59°, <$\Delta V$>=-0.1m/s and <$\Delta D$>=1.93°
$\Delta D=D_{sensor}-D_t-<X_{off}>$ (°)
$\Delta V=V_{sensor}-V_t$ (m/s)
$D_t$ (°)
5
4
3
2
1
0
-1
-2
-3
-4
-5
0.5
0.4
0.3
0.2
0.1
0.0
-0.1
-0.2
-0.3
-0.4
-0.5
-180
-150
-120
-90
-60
-30
0
30
60
90
120
150
180

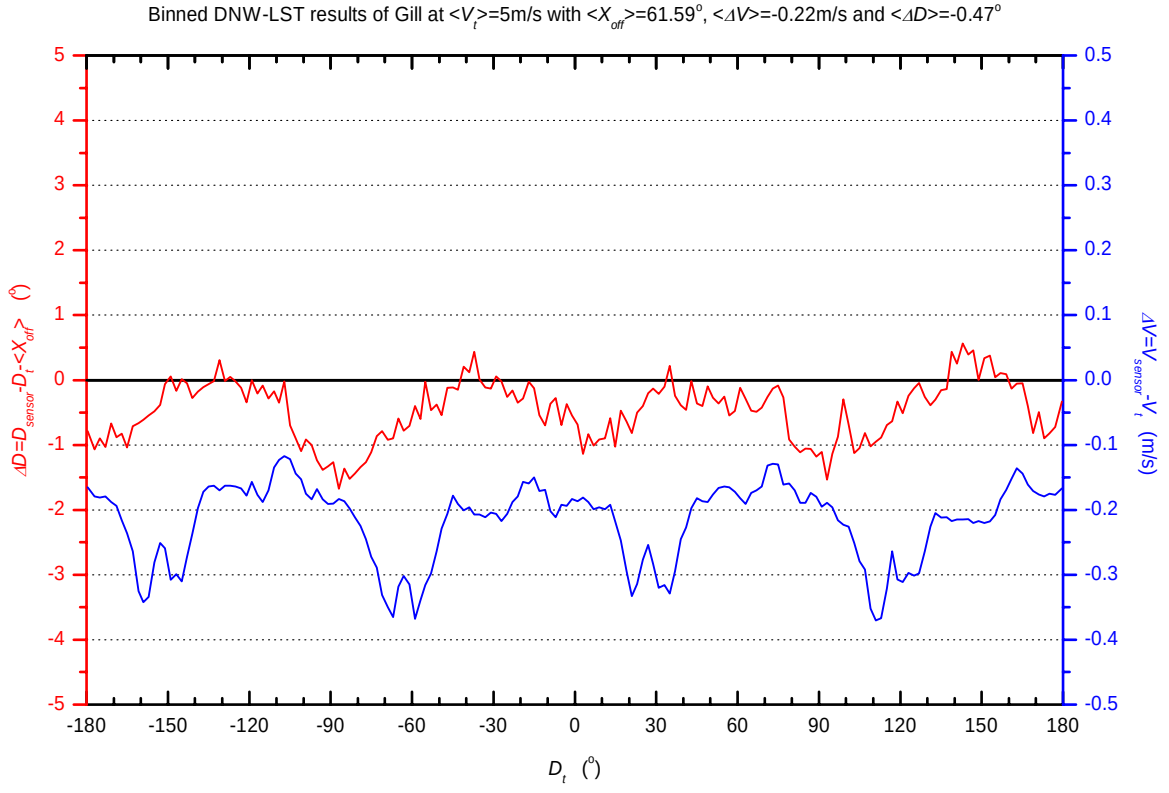
Binned DNW-LST results of Gill at <$V_t$>=5m/s with <$X_{off}$>=61.59°, <$\Delta V$>=-0.22m/s and <$\Delta D$>=-0.47°
$\Delta D=D_{sensor}-D_t-<X_{off}>$ (°)
$\Delta V=V_{sensor}-V_t$ (m/s)
$D_t$ (°)
5
4
3
2
1
0
-1
-2
-3
-4
-5
0.5
0.4
0.3
0.2
0.1
0.0
-0.1
-0.2
-0.3
-0.4
-0.5
-180
-150
-120
-90
-60
-30
0
30
60
90
120
150
180

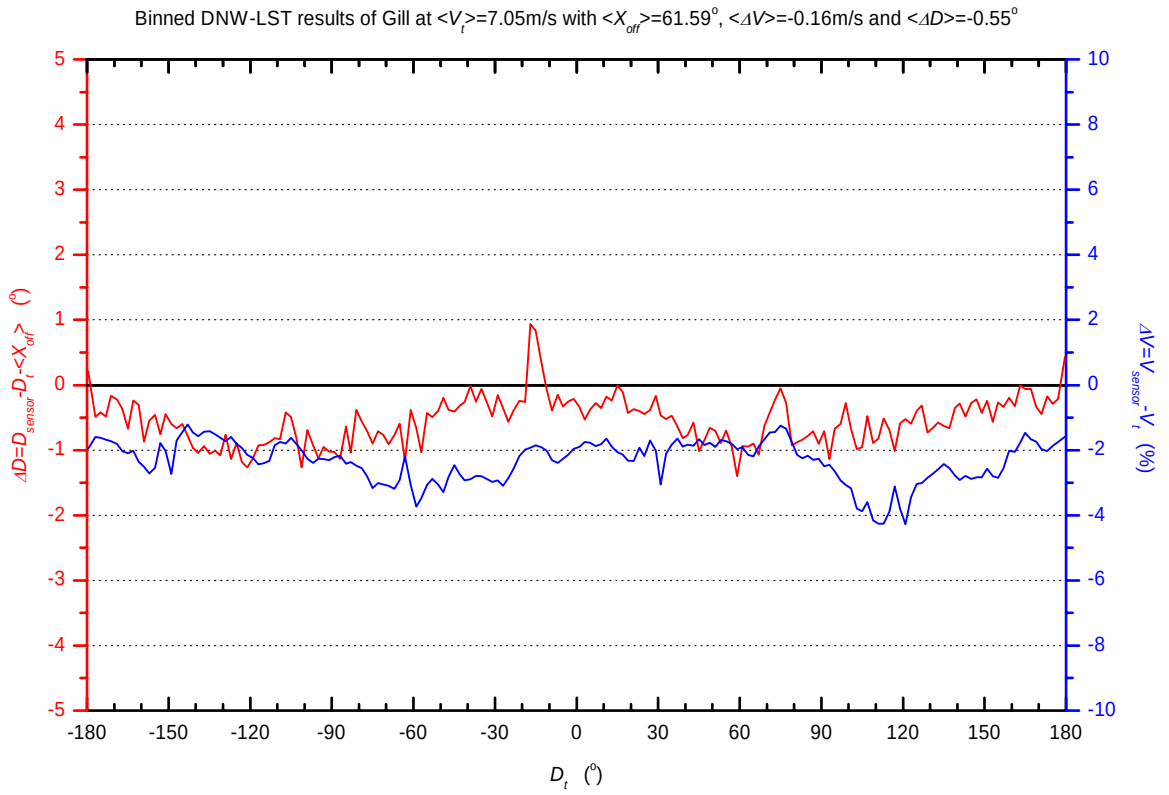
Binned DNW-LST results of Gill at <$V_t$>=7.05m/s with <$X_{off}$>=61.59°, <$\Delta V$>=-0.16m/s and <$\Delta D$>=-0.55°
$\Delta D=D_{sensor}-D_t-<X_{off}>$ (°)
$\Delta V=V_{sensor}-V_t$ (%)
$D_t$ (°)

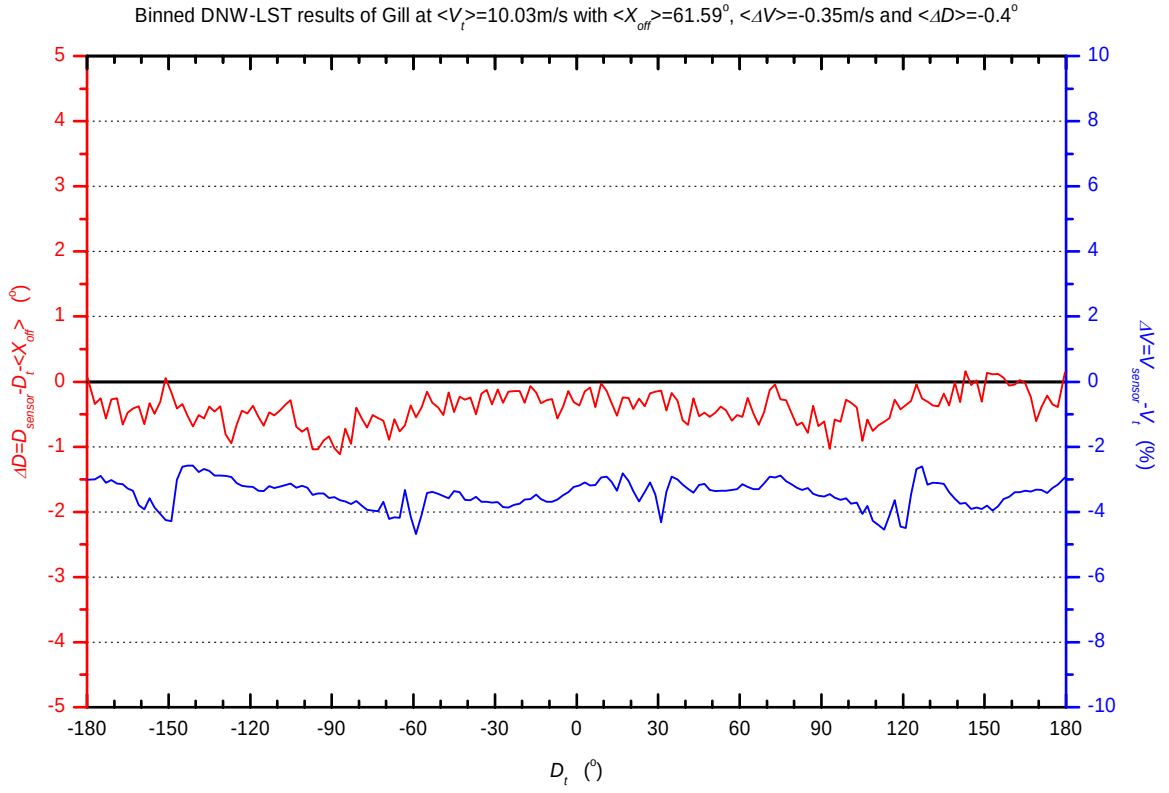
Binned DNW-LST results of Gill at <$V_t$>=10.03m/s with <$X_{off}$>=61.59°, <$\Delta V$>=-0.35m/s and <$\Delta D$>=-0.4°
$\Delta D=D_{sensor}-D_t-<X_{off}>$ (°)
$\Delta V=V_{sensor}-V_t$ (%)
$D_t$ (°)

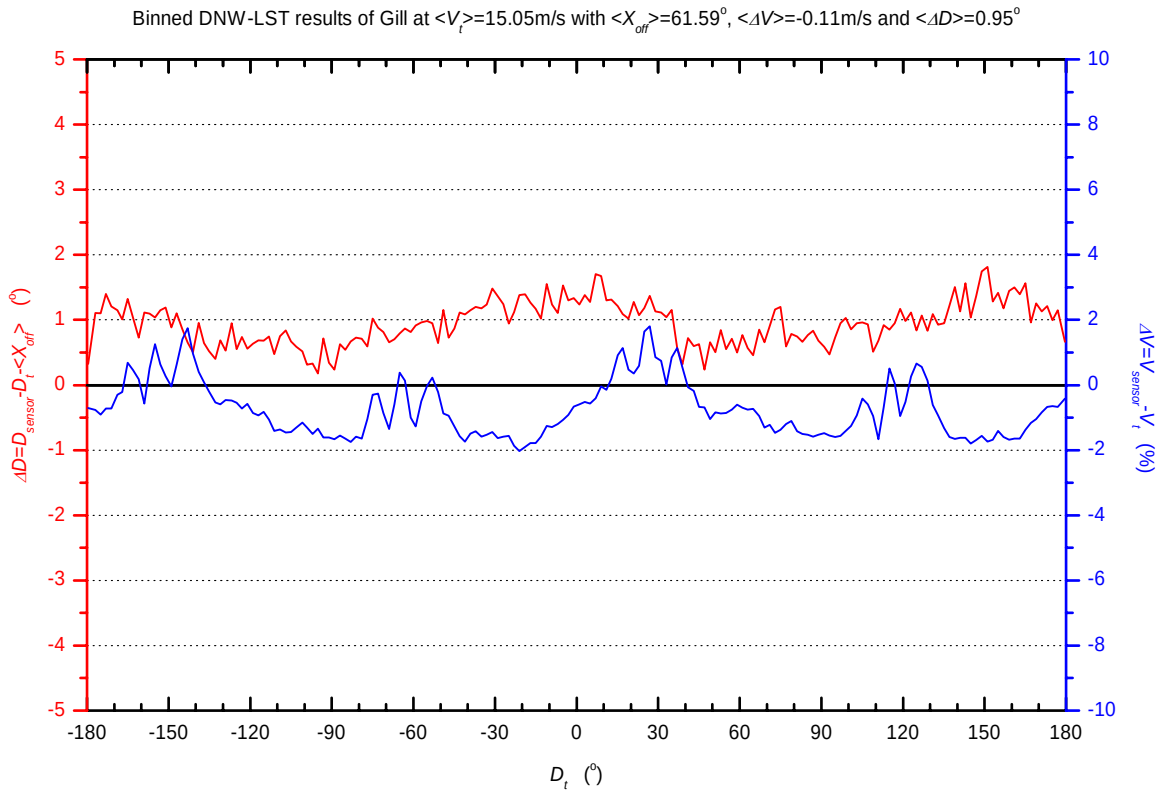
Binned DNW-LST results of Gill at <$V_t$>=15.05m/s with <$X_{off}$>=61.59°, <$\Delta V$>=-0.11m/s and <$\Delta D$>=0.95°
$\Delta D=D_{sensor}-D_t-<X_{off}>$ (°)
$\Delta V=V_{sensor}-V_t$ (%)
$D_t$ (°)

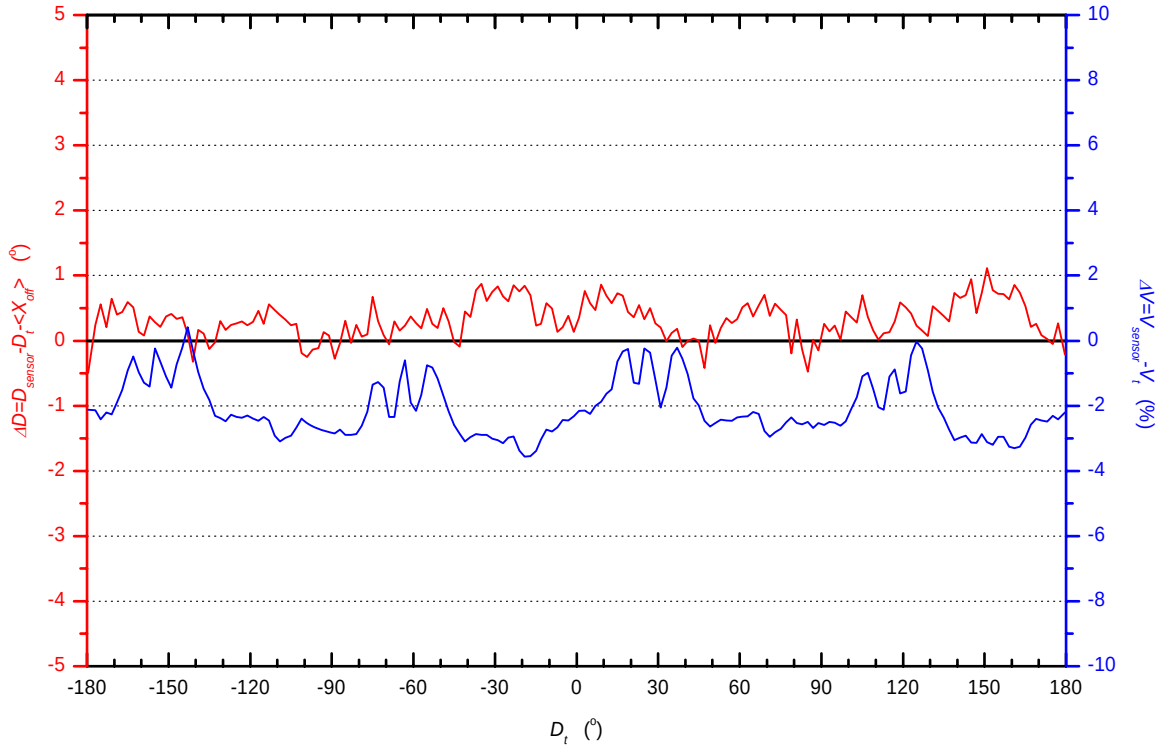
Binned DNW-LST results of Gill at <$V_t$>=20.04m/s with <$X_{off}$>=61.59°, <$\Delta V$>=-0.42m/s and <$\Delta D$>=0.32°
$\Delta D=D_{sensor}-D_t-<X_{off}>$ (°)
$\Delta V=V_{sensor}-V_t$ (%)
$D_t$ (°)

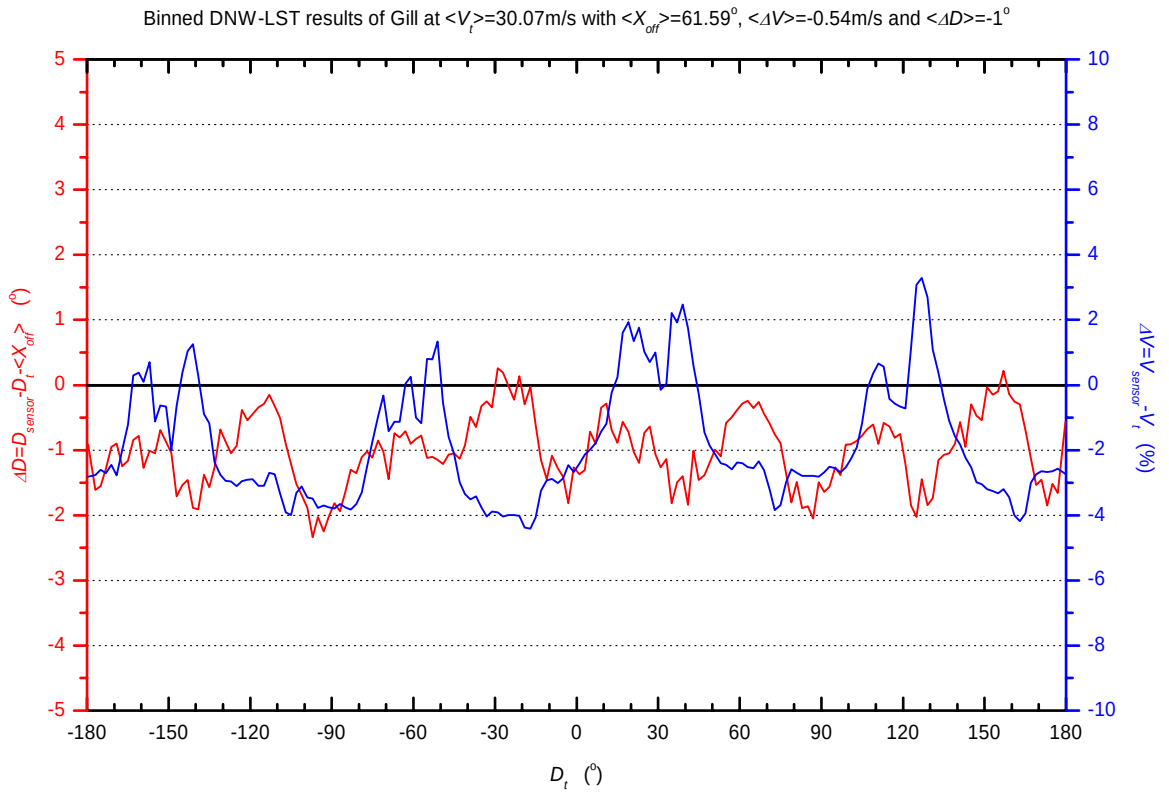
Binned DNW-LST results of Gill at <$V_t$>=30.07m/s with <$X_{off}$>=61.59°, <$\Delta V$>=-0.54m/s and <$\Delta D$>=-1°
$\Delta D=D_{sensor}-D_t-<X_{off}>$ (°)
$\Delta V=V_{sensor}-V_t$ (%)
$D_t$ (°)

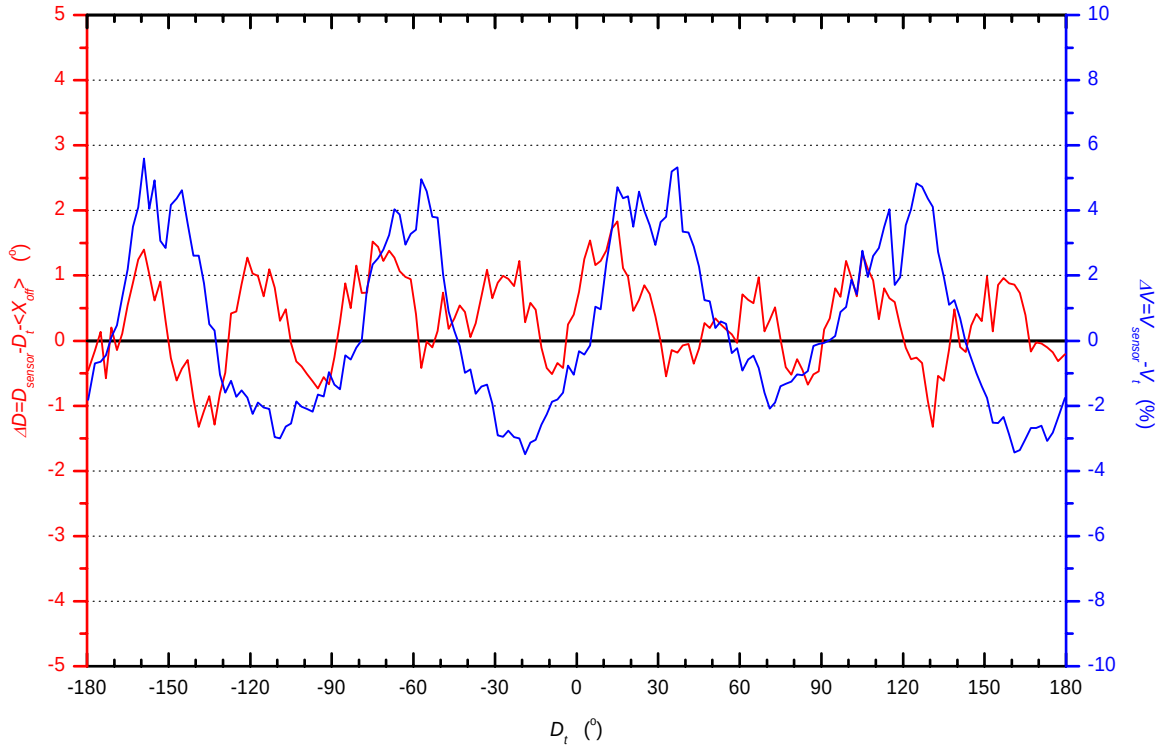
Binned DNW-LST results of Gill at <$V_t$>=50.07m/s with <$X_{off}$>=61.59°, <$\Delta V$>=0.24m/s and <$\Delta D$>=0.3°
$\Delta D=D_{sensor}-D_t-<X_{off}>$ (°)
$\Delta V=V_{sensor}-V_t$ (%)
$D_t$ (°)

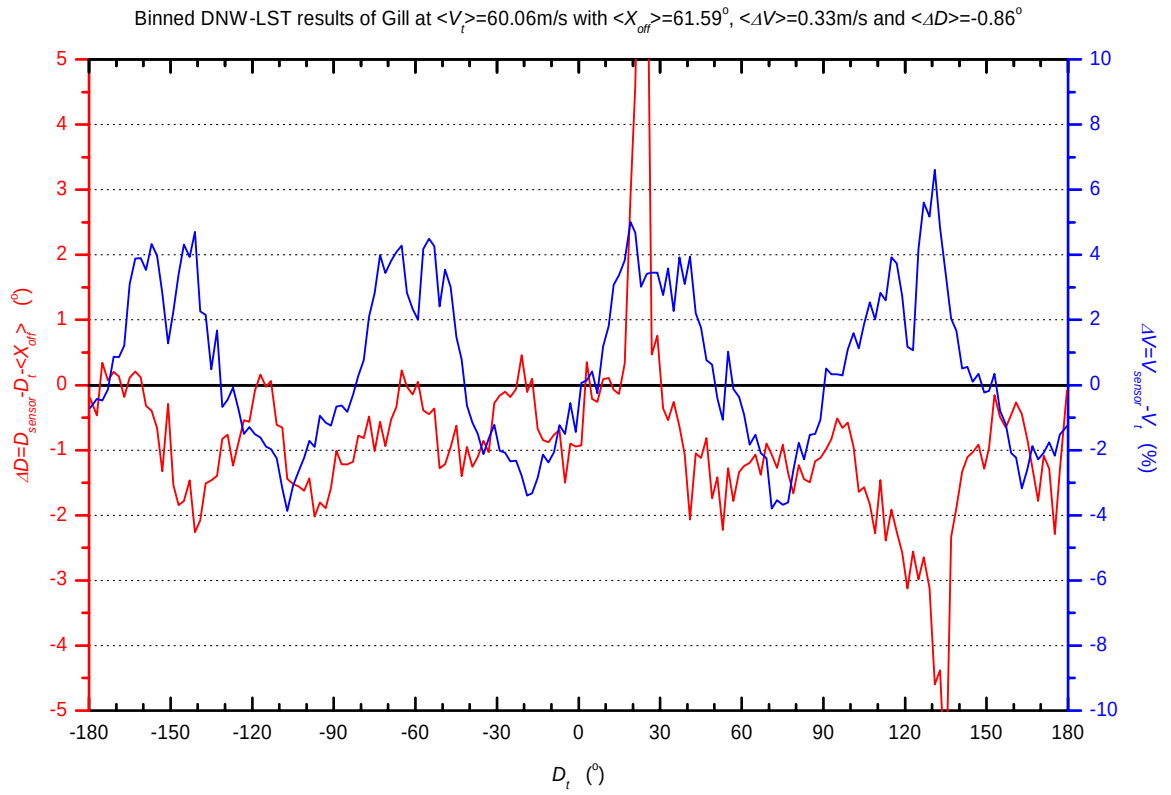
Binned DNW-LST results of Gill at <$V_t$>=60.06m/s with <$X_{off}$>=61.59°, <$\Delta V$>=0.33m/s and <$\Delta D$>=-0.86°
$\Delta D=D_{sensor}-D_t-<X_{off}>$ (°)
$\Delta V=V_{sensor}-V_t$ (%)
$D_t$ (°)

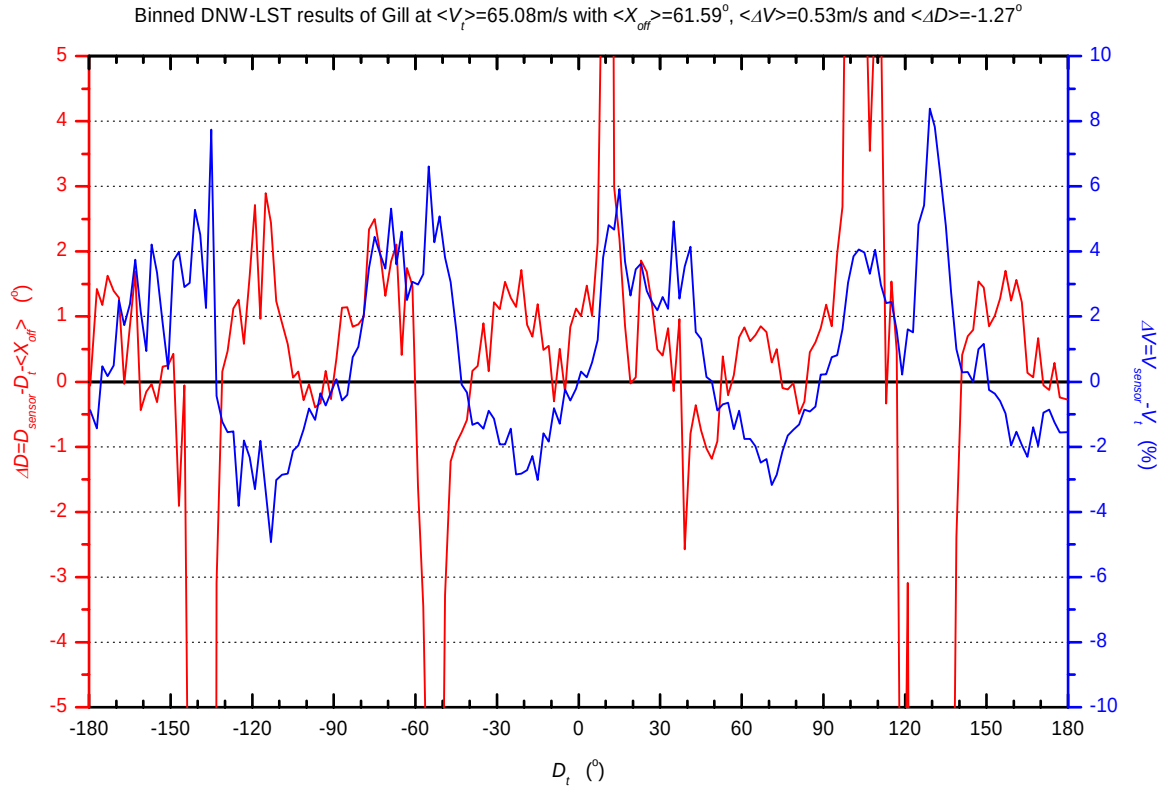
Binned DNW-LST results of Gill at <$V_t$>=65.08m/s with <$X_{off}$>=61.59°, <$\Delta V$>=0.53m/s and <$\Delta D$>=-1.27°
$\Delta D=D_{sensor}-D_t-<X_{off}>$ (°)
$\Delta V=V_{sensor}-V_t$ (%)
$D_t$ (°)

## *Thies sonic anemometer*

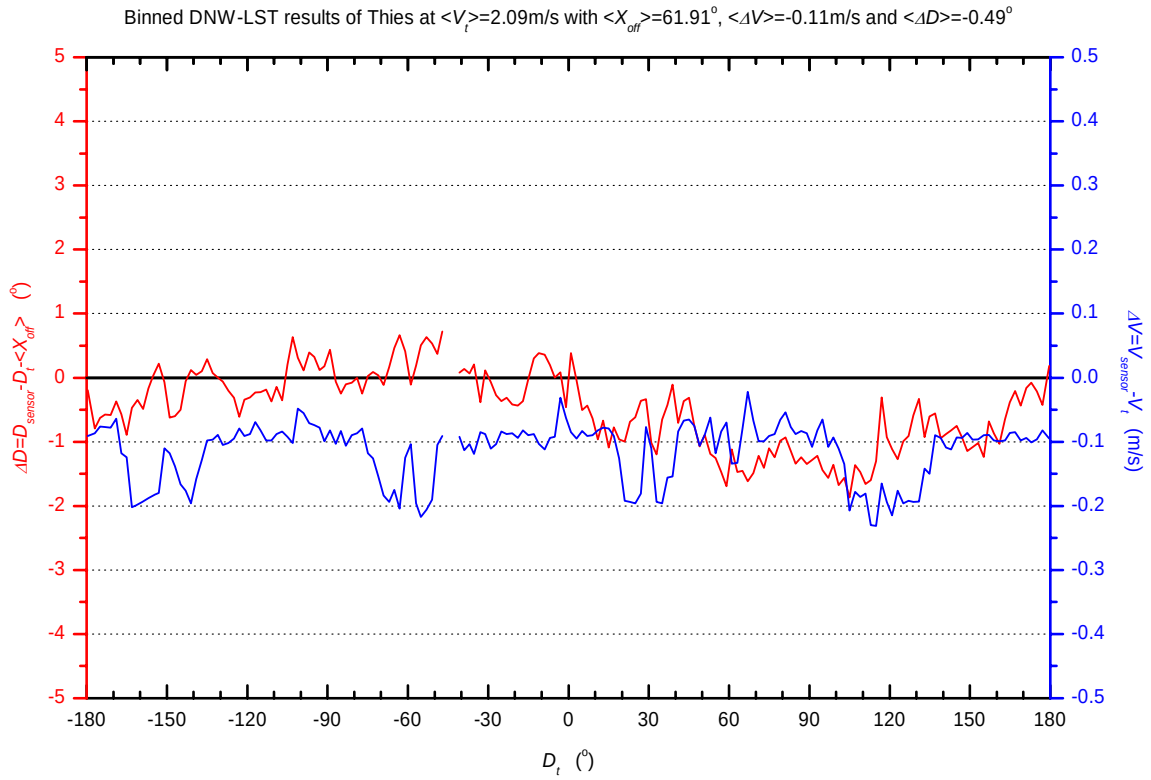


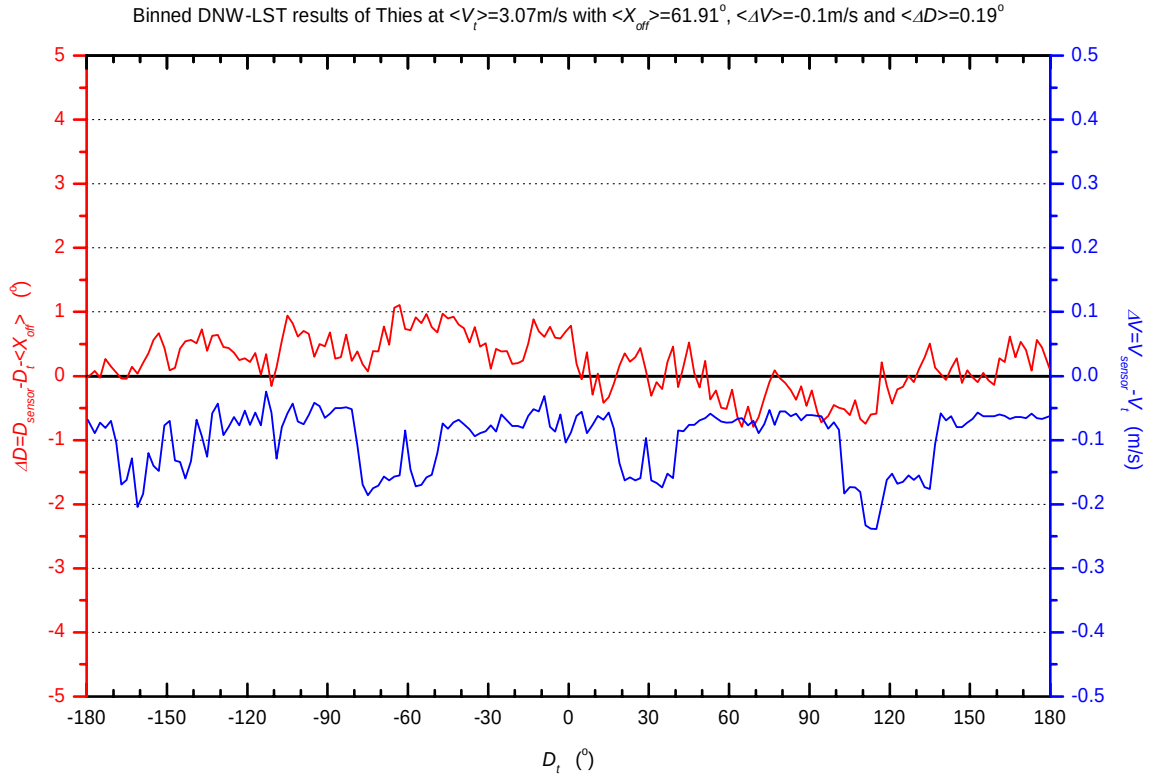

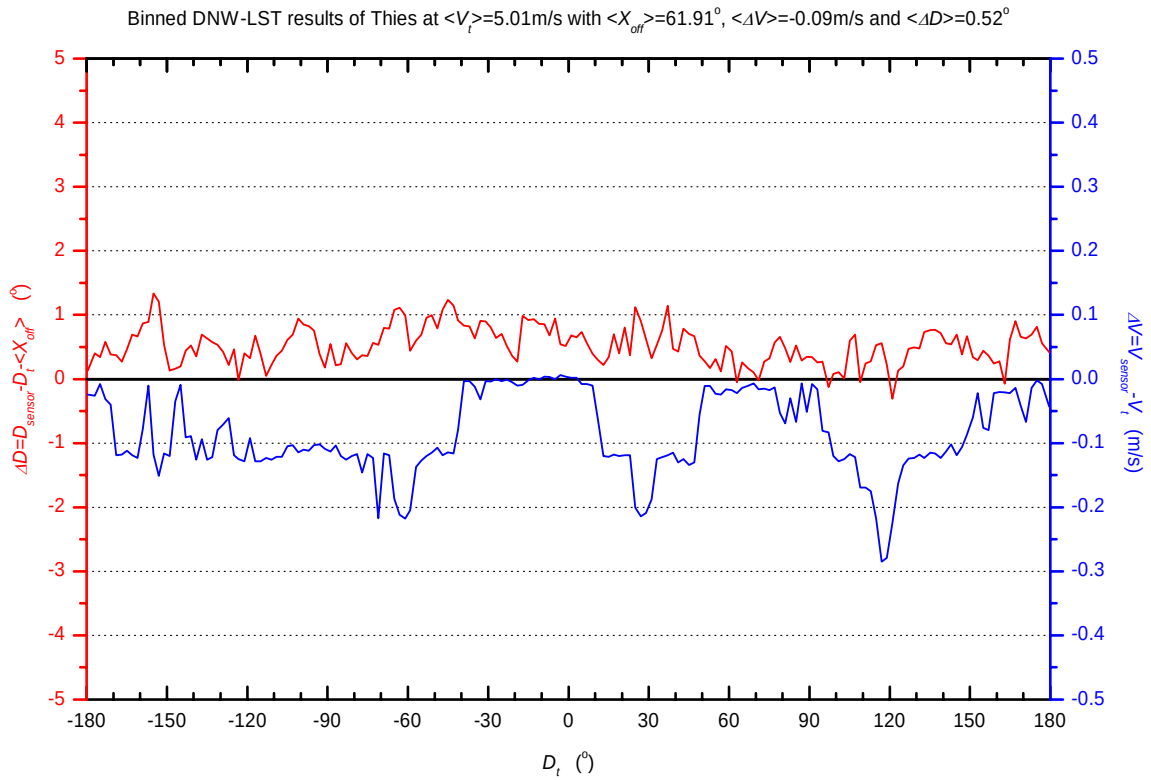
Binned DNW-LST results of Thies at <$V_t$>=5.01m/s with <$X_{off}$>=61.91°, <$\Delta V$>=-0.09m/s and <$\Delta D$>=0.52°
$\Delta D=D_{sensor}-D_t-<X_{off}>$ (°)
$\Delta V=V_{sensor}-V_t$ (m/s)
$D_t$ (°)

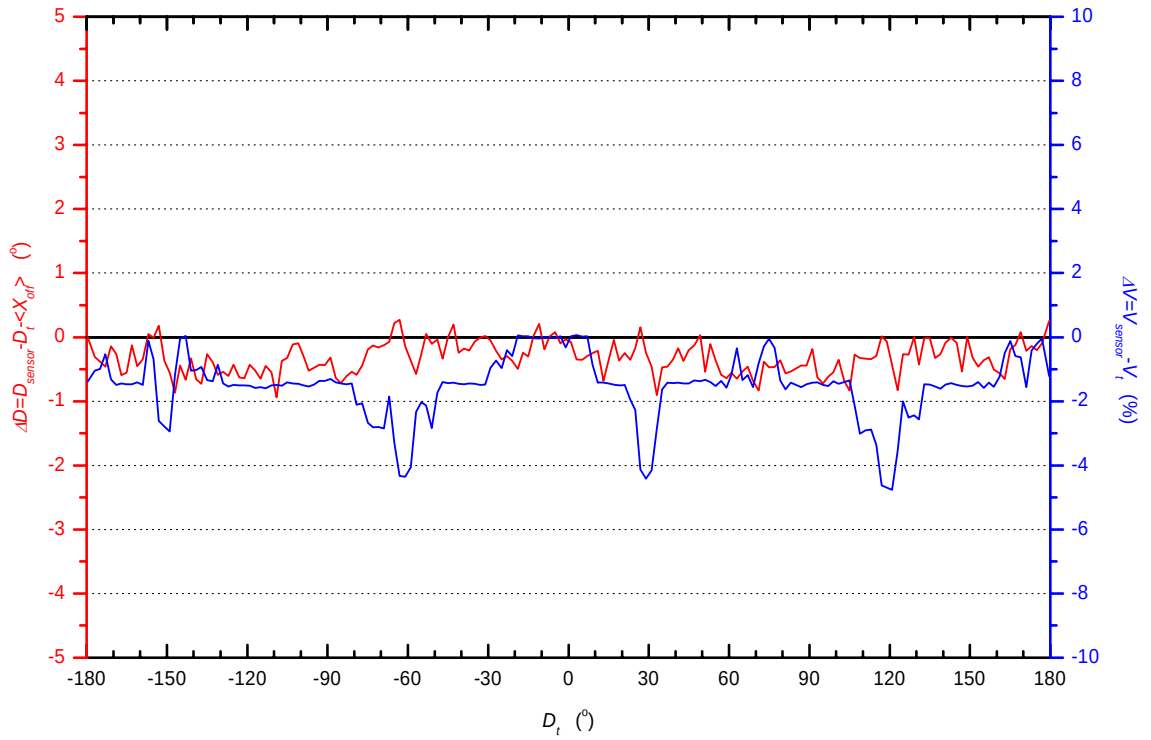
Binned DNW-LST results of Thies at <$V_t$>=7m/s with <$X_{off}$>=61.91°, <$\Delta V$>=-0.11m/s and <$\Delta D$>=-0.32°
$\Delta D=D_{sensor}-D_t-<X_{off}>$ (°)
$\Delta V=V_{sensor}-V_t$ (%)
$D_t$ (°)

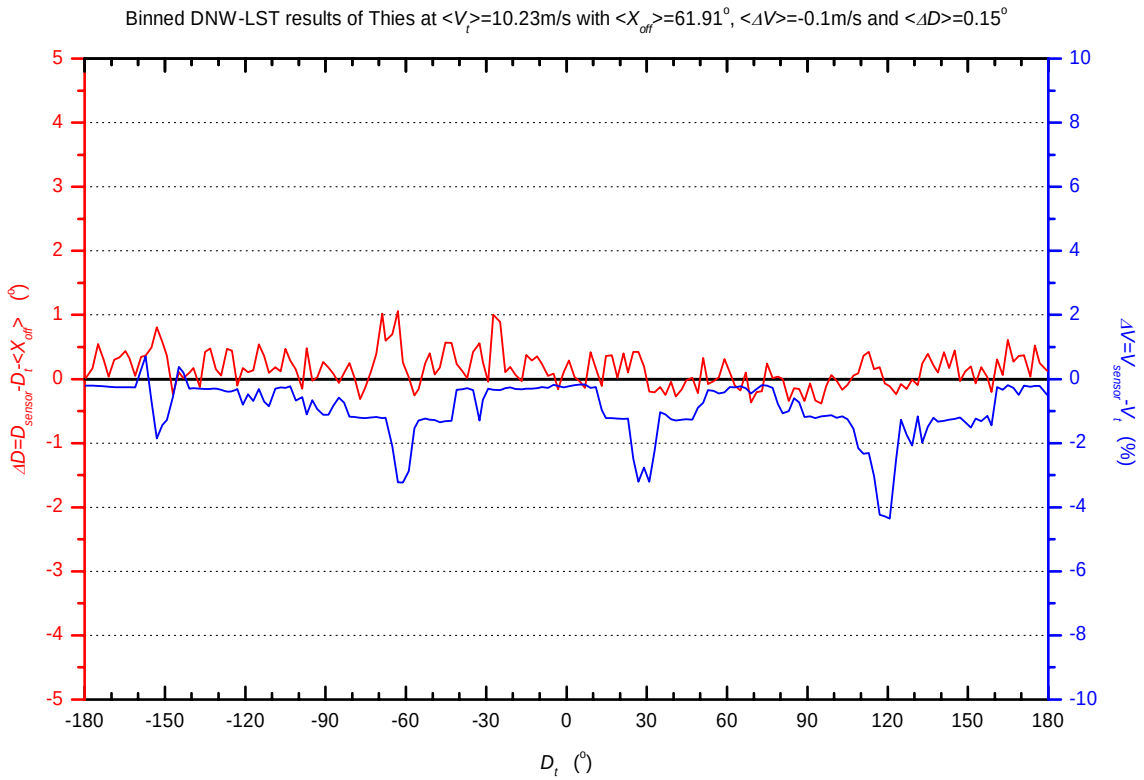
Binned DNW-LST results of Thies at <$V_t$>=10.23m/s with <$X_{off}$>=61.91°, <$\Delta V$>=-0.1m/s and <$\Delta D$>=0.15°
$\Delta D=D_{sensor}-D_t-<X_{off}>$ (°)
$\Delta V=V_{sensor}-V_t$ (%)
$D_t$ (°)

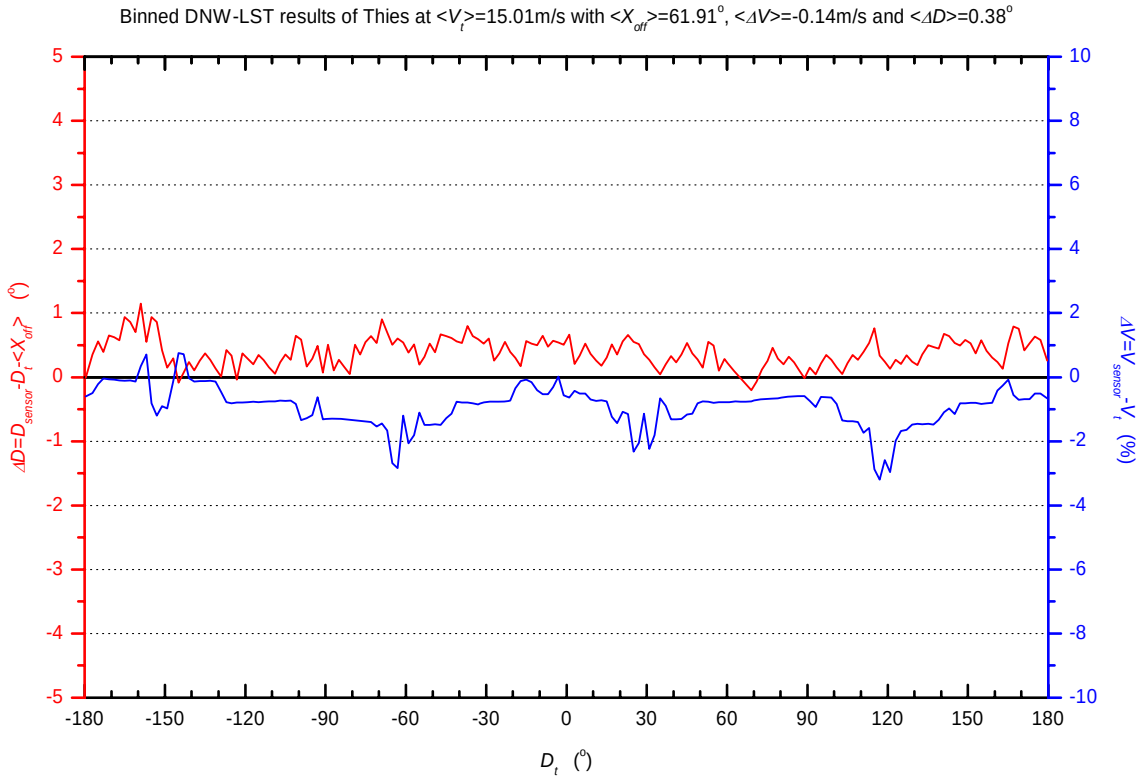
Binned DNW-LST results of Thies at <$V_t$>=15.01m/s with <$X_{off}$>=61.91°, <$\Delta V$>=-0.14m/s and <$\Delta D$>=0.38°
$\Delta D=D_{sensor}-D_t-<X_{off}>$ (°)
$\Delta V=V_{sensor}-V_t$ (%)
$D_t$ (°)

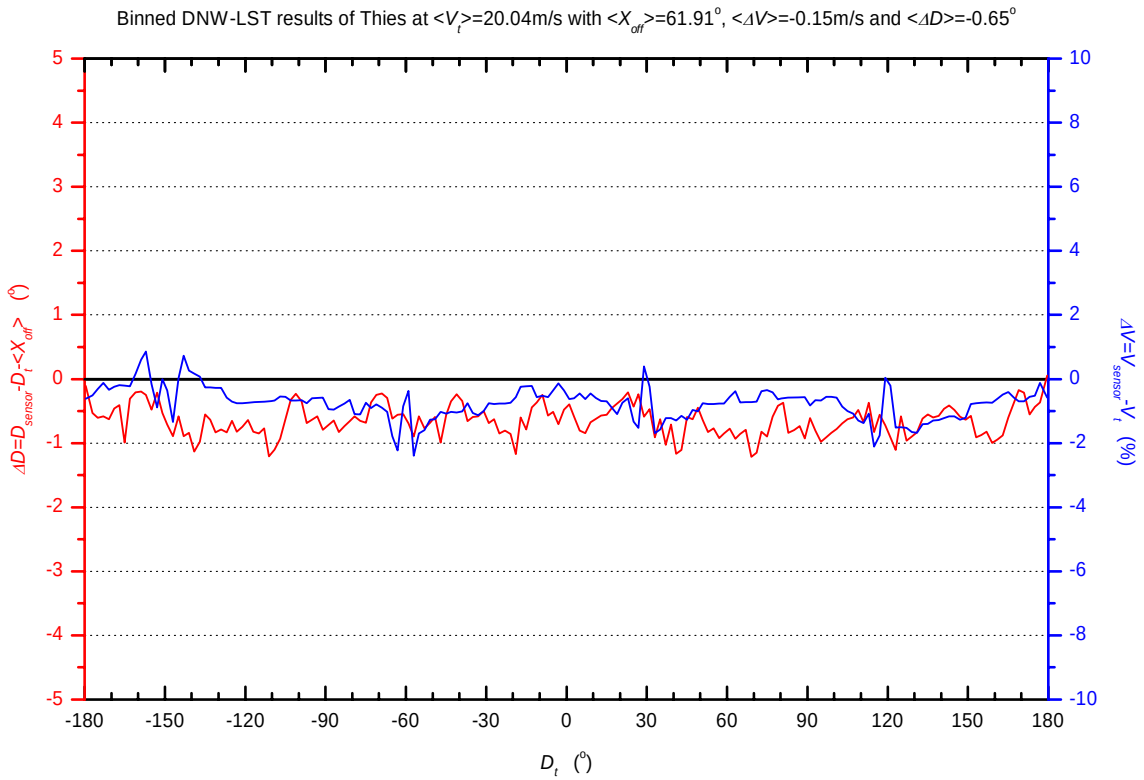
Binned DNW-LST results of Thies at <$V_t$>=20.04m/s with <$X_{off}$>=61.91°, <$\Delta V$>=-0.15m/s and <$\Delta D$>=-0.65°
$\Delta D=D_{sensor}-D_t-<X_{off}>$ (°)
$\Delta V=V_{sensor}-V_t$ (%)
$D_t$ (°)

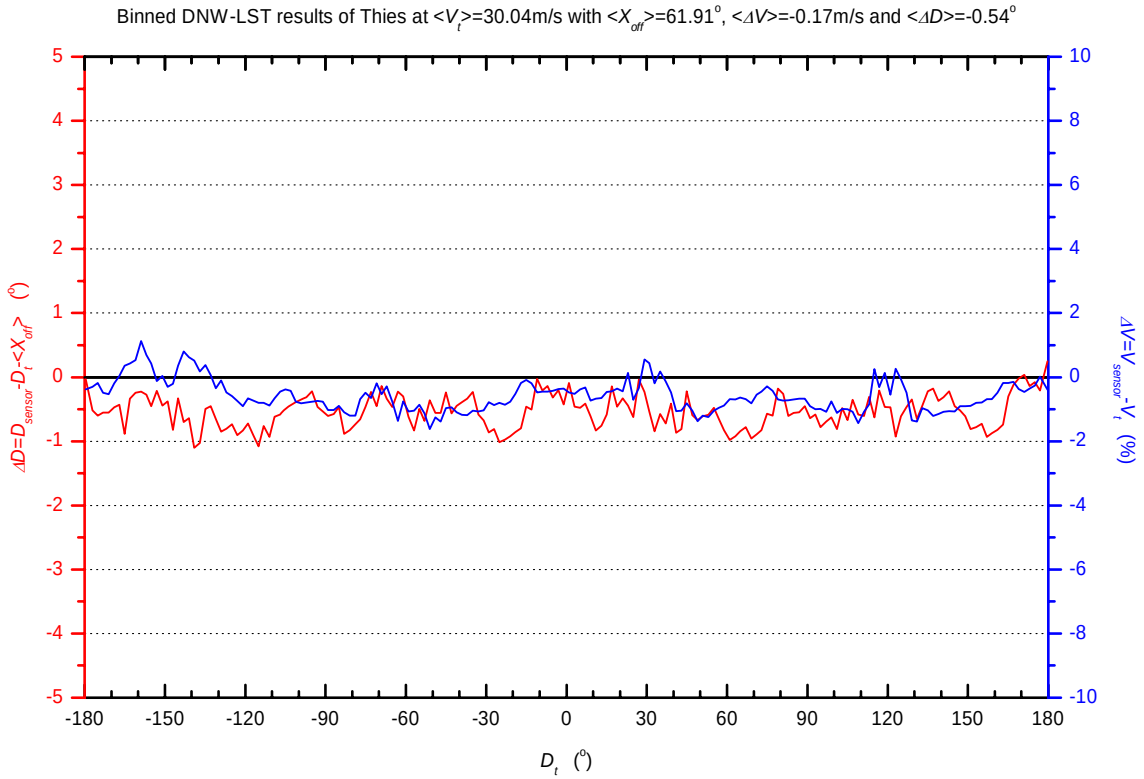
Binned DNW-LST results of Thies at <$V_t$>=30.04m/s with <$X_{off}$>=61.91°, <$\Delta V$>=-0.17m/s and <$\Delta D$>=-0.54°
$\Delta D=D_{sensor}-D_t-<X_{off}>$ (°)
$\Delta V=V_{sensor}-V_t$ (%)
$D_t$ (°)

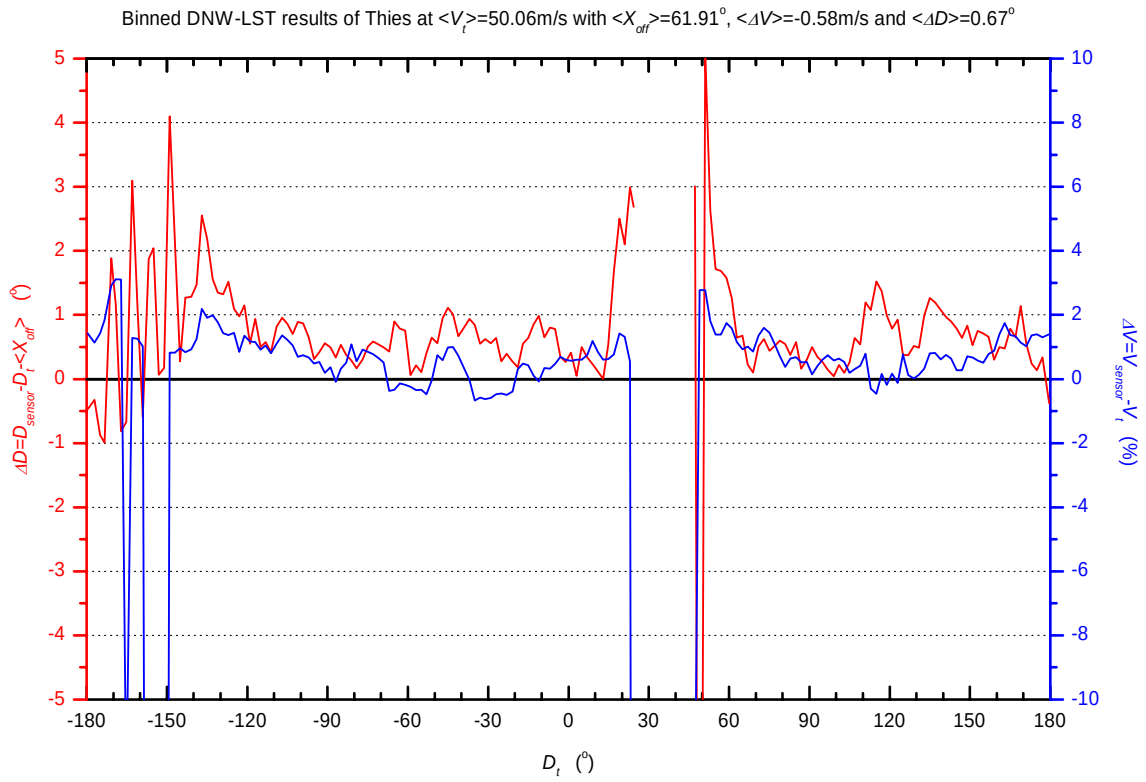
Binned DNW-LST results of Thies at <$V_t$>=50.06m/s with <$X_{off}$>=61.91°, <$\Delta V$>=-0.58m/s and <$\Delta D$>=0.67°
$\Delta D=D_{sensor}-D_t-<X_{off}>$ (°)
$\Delta V=V_{sensor}-V_t$ (%)
$D_t$ (°)
5
4
3
2
1
0
-1
-2
-3
-4
-5
10
8
6
4
2
0
-2
-4
-6
-8
-10
-180
-150
-120
-90
-60
-30
0
30
60
90
120
150
180

## *Vaisala sonic anemometer*

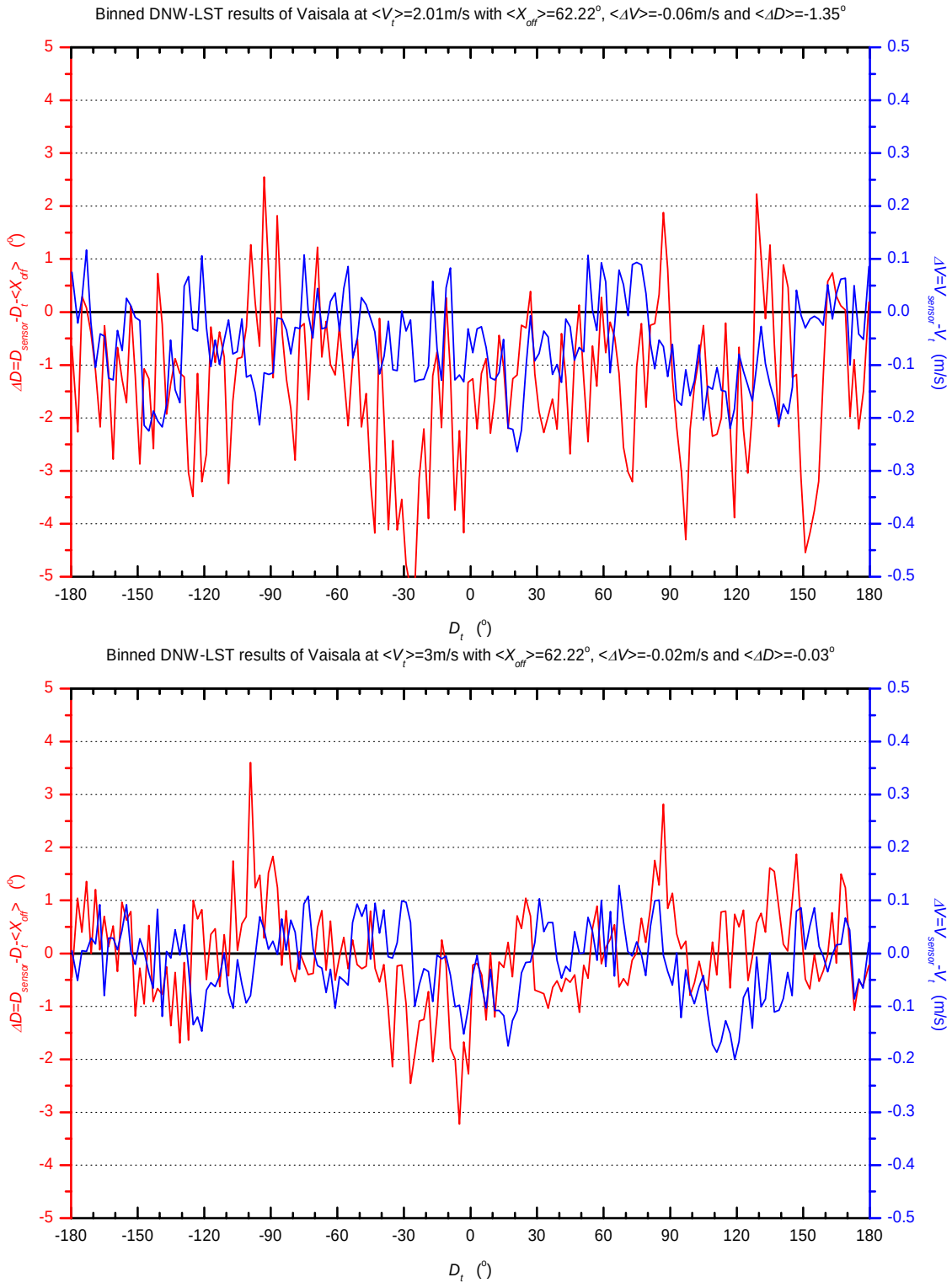

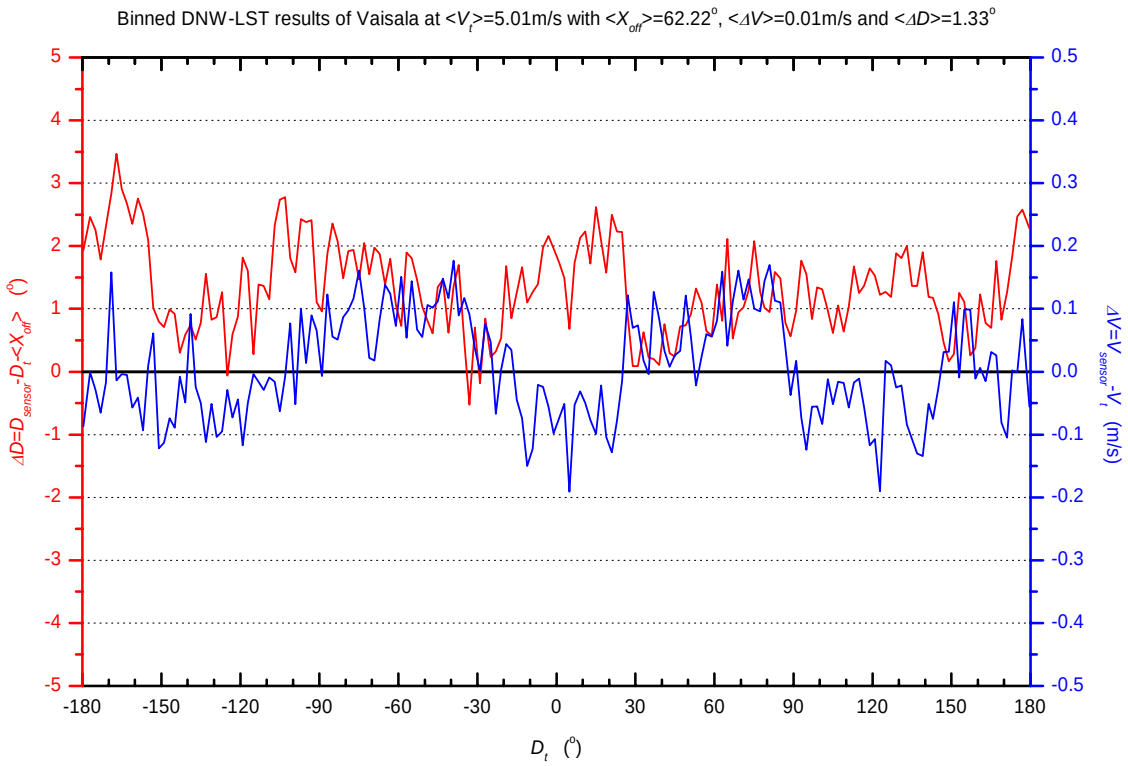
Binned DNW-LST results of Vaisala at <$V_t$>=5.01m/s with <$X_{off}$>=62.22°, <$\Delta V$>=0.01m/s and <$\Delta D$>=1.33°
$\Delta D=D_{sensor}-D_t-<X_{off}>$ (°)
$\Delta V=V_{sensor}-V_t$ (m/s)
$D_t$ (°)

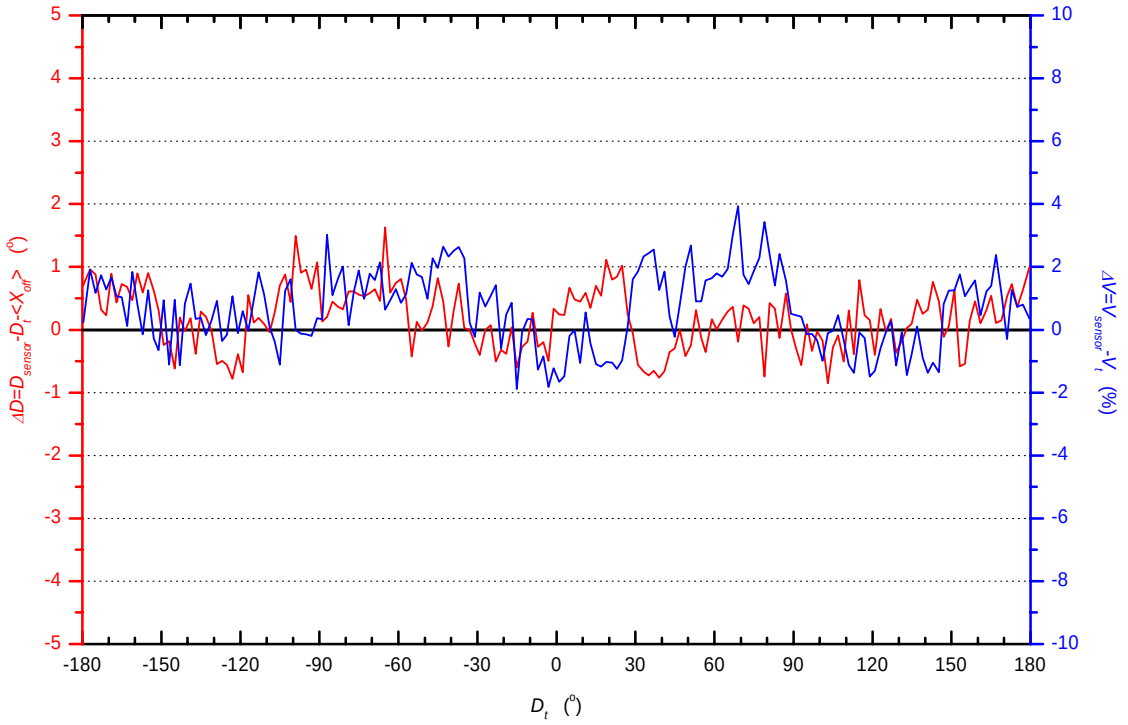
Binned DNW-LST results of Vaisala at <$V_t$>=7.03m/s with <$X_{off}$>=62.22°, <$\Delta V$>=0.05m/s and <$\Delta D$>=0.18°
$\Delta D=D_{sensor}-D_t-<X_{off}>$ (°)
$\Delta V=V_{sensor}-V_t$ (%)
$D_t$ (°)

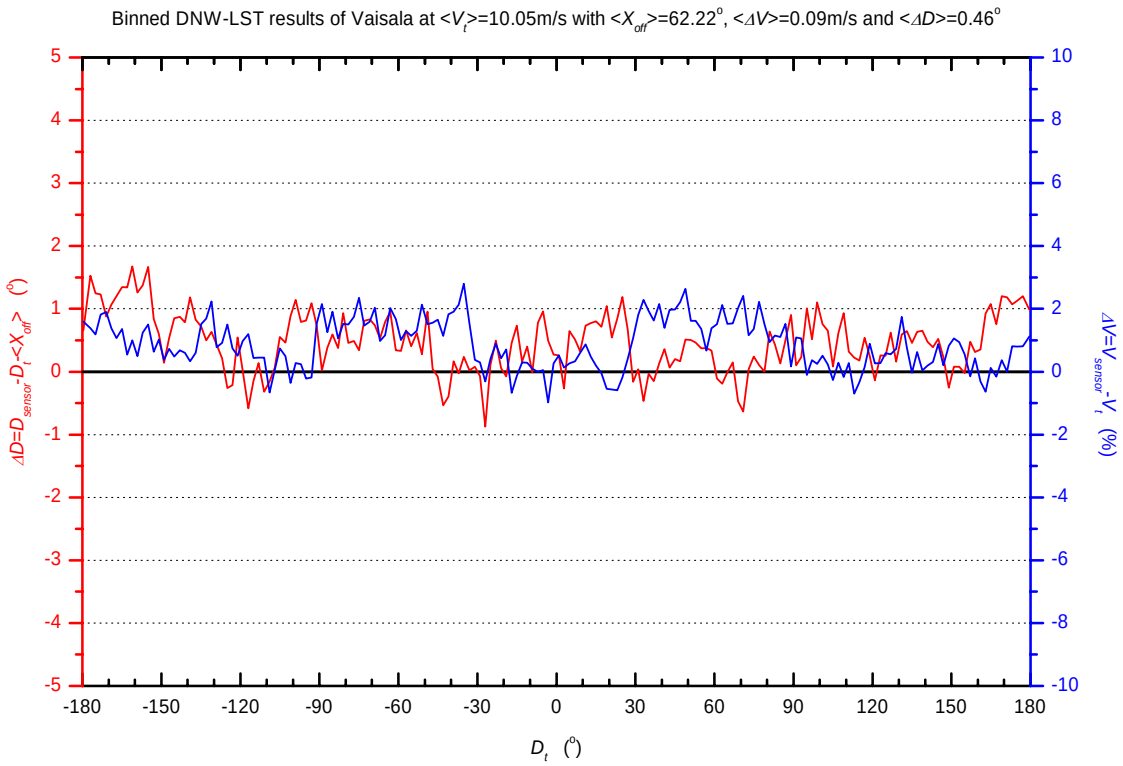
Binned DNW-LST results of Vaisala at <$V_t$>=10.05m/s with <$X_{off}$>=62.22°, <$\Delta V$>=0.09m/s and <$\Delta D$>=0.46°
$\Delta D=D_{sensor}-D_t-<X_{off}>$ (°)
$\Delta V=V_{sensor}-V_t$ (%)
$D_t$ (°)

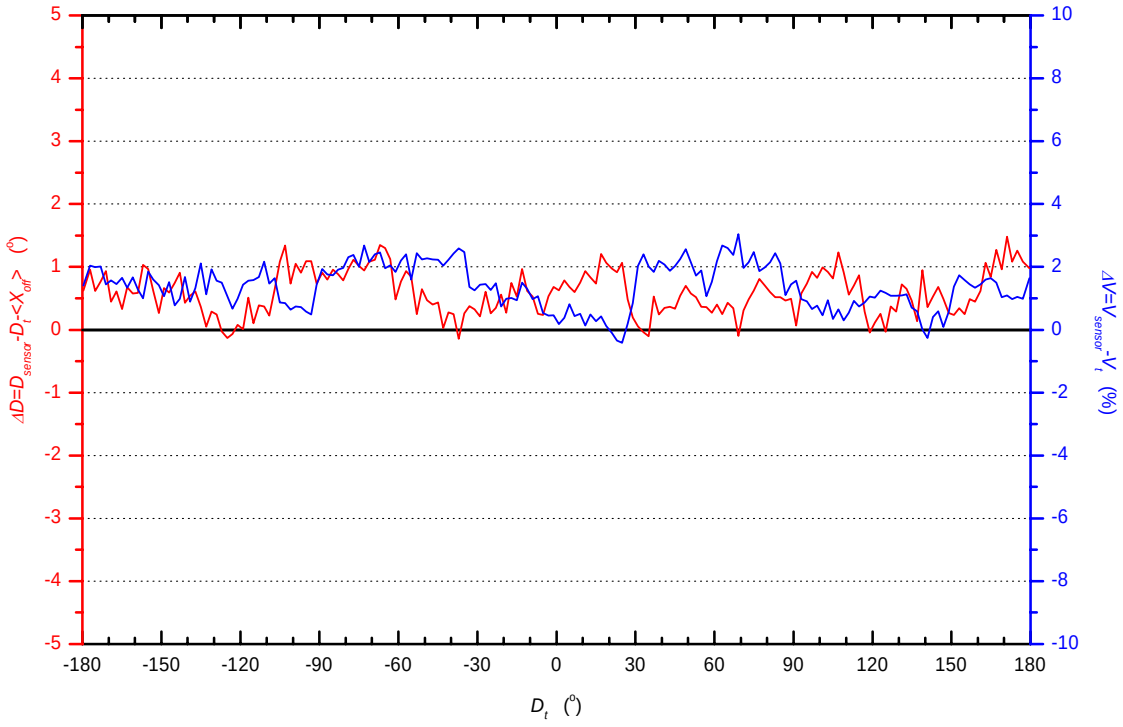
Binned DNW-LST results of Vaisala at <$V_t$>=15.03m/s with <$X_{off}$>=62.22°, <$\Delta V$>=0.21m/s and <$\Delta D$>=0.59°
$\Delta D=D_{sensor}-D_t-<X_{off}>$ (°)
$\Delta V=V_{sensor}-V_t$ (%)
$D_t$ (°)

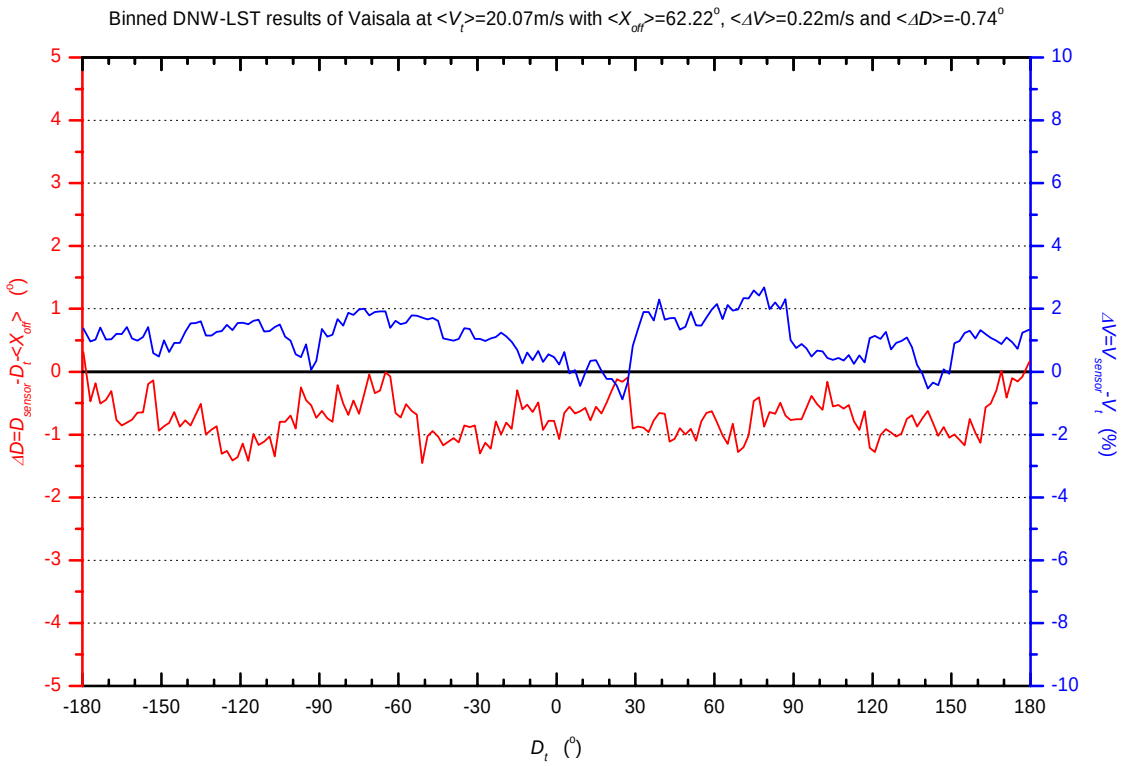
Binned DNW-LST results of Vaisala at <$V_t$>=20.07m/s with <$X_{off}$>=62.22°, <$\Delta V$>=0.22m/s and <$\Delta D$>=-0.74°
$\Delta D=D_{sensor}-D_t-<X_{off}>$ (°)
$\Delta V=V_{sensor}-V_t$ (%)
$D_t$ (°)

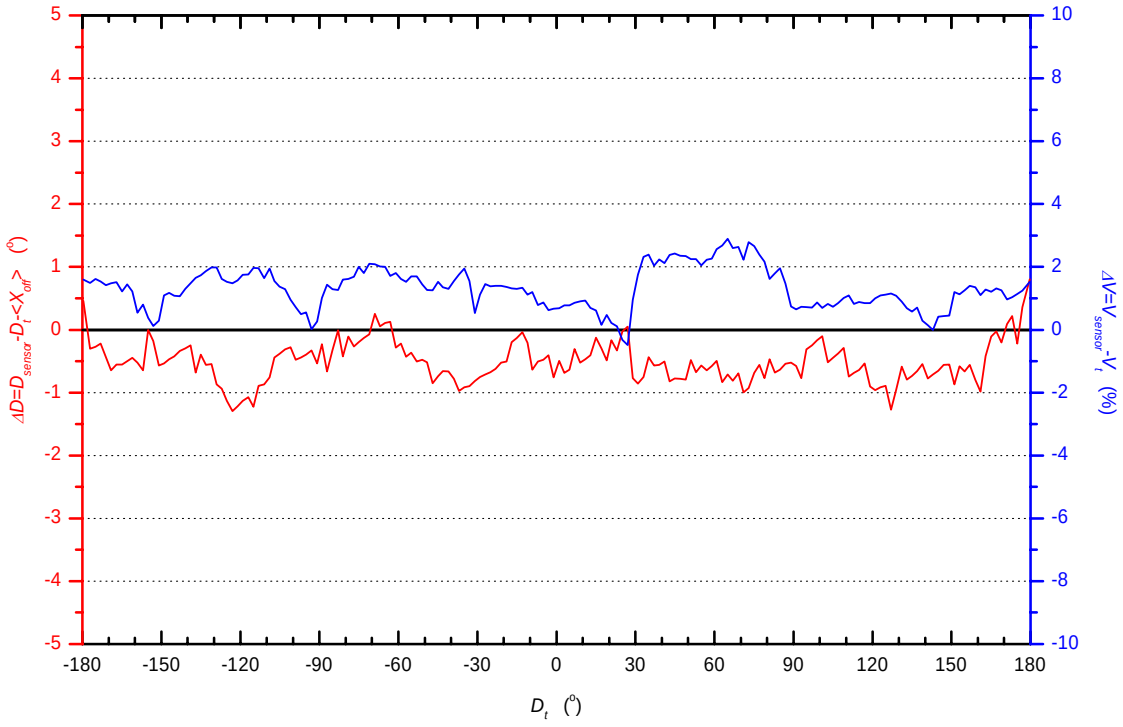
Binned DNW-LST results of Vaisala at <$V_t$>=30.04m/s with <$X_{off}$>=62.22°, <$\Delta V$>=0.4m/s and <$\Delta D$>=-0.51°
$\Delta D=D_{sensor}-D_t-<X_{off}>$ (°)
$\Delta V=V_{sensor}-V_t$ (%)
$D_t$ (°)

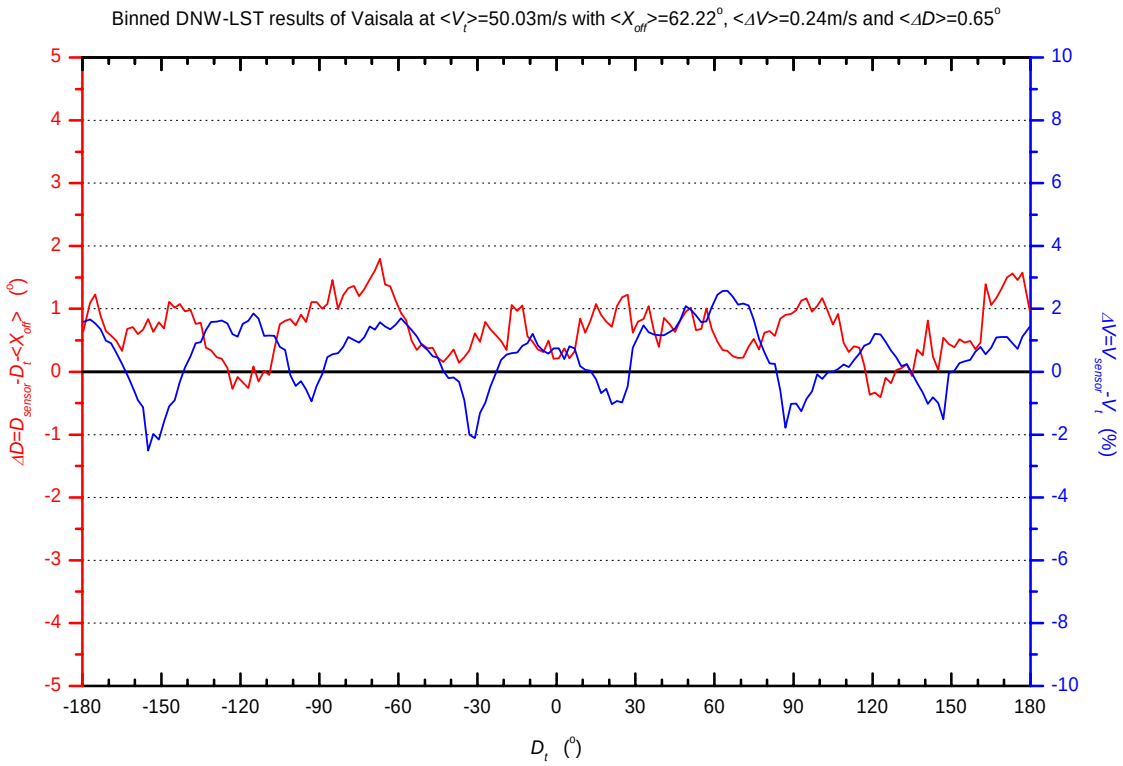
Binned DNW-LST results of Vaisala at <$V_t$>=50.03m/s with <$X_{off}$>=62.22°, <$\Delta V$>=0.24m/s and <$\Delta D$>=0.65°
$\Delta D=D_{sensor}-D_t-<X_{off}>$ (°)
$\Delta V=V_{sensor}-V_t$ (%)
$D_t$ (°)

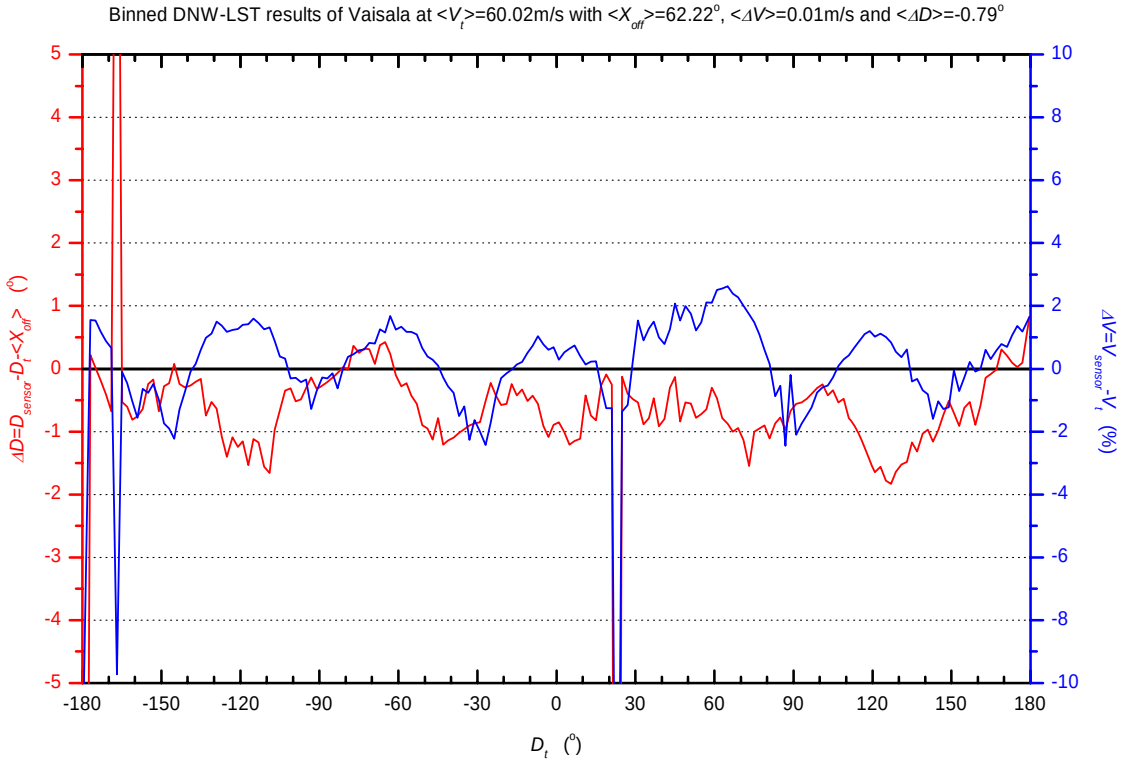
Binned DNW-LST results of Vaisala at <$V_t$>=60.02m/s with <$X_{off}$>=62.22°, <$\Delta V$>=0.01m/s and <$\Delta D$>=-0.79°
$\Delta D=D_{sensor}-D_t-<X_{off}>$ (°)
$\Delta V=V_{sensor}-V_t$ (%)
$D_t$ (°)

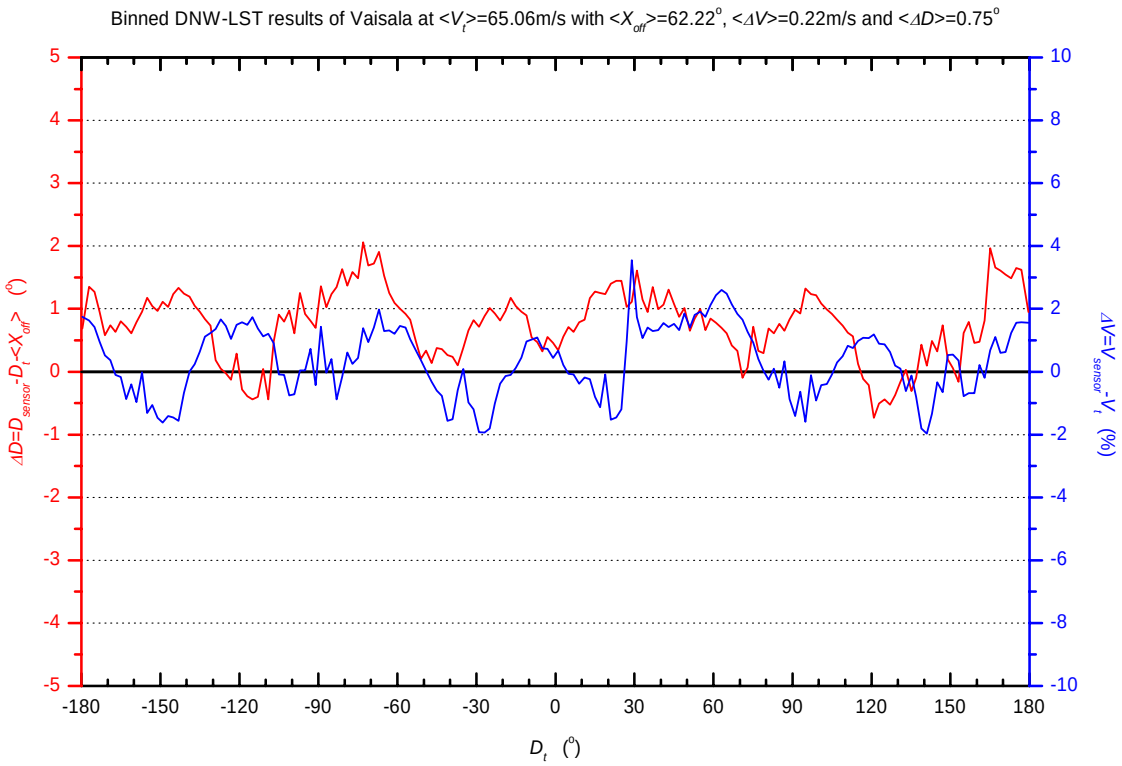
Binned DNW-LST results of Vaisala at <$V_t$>=65.06m/s with <$X_{off}$>=62.22°, <$\Delta V$>=0.22m/s and <$\Delta D$>=0.75°
$\Delta D=D_{sensor}-D_t-<X_{off}>$ (°)
$\Delta V=V_{sensor}-V_t$ (%)
$D_t$ (°)
5
4
3
2
1
0
-1
-2
-3
-4
-5
10
8
6
4
2
0
-2
-4
-6
-8
-10
-180
-150
-120
-90
-60
-30
0
30
60
90
120
150
180

# Appendix B1: Overview KNMI wind tunnel results

The table below gives an overview of the azimuth-averaged results of the KNMI wind tunnel measurements. See section 4.2 for details.

| *Date* | *Sensor* | $V_{tunnel}$ | *Azimuth*[2] | $<V_t>$ | $<\Delta V>$ | $<WR_{off}>$ | $<\Delta D>$[3] | # | *Comment* |
|---|---|---|---|---|---|---|---|---|---|
| 031201 | Vaisala | 2 | -180,5,180 | 2.10 | 0.11 | 177.8 | 0.46 | 5 | 5 of 365 missing |
| 031201 | Vaisala | 5 | -180,5,180 | 5.10 | 0.19 | 177.0 | -0.34 | 5 | |
| 031201 | Vaisala | 10 | -180,5,180 | 9.93 | 0.35 | 177.2 | -0.14 | 5 | 2 of 365 missing |
| 031201 | Vaisala | 20 | -180,5,180 | 20.20 | 0.66 | 177.5 | 0.16 | 5 | 1 of 365 missing |
| 031201 | Vaisala | 15 | -180,5,180 | 14.92 | 0.52 | 177.5 | 0.16 | 5 | 1 of 365 missing |
| 031201 | Vaisala | 7 | -180,5,180 | 7.07 | 0.22 | 177.3 | -0.04 | 5 | 4 of 365 missing |
| 031201 | Vaisala | 3 | -180,5,180 | 3.01 | 0.09 | 177.1 | -0.24 | 5 | |
| 031201 | Vaisala | 1 | -180,5,180 | 1.06 | -0.03 | 177.3 | -0.04 | 5 | |
| 031201 | Vaisala | 5 | -180,2,180 | 5.10 | 0.18 | 177.4 | 0.06 | 5 | |
| 031201 | Gill | 2 | -180,5,180 | 1.98 | 0.05 | 176.8 | -0.04 | 5 | |
| 031202 | Gill | 5 | -180,5,180 | 4.94 | 0.02 | 176.8 | -0.04 | 5 | |
| 031202 | Gill | 10 | -180,5,180 | 9.99 | -0.09 | 176.9 | 0.06 | 5 | |
| 031202 | Gill | 20 | -180,5,180 | 20.25 | 0.05 | 176.9 | 0.06 | 5 | |
| 031202 | Gill | 15 | -180,5,180 | 14.98 | 0.00 | 176.9 | 0.06 | 5 | |
| 031202 | Gill | 7 | -180,5,180 | 7.03 | -0.09 | 176.9 | 0.06 | 5 | |
| 031202 | Gill | 3 | -180,5,180 | 2.98 | 0.05 | 176.8 | -0.04 | 5 | |
| 031202 | Gill | 1 | -180,5,180 | 0.96 | -0.01 | 176.7 | -0.14 | 5 | |
| 031201 | Gill | 5 | -180,2,180 | 5.11 | 0.03 | 176.9 | 0.06 | 5 | |
| 031202 | Thies | 2 | -180,5,180 | 2.06 | -0.02 | 177.0 | 0.01 | 5 | |
| 031202 | Thies | 5 | -180,5,180 | 5.01 | -0.02 | 177.0 | 0.01 | 5 | |
| 031202 | Thies | 10 | -180,5,180 | 10.05 | 0.02 | 177.0 | 0.01 | 5 | |
| 031202 | Thies | 20 | -180,5,180 | 20.16 | 0.04 | 177.0 | 0.01 | 5 | |
| 031202 | Thies | 15 | -180,5,180 | 14.91 | 0.07 | 177.0 | 0.01 | 5 | |

[2] Reported is the minimum, step and maximum azimuth angle of the rotation device.

[3] Note that $<\Delta D>$ is determined w.r.t. the sensor averaged offset for all tunnel speeds $<X_{off}>$ which is 176.99° for the Thies; 177.34° for the Vaisala; 176.84° for the Gill sonic anemometer.

| *Date* | *Sensor* | $V_{tunnel}$ | *Azimuth*[2] | $<V_t>$ | $<\Delta V>$ | $<WR_{off}>$ | $<\Delta D>$[3] | # | *Comment* |
|---|---|---|---|---|---|---|---|---|---|
| 031202 | Thies | 7 | -180,5,180 | 7.02 | -0.01 | 177.0 | 0.01 | 5 | |
| 031202 | Thies | 3 | -180,5,180 | 2.93 | -0.03 | 177.0 | 0.01 | 5 | |
| 031202 | Thies | 1 | -180,5,180 | 1.05 | -0.02 | 177.0 | 0.01 | 5 | |
| 031201 | Thies | 5 | -180,2,180 | 5.11 | -0.01 | 176.9 | -0.09 | 5 | |
| 031204 | Cup-133 | 2 | - | 1.90 | 0.00 | - | - | 11 | |
| 031204 | Cup-133 | 5 | - | 5.12 | 0.03 | - | - | 10 | |
| 031204 | Cup-133 | 10 | - | 10.22 | 0.06 | - | - | 10 | |
| 031204 | Cup-133 | 20 | - | 20.22 | 0.17 | - | - | 10 | |
| 031204 | Cup-133 | 15 | - | 15.21 | 0.20 | - | - | 10 | |
| 031204 | Cup-133 | 7 | - | 7.09 | 0.01 | - | - | 10 | |
| 031204 | Cup-133 | 3 | - | 3.09 | -0.01 | - | - | 10 | |
| 031204 | Cup-133 | 1 | - | 1.00 | 0.03 | - | - | 10 | |
| 031204 | Cup-115 | 2 | - | 1.89 | 0.00 | - | - | 10 | |
| 031204 | Cup-115 | 5 | - | 4.91 | 0.02 | - | - | 10 | |
| 031204 | Cup-115 | 10 | - | 10.23 | 0.09 | - | - | 10 | |
| 031204 | Cup-115 | 20 | - | 19.94 | 0.05 | - | - | 10 | |
| 031204 | Cup-115 | 15 | - | 15.21 | 0.09 | - | - | 10 | |
| 031204 | Cup-115 | 7 | - | 7.05 | 0.02 | - | - | 10 | |
| 031204 | Cup-115 | 3 | - | 3.11 | 0.00 | - | - | 10 | |
| 031204 | Cup-115 | 1 | - | 0.84 | 0.03 | - | - | 10 | |

# Appendix B2: KNMI wind tunnel measurements

In this appendix the averaged binned results of the 360° rotation test in the KNMI wind tunnel are presented for the Gill, Thies and Vaisala sonic anemometers with increasing tunnel speed. For that purpose 5 1-second sensor measurements and tunnel readings are averaged for each orietation of the rotation device and presented as a function of the azimuth angle $D_r$ of the turntable. The figures show for each sensor and tunnel speed the angular dependence of the differerences between sensor wind speed and the tunnel value ($WS_{sensor}$-$WS_{tunnel}$) and the diffference between the sensor wind direction and the turntable reference value compensated for the offset of the sonic anemometer ($WR_{sensor}$-$WR_{tunnel}$-$WR_{offset}$). The full scale of the figures are fixed at the WMO accuracy requirements, i.e. ±5° for wind direction and ±0.5m/s or ±10% for wind speeds below and above 5m/s, respectively. Note that the results for the sonic anemometers obtained for a tunnel speed of 5m/s and an azimtuh step angle of 2° are given in section 4.2.

## *Gill sonic anemometer*

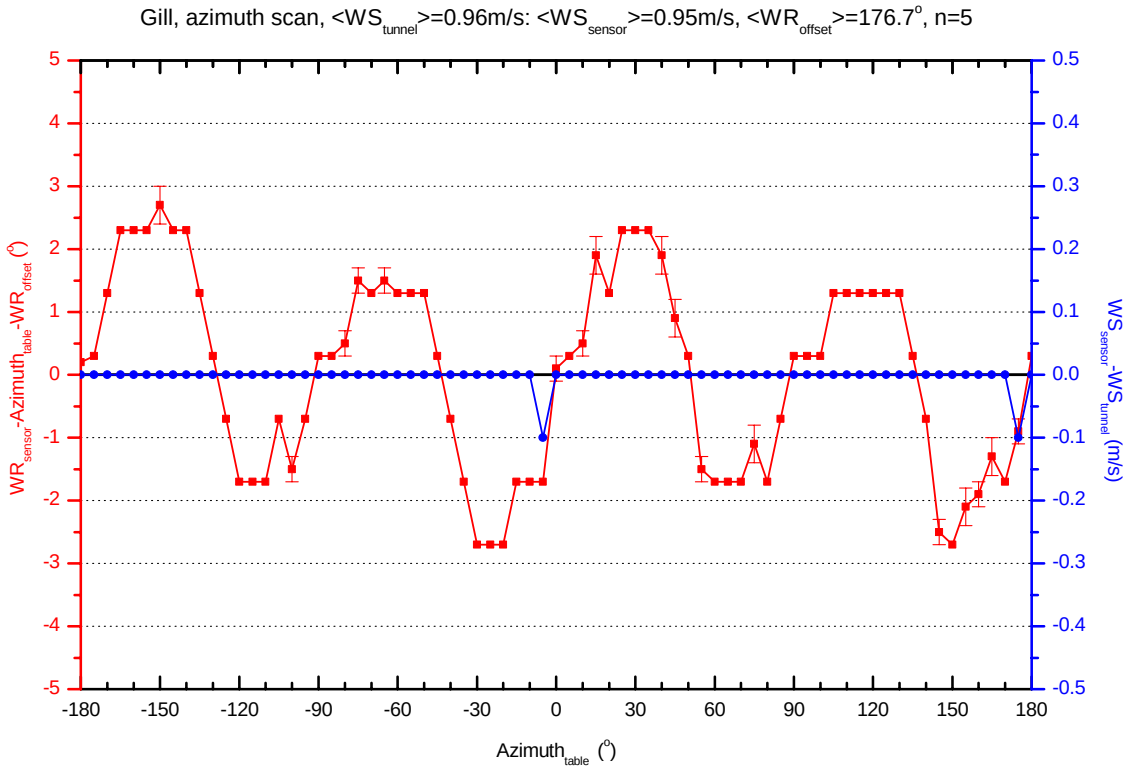

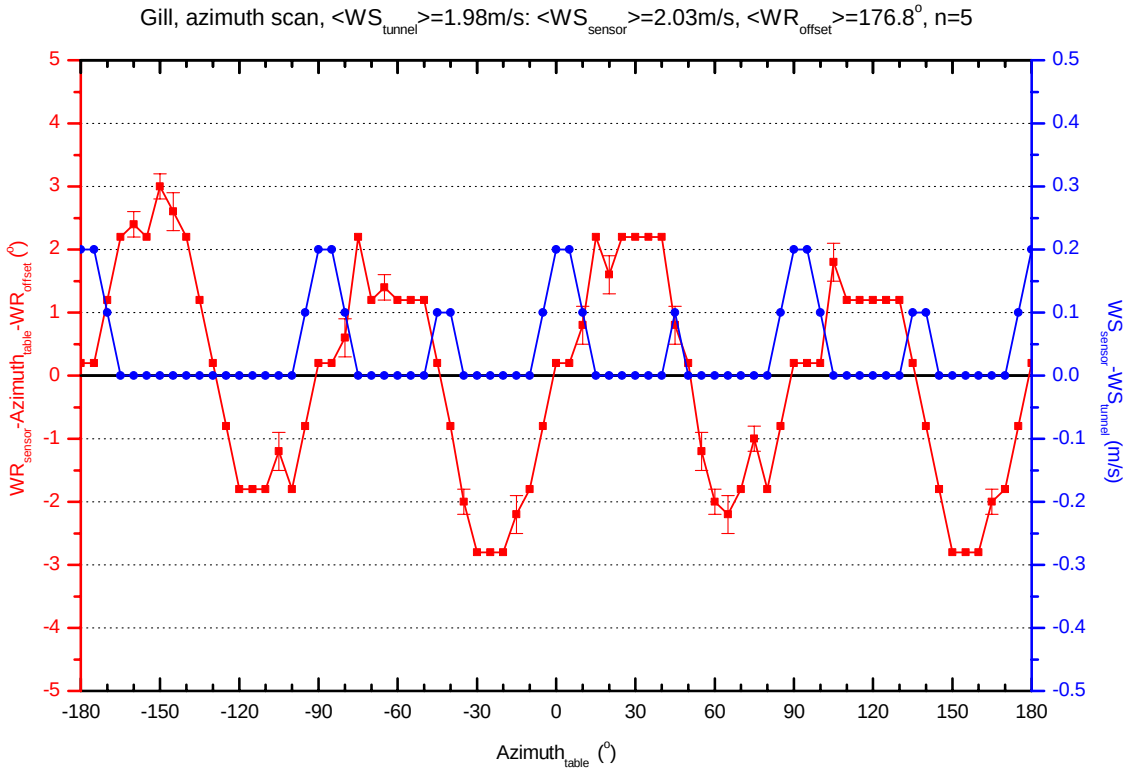
Gill, azimuth scan, <WS_tunnel>=1.98m/s: <WS_sensor>=2.03m/s, <WR_offset>=176.8°, n=5
WR_sensor-Azimuth_table-WR_offset (°)
WS_sensor-WS_tunnel (m/s)
Azimuth_table (°)
5
4
3
2
1
0
-1
-2
-3
-4
-5
0.5
0.4
0.3
0.2
0.1
0.0
-0.1
-0.2
-0.3
-0.4
-0.5
-180
-150
-120
-90
-60
-30
0
30
60
90
120
150
180

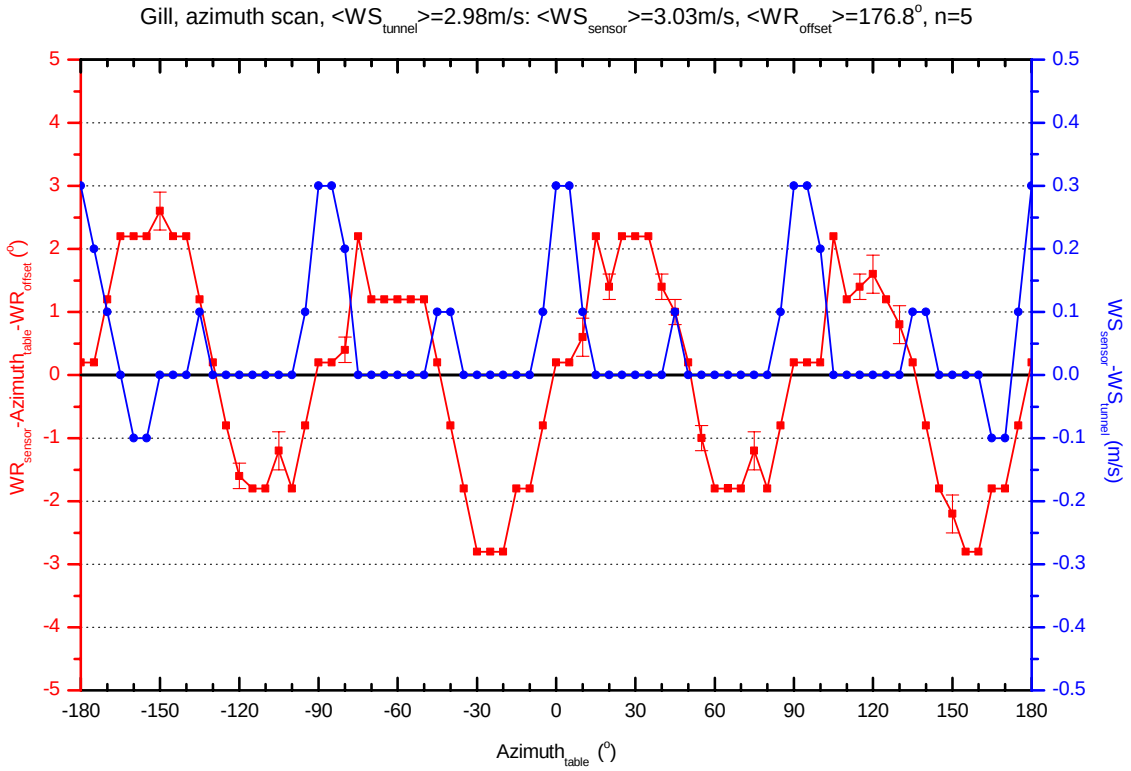
Gill, azimuth scan, <WS_tunnel>=2.98m/s: <WS_sensor>=3.03m/s, <WR_offset>=176.8°, n=5
WR_sensor-Azimuth_table-WR_offset (°)
WS_sensor-WS_tunnel (m/s)
Azimuth_table (°)
5
4
3
2
1
0
-1
-2
-3
-4
-5
0.5
0.4
0.3
0.2
0.1
0.0
-0.1
-0.2
-0.3
-0.4
-0.5
-180
-150
-120
-90
-60
-30
0
30
60
90
120
150
180

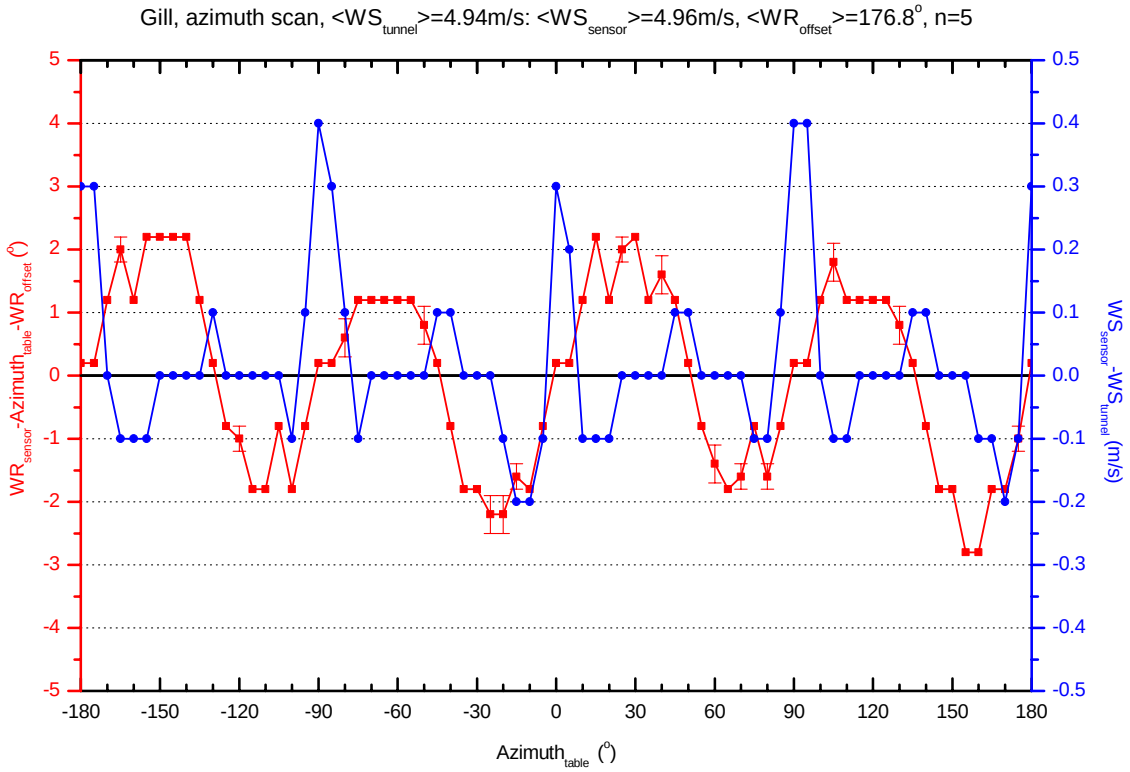
Gill, azimuth scan, <WS_tunnel>=4.94m/s: <WS_sensor>=4.96m/s, <WR_offset>=176.8°, n=5
WR_sensor-Azimuth_table-WR_offset (°)
WS_sensor-WS_tunnel (m/s)
Azimuth_table (°)

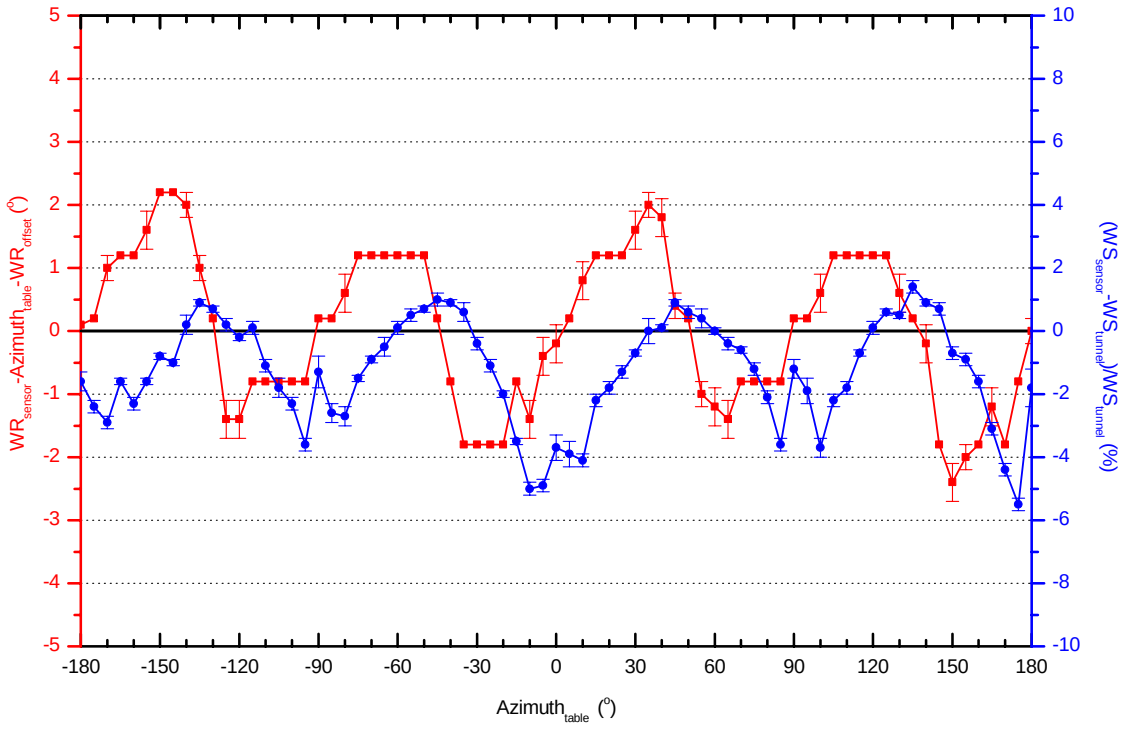
Gill, azimuth scan, <WS_tunnel>=7.03m/s: <WS_sensor>=6.94m/s, <WR_offset>=176.9°, n=5
WR_sensor-Azimuth_table-WR_offset (°)
(WS_sensor-WS_tunnel)/WS_tunnel (%)
Azimuth_table (°)

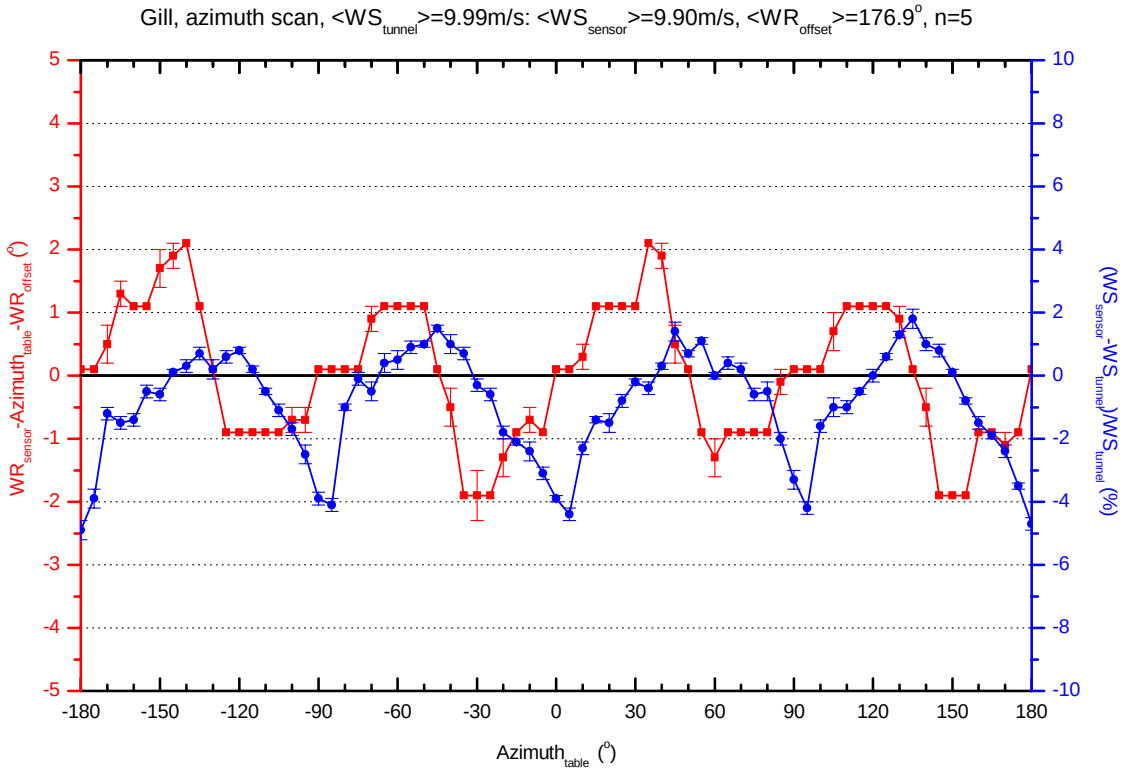
Gill, azimuth scan, <WS_tunnel>=9.99m/s: <WS_sensor>=9.90m/s, <WR_offset>=176.9°, n=5
WR_sensor-Azimuth_table-WR_offset (°)
(WS_sensor-WS_tunnel)/WS_tunnel (%)
Azimuth_table (°)
5
4
3
2
1
0
-1
-2
-3
-4
-5
10
8
6
4
2
0
-2
-4
-6
-8
-10
-180
-150
-120
-90
-60
-30
0
30
60
90
120
150
180

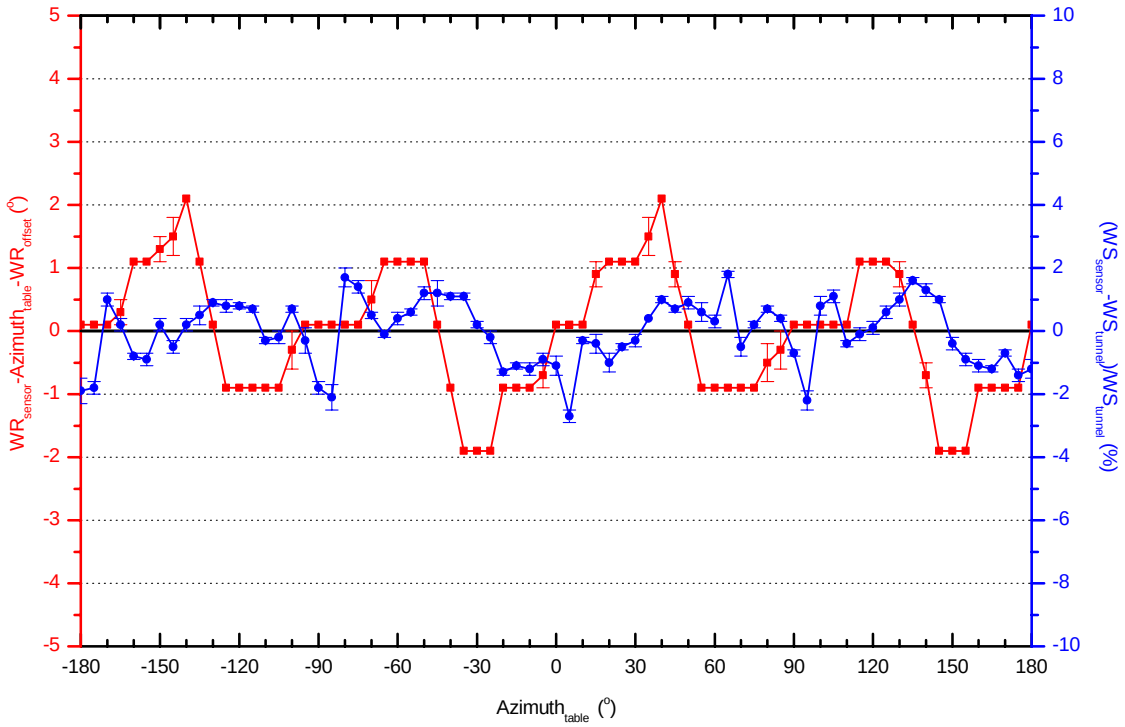
Gill, azimuth scan, <WS_tunnel>=14.98m/s: <WS_sensor>=14.98m/s, <WR_offset>=176.9°, n=5
WR_sensor-Azimuth_table-WR_offset (°)
(WS_sensor-WS_tunnel)/WS_tunnel (%)
Azimuth_table (°)
5
4
3
2
1
0
-1
-2
-3
-4
-5
10
8
6
4
2
0
-2
-4
-6
-8
-10
-180
-150
-120
-90
-60
-30
0
30
60
90
120
150
180

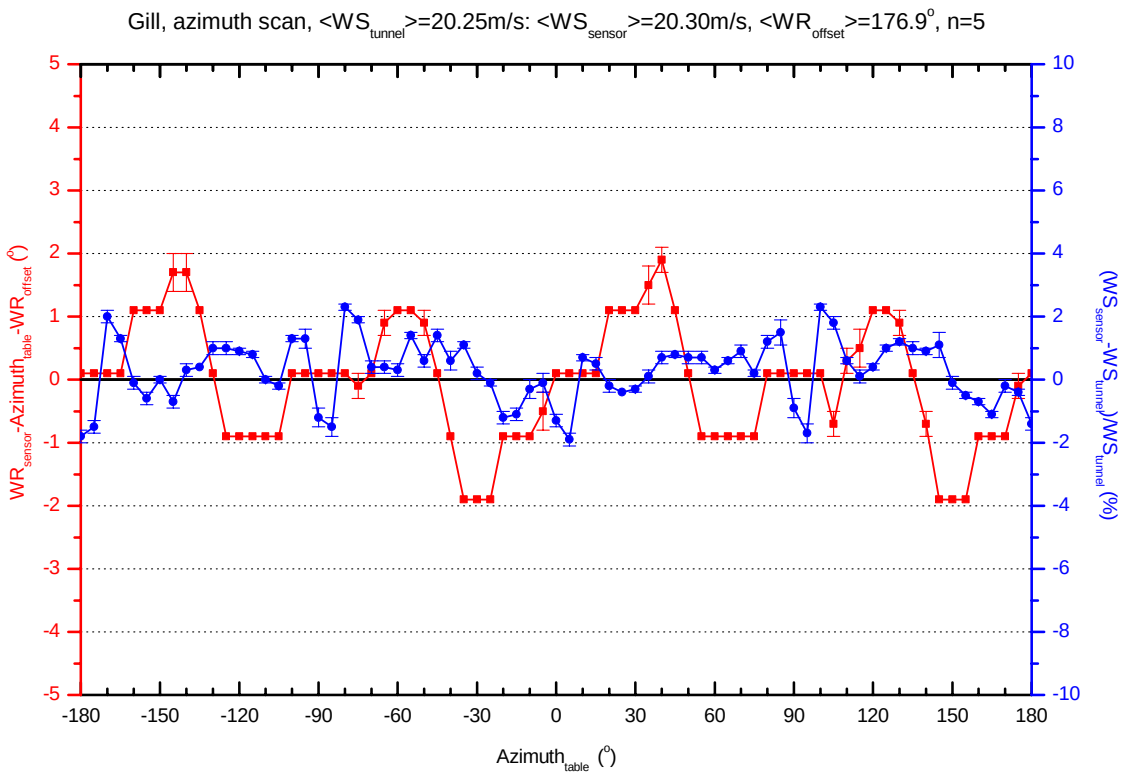
Gill, azimuth scan, <WS_tunnel>=20.25m/s: <WS_sensor>=20.30m/s, <WR_offset>=176.9°, n=5
WR_sensor-Azimuth_table-WR_offset (°)
(WS_sensor-WS_tunnel)/WS_tunnel (%)
Azimuth_table (°)
5
4
3
2
1
0
-1
-2
-3
-4
-5
10
8
6
4
2
0
-2
-4
-6
-8
-10
-180
-150
-120
-90
-60
-30
0
30
60
90
120
150
180

## *Thies sonic anemometer*

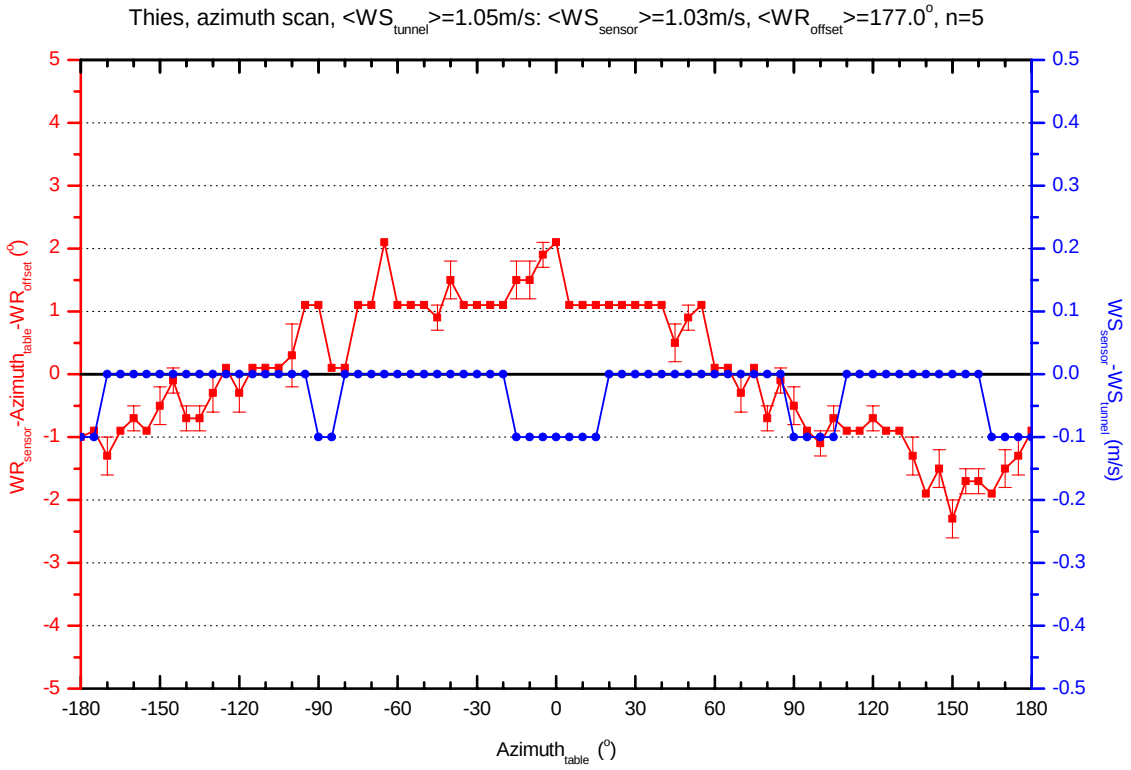


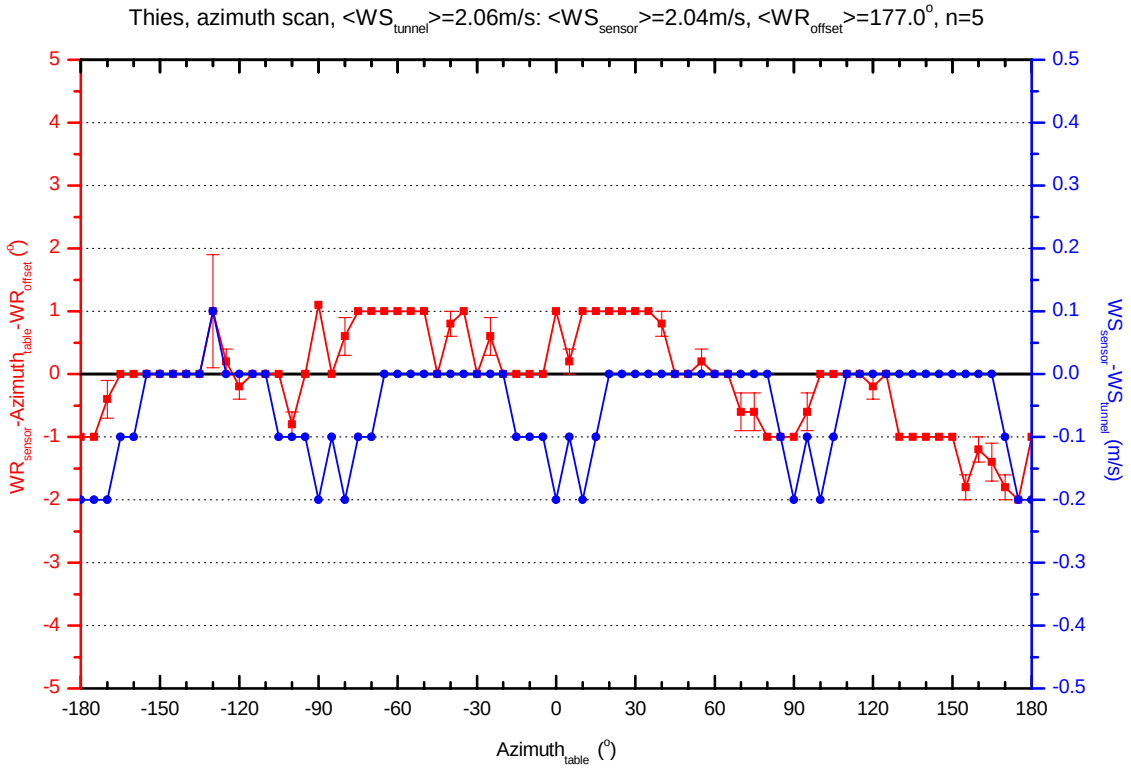

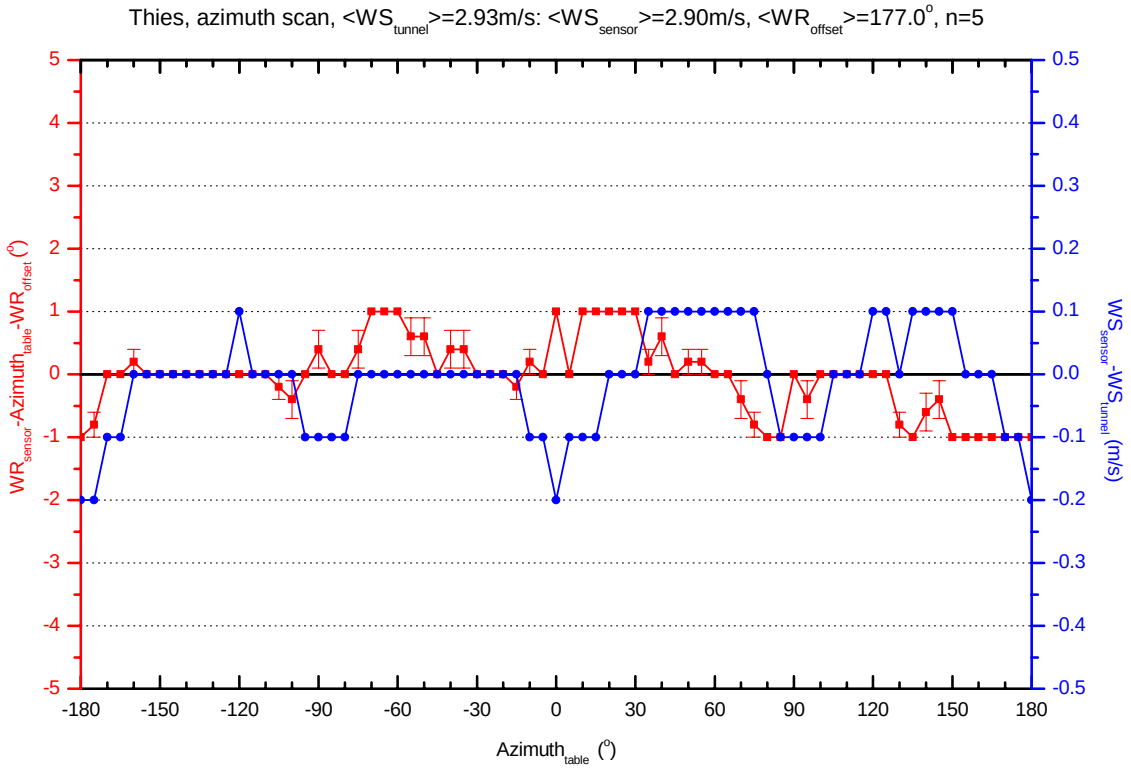
Thies, azimuth scan, <WS_tunnel>=2.93m/s: <WS_sensor>=2.90m/s, <WR_offset>=177.0°, n=5
WR_sensor-Azimuth_table-WR_offset (°)
WS_sensor-WS_tunnel (m/s)
Azimuth_table (°)
5
4
3
2
1
0
-1
-2
-3
-4
-5
0.5
0.4
0.3
0.2
0.1
0.0
-0.1
-0.2
-0.3
-0.4
-0.5
-180
-150
-120
-90
-60
-30
0
30
60
90
120
150
180

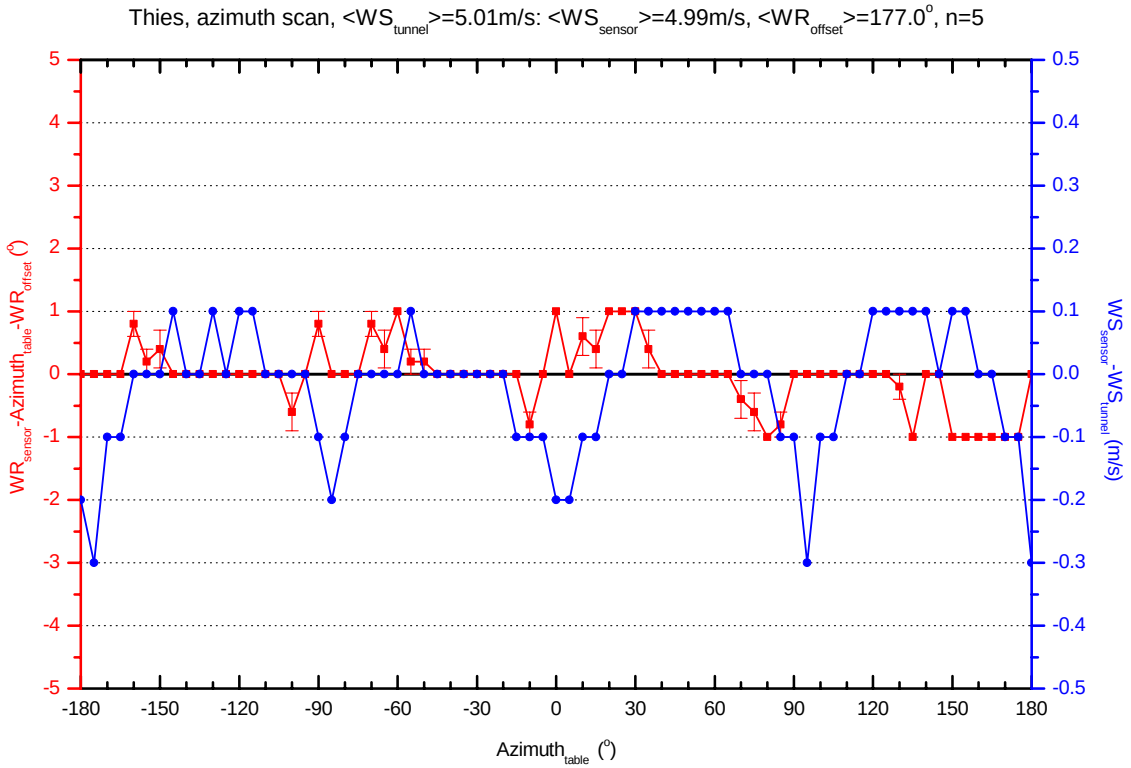
Thies, azimuth scan, <WS_tunnel>=5.01m/s: <WS_sensor>=4.99m/s, <WR_offset>=177.0°, n=5
WR_sensor-Azimuth_table-WR_offset (°)
WS_sensor-WS_tunnel (m/s)
Azimuth_table (°)
5
4
3
2
1
0
-1
-2
-3
-4
-5
0.5
0.4
0.3
0.2
0.1
0.0
-0.1
-0.2
-0.3
-0.4
-0.5
-180
-150
-120
-90
-60
-30
0
30
60
90
120
150
180

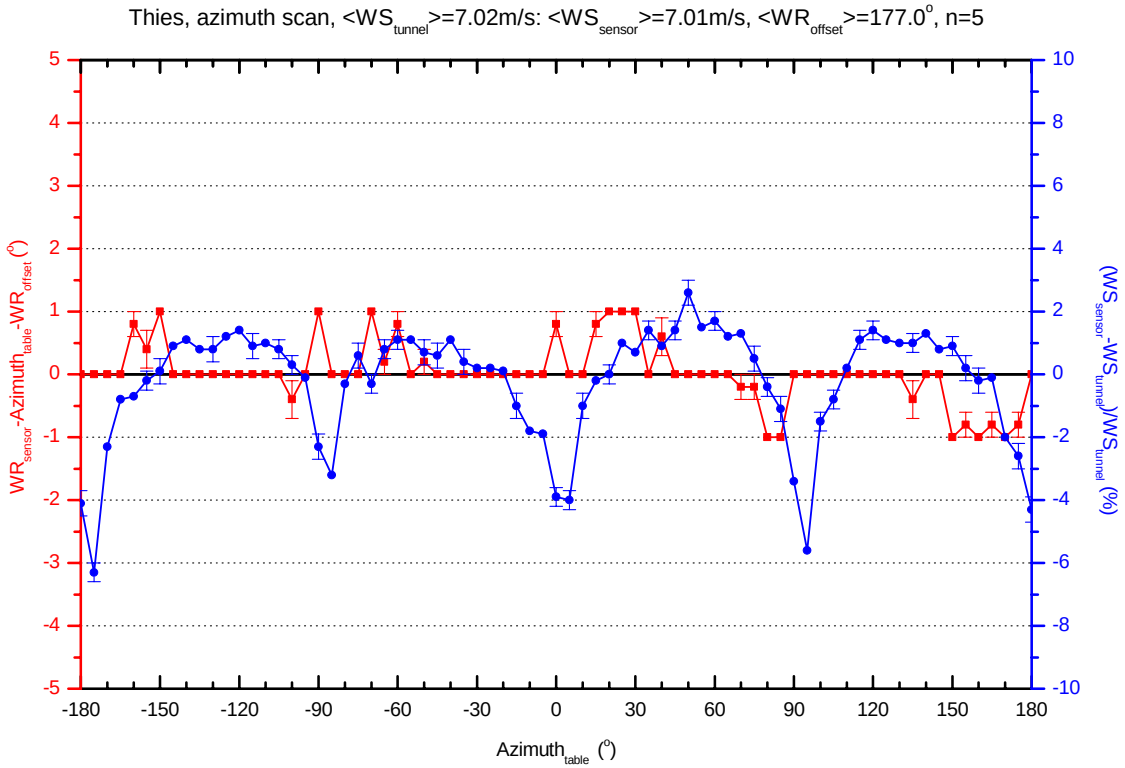
Thies, azimuth scan, <WS$_{tunnel}$>=7.02m/s: <WS$_{sensor}$>=7.01m/s, <WR$_{offset}$>=177.0°, n=5
WR$_{sensor}$-Azimuth$_{table}$-WR$_{offset}$ (°)
(WS$_{sensor}$-WS$_{tunnel}$)/WS$_{tunnel}$ (%)
Azimuth$_{table}$ (°)

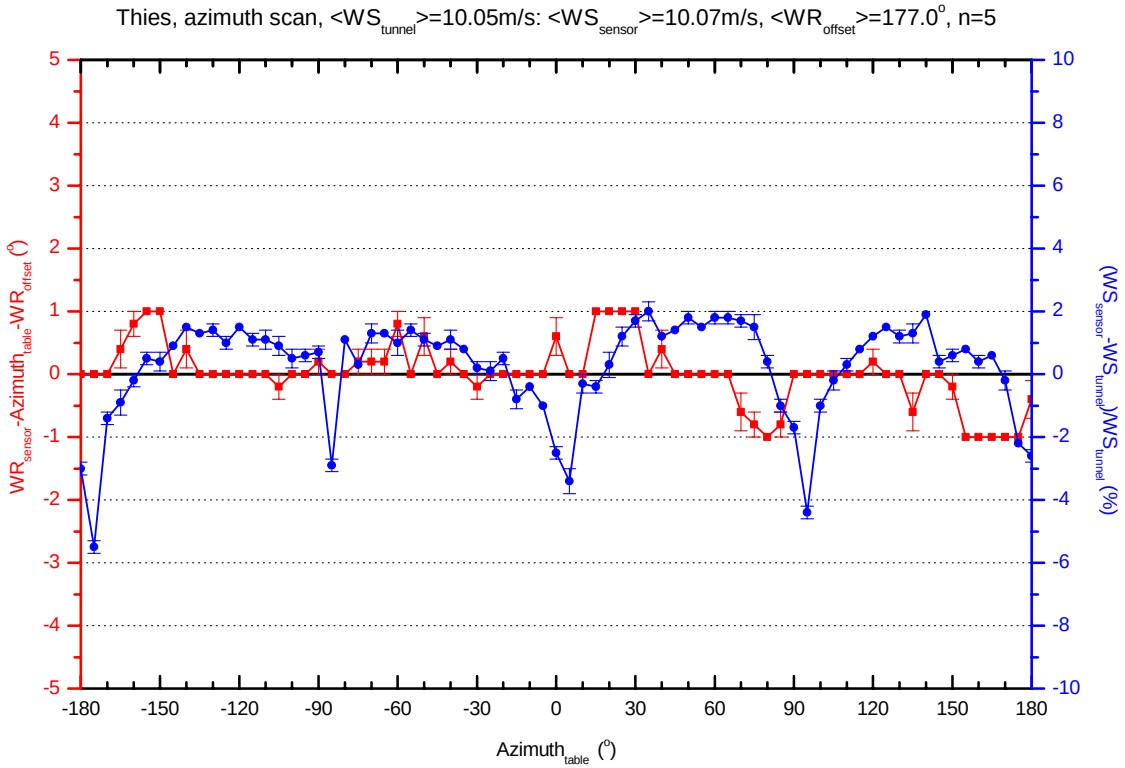
Thies, azimuth scan, <WS$_{tunnel}$>=10.05m/s: <WS$_{sensor}$>=10.07m/s, <WR$_{offset}$>=177.0°, n=5
WR$_{sensor}$-Azimuth$_{table}$-WR$_{offset}$ (°)
(WS$_{sensor}$-WS$_{tunnel}$)/WS$_{tunnel}$ (%)
Azimuth$_{table}$ (°)

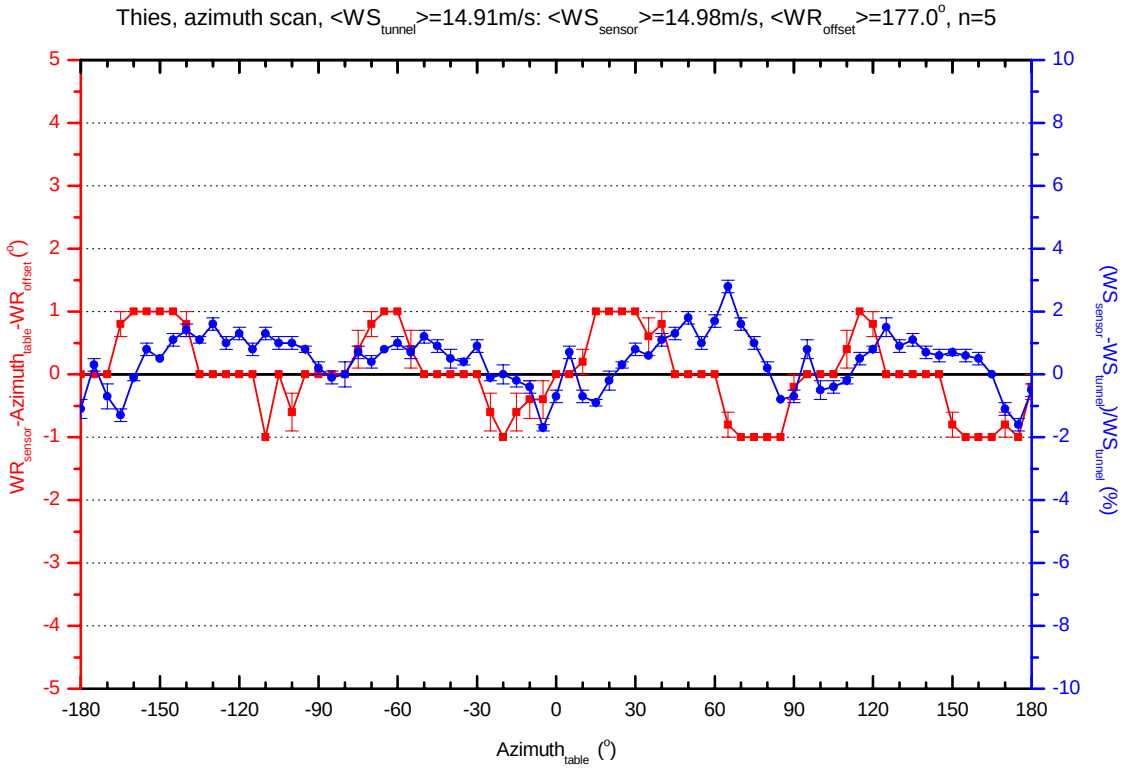
Thies, azimuth scan, <WS_tunnel>=14.91m/s: <WS_sensor>=14.98m/s, <WR_offset>=177.0°, n=5
WR_sensor-Azimuth_table-WR_offset (°)
(WS_sensor-WS_tunnel)/WS_tunnel (%)
Azimuth_table (°)
5
4
3
2
1
0
-1
-2
-3
-4
-5
10
8
6
4
2
0
-2
-4
-6
-8
-10
-180
-150
-120
-90
-60
-30
0
30
60
90
120
150
180

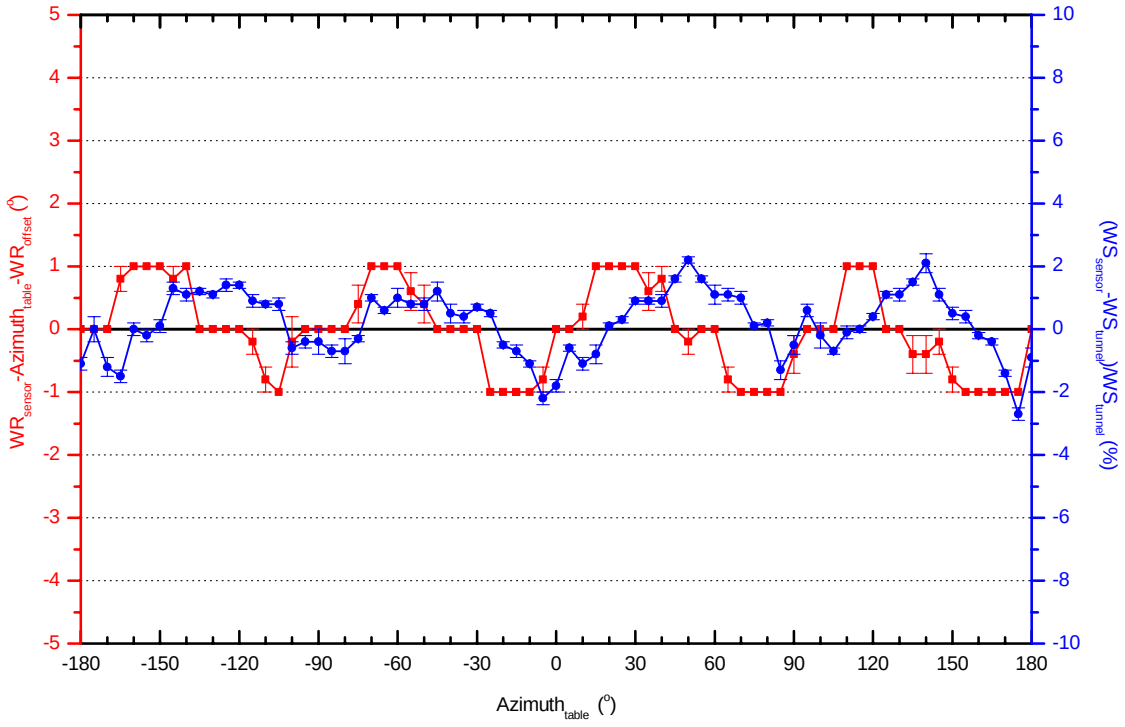
Thies, azimuth scan, <WS_tunnel>=20.16m/s: <WS_sensor>=20.20m/s, <WR_offset>=177.0°, n=5
WR_sensor-Azimuth_table-WR_offset (°)
(WS_sensor-WS_tunnel)/WS_tunnel (%)
Azimuth_table (°)
5
4
3
2
1
0
-1
-2
-3
-4
-5
10
8
6
4
2
0
-2
-4
-6
-8
-10
-180
-150
-120
-90
-60
-30
0
30
60
90
120
150
180

## *Vaisala sonic anemometer*

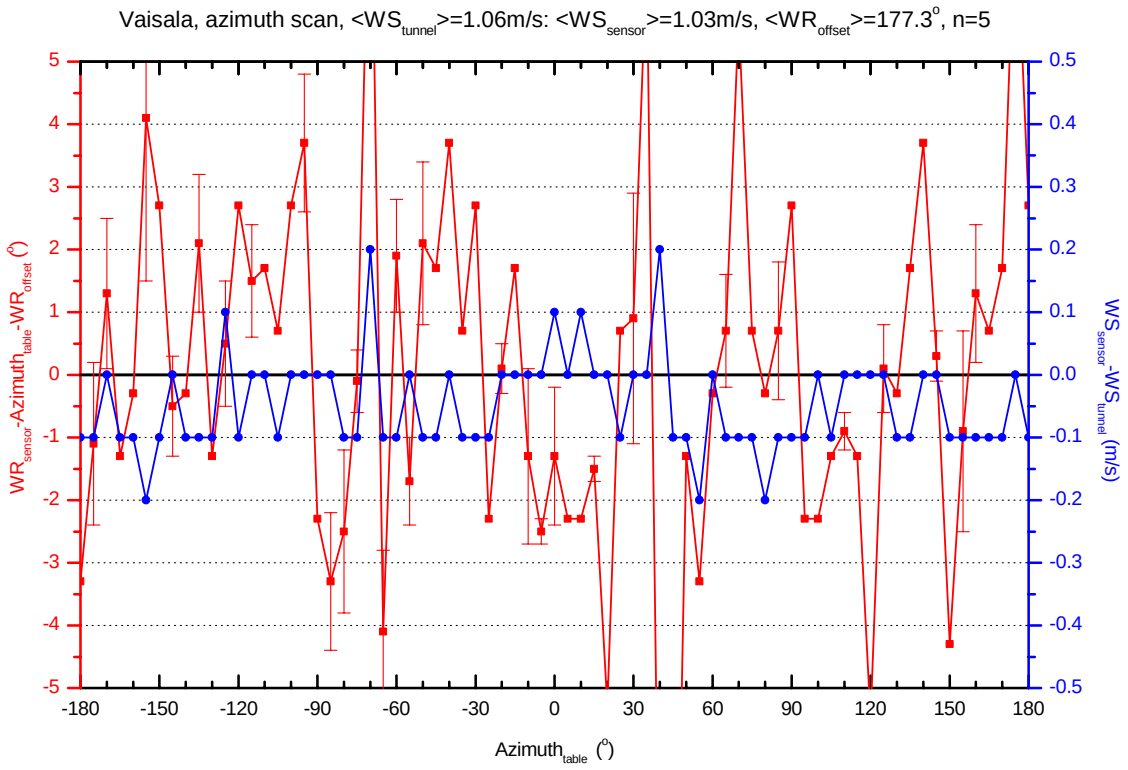


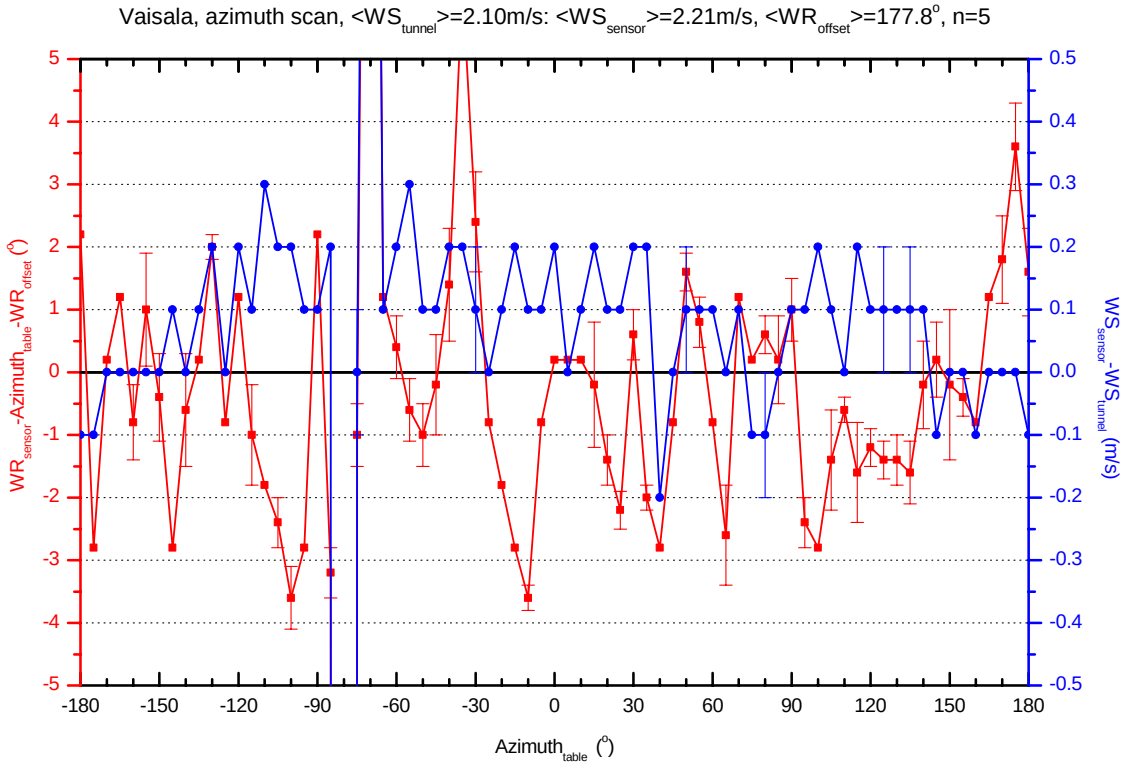

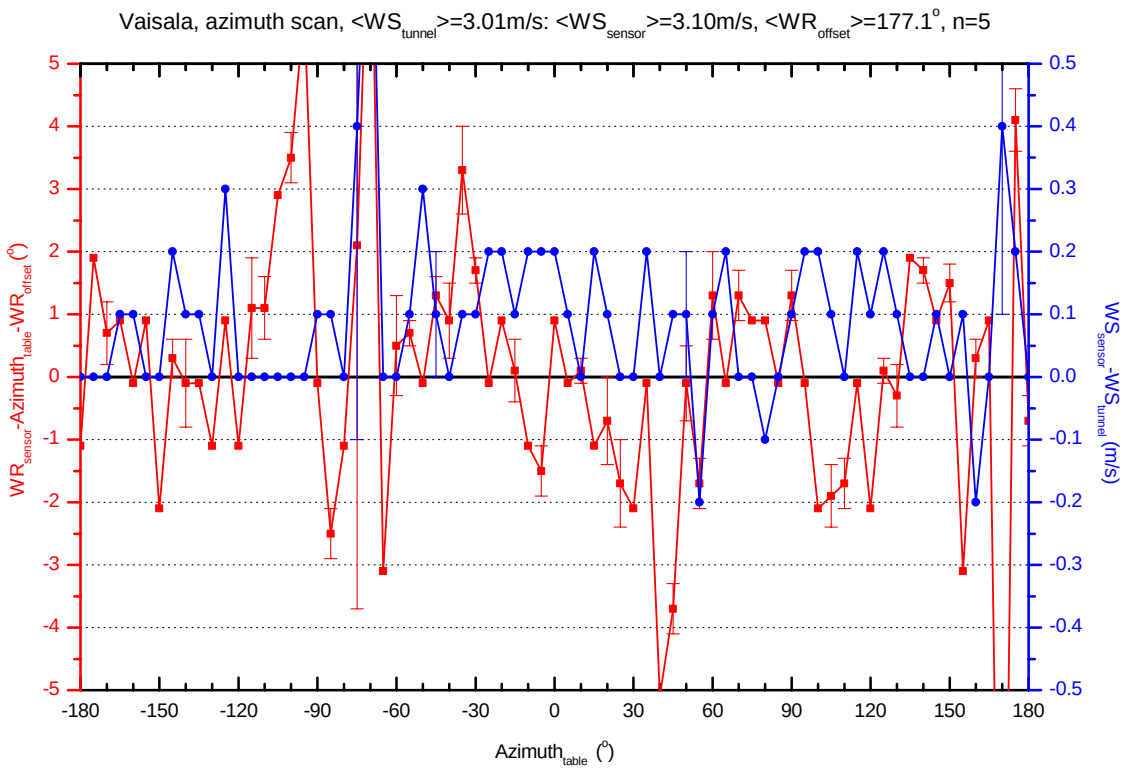
Vaisala, azimuth scan, <WS$_{tunnel}$>=3.01m/s: <WS$_{sensor}$>=3.10m/s, <WR$_{offset}$>=177.1°, n=5
WR$_{sensor}$-Azimuth$_{table}$-WR$_{offset}$ (°)
WS$_{sensor}$-WS$_{tunnel}$ (m/s)
Azimuth$_{table}$ (°)

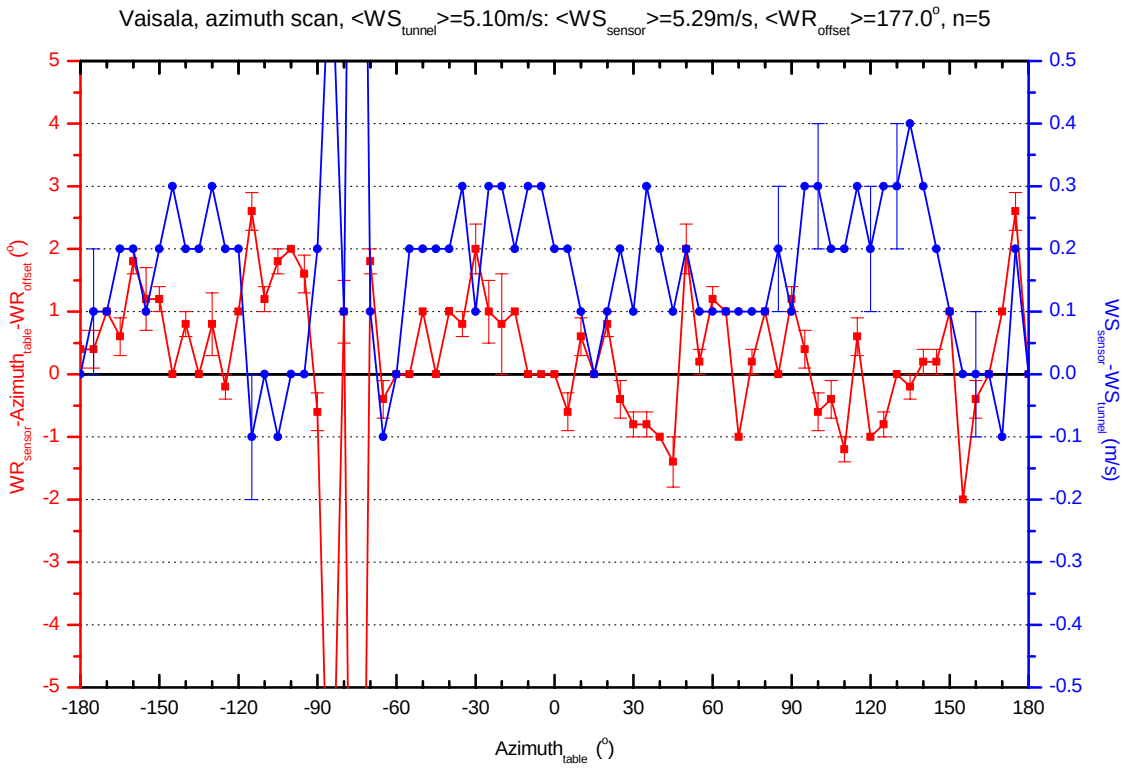
Vaisala, azimuth scan, <WS$_{tunnel}$>=5.10m/s: <WS$_{sensor}$>=5.29m/s, <WR$_{offset}$>=177.0°, n=5
WR$_{sensor}$-Azimuth$_{table}$-WR$_{offset}$ (°)
WS$_{sensor}$-WS$_{tunnel}$ (m/s)
Azimuth$_{table}$ (°)

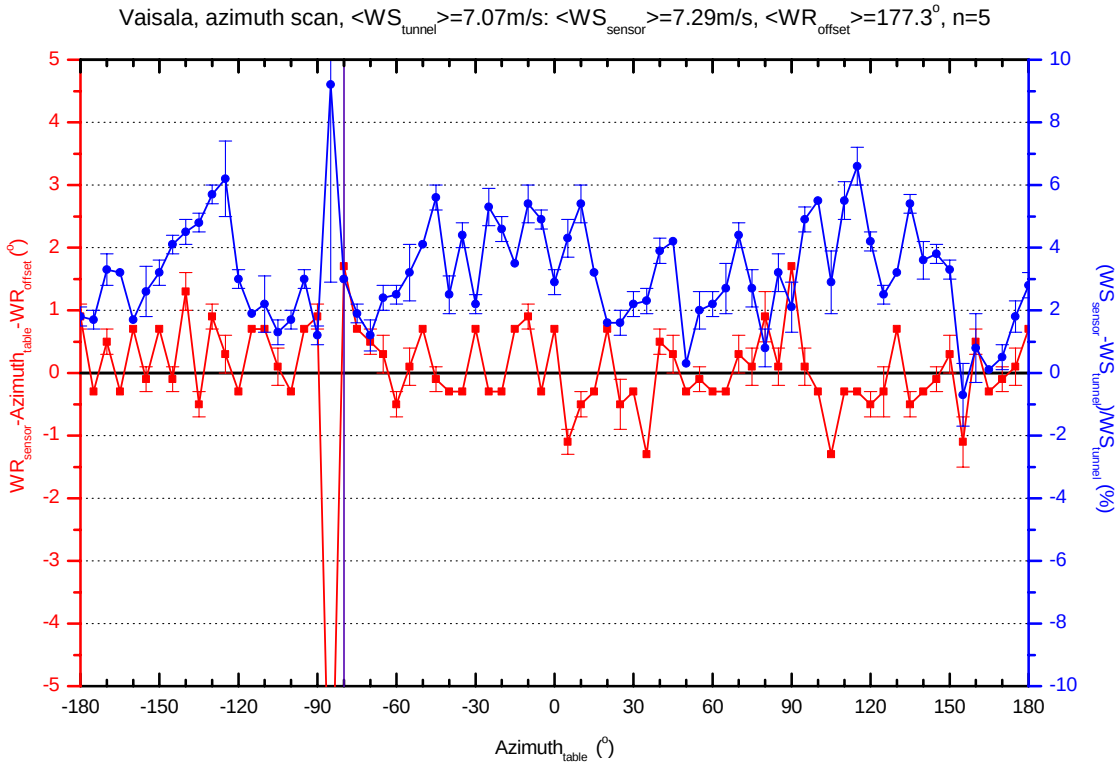
Vaisala, azimuth scan, <WS_tunnel>=7.07m/s: <WS_sensor>=7.29m/s, <WR_offset>=177.3°, n=5
WR_sensor-Azimuth_table-WR_offset (°)
WS_sensor-WS_tunnel/WS_tunnel (%)
Azimuth_table (°)
5
4
3
2
1
0
-1
-2
-3
-4
-5
10
8
6
4
2
0
-2
-4
-6
-8
-10
-180
-150
-120
-90
-60
-30
0
30
60
90
120
150
180

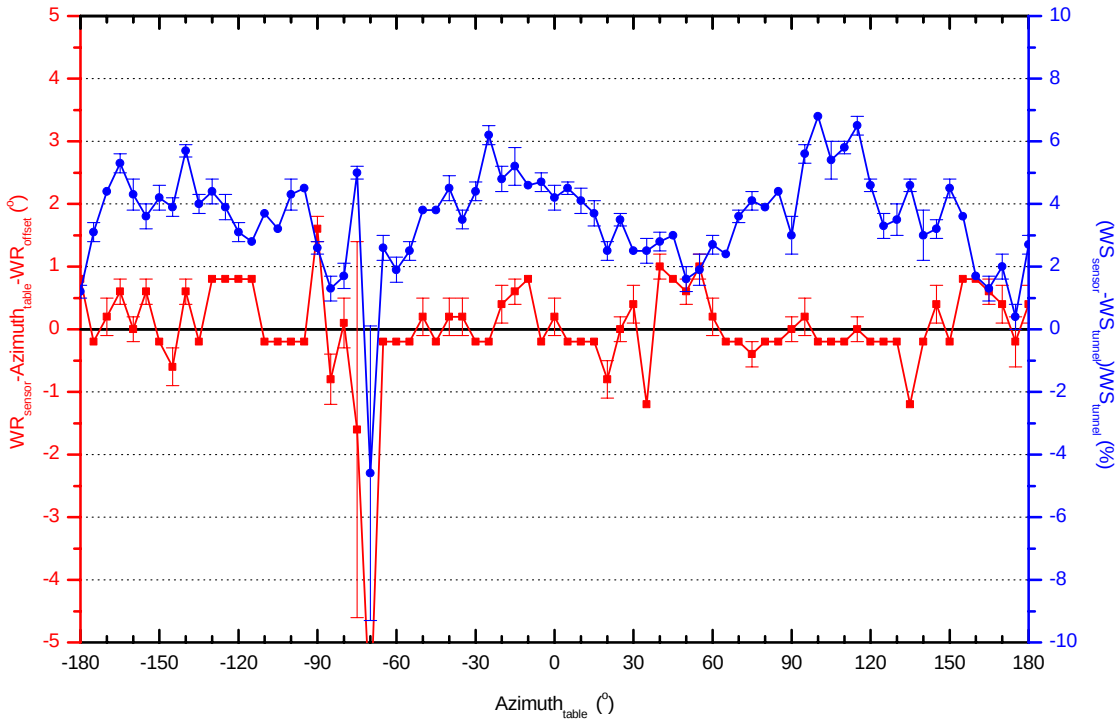
Vaisala, azimuth scan, <WS_tunnel>=9.93m/s: <WS_sensor>=10.28m/s, <WR_offset>=177.2°, n=5
WR_sensor-Azimuth_table-WR_offset (°)
WS_sensor-WS_tunnel/WS_tunnel (%)
Azimuth_table (°)
5
4
3
2
1
0
-1
-2
-3
-4
-5
10
8
6
4
2
0
-2
-4
-6
-8
-10
-180
-150
-120
-90
-60
-30
0
30
60
90
120
150
180

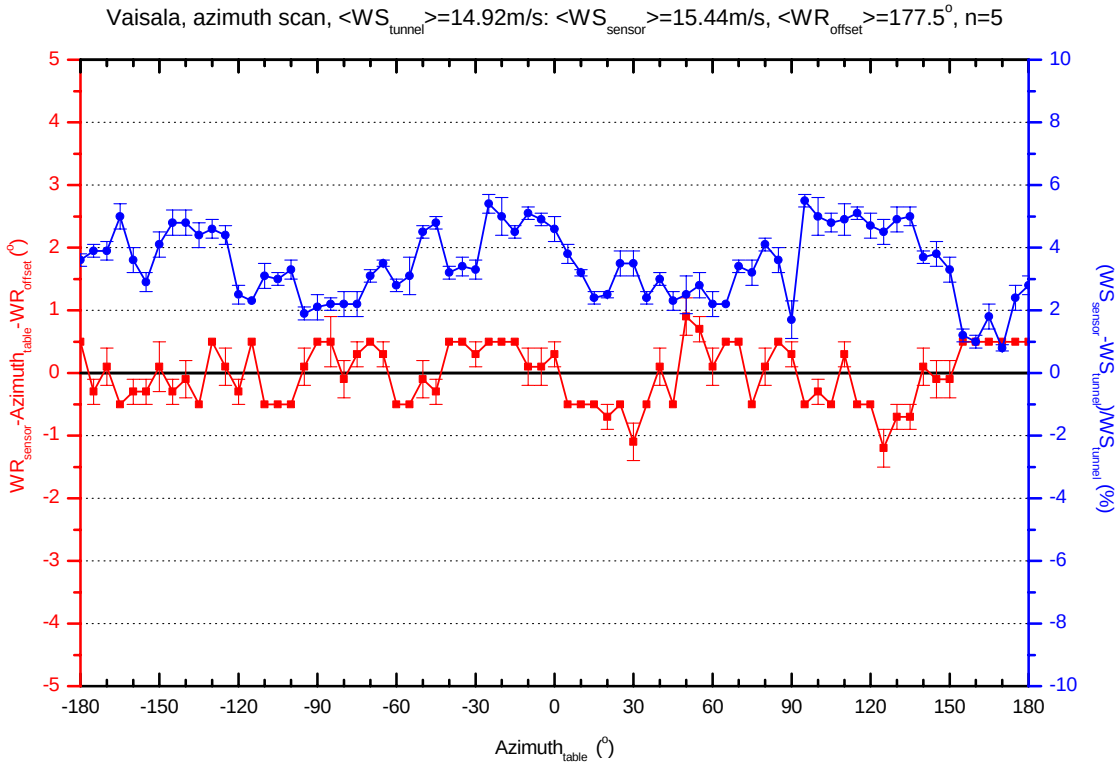
Vaisala, azimuth scan, <WS_tunnel>=14.92m/s: <WS_sensor>=15.44m/s, <WR_offset>=177.5°, n=5
WR_sensor-Azimuth_table-WR_offset (°)
(WS_sensor-WS_tunnel)/WS_tunnel (%)
Azimuth_table (°)

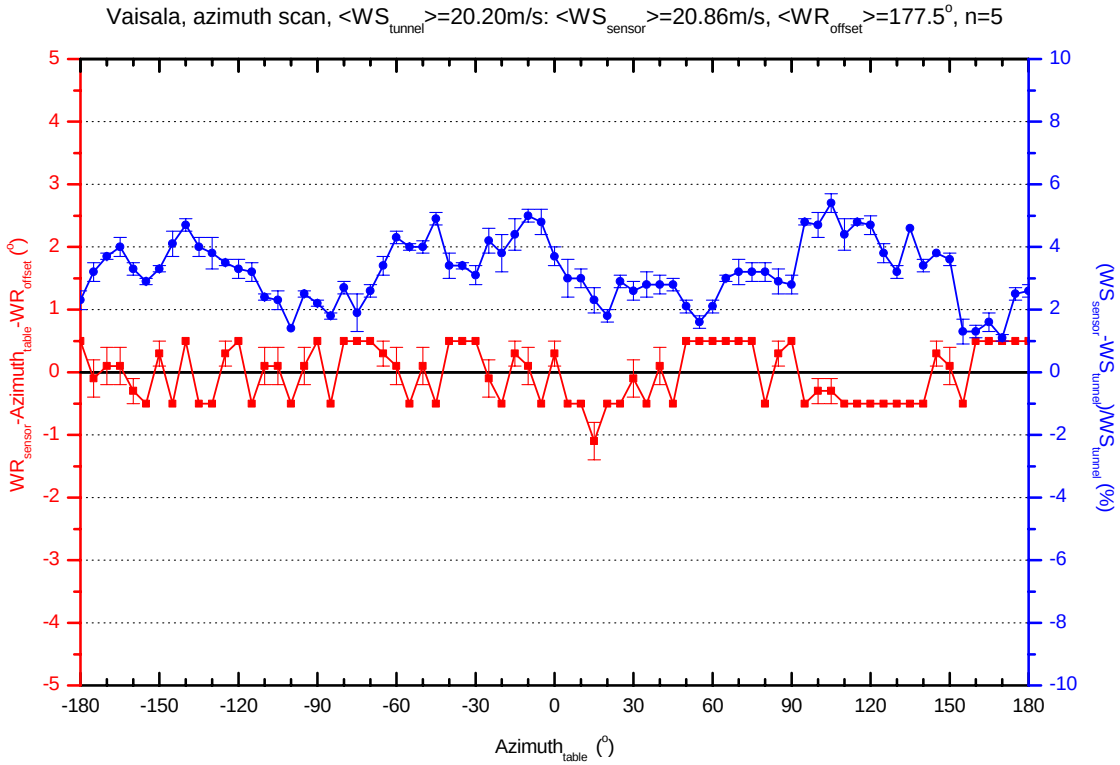
Vaisala, azimuth scan, <WS_tunnel>=20.20m/s: <WS_sensor>=20.86m/s, <WR_offset>=177.5°, n=5
WR_sensor-Azimuth_table-WR_offset (°)
(WS_sensor-WS_tunnel)/WS_tunnel (%)
Azimuth_table (°)

# Appendix C: TNO wind tunnel measurements

In this appendix the results of the TNO wind tunnel measuremenst at 5m/s are shown. The full set of measuremtns is given by Wauben and Beekhuis (2001). Since the sensors were changed after the TNO tunnel test, only the results relevant for the inclination scans performed at 5m/s are presented here. For each of the three sonic anemometers the azimuth scans are shown (performed with an azimuth resolution of 2° for Gill and Vasiala and 1° for Thies) and the results for wind speed and wind direction for the inclination scans. The results for the inclination scans are given as contour plots. The wind speed results show the relative deviation (in %) from the expected cosine behaviour whereas the wind direction gives the absolute diffrerence. Blue contour lines denote negative values and red indicates zero. Note that the azimuth scans are corrected for the direction offset between the sensor and the rotation device, but not the incliantion scans. Hence the 0° to 90° azimuth angles of the inclination scan correspond roughly with the –180° to –90 azimuth angles of the azimuth scan. Also note that the fine structure and extremes of the differences are missing in the inclination scans due to the 15° resolution of the azimuth step (e.g. the disturbance by the transducers for the Gill anemometer).

## *Gill sonic anemometer*

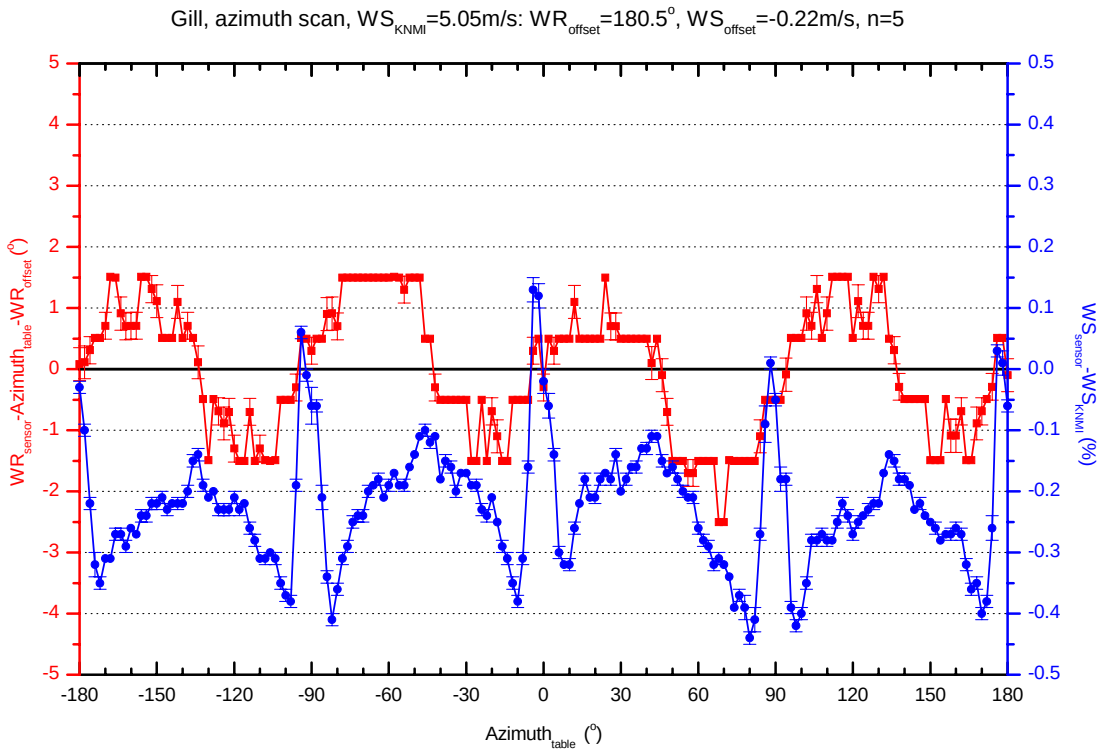

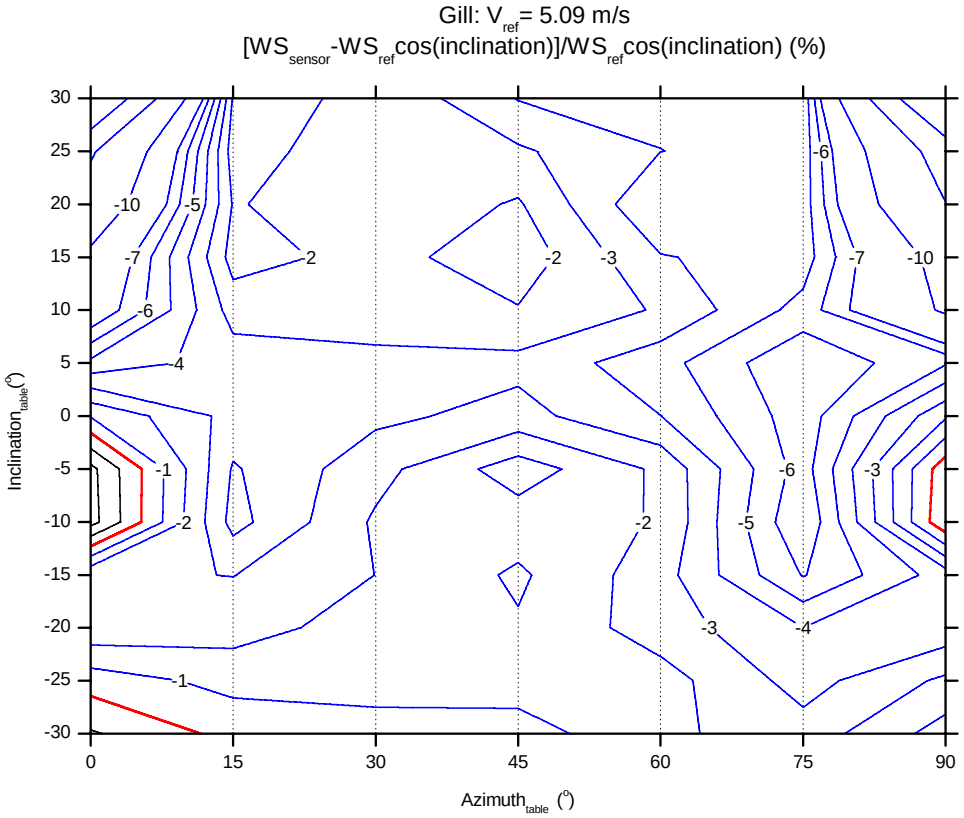
Gill: V_ref = 5.09 m/s
[WS_sensor-WS_ref cos(inclination)]/WS_ref cos(inclination) (%)
Inclination_table (°)
Azimuth_table (°)
-10
-5
-7
-2
-2
-3
-6
-7
-10
-6
-4
-1
-2
-2
-5
-6
-3
-3
-4
-1

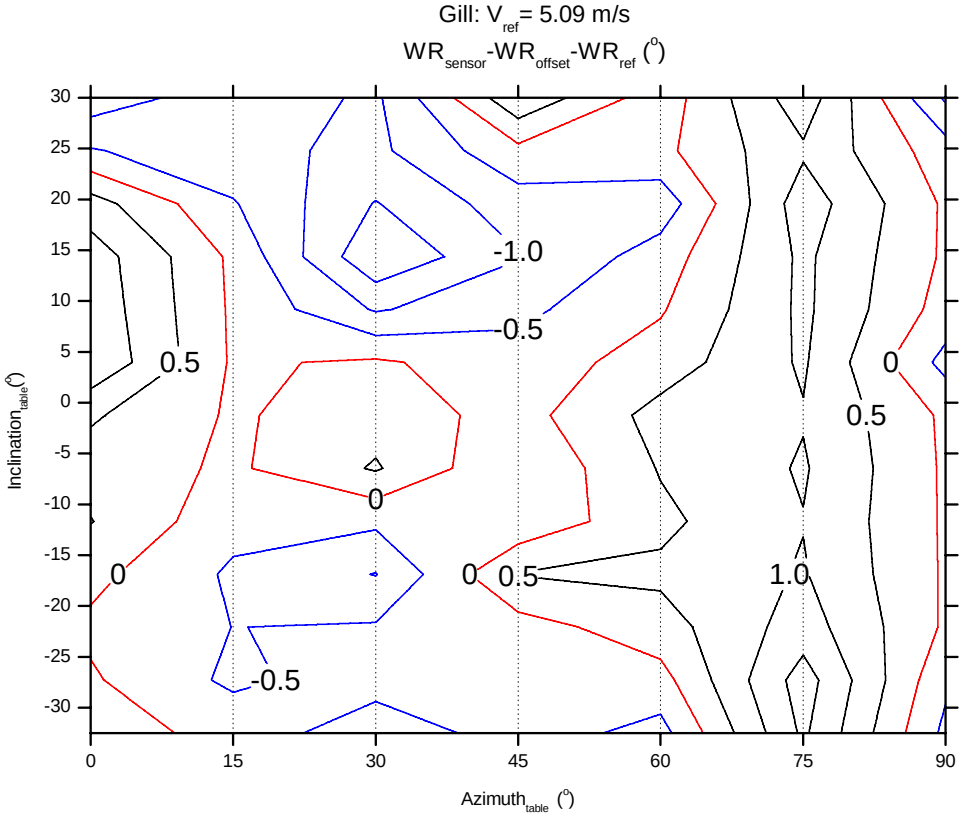
Gill: V_ref = 5.09 m/s
WR_sensor-WR_offset-WR_ref (°)
Inclination_table (°)
Azimuth_table (°)
-1.0
-0.5
0.5
0
0.5
0
0
0
0.5
1.0
-0.5

## *Thies sonic anemometer*

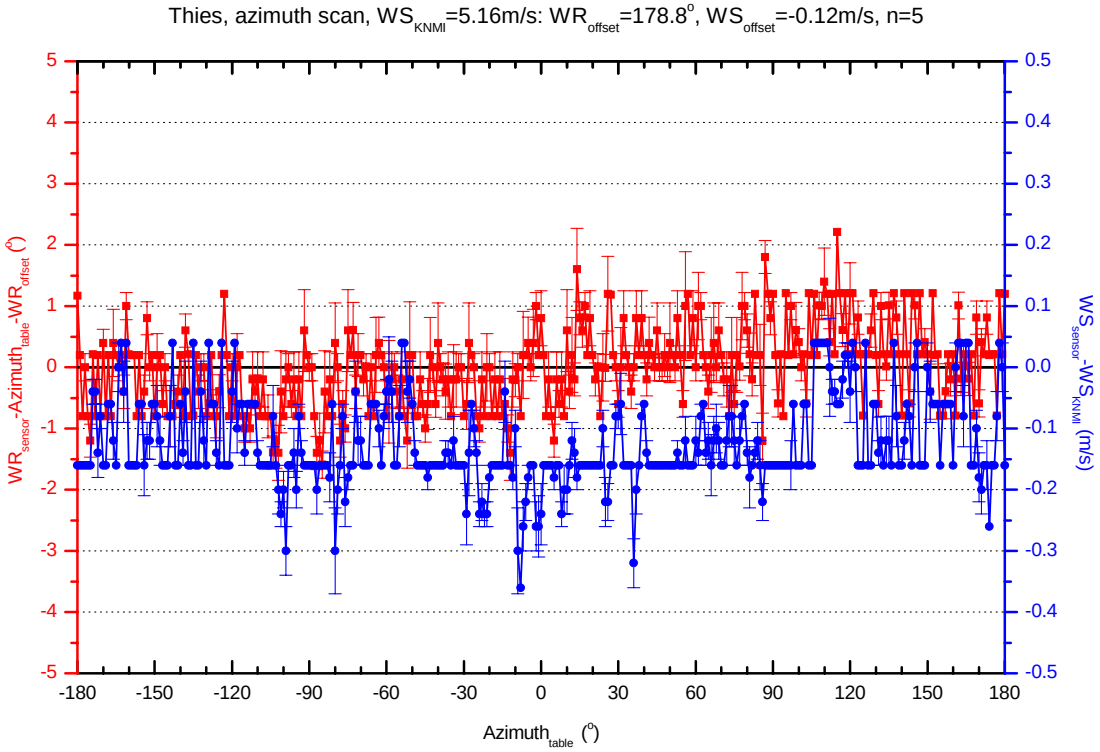


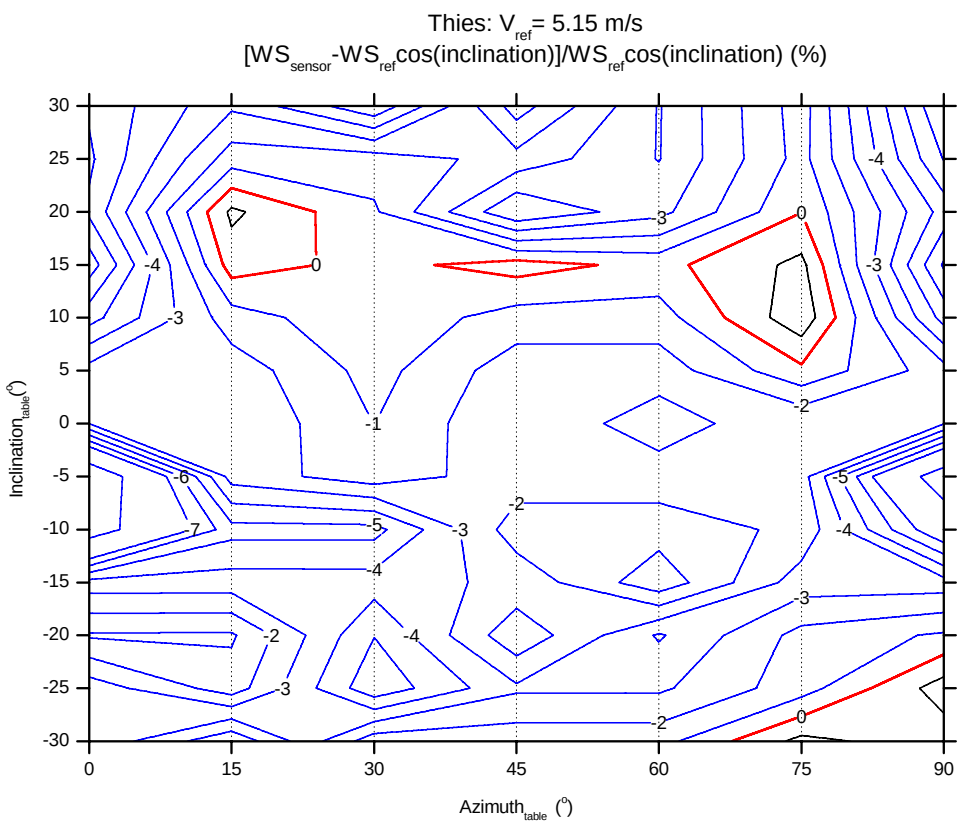

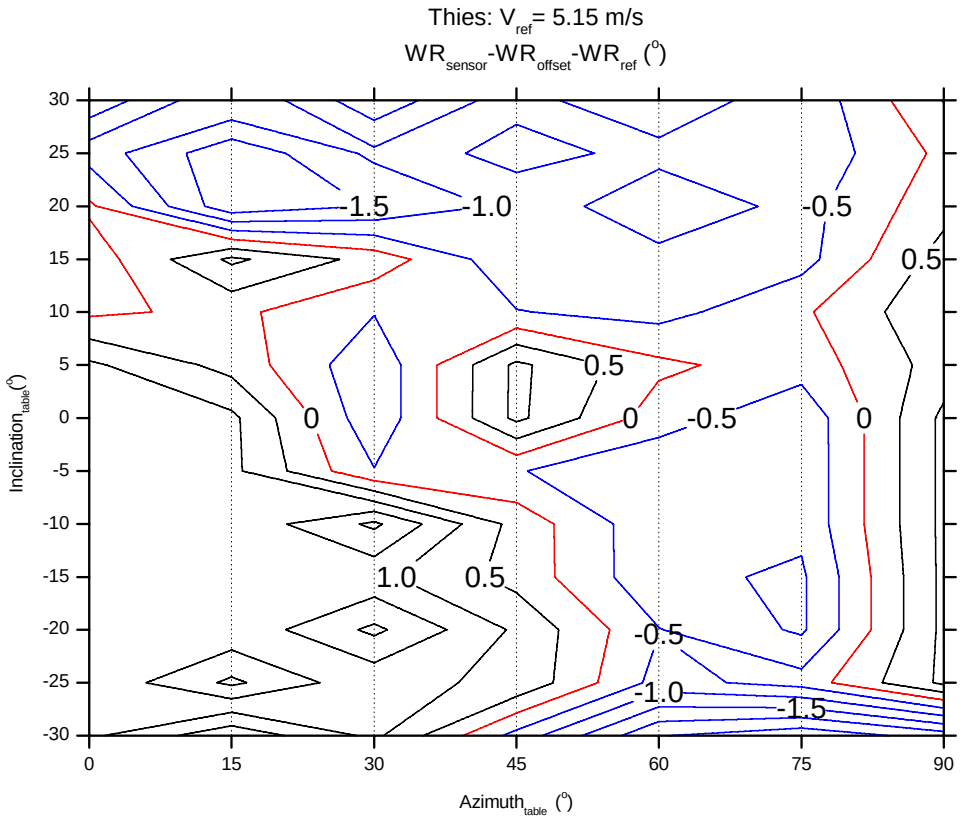


## *Vaisala sonic anemometer*

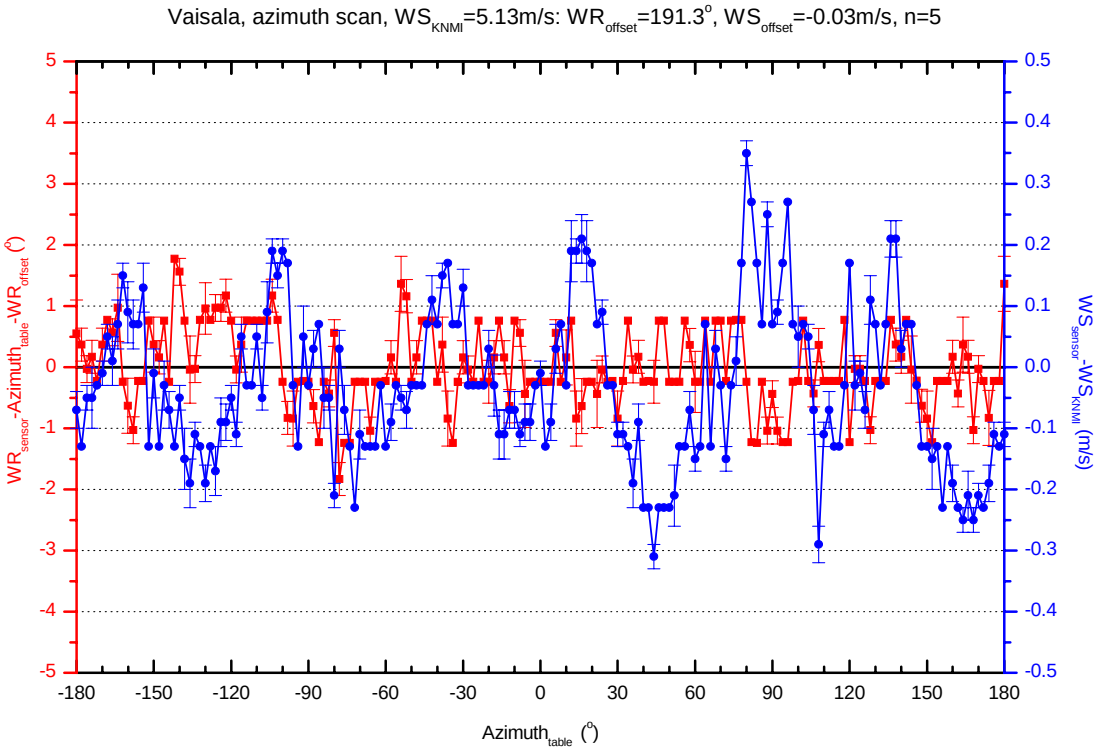

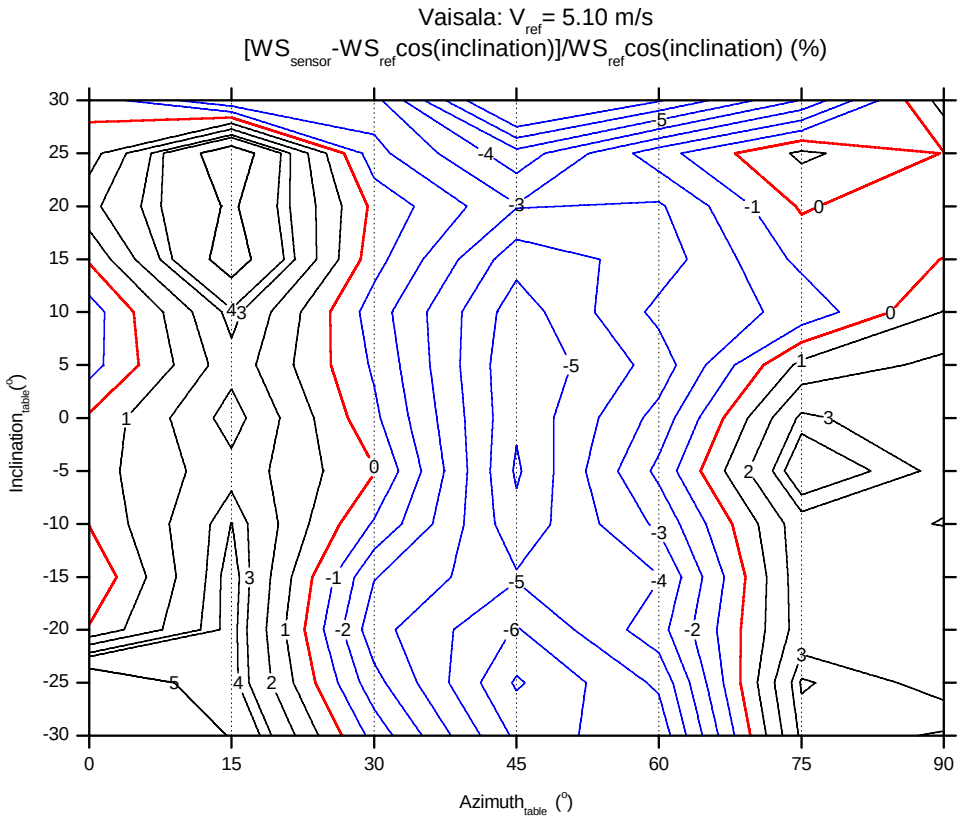
Vaisala: V_ref = 5.10 m/s
[WS_sensor-WS_ref cos(inclination)]/WS_ref cos(inclination) (%)
Inclination_table (°)
Azimuth_table (°)

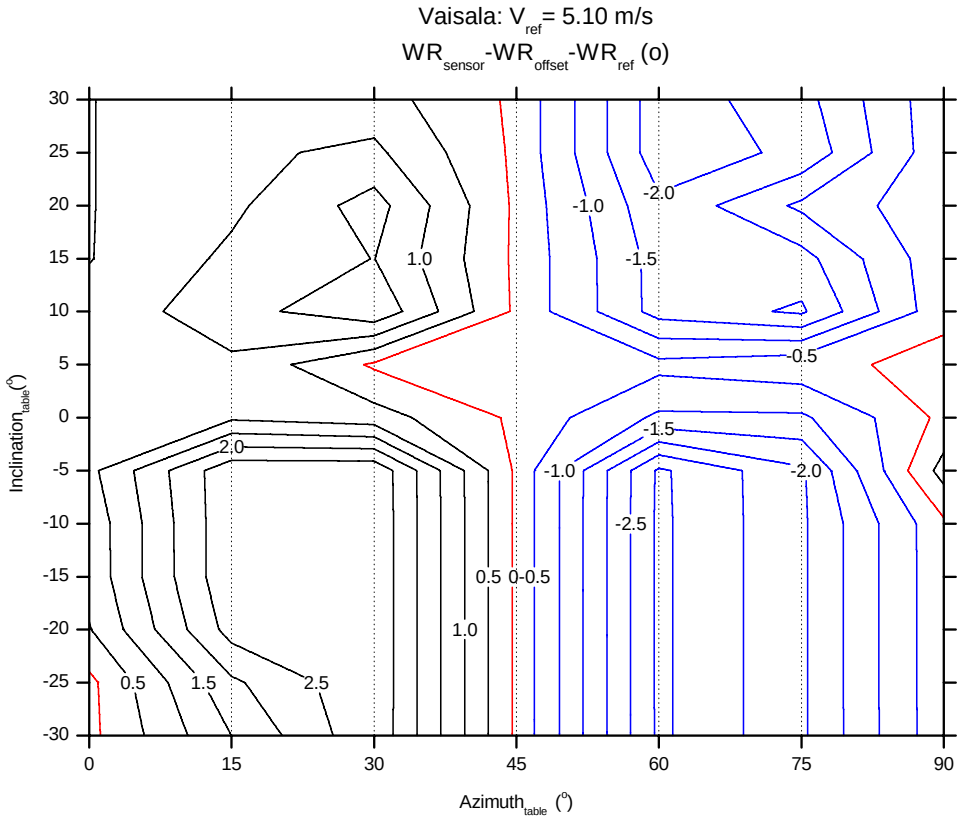
Vaisala: V_ref = 5.10 m/s
WR_sensor-WR_offset-WR_ref (o)
Inclination_table (°)
Azimuth_table (°)

# Appendix D1: Field data as a function of wind direction

In this appendix the field test results for the 10-minute averaged wind direction, wind speed and wind gust are presented as a function of wind direction. For that purpose, the results are binned in 10° intervals, centred around 5°, 15°, …, 355°, w.r.t. the wind direction reported by the KNMI wind vane. All 10-minute intervals are considered where the wind variables of all 4 sensors are valid, i.e. less than 10% of the data is missing. The number of cases for each wind sector are given in the figure below. For each 10° bin between about 700 and 2000 measurements are available.

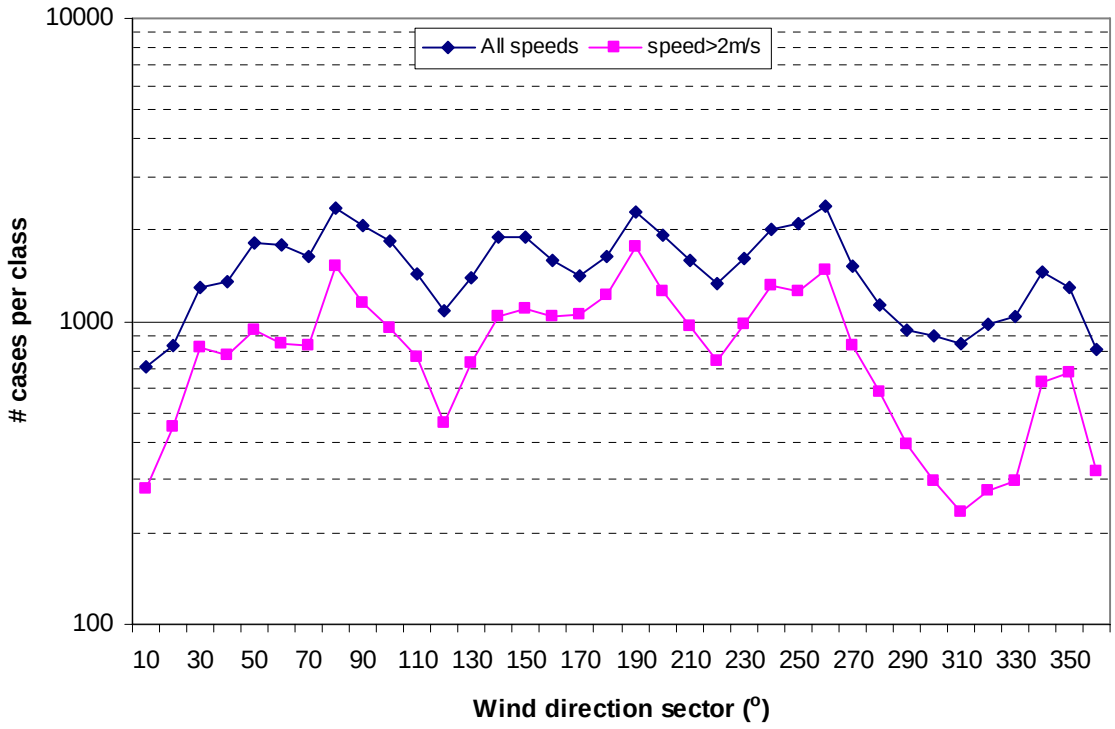


In the sections below the results for wind direction, wind speed and wind gust are reported, respectively. The differences between the sonic anemometers and the conventional wind vane and cup anemometer are presented as well as the differences between the sonics themselves. For each of the three wind parameter is shown: (i) the fraction of the cases with differences within the WMO limits; (ii) the averaged differences; (iii) the averaged absolute differences and; (iv) the standard deviation of the differences. The results are given for all wind speeds and for 10-minute averaged wind speeds of the KNMI cup anemometer above 2m/s. The latter is considered since at variable wind conditions the wind direction is generally not relevant.

## *Wind direction (all wind speeds)*

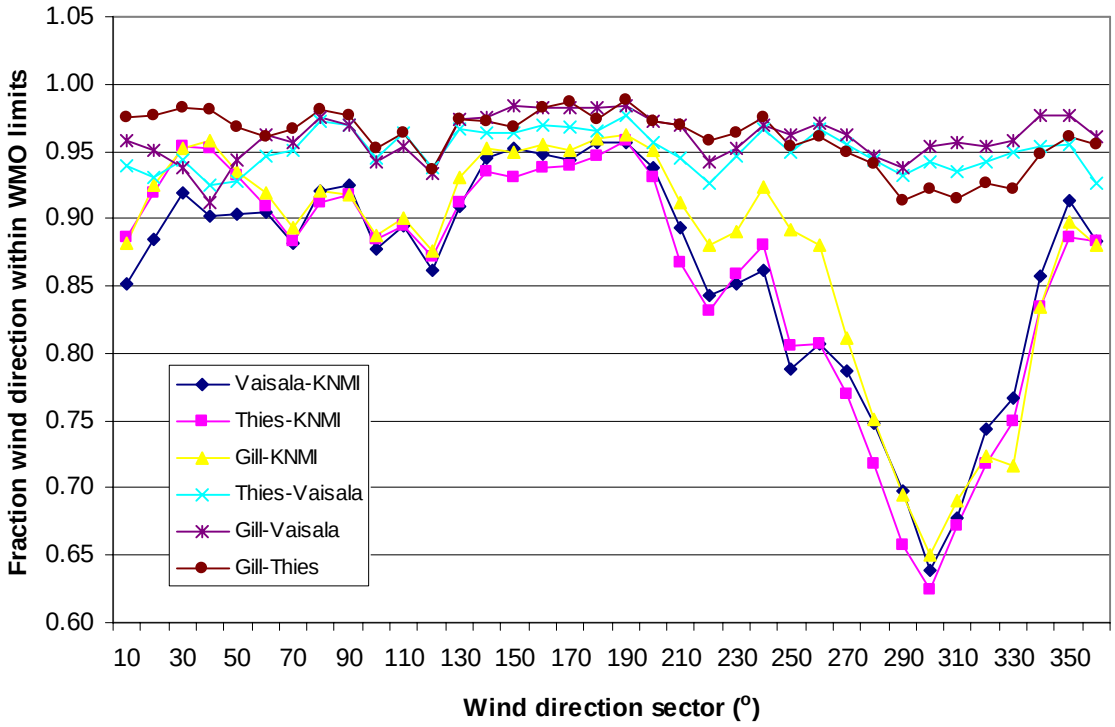


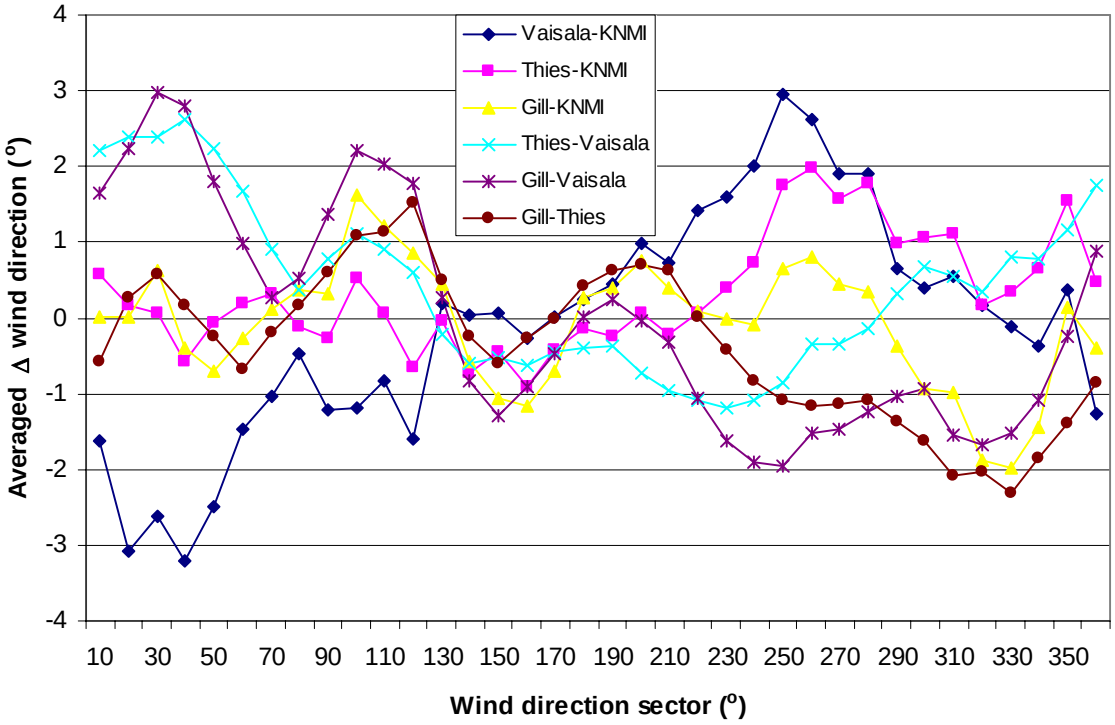

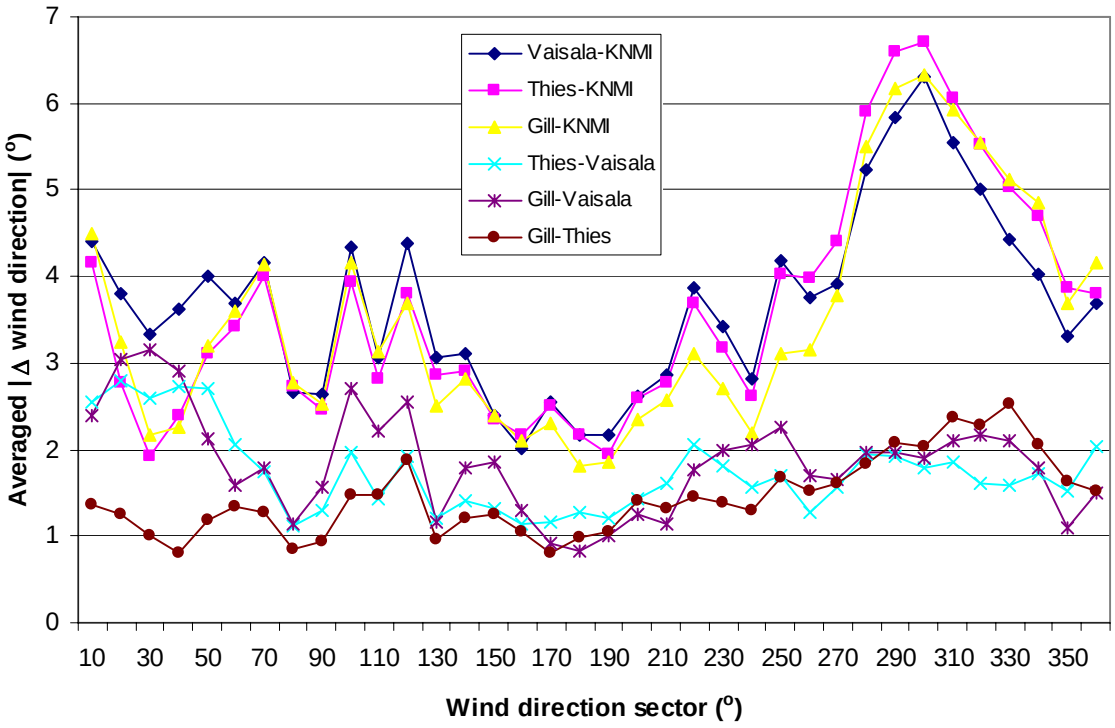
Vaisala-KNMI
Thies-KNMI
Gill-KNMI
Thies-Vaisala
Gill-Vaisala
Gill-Thies
Averaged | Δ wind direction| (°)
Wind direction sector (°)
0
1
2
3
4
5
6
7
10 30 50 70 90 110 130 150 170 190 210 230 250 270 290 310 330 350

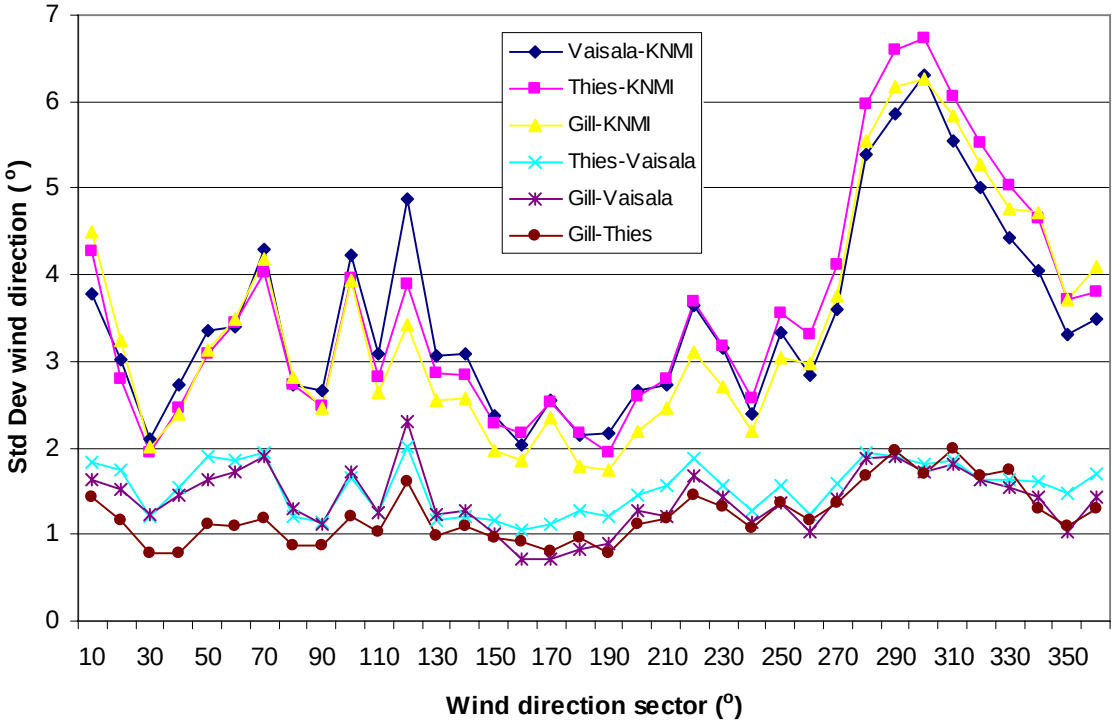
Vaisala-KNMI
Thies-KNMI
Gill-KNMI
Thies-Vaisala
Gill-Vaisala
Gill-Thies
Std Dev wind direction (°)
Wind direction sector (°)
0
1
2
3
4
5
6
7
10 30 50 70 90 110 130 150 170 190 210 230 250 270 290 310 330 350

## *Wind direction (wind speed>2m/s)*

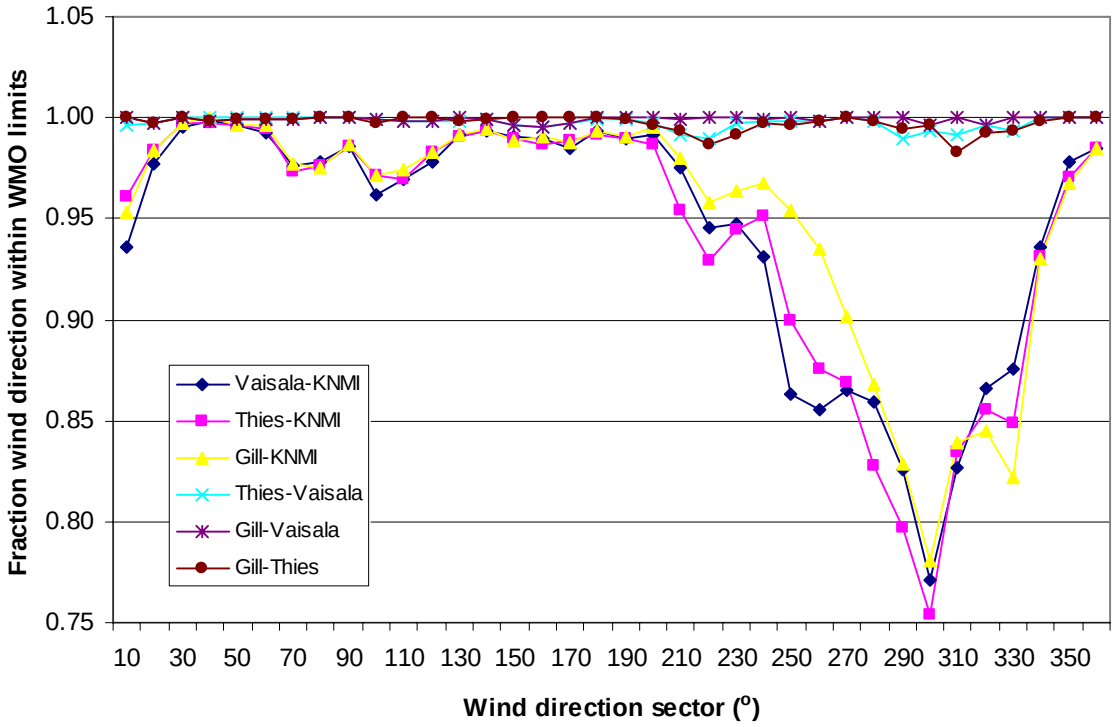


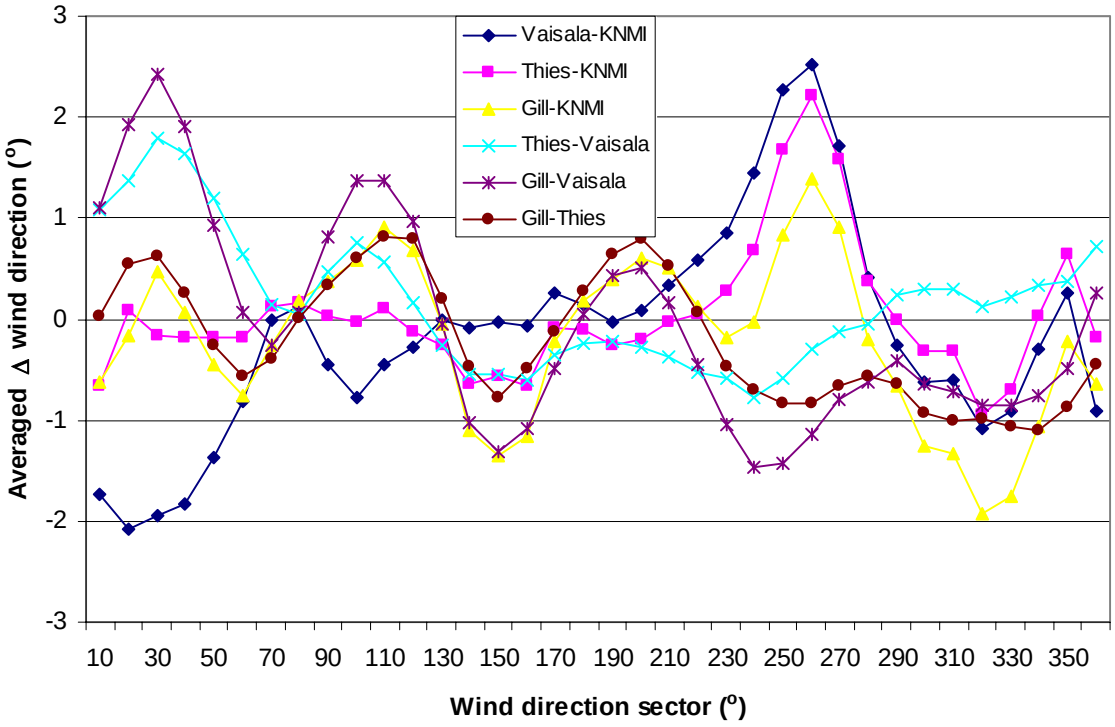

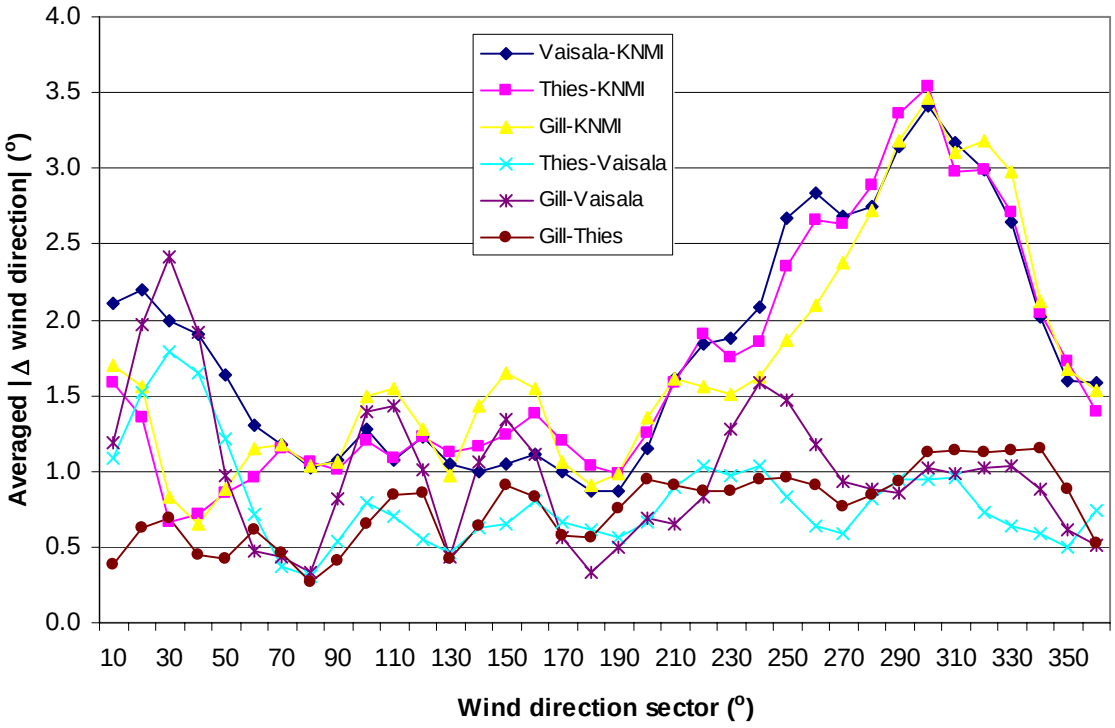
Vaisala-KNMI
Thies-KNMI
Gill-KNMI
Thies-Vaisala
Gill-Vaisala
Gill-Thies
Averaged | Δ wind direction| (°)
Wind direction sector (°)
0.0
0.5
1.0
1.5
2.0
2.5
3.0
3.5
4.0
10 30 50 70 90 110 130 150 170 190 210 230 250 270 290 310 330 350

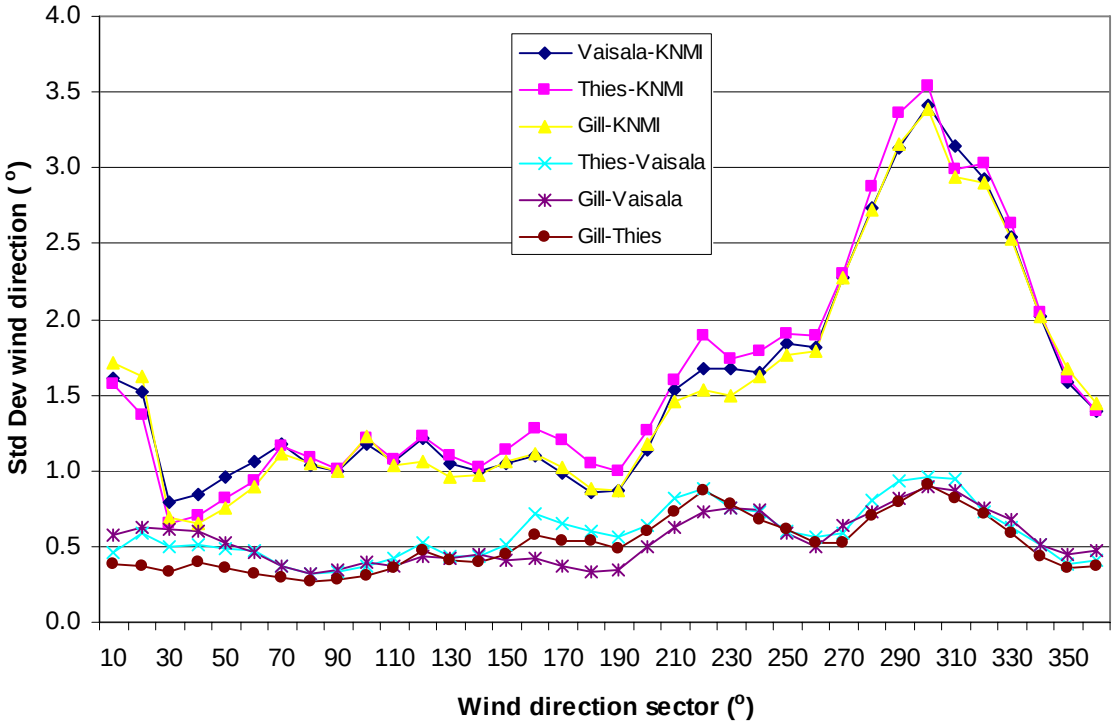
Vaisala-KNMI
Thies-KNMI
Gill-KNMI
Thies-Vaisala
Gill-Vaisala
Gill-Thies
Std Dev wind direction (°)
Wind direction sector (°)
0.0
0.5
1.0
1.5
2.0
2.5
3.0
3.5
4.0
10 30 50 70 90 110 130 150 170 190 210 230 250 270 290 310 330 350

## *Wind speed (all wind speeds)*

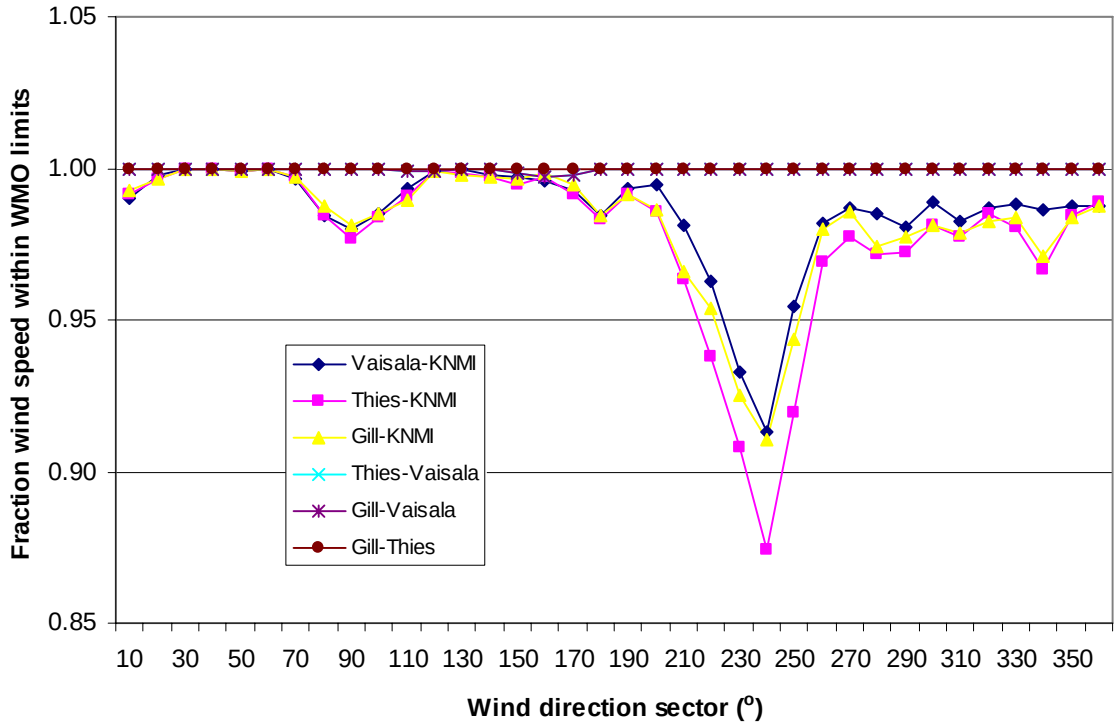


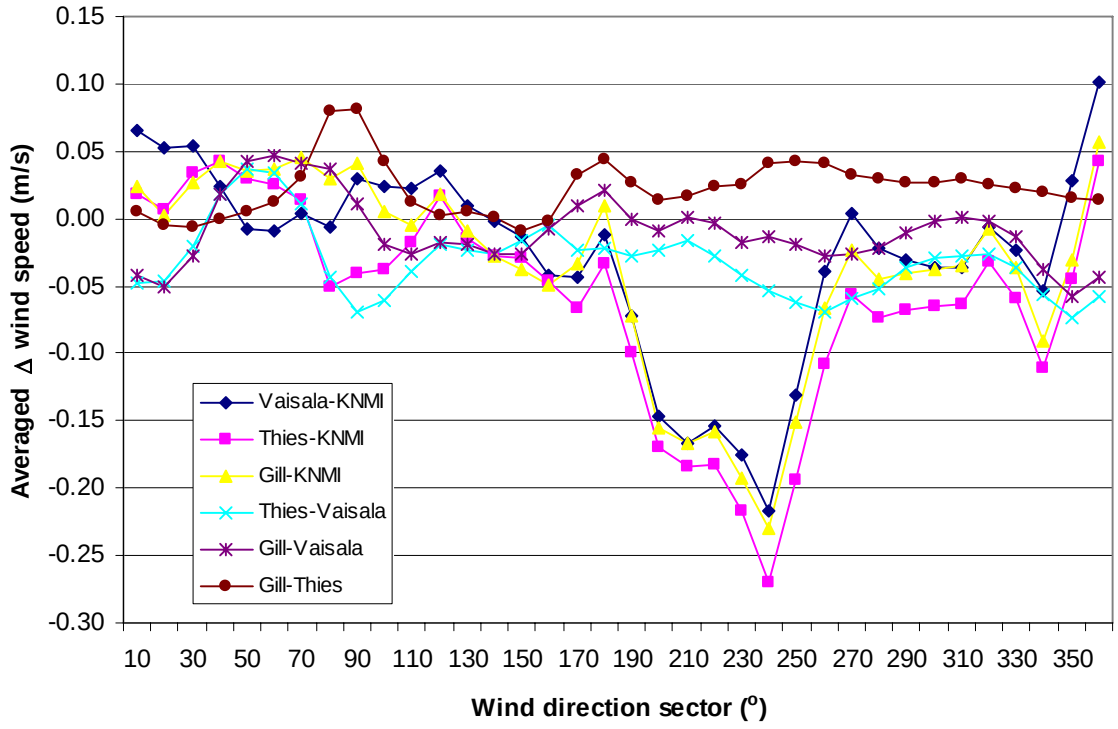

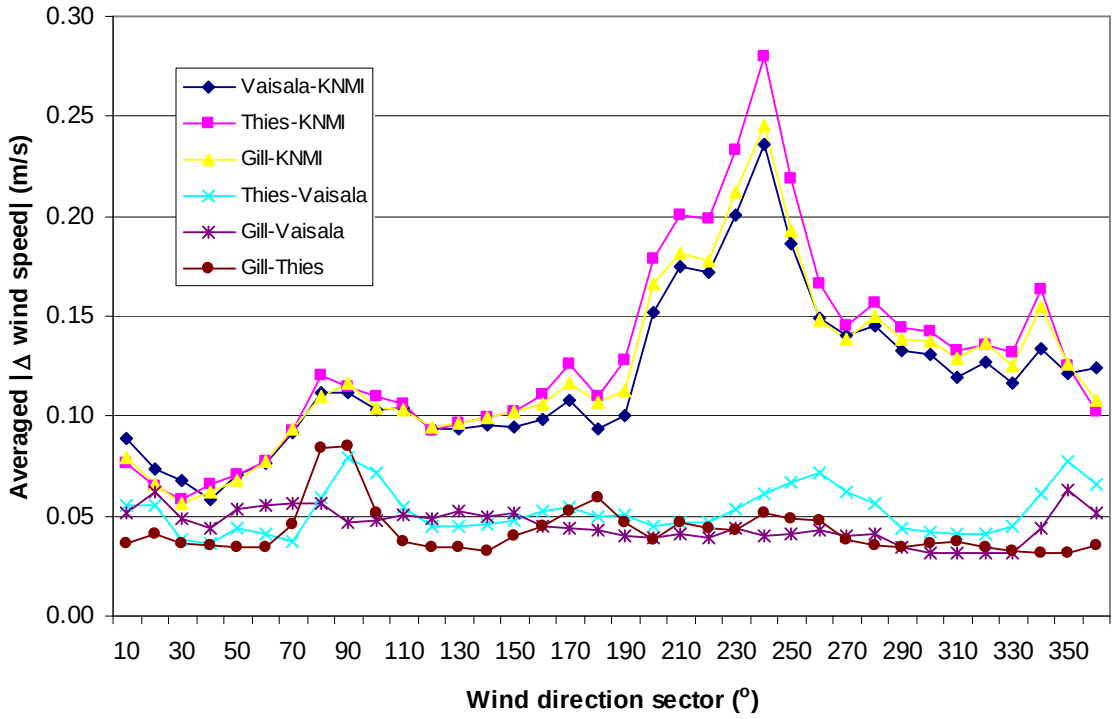
Averaged |Δ wind speed| (m/s)
0.30
0.25
0.20
0.15
0.10
0.05
0.00
Vaisala-KNMI
Thies-KNMI
Gill-KNMI
Thies-Vaisala
Gill-Vaisala
Gill-Thies
10 30 50 70 90 110 130 150 170 190 210 230 250 270 290 310 330 350
Wind direction sector (°)

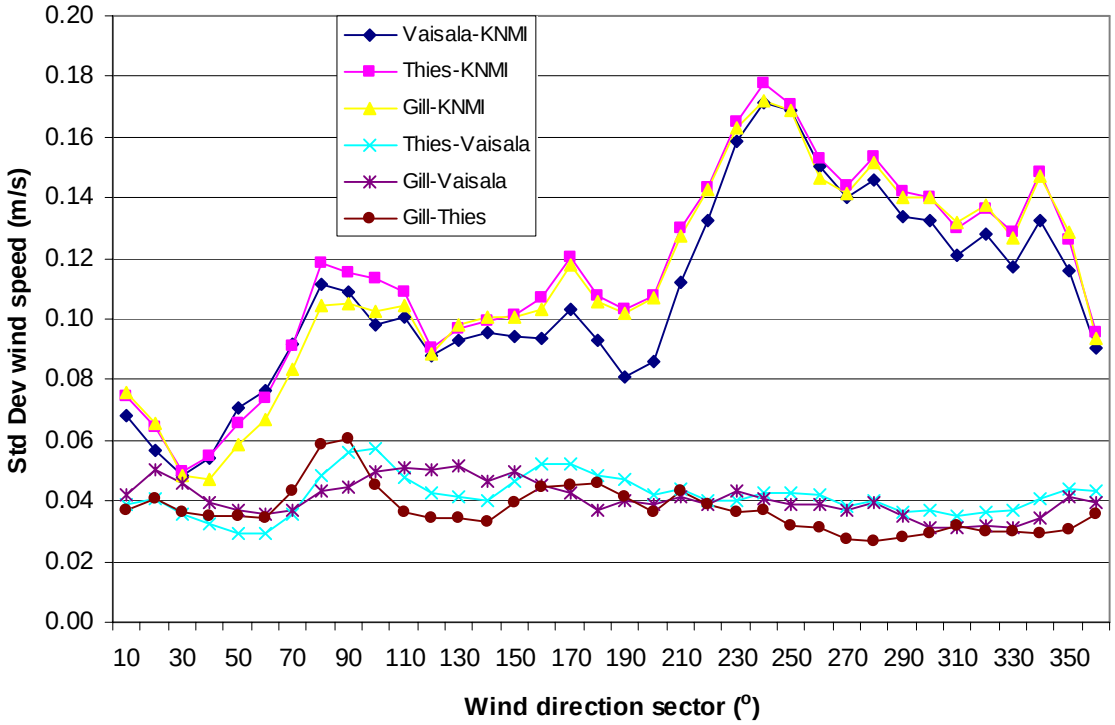
Std Dev wind speed (m/s)
0.20
0.18
0.16
0.14
0.12
0.10
0.08
0.06
0.04
0.02
0.00
Vaisala-KNMI
Thies-KNMI
Gill-KNMI
Thies-Vaisala
Gill-Vaisala
Gill-Thies
10 30 50 70 90 110 130 150 170 190 210 230 250 270 290 310 330 350
Wind direction sector (°)

## *Wind speed (wind speed>2m/s)*

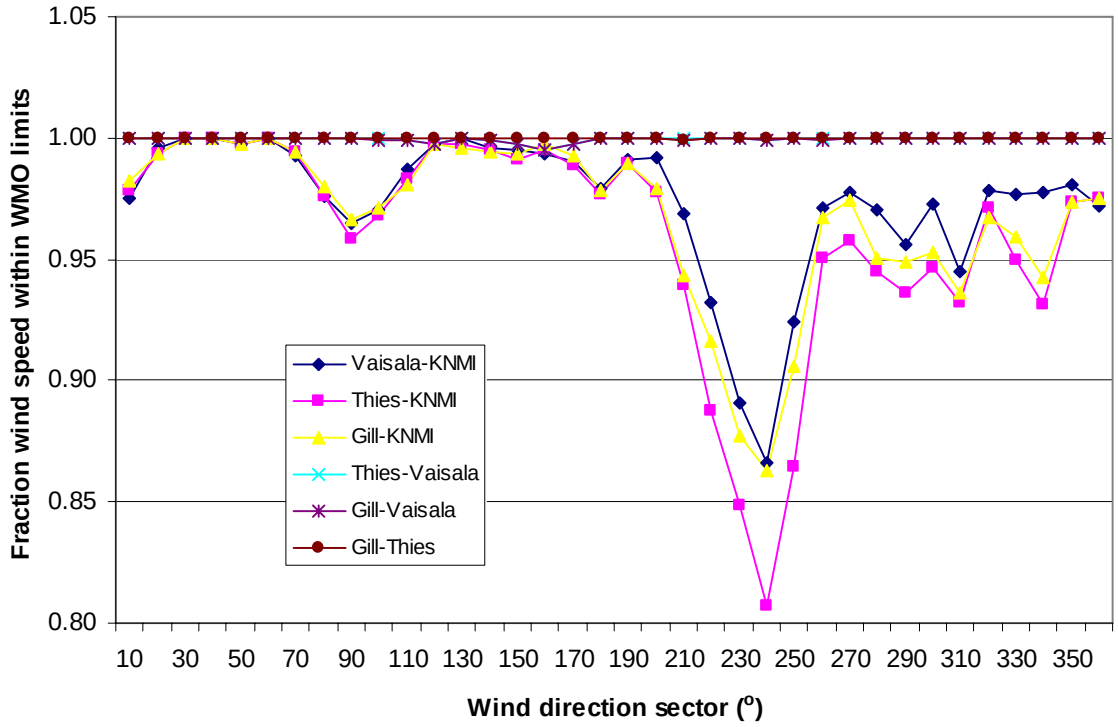


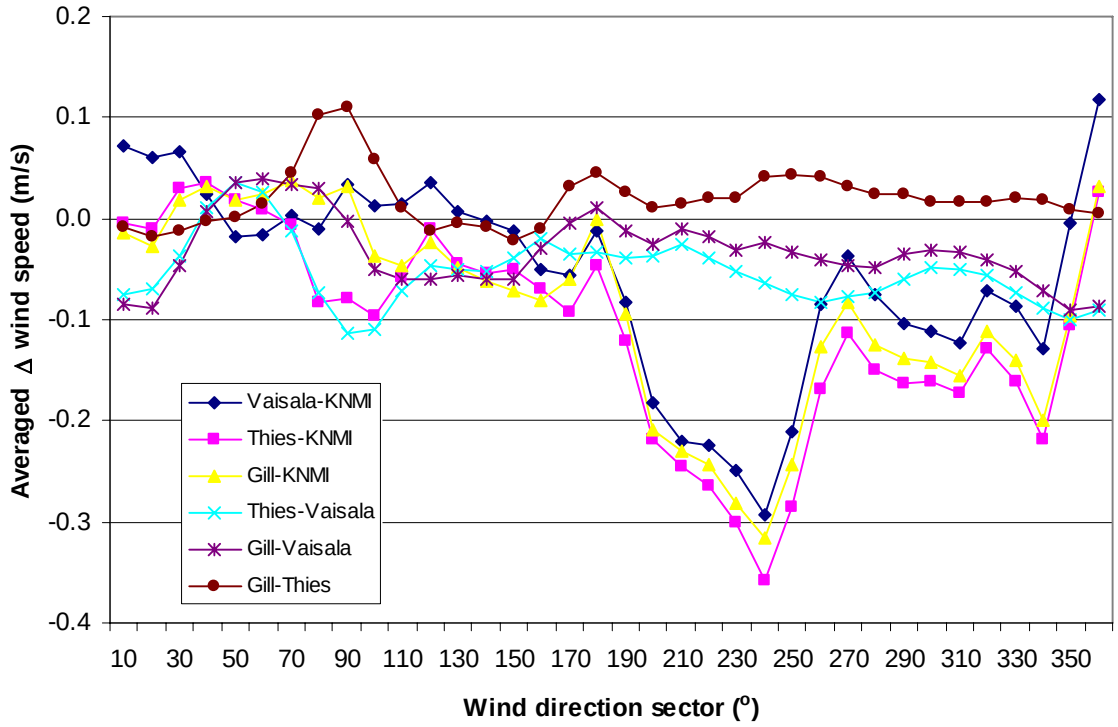

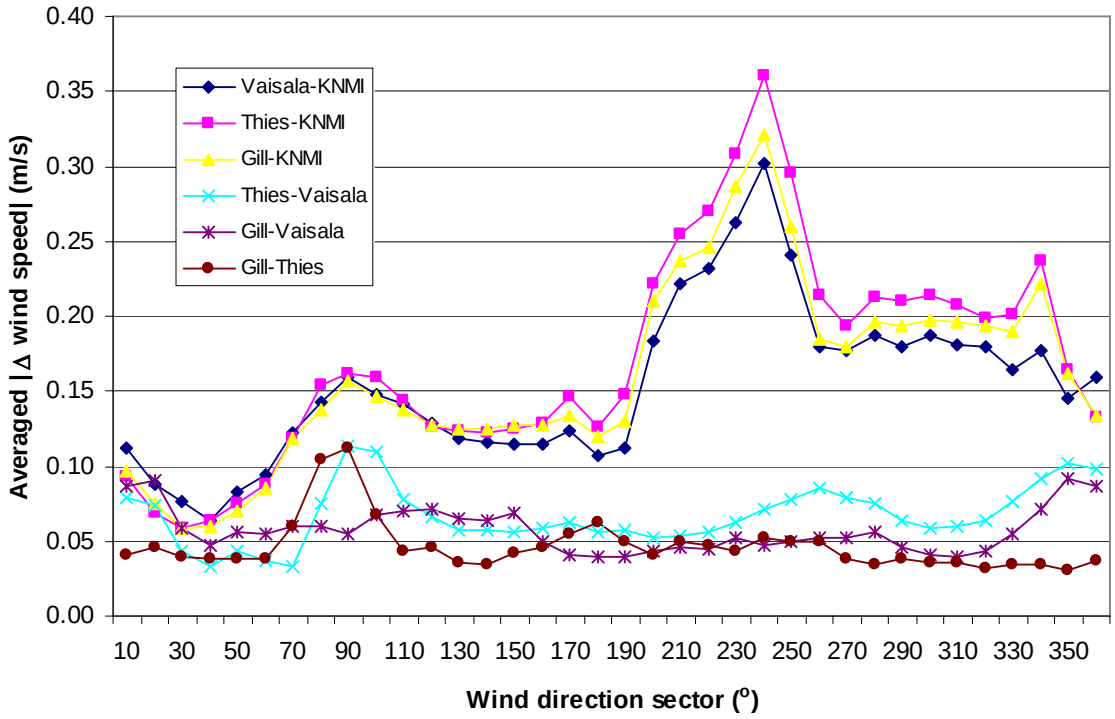
Averaged |Δ wind speed| (m/s)
0.40
0.35
0.30
0.25
0.20
0.15
0.10
0.05
0.00
Vaisala-KNMI
Thies-KNMI
Gill-KNMI
Thies-Vaisala
Gill-Vaisala
Gill-Thies
10 30 50 70 90 110 130 150 170 190 210 230 250 270 290 310 330 350
Wind direction sector (°)

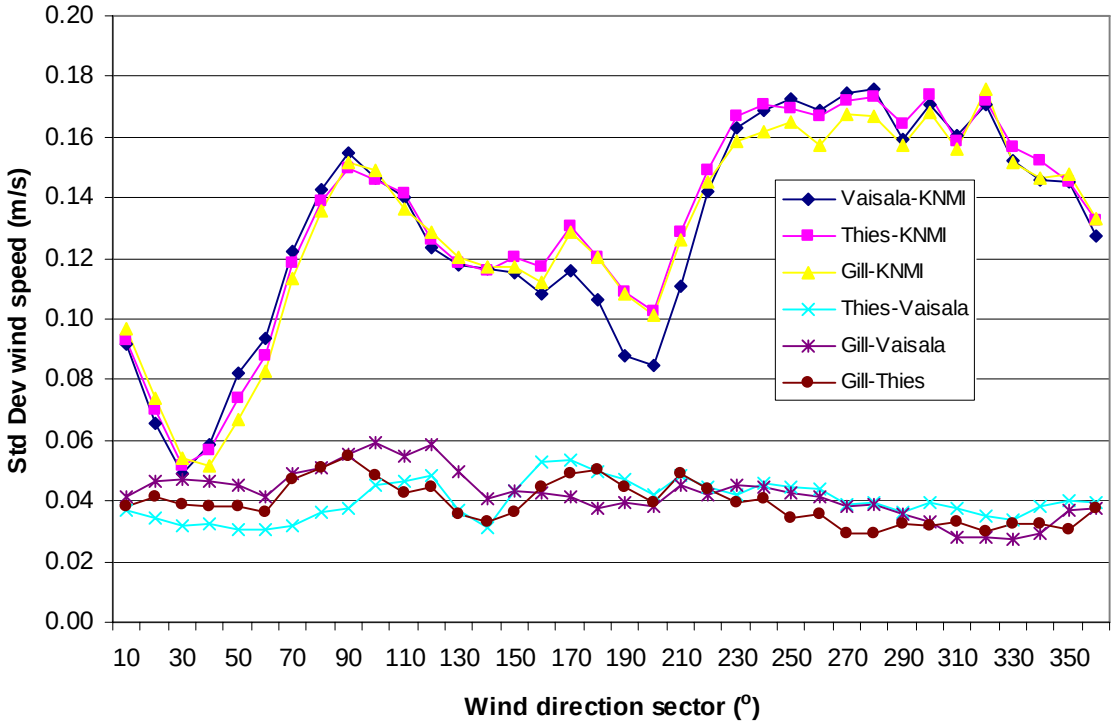
Std Dev wind speed (m/s)
0.20
0.18
0.16
0.14
0.12
0.10
0.08
0.06
0.04
0.02
0.00
Vaisala-KNMI
Thies-KNMI
Gill-KNMI
Thies-Vaisala
Gill-Vaisala
Gill-Thies
10 30 50 70 90 110 130 150 170 190 210 230 250 270 290 310 330 350
Wind direction sector (°)

## *Wind gust (all wind speeds)*

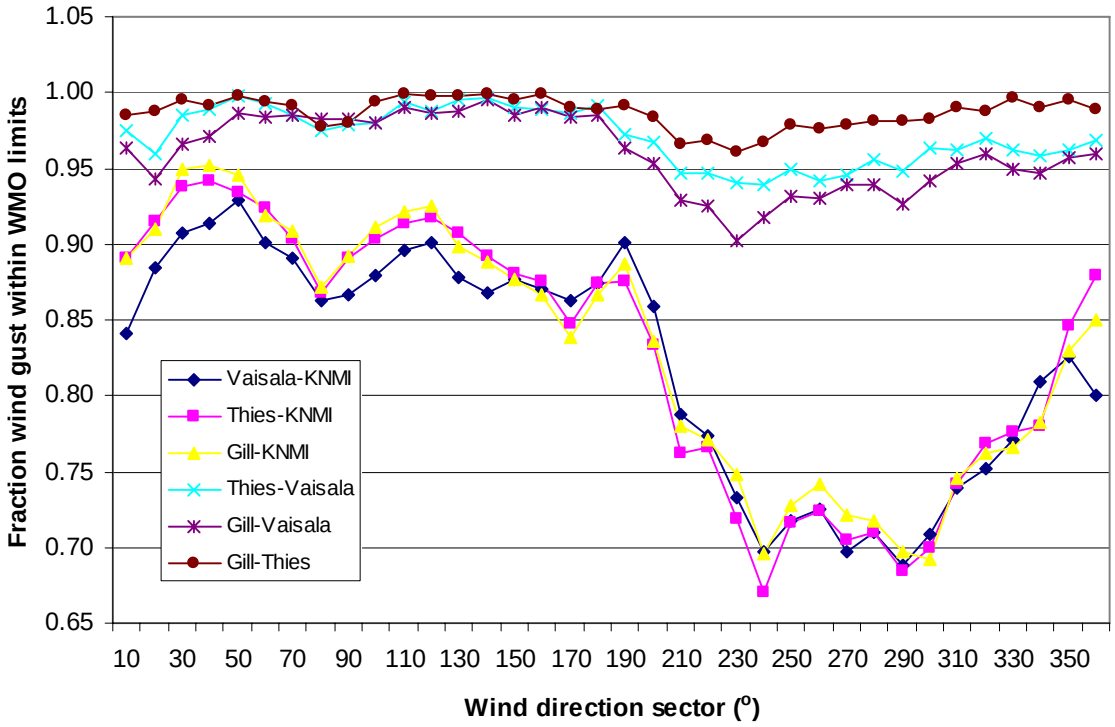


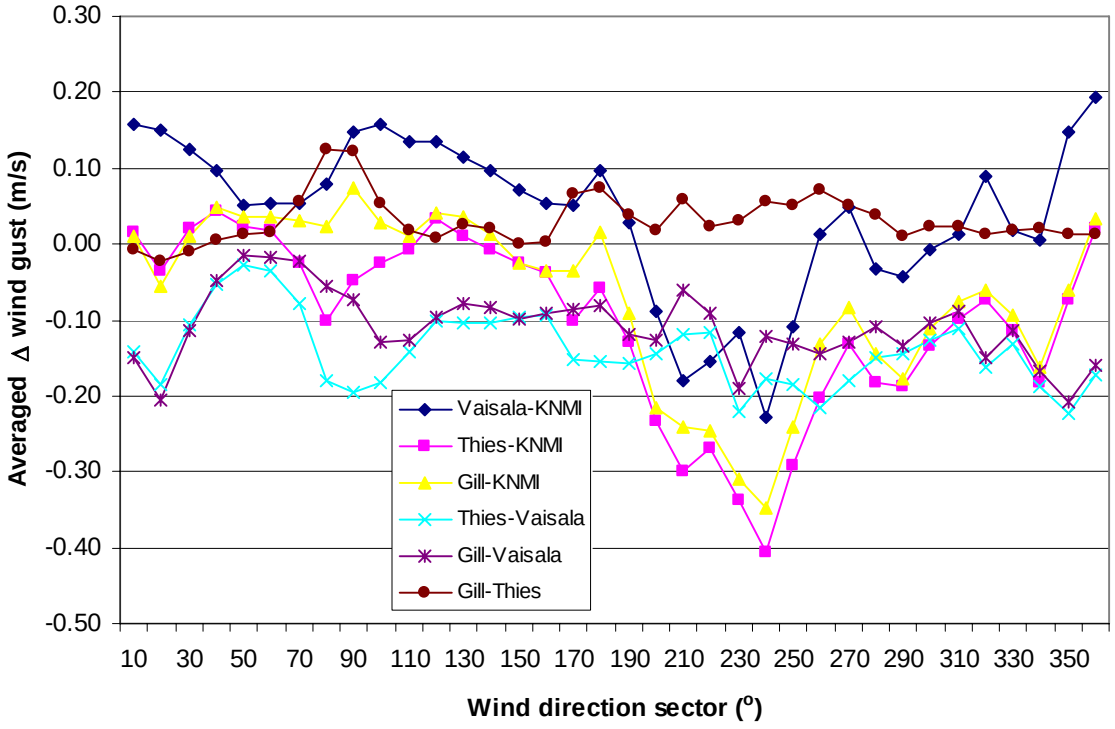

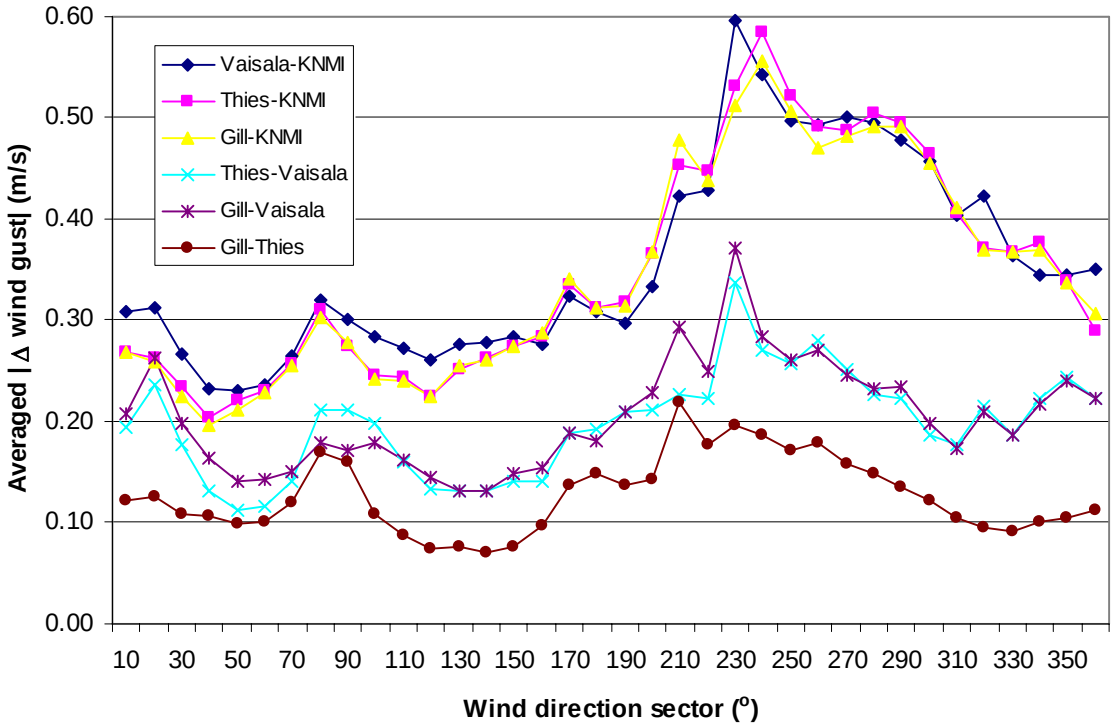
Vaisala-KNMI
Thies-KNMI
Gill-KNMI
Thies-Vaisala
Gill-Vaisala
Gill-Thies
Averaged | Δ wind gust| (m/s)
0.00
0.10
0.20
0.30
0.40
0.50
0.60
10 30 50 70 90 110 130 150 170 190 210 230 250 270 290 310 330 350
Wind direction sector (°)

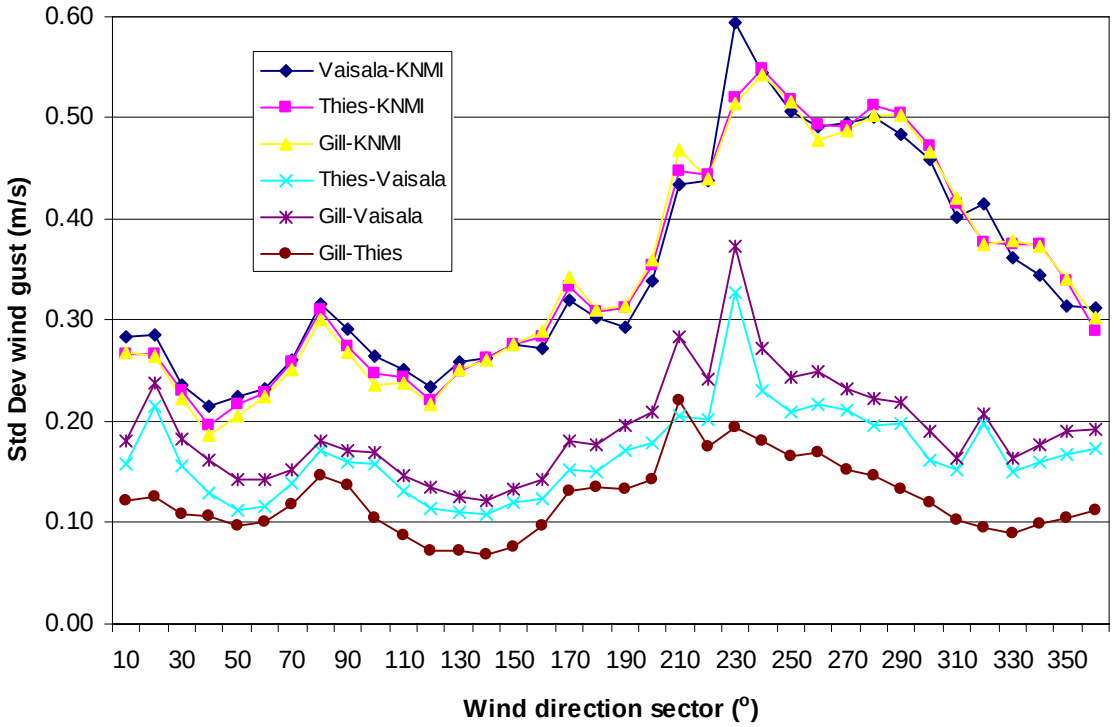
Vaisala-KNMI
Thies-KNMI
Gill-KNMI
Thies-Vaisala
Gill-Vaisala
Gill-Thies
Std Dev wind gust (m/s)
0.00
0.10
0.20
0.30
0.40
0.50
0.60
10 30 50 70 90 110 130 150 170 190 210 230 250 270 290 310 330 350
Wind direction sector (°)

## *Wind gust (wind speed>2m/s)*

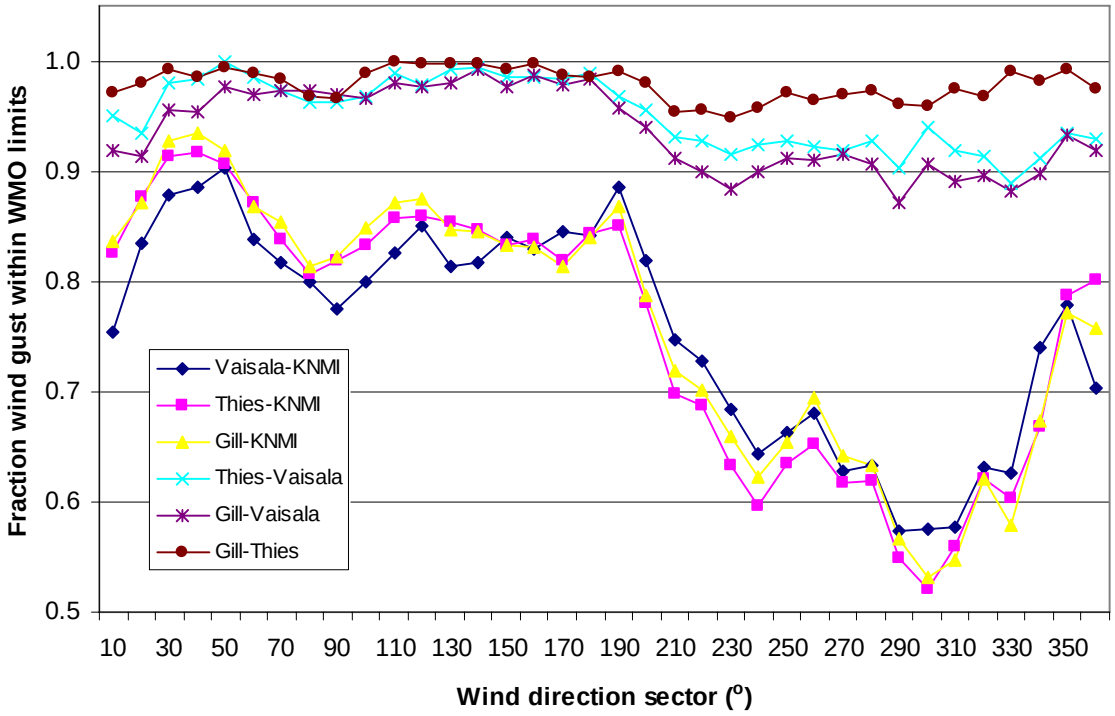


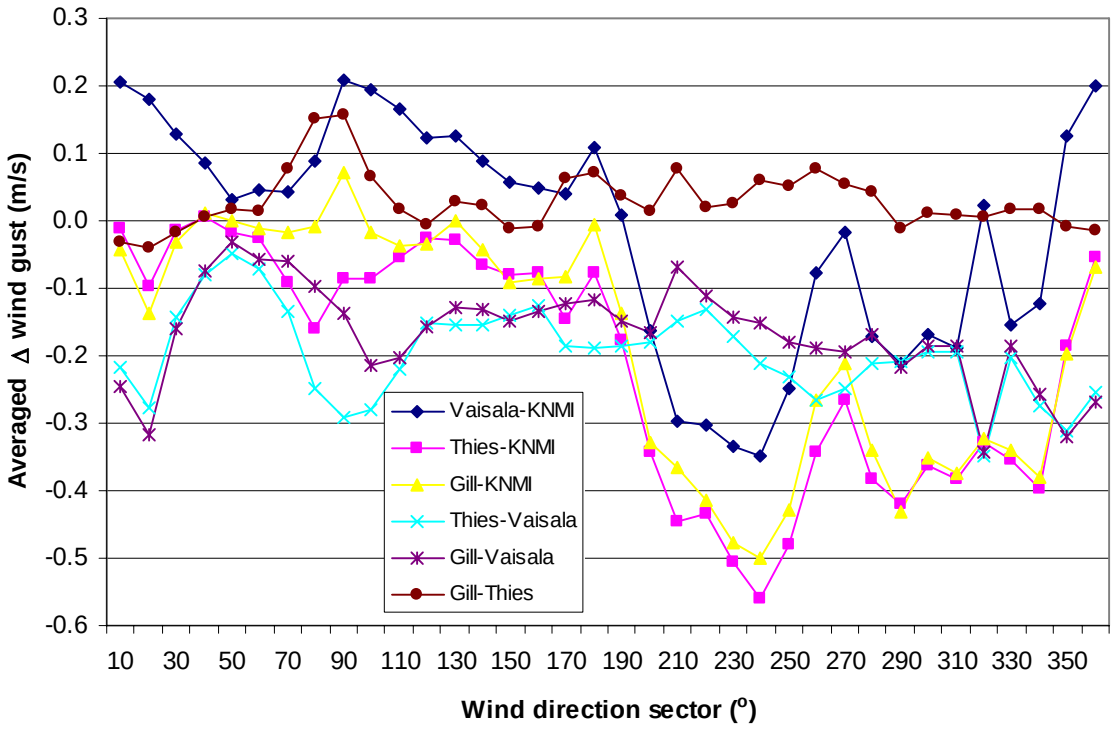

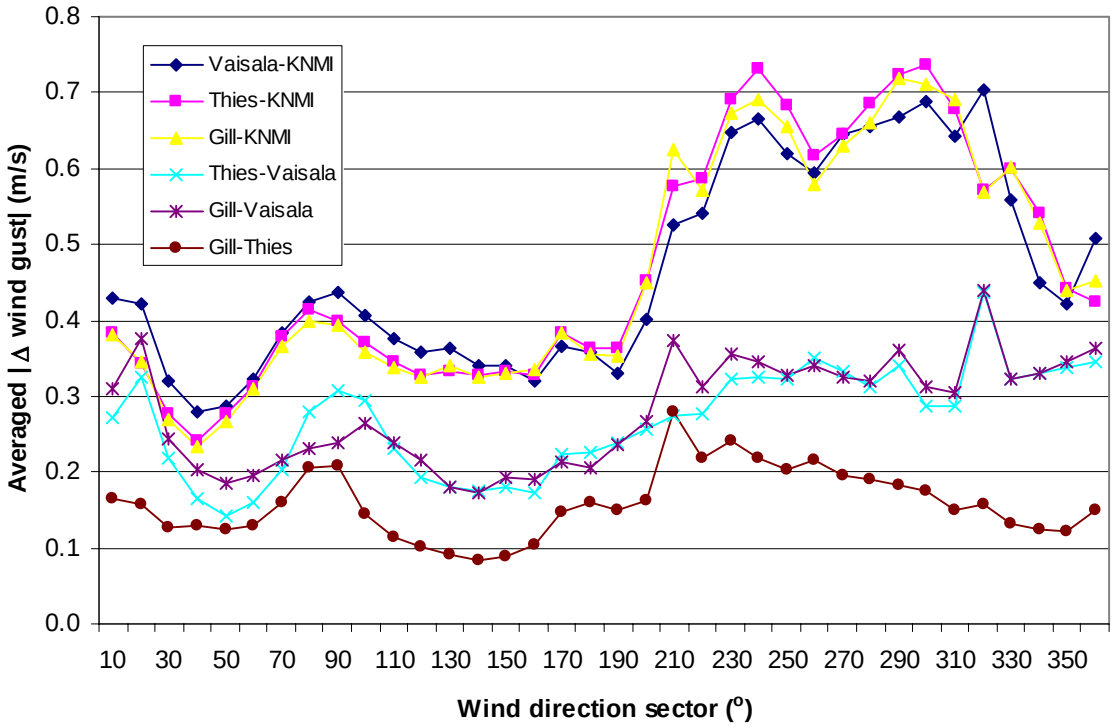
Vaisala-KNMI
Thies-KNMI
Gill-KNMI
Thies-Vaisala
Gill-Vaisala
Gill-Thies
Averaged | Δ wind gust| (m/s)
0.0
0.1
0.2
0.3
0.4
0.5
0.6
0.7
0.8
10 30 50 70 90 110 130 150 170 190 210 230 250 270 290 310 330 350
Wind direction sector (°)

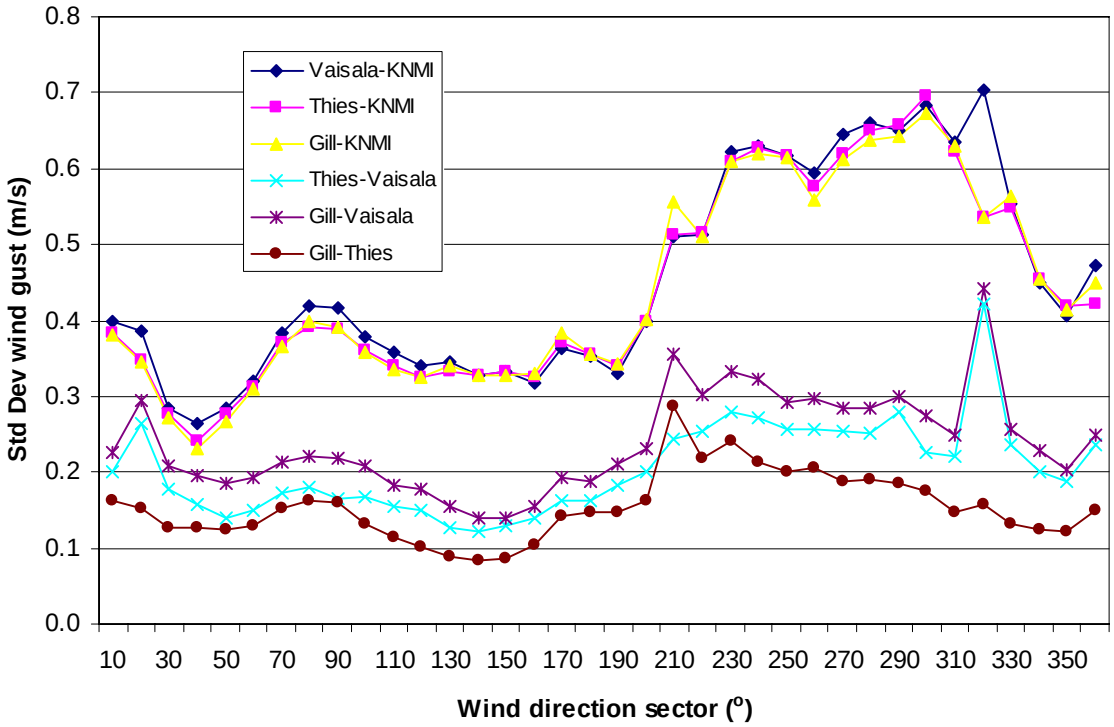
Vaisala-KNMI
Thies-KNMI
Gill-KNMI
Thies-Vaisala
Gill-Vaisala
Gill-Thies
Std Dev wind gust (m/s)
0.0
0.1
0.2
0.3
0.4
0.5
0.6
0.7
0.8
10 30 50 70 90 110 130 150 170 190 210 230 250 270 290 310 330 350
Wind direction sector (°)

# Appendix D2: Field data as a function of wind speed

In this appendix the field test results for the 10-minute averaged wind direction, wind speed and wind gust are presented as a function of wind speed. For that purpose, the results are binned in 0.5m/s intervals, w.r.t. the wind speed reported by the KNMI cup anemometer. All 10-minute intervals are considered where the wind variables of all 4 sensors are valid, i.e. less than 10% of the data is missing. The number of cases for each wind sector are given in the figure below. Note that for wind speeds exceeding 6.5m/s less than 100 cases are available for each bin.

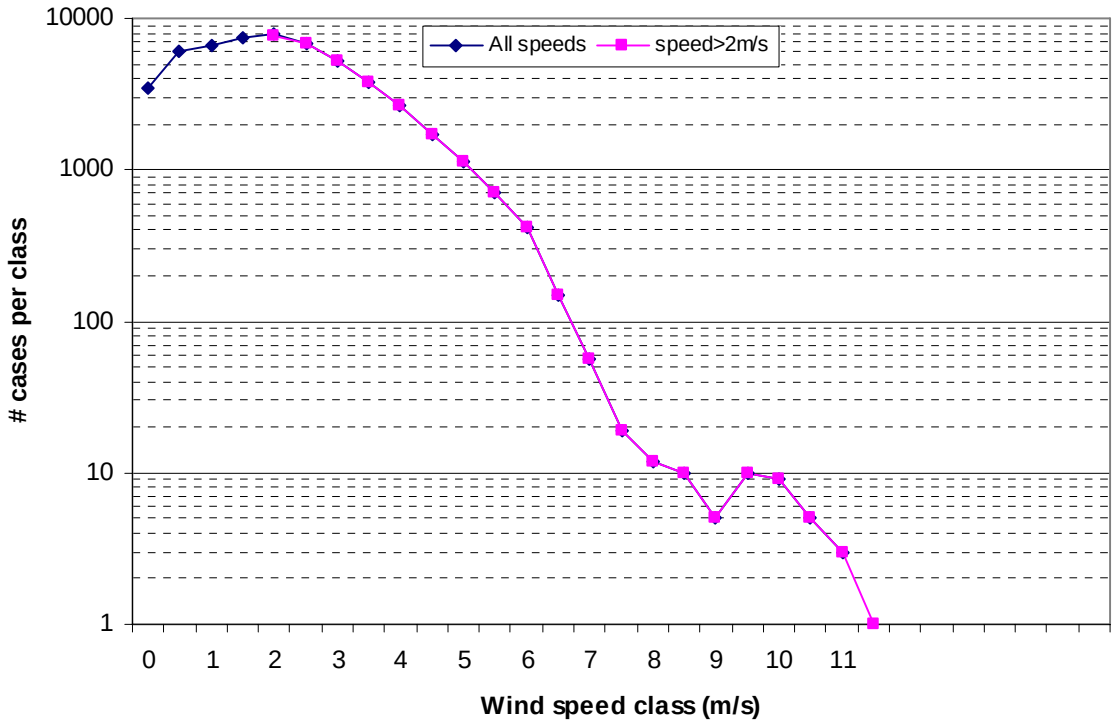


In the sections below the results for wind direction, wind speed and wind gust are reported, respectively. The differences between the sonic anemometers and the conventional wind vane and cup anemometer are presented as well as the differences between the sonics themselves. For each of the three wind parameter is shown: (i) the fraction of the cases with differences within the WMO limits; (ii) the averaged differences; (iii) the averaged absolute differences and; (iv) the standard deviation of the differences.

## *Wind direction*

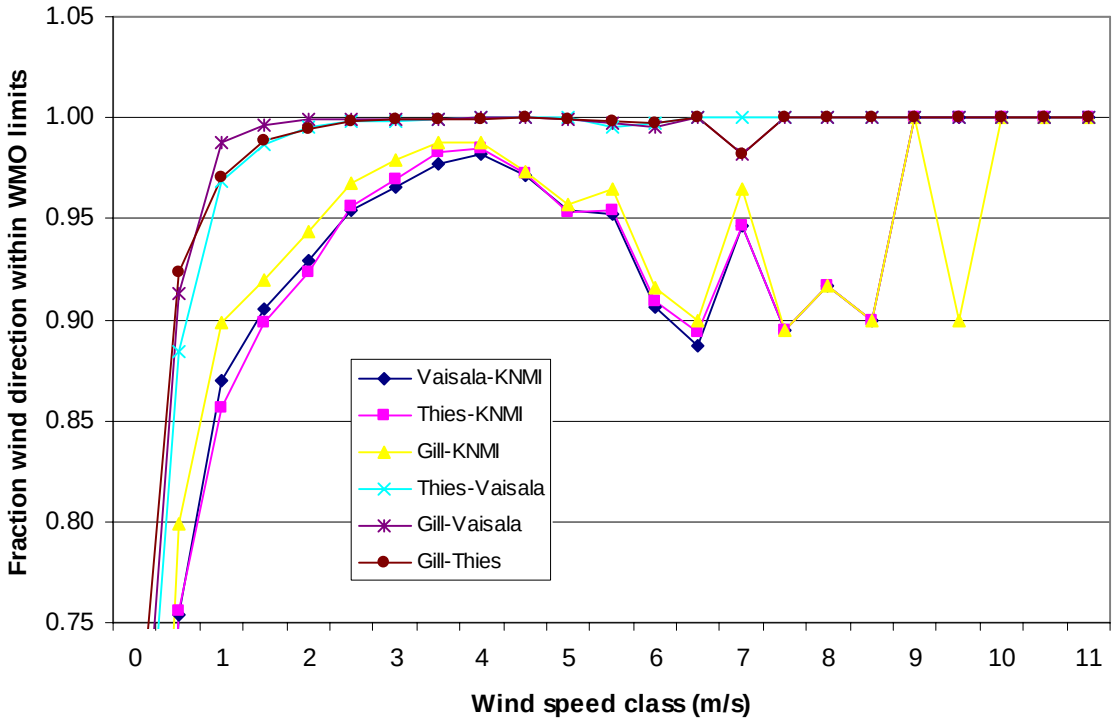


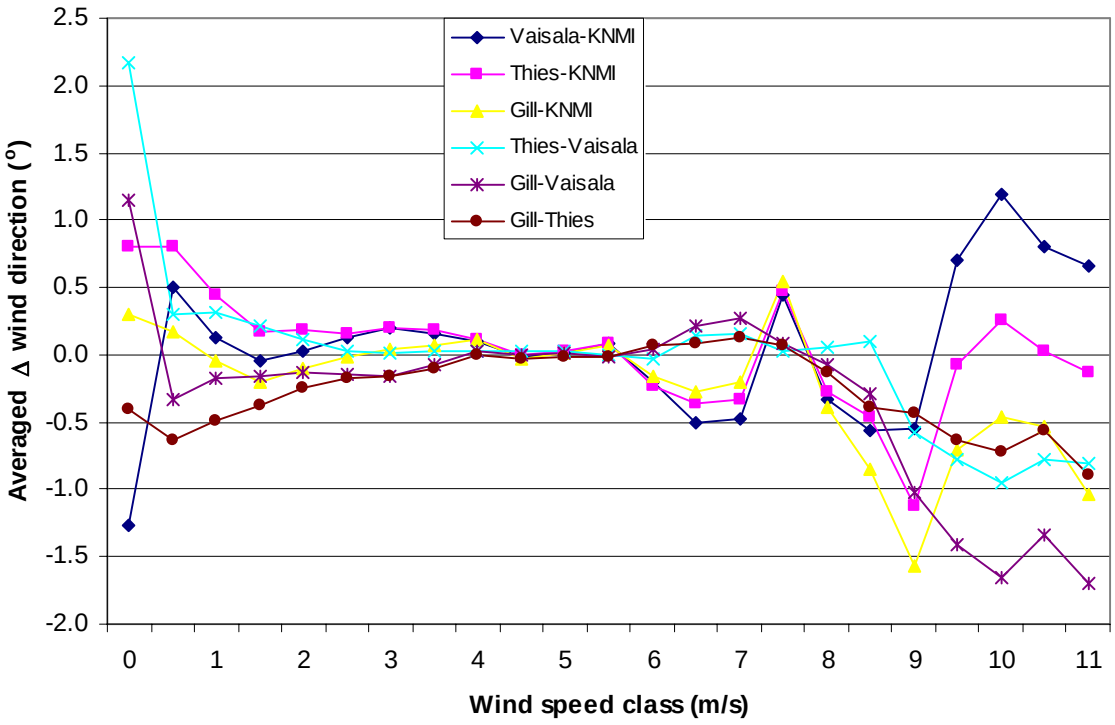

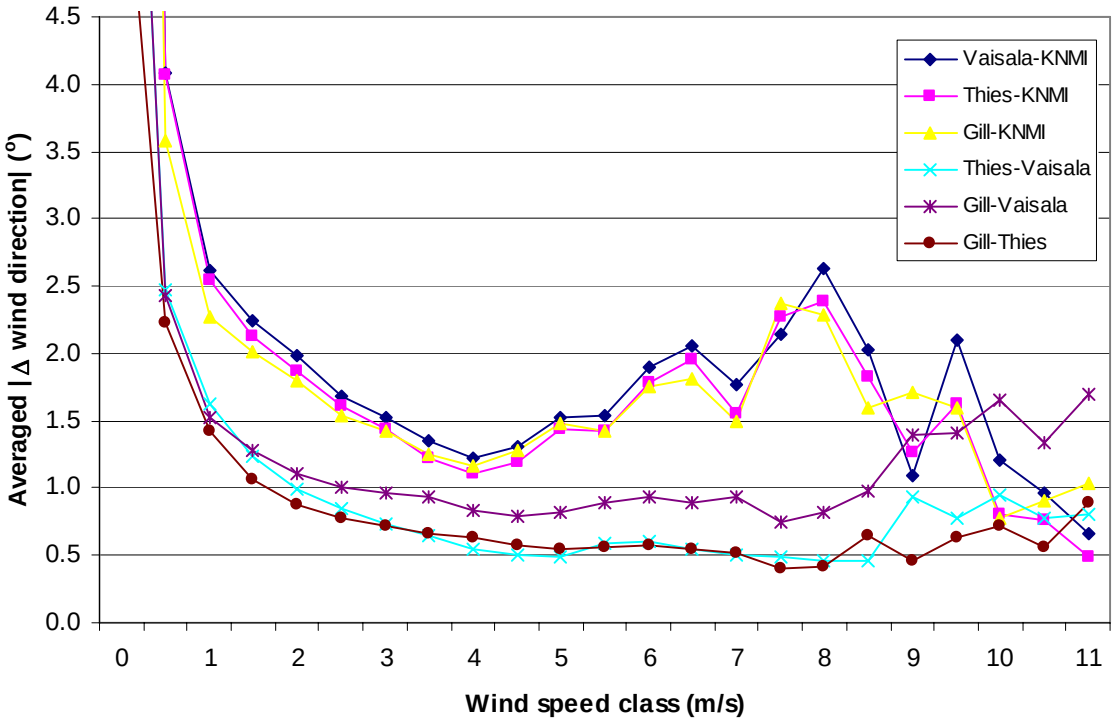
Averaged | Δ wind direction| (°)
Wind speed class (m/s)
Vaisala-KNMI
Thies-KNMI
Gill-KNMI
Thies-Vaisala
Gill-Vaisala
Gill-Thies

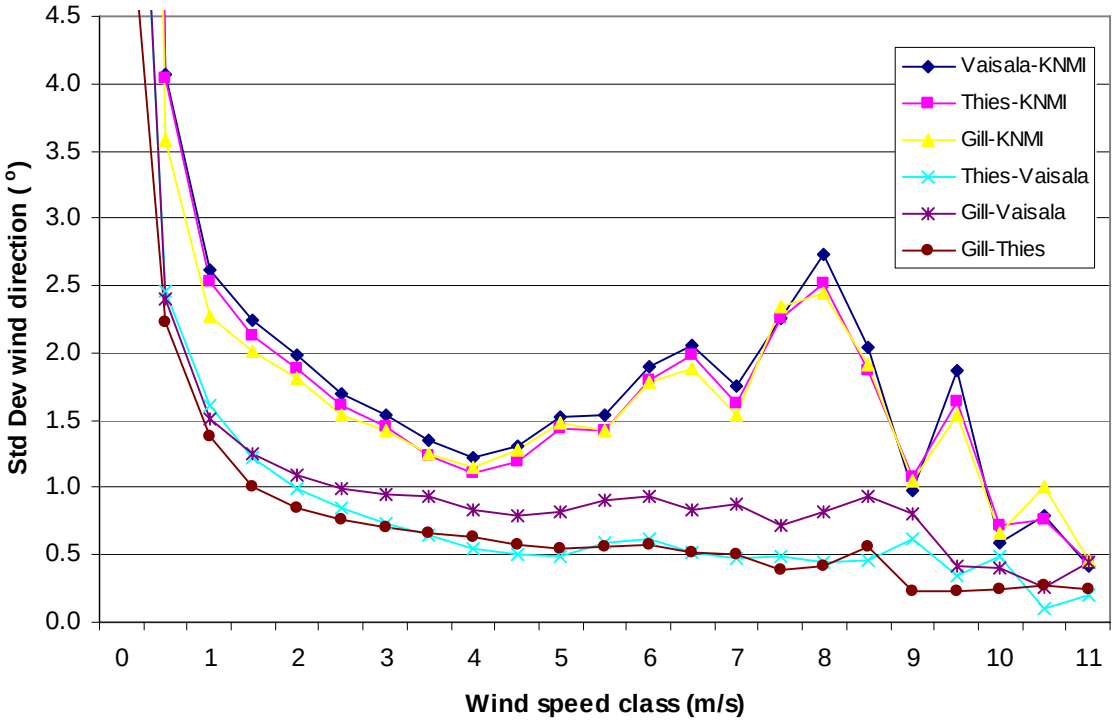
Std Dev wind direction (°)
Wind speed class (m/s)
Vaisala-KNMI
Thies-KNMI
Gill-KNMI
Thies-Vaisala
Gill-Vaisala
Gill-Thies

## *Wind speed*

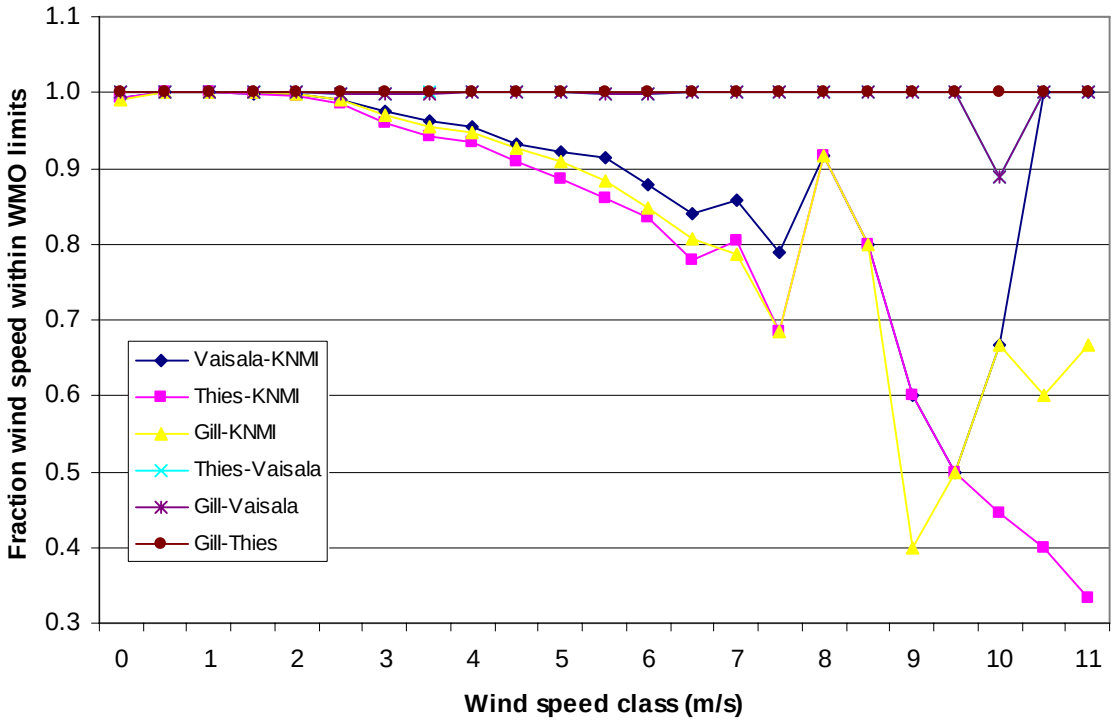
Fraction wind speed within WMO limits
1.1
1.0
0.9
0.8
0.7
0.6
0.5
0.4
0.3
0
1
2
3
4
5
6
7
8
9
10
11
Wind speed class (m/s)
Vaisala-KNMI
Thies-KNMI
Gill-KNMI
Thies-Vaisala
Gill-Vaisala
Gill-Thies

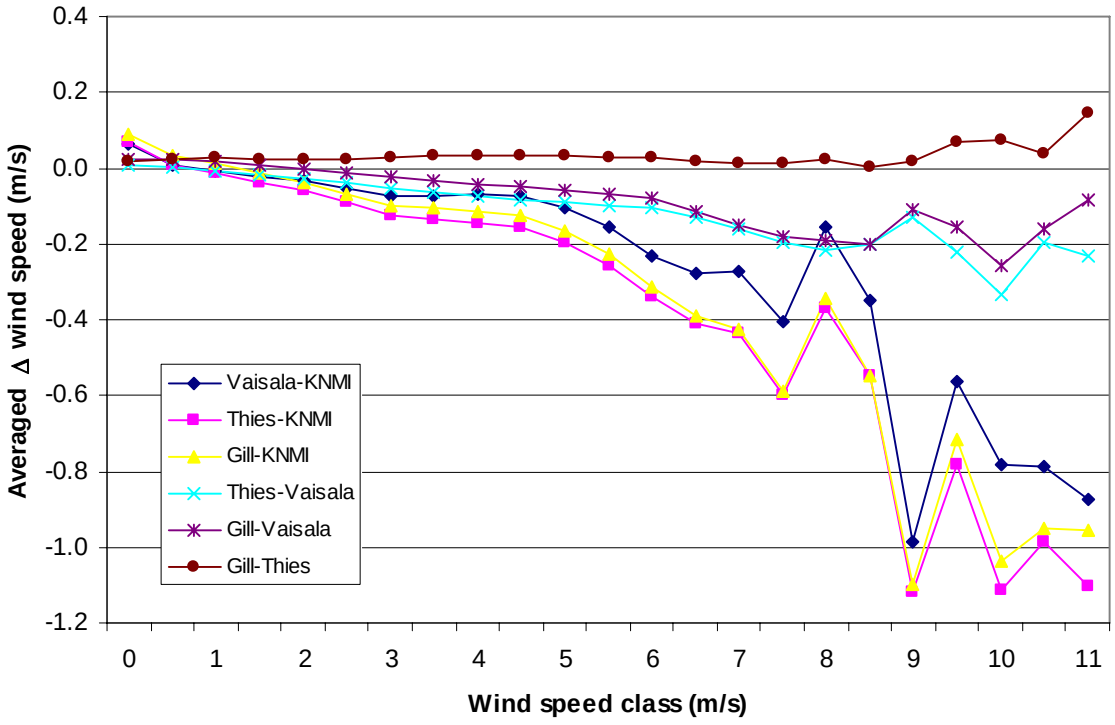
Averaged Δ wind speed (m/s)
0.4
0.2
0.0
-0.2
-0.4
-0.6
-0.8
-1.0
-1.2
0
1
2
3
4
5
6
7
8
9
10
11
Wind speed class (m/s)
Vaisala-KNMI
Thies-KNMI
Gill-KNMI
Thies-Vaisala
Gill-Vaisala
Gill-Thies

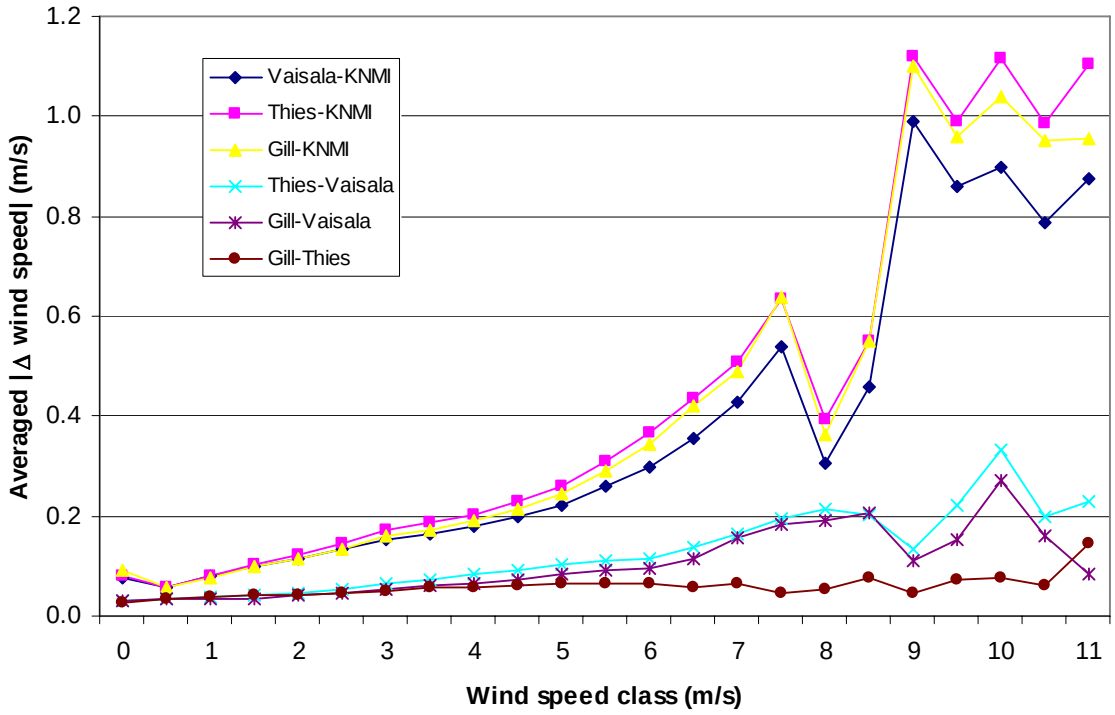
Vaisala-KNMI
Thies-KNMI
Gill-KNMI
Thies-Vaisala
Gill-Vaisala
Gill-Thies
Averaged |Δ wind speed| (m/s)
Wind speed class (m/s)
0.0
0.2
0.4
0.6
0.8
1.0
1.2
0
1
2
3
4
5
6
7
8
9
10
11

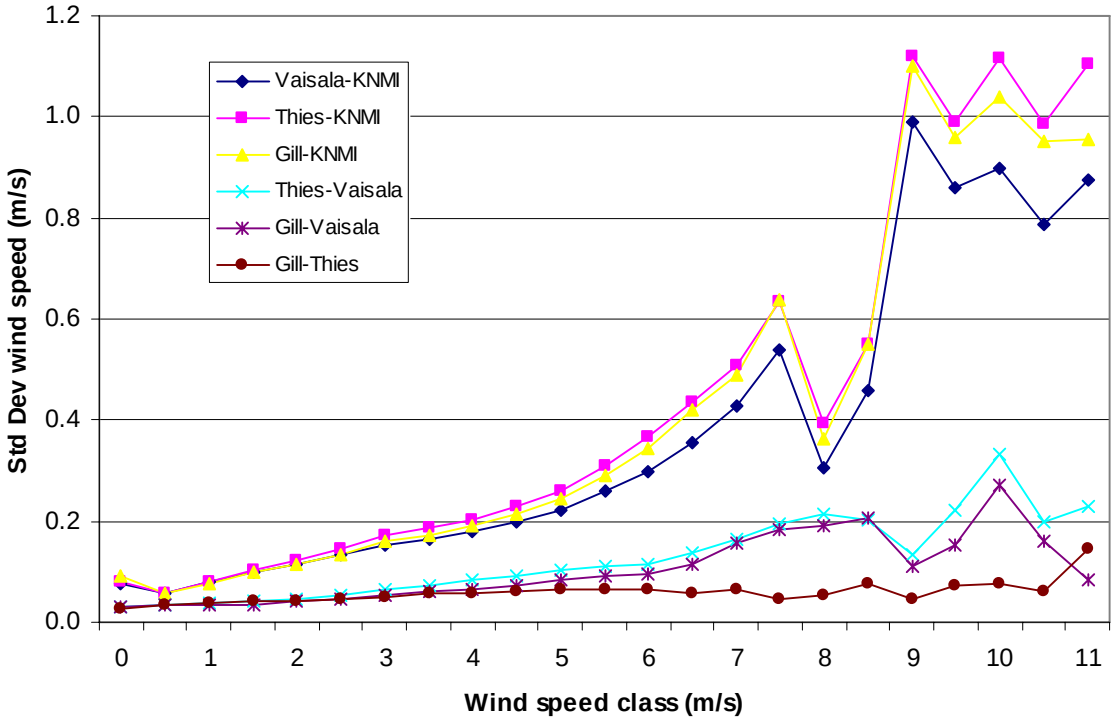
Vaisala-KNMI
Thies-KNMI
Gill-KNMI
Thies-Vaisala
Gill-Vaisala
Gill-Thies
Std Dev wind speed (m/s)
Wind speed class (m/s)
0.0
0.2
0.4
0.6
0.8
1.0
1.2
0
1
2
3
4
5
6
7
8
9
10
11

## *Wind gust*

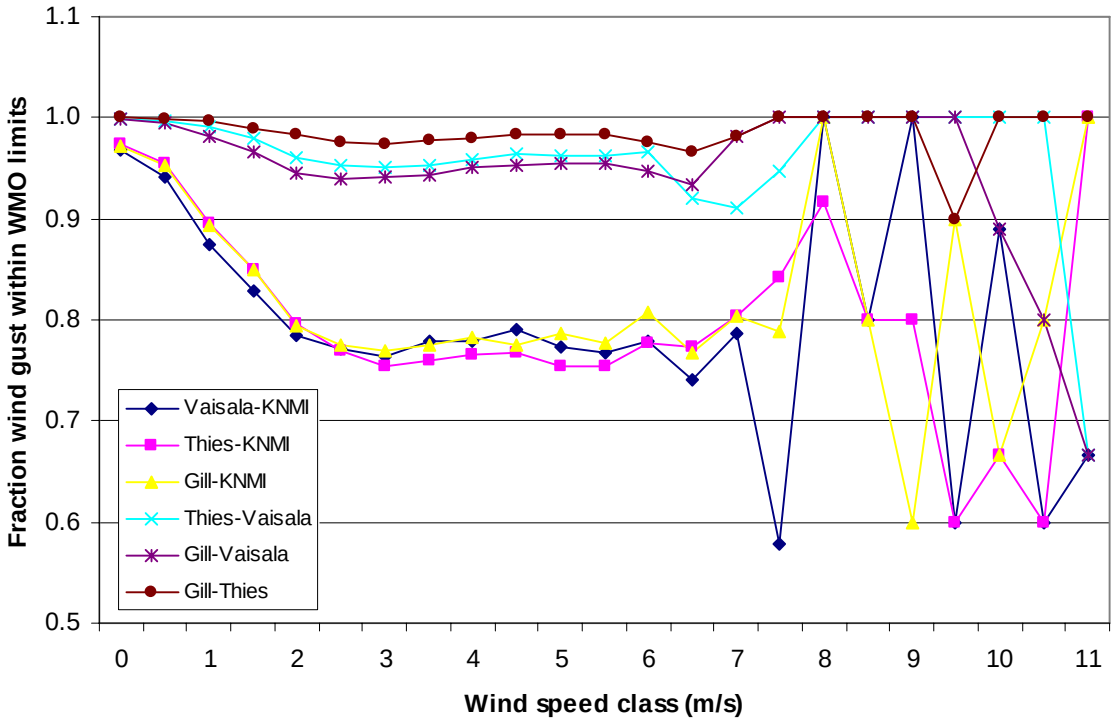
Fraction wind gust within WMO limits
1.1
1.0
0.9
0.8
0.7
0.6
0.5
0
1
2
3
4
5
6
7
8
9
10
11
Wind speed class (m/s)
Vaisala-KNMI
Thies-KNMI
Gill-KNMI
Thies-Vaisala
Gill-Vaisala
Gill-Thies

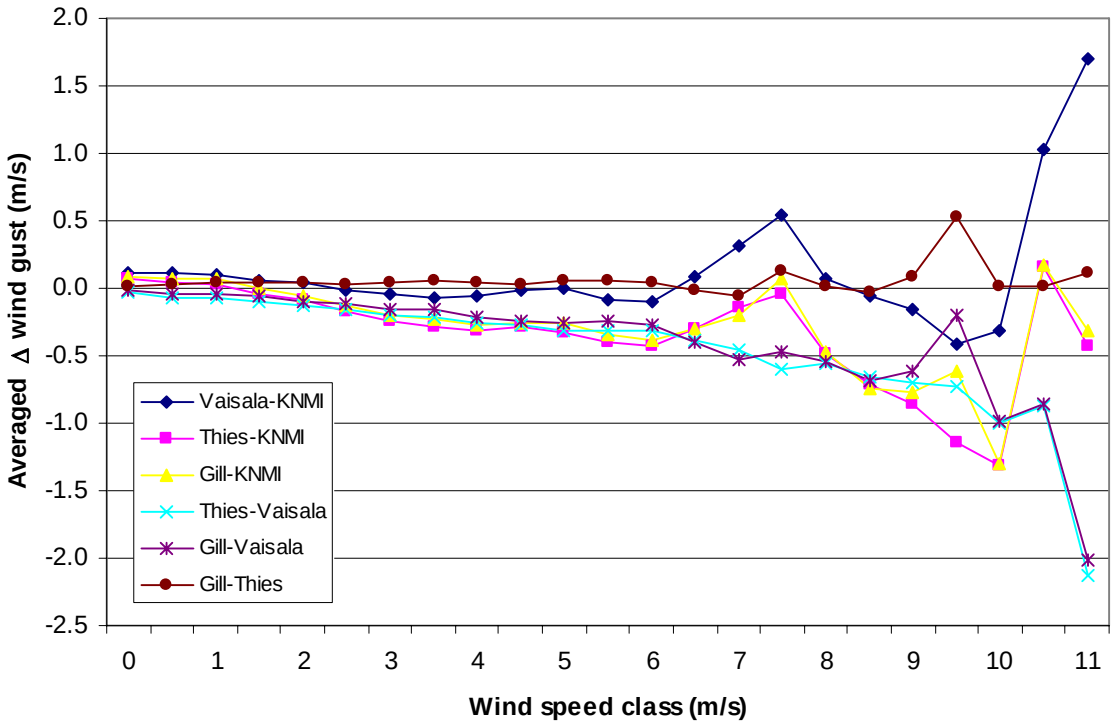
Averaged Δ wind gust (m/s)
2.0
1.5
1.0
0.5
0.0
-0.5
-1.0
-1.5
-2.0
-2.5
0
1
2
3
4
5
6
7
8
9
10
11
Wind speed class (m/s)
Vaisala-KNMI
Thies-KNMI
Gill-KNMI
Thies-Vaisala
Gill-Vaisala
Gill-Thies

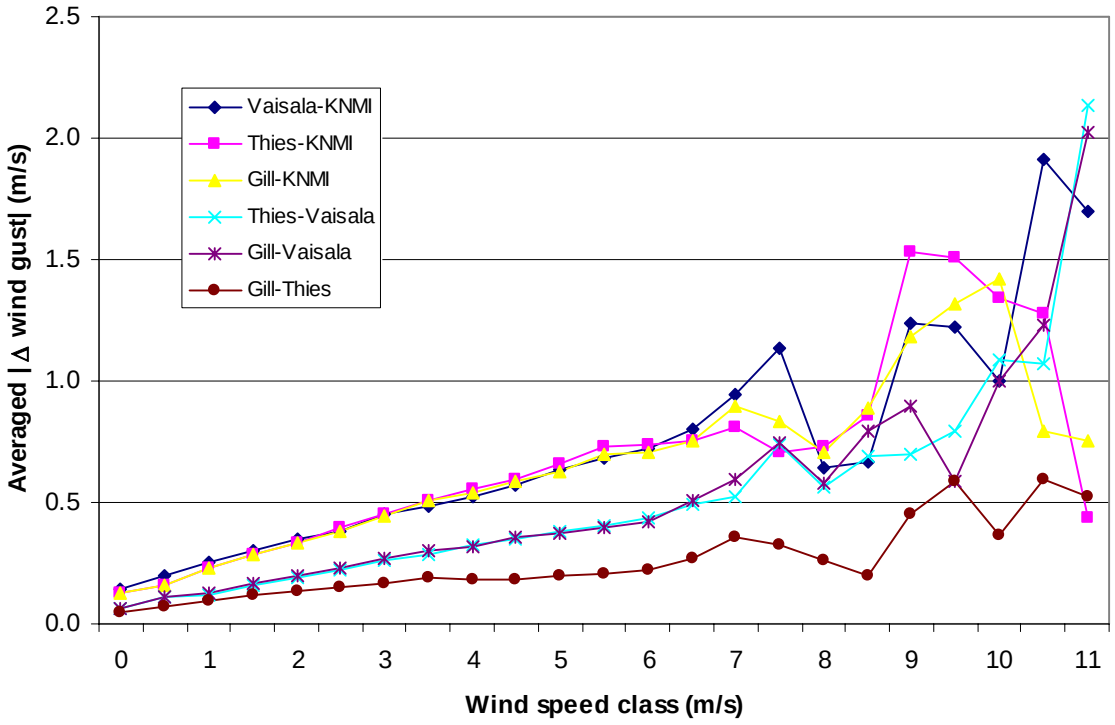
Averaged | Δ wind gust| (m/s)
Wind speed class (m/s)
Vaisala-KNMI
Thies-KNMI
Gill-KNMI
Thies-Vaisala
Gill-Vaisala
Gill-Thies

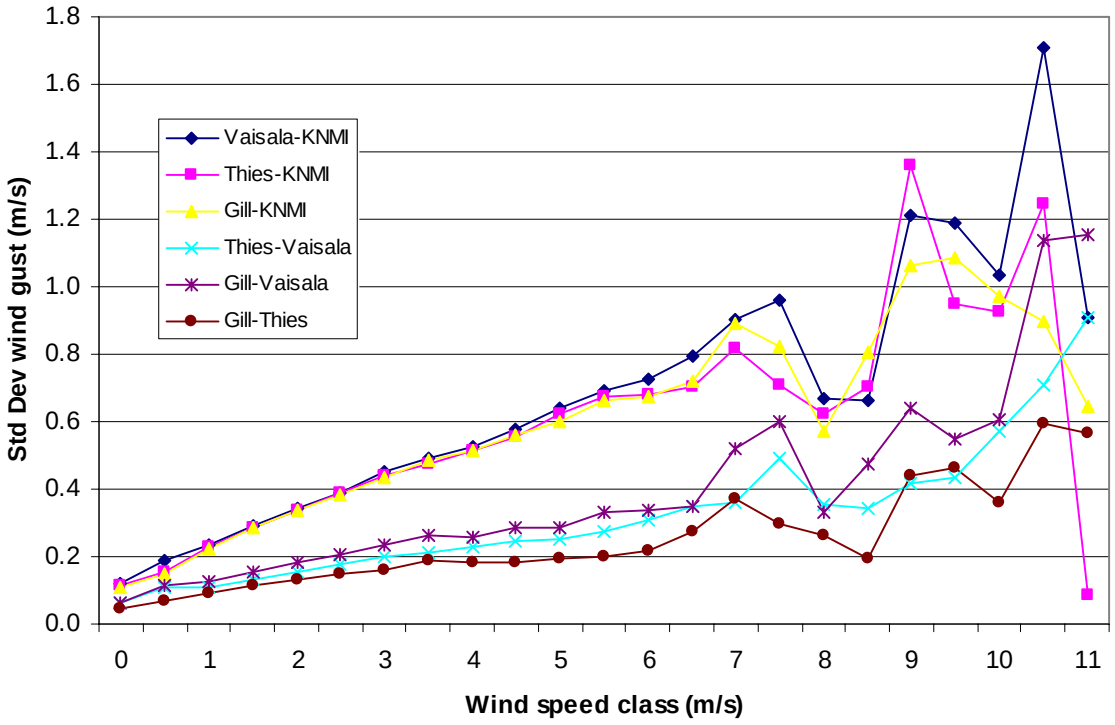
Std Dev wind gust (m/s)
Wind speed class (m/s)
Vaisala-KNMI
Thies-KNMI
Gill-KNMI
Thies-Vaisala
Gill-Vaisala
Gill-Thies

# Appendix D3: Field data as a function of precipitation intensity and type

In this appendix the field test results for the 10-minute averaged wind direction, wind speed and wind gust are presented as a function of precipitation intensity and type. For that purpose, the results are binned w.r.t. the 10-minute precipitation intensiy and type reported by the Vaisala FD12P present waether sensor. All 10-minute intervals are considered where the wind variables of all 4 sensors and the present waether sensor are valid, i.e. less than 10% of the data is missing. The precipiation intensity classes considered here are: NP (no precipitation, intensity=0), TR (traces, intensity<0.05mm/h), 0 (intensity ≥0.05 and less than 0.5mm/h, i.e. rounded down to 0), 1-10 (intensity rounded to 1mm/h intervals, where the largest intensity class 10 also includes all higher intensities). The precipiation type classes considered are: AP (all precipitation types), LP (liquid precipitation); SP (solid precipitation, including mixtures); UP (unidentified precipitation). Finally the class All denotes the results for all cases regardless the precipitation intensity or type class. Note that the number of cases in bins with intensities exceeding 5mm/h is less than 100, and the number of cases with solid or unidentified preciptiation type is only about 200.

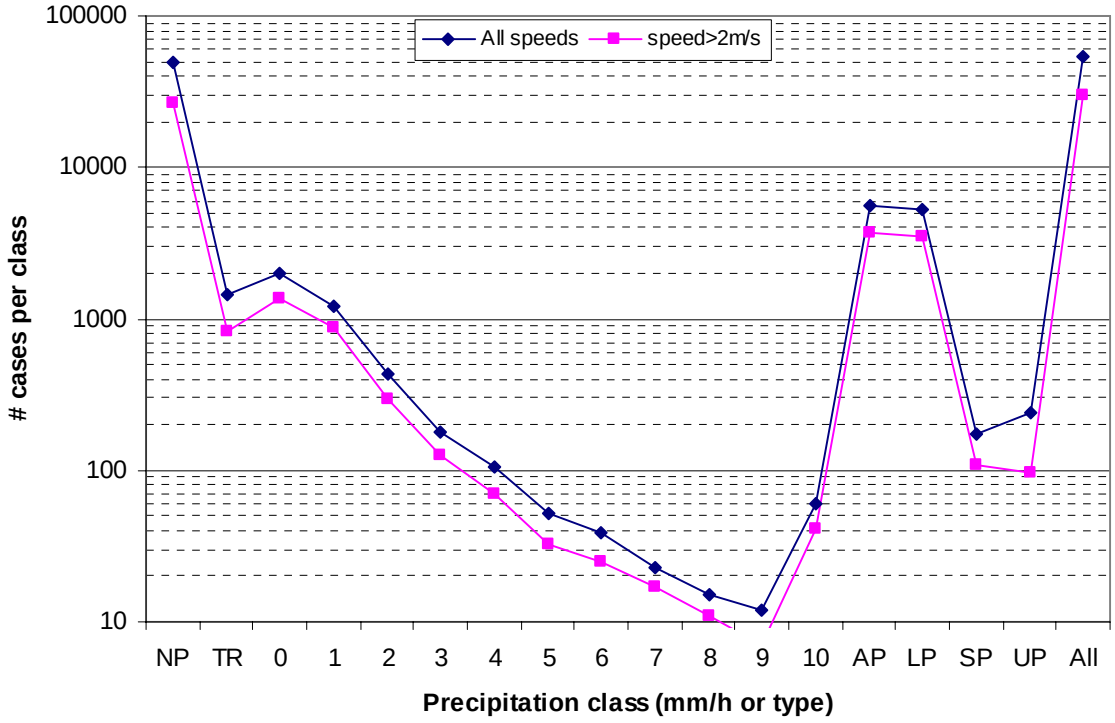


In the sections below the results for wind direction, wind speed and wind gust are reported, respectively. The differences between the sonic anemometers and the conventional wind vane and cup anemometer are presented as well as the differences between the sonics themselves. For each of the three wind parameter is shown: (i) the fraction of the cases with differences within the WMO limits; (ii) the averaged differences; (iii) the averaged absolute differences and; (iv) the standard deviation of the

differences. The results are given for all wind speeds and for 10-minute averaged wind speeds of the KNMI cup anemometer above 2m/s.

## *Wind direction (all wind speeds)*

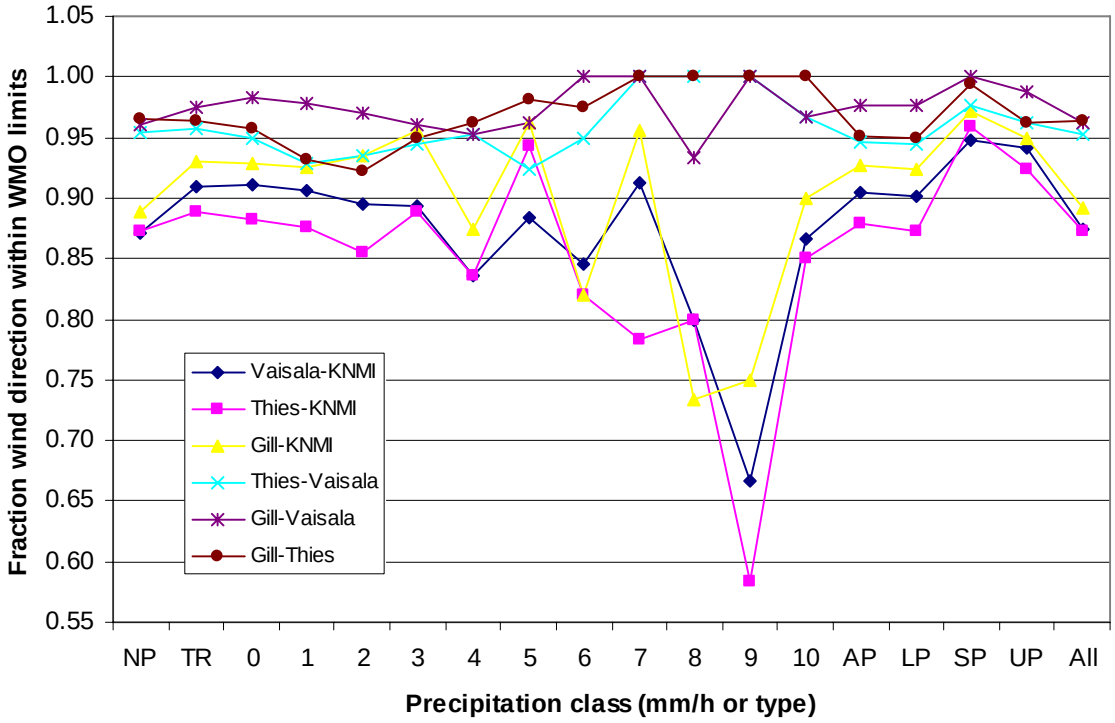


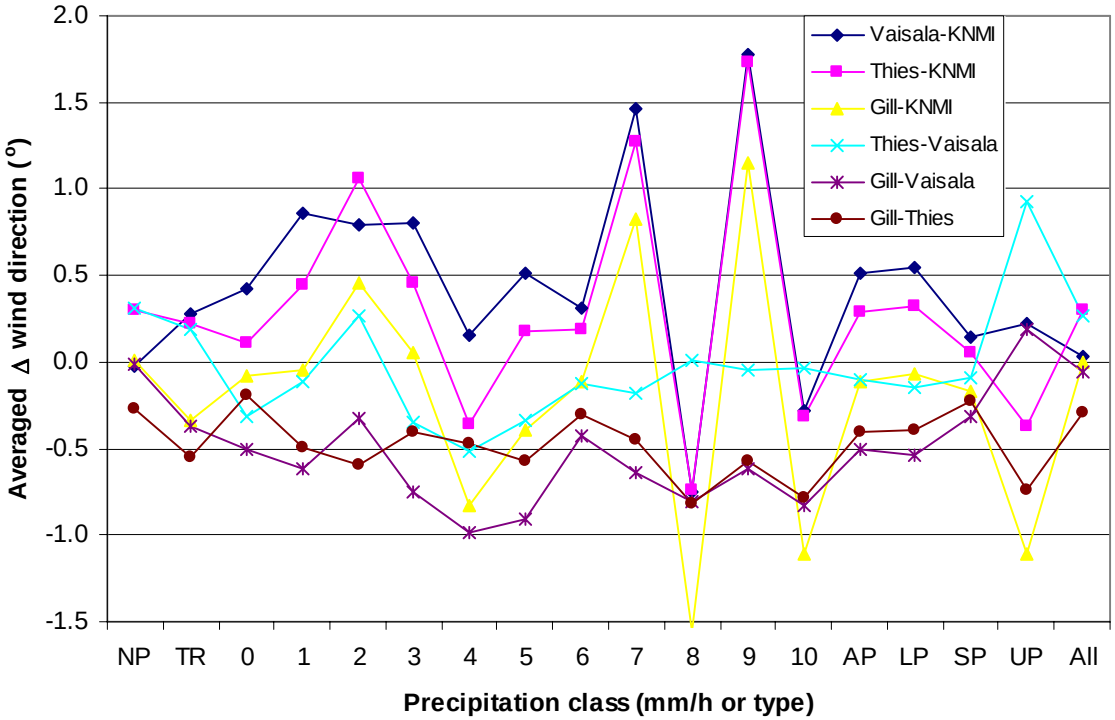

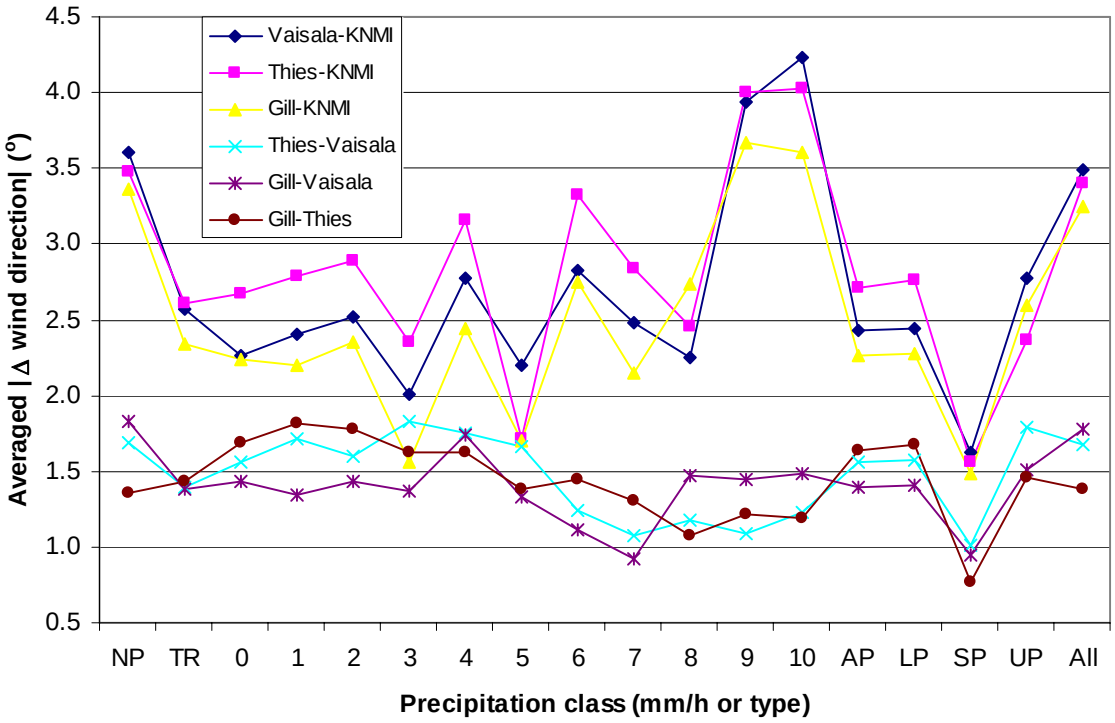
Vaisala-KNMI
Thies-KNMI
Gill-KNMI
Thies-Vaisala
Gill-Vaisala
Gill-Thies
Averaged | Δ wind direction| (°)
4.5
4.0
3.5
3.0
2.5
2.0
1.5
1.0
0.5
NP TR 0 1 2 3 4 5 6 7 8 9 10 AP LP SP UP All
Precipitation class (mm/h or type)

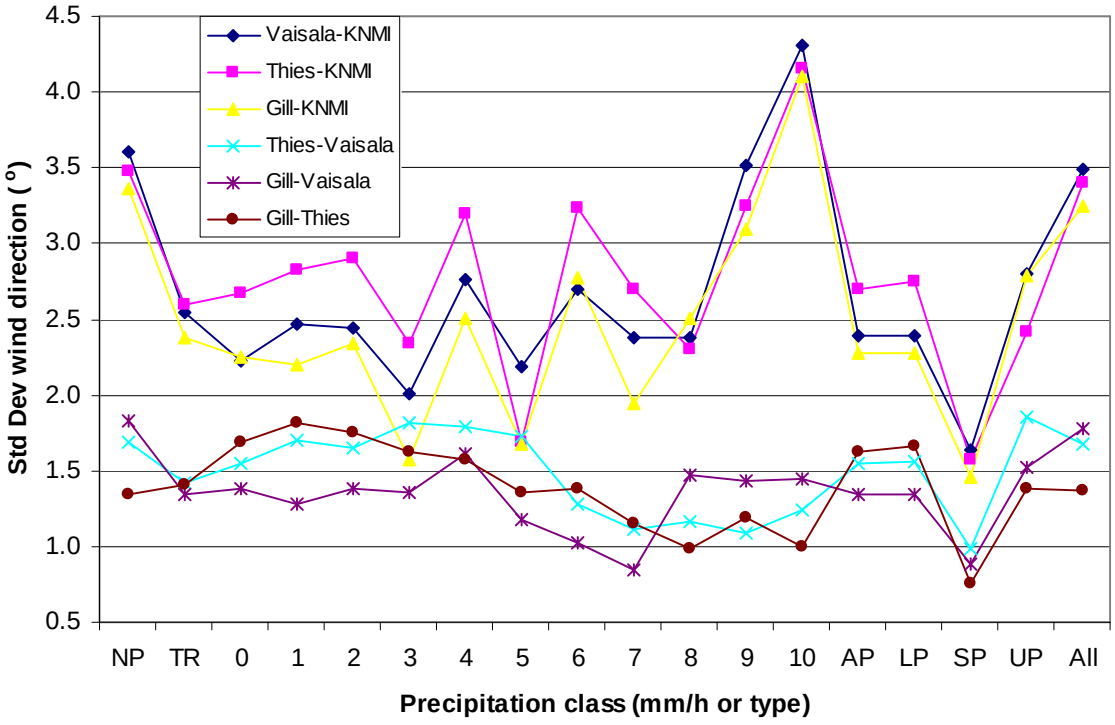
Vaisala-KNMI
Thies-KNMI
Gill-KNMI
Thies-Vaisala
Gill-Vaisala
Gill-Thies
Std Dev wind direction (°)
4.5
4.0
3.5
3.0
2.5
2.0
1.5
1.0
0.5
NP TR 0 1 2 3 4 5 6 7 8 9 10 AP LP SP UP All
Precipitation class (mm/h or type)

## *Wind direction (wind >2m/s)*

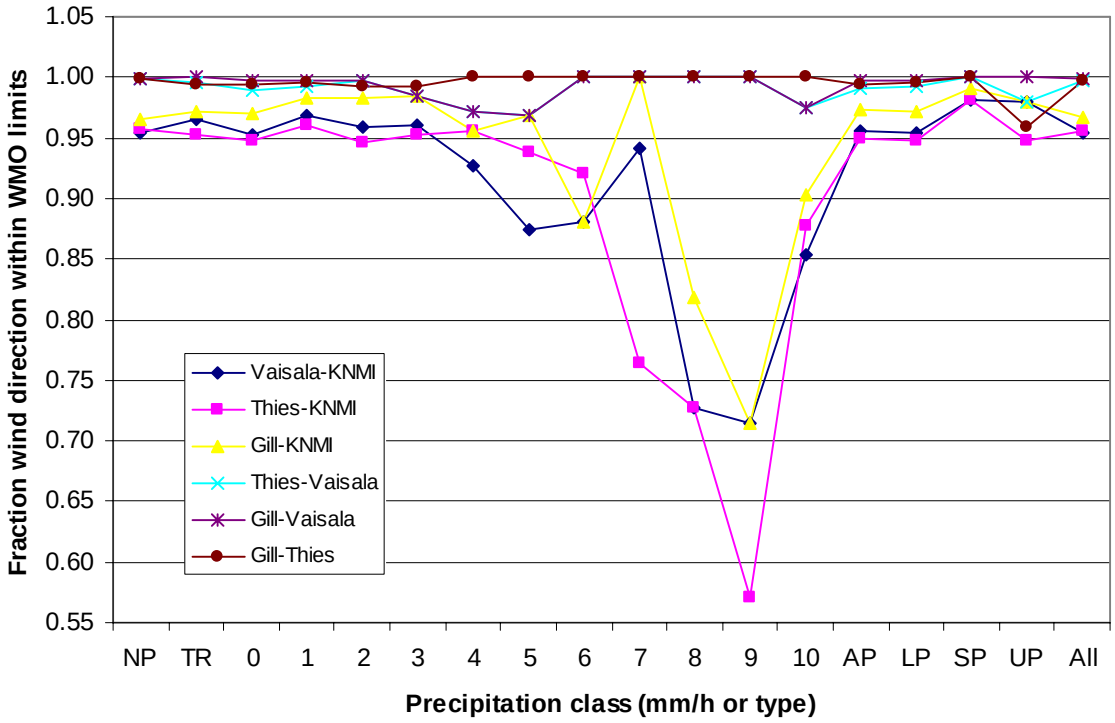


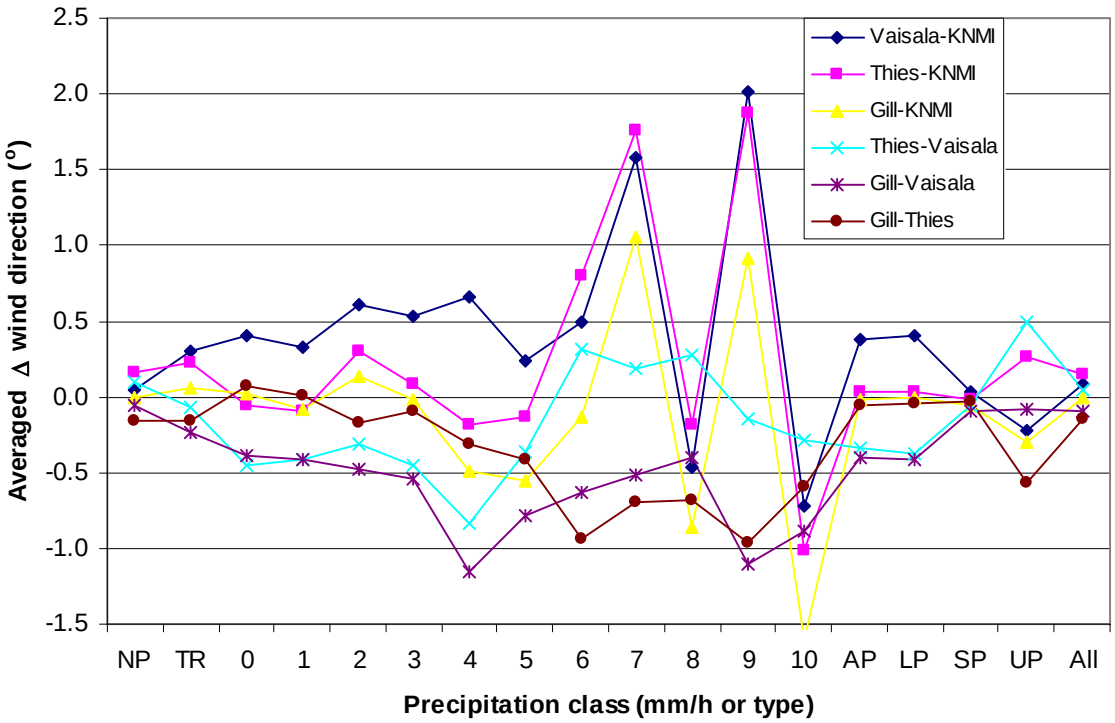

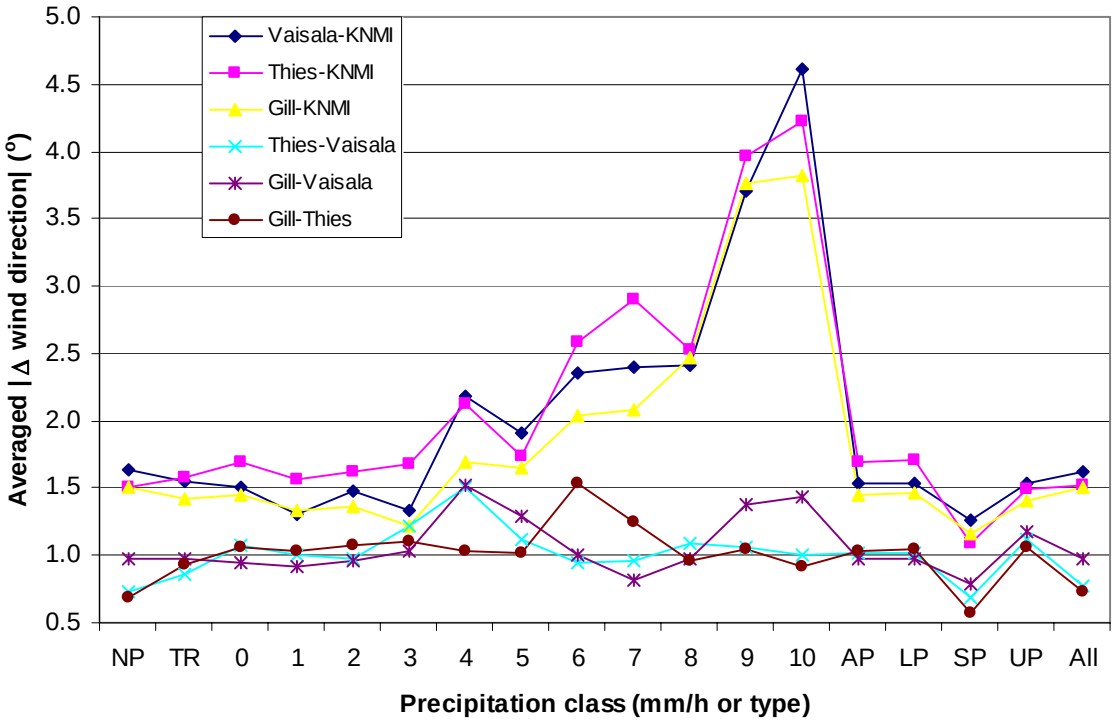
Vaisala-KNMI
Thies-KNMI
Gill-KNMI
Thies-Vaisala
Gill-Vaisala
Gill-Thies
Averaged | Δ wind direction| (°)
5.0
4.5
4.0
3.5
3.0
2.5
2.0
1.5
1.0
0.5
NP TR 0 1 2 3 4 5 6 7 8 9 10 AP LP SP UP All
Precipitation class (mm/h or type)

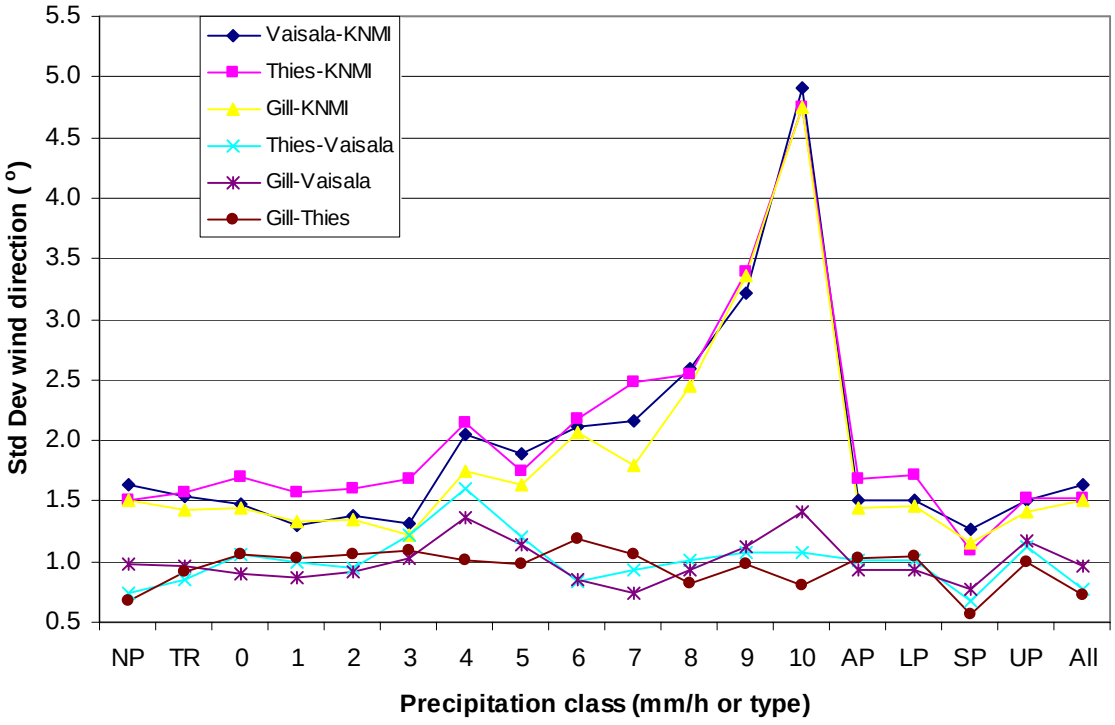
Vaisala-KNMI
Thies-KNMI
Gill-KNMI
Thies-Vaisala
Gill-Vaisala
Gill-Thies
Std Dev wind direction (°)
5.5
5.0
4.5
4.0
3.5
3.0
2.5
2.0
1.5
1.0
0.5
NP TR 0 1 2 3 4 5 6 7 8 9 10 AP LP SP UP All
Precipitation class (mm/h or type)

## *Wind speed (all wind speeds)*

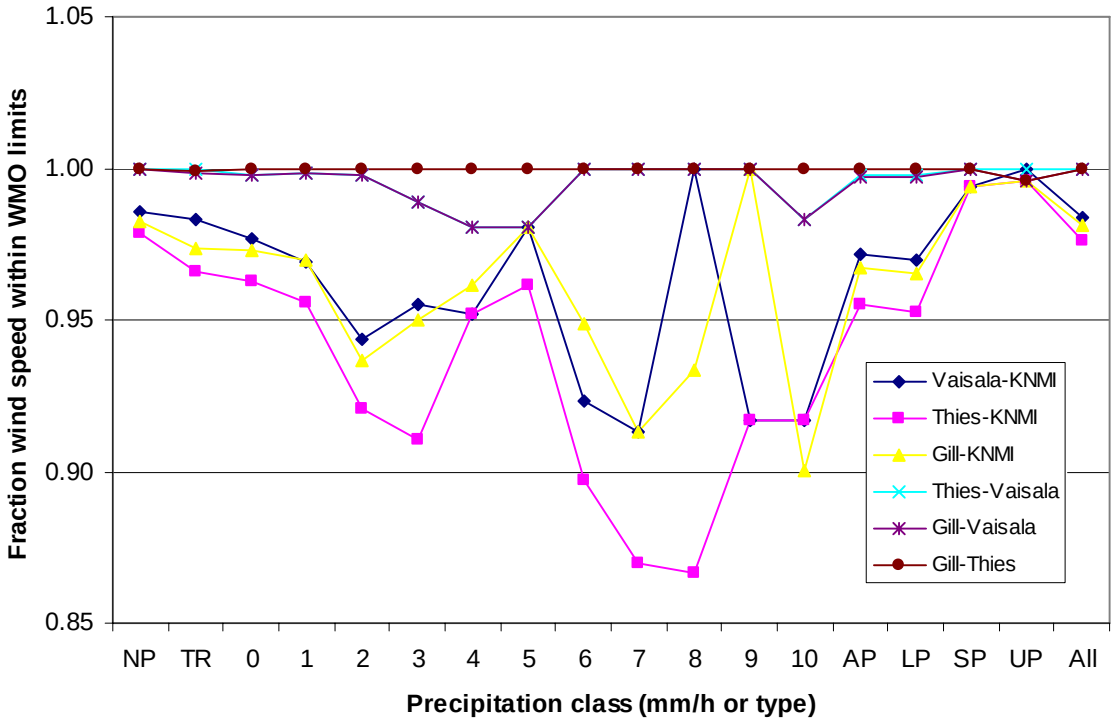


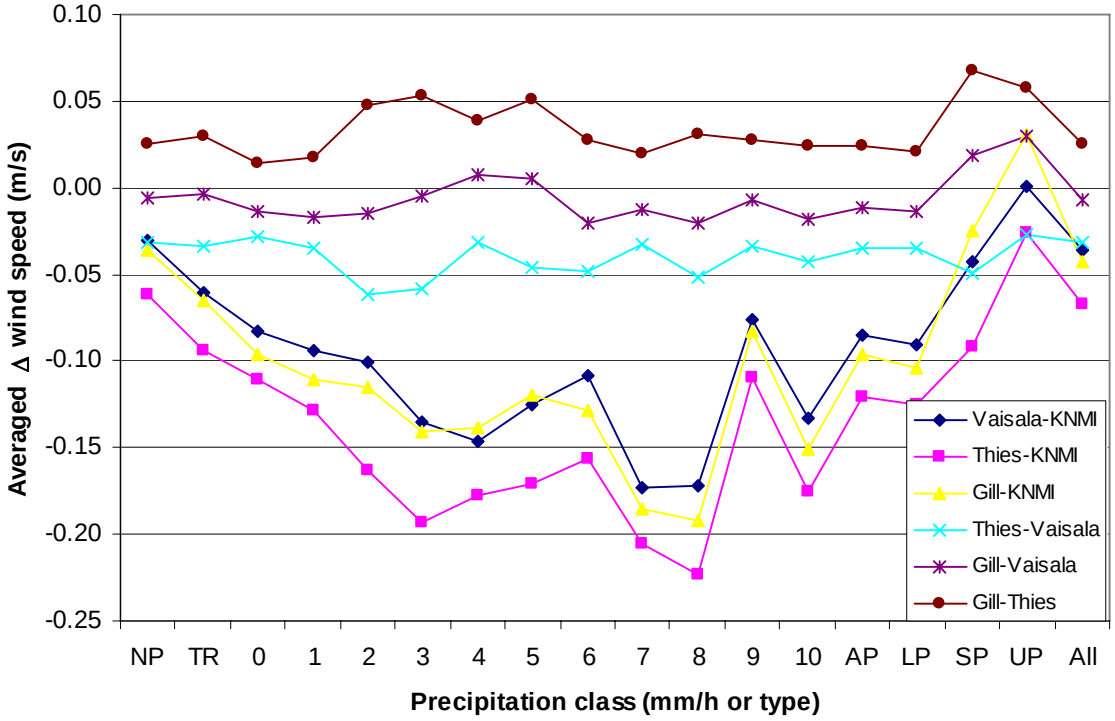

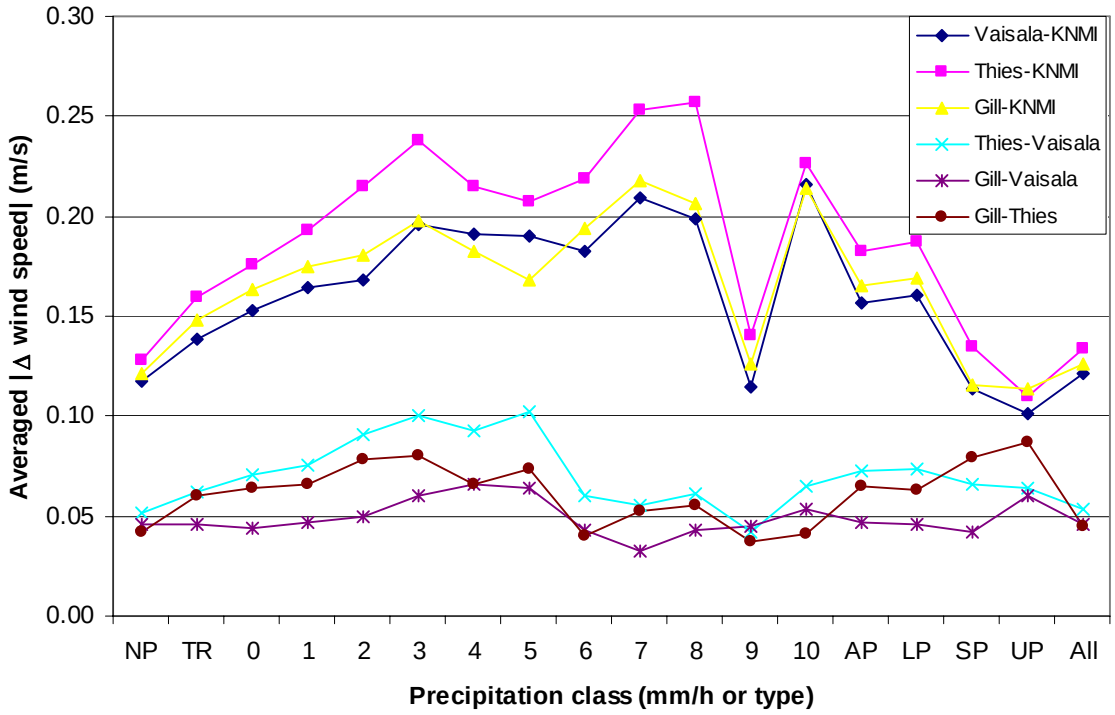
0.30
0.25
0.20
0.15
0.10
0.05
0.00
Averaged |Δ wind speed| (m/s)
Vaisala-KNMI
Thies-KNMI
Gill-KNMI
Thies-Vaisala
Gill-Vaisala
Gill-Thies
NP TR 0 1 2 3 4 5 6 7 8 9 10 AP LP SP UP All
Precipitation class (mm/h or type)

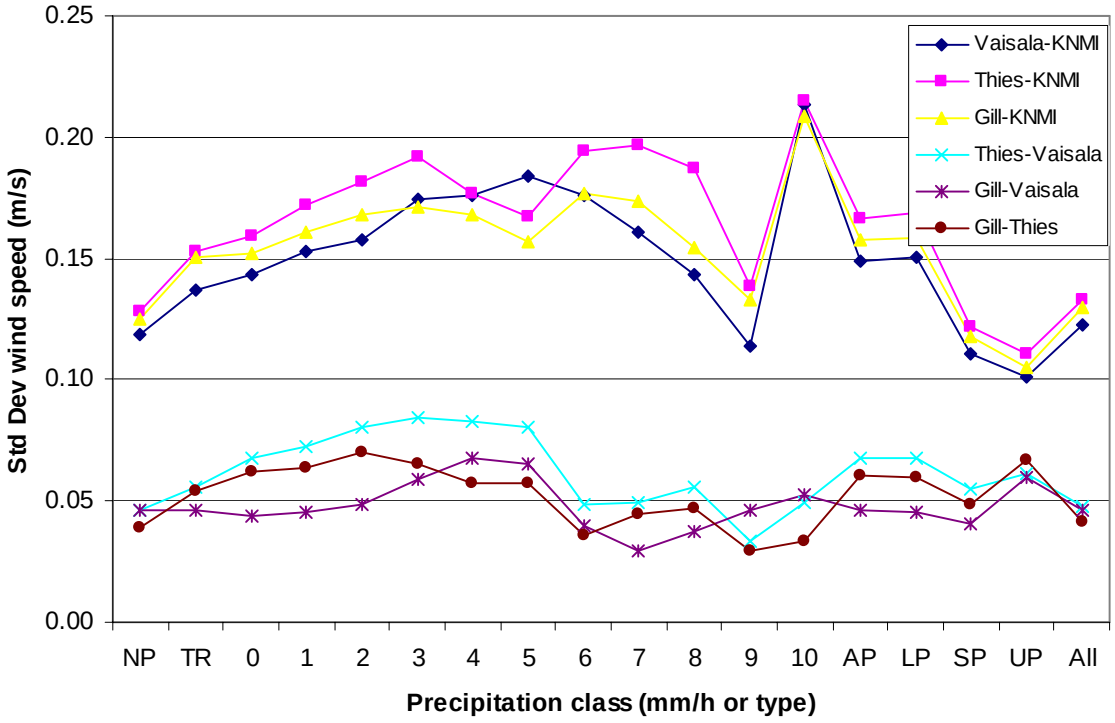
0.25
0.20
0.15
0.10
0.05
0.00
Std Dev wind speed (m/s)
Vaisala-KNMI
Thies-KNMI
Gill-KNMI
Thies-Vaisala
Gill-Vaisala
Gill-Thies
NP TR 0 1 2 3 4 5 6 7 8 9 10 AP LP SP UP All
Precipitation class (mm/h or type)

## *Wind speed (wind >2m/s)*

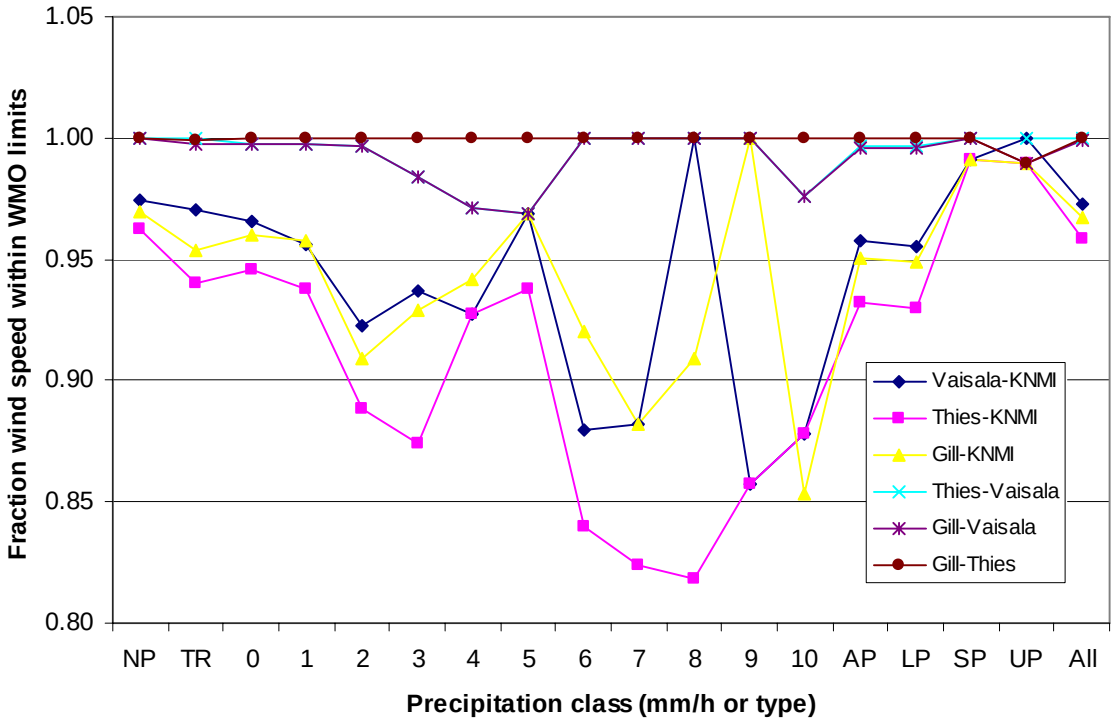


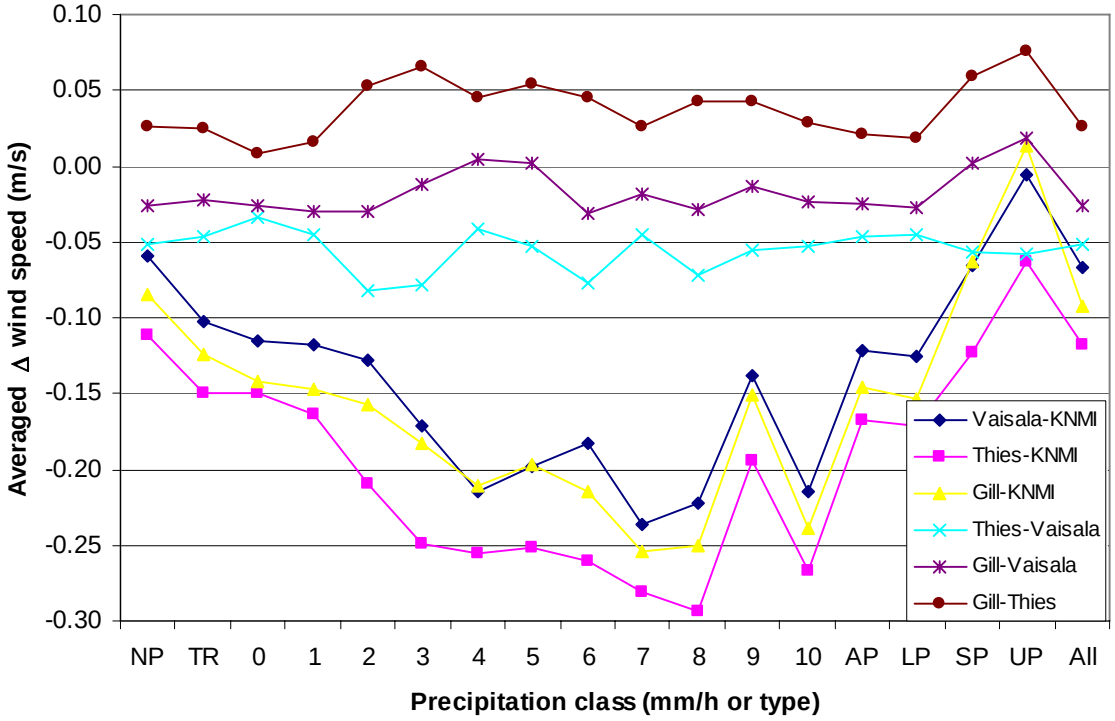

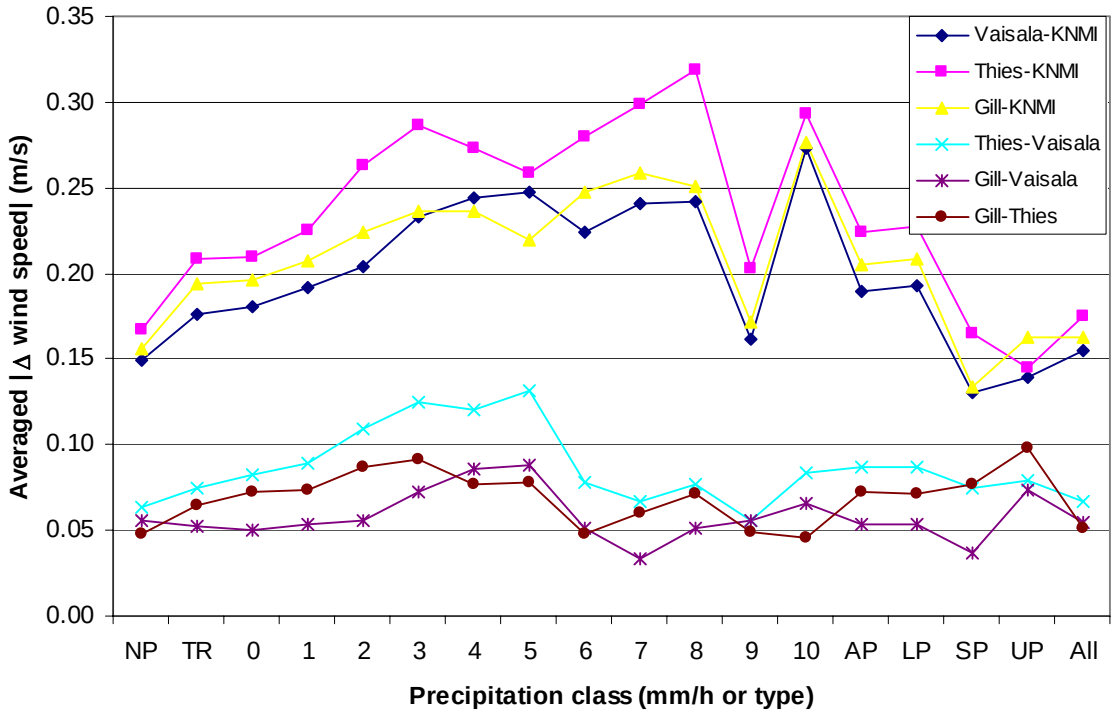
Averaged |Δ wind speed| (m/s)
0.35
0.30
0.25
0.20
0.15
0.10
0.05
0.00
NP TR 0 1 2 3 4 5 6 7 8 9 10 AP LP SP UP All
Precipitation class (mm/h or type)
Vaisala-KNMI
Thies-KNMI
Gill-KNMI
Thies-Vaisala
Gill-Vaisala
Gill-Thies

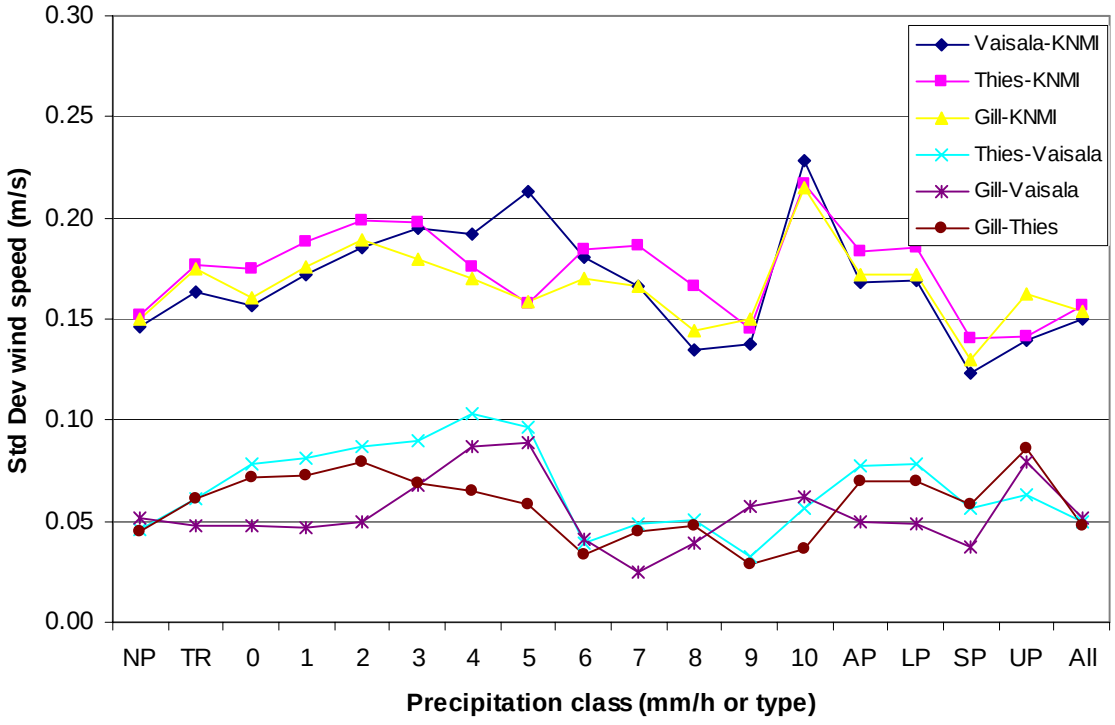
Std Dev wind speed (m/s)
0.30
0.25
0.20
0.15
0.10
0.05
0.00
NP TR 0 1 2 3 4 5 6 7 8 9 10 AP LP SP UP All
Precipitation class (mm/h or type)
Vaisala-KNMI
Thies-KNMI
Gill-KNMI
Thies-Vaisala
Gill-Vaisala
Gill-Thies

## *Wind gust (all wind speeds)*

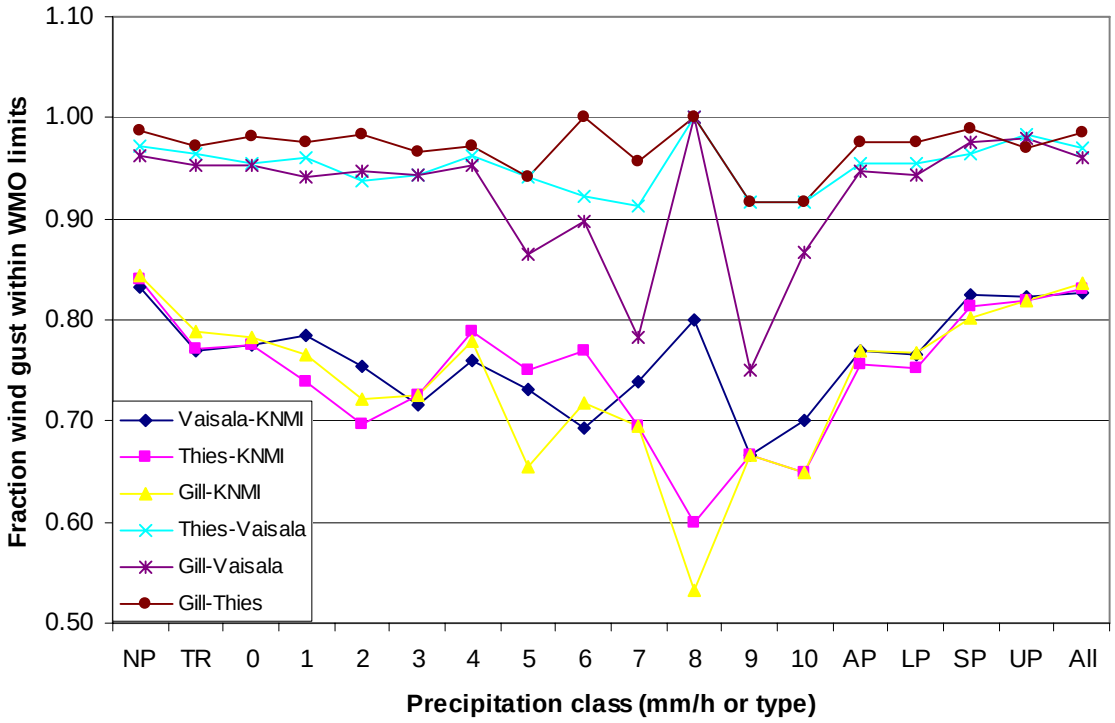


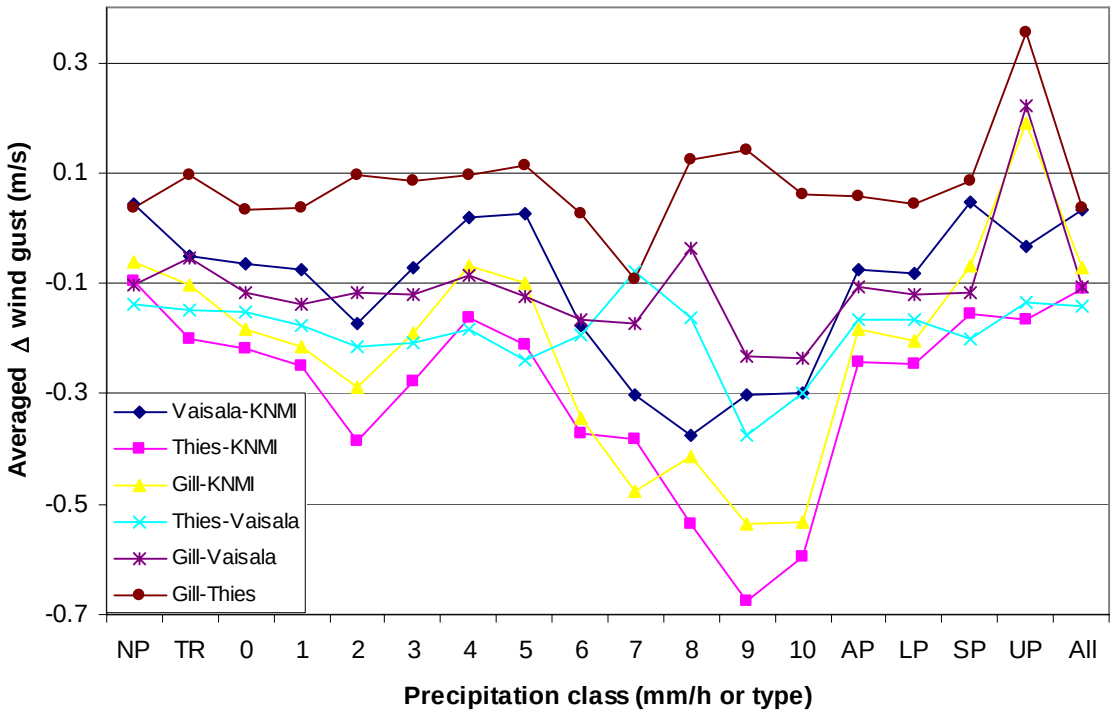

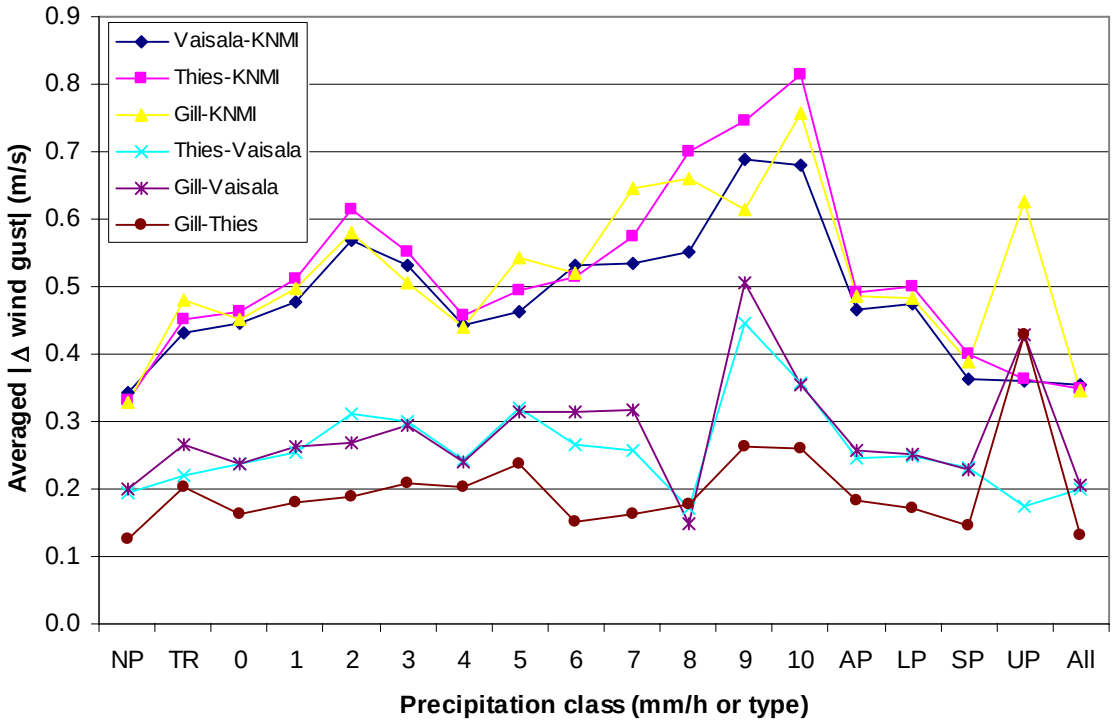
Vaisala-KNMI
Thies-KNMI
Gill-KNMI
Thies-Vaisala
Gill-Vaisala
Gill-Thies
Averaged | Δ wind gust| (m/s)
0.0
0.1
0.2
0.3
0.4
0.5
0.6
0.7
0.8
0.9
NP TR 0 1 2 3 4 5 6 7 8 9 10 AP LP SP UP All
Precipitation class (mm/h or type)

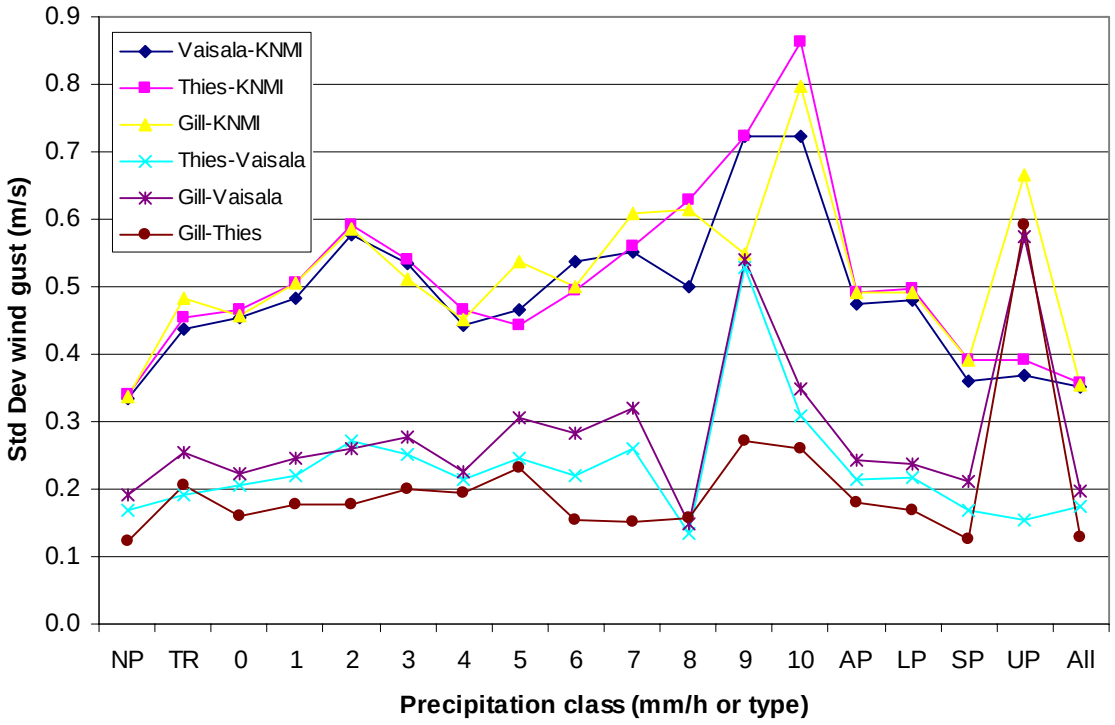
Vaisala-KNMI
Thies-KNMI
Gill-KNMI
Thies-Vaisala
Gill-Vaisala
Gill-Thies
Std Dev wind gust (m/s)
0.0
0.1
0.2
0.3
0.4
0.5
0.6
0.7
0.8
0.9
NP TR 0 1 2 3 4 5 6 7 8 9 10 AP LP SP UP All
Precipitation class (mm/h or type)

## *Wind gust (wind speed>2m/s)*

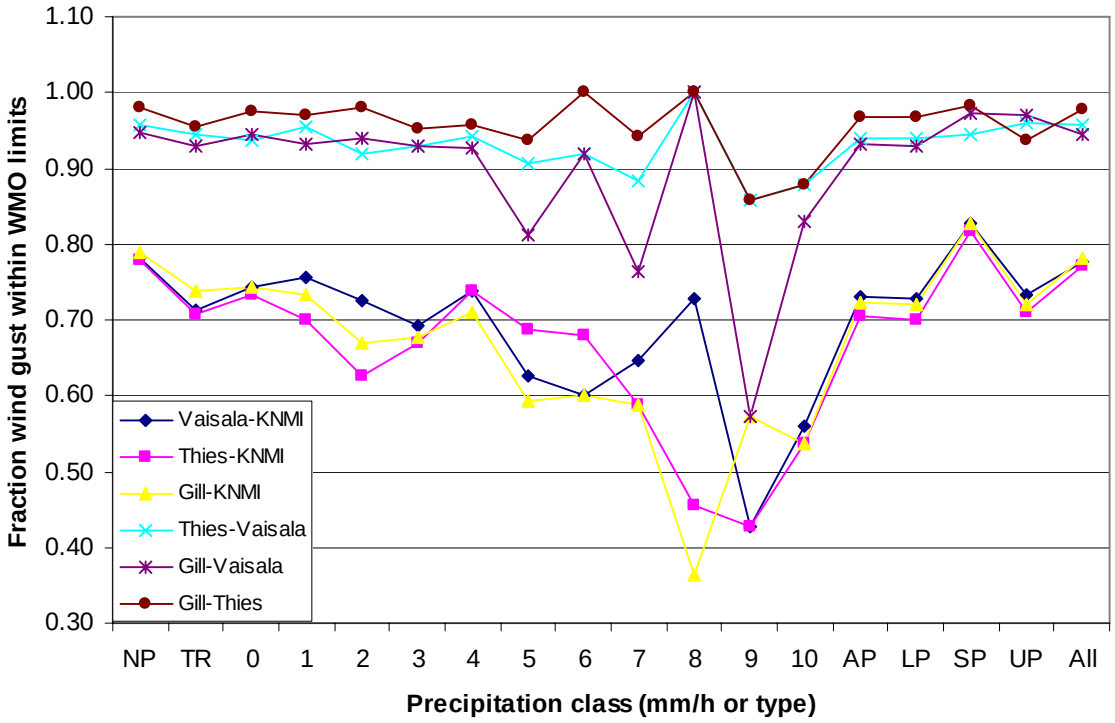


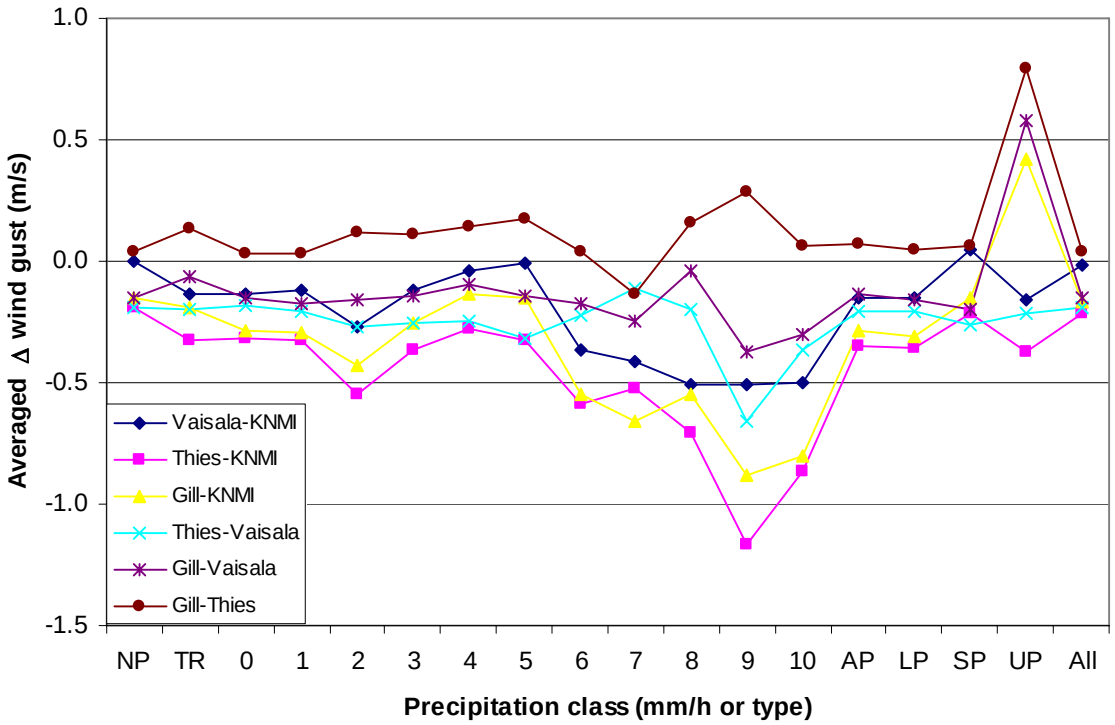

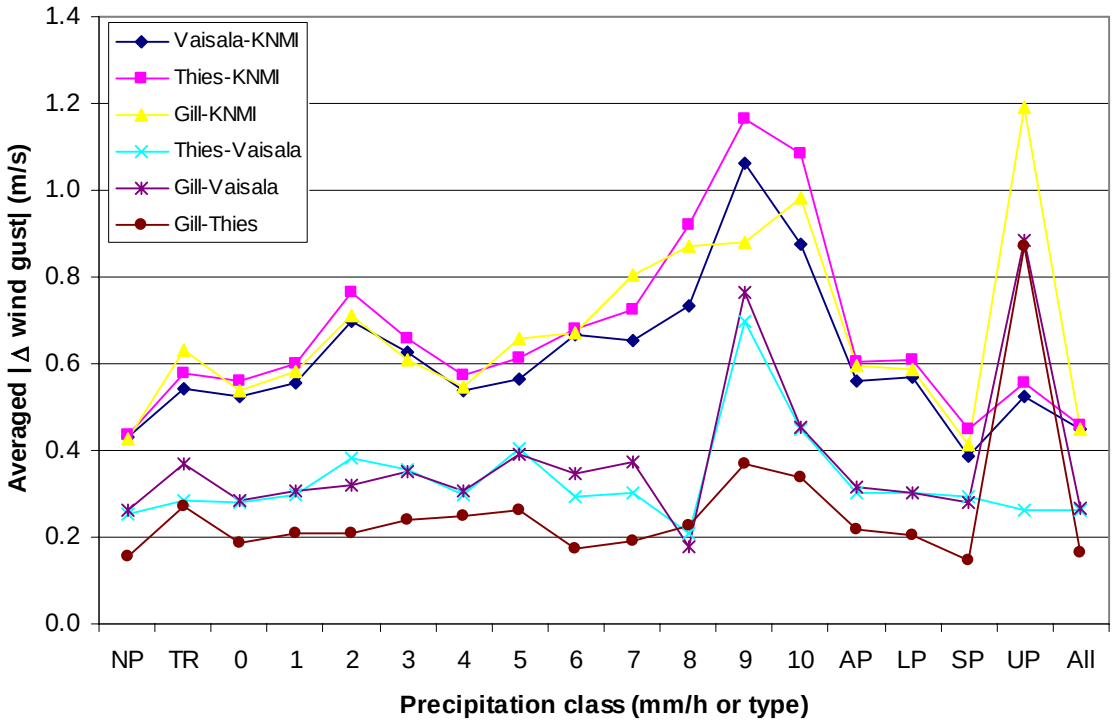
Vaisala-KNMI
Thies-KNMI
Gill-KNMI
Thies-Vaisala
Gill-Vaisala
Gill-Thies
Averaged | Δ wind gust| (m/s)
1.4
1.2
1.0
0.8
0.6
0.4
0.2
0.0
NP TR 0 1 2 3 4 5 6 7 8 9 10 AP LP SP UP All
Precipitation class (mm/h or type)

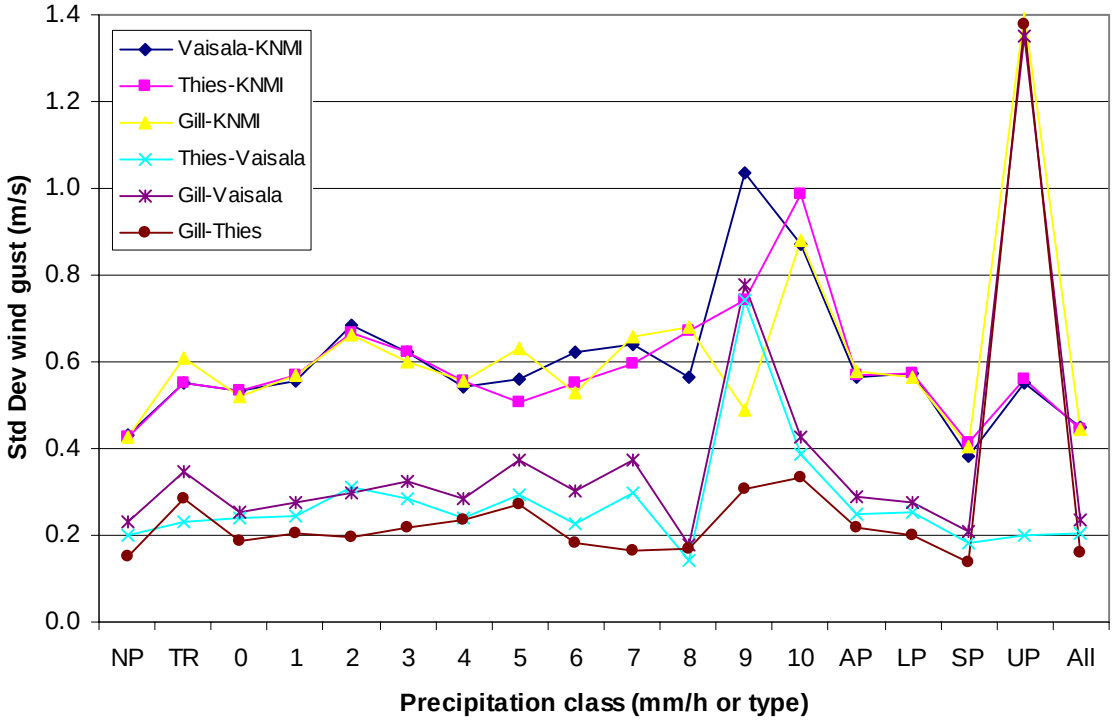
Vaisala-KNMI
Thies-KNMI
Gill-KNMI
Thies-Vaisala
Gill-Vaisala
Gill-Thies
Std Dev wind gust (m/s)
1.4
1.2
1.0
0.8
0.6
0.4
0.2
0.0
NP TR 0 1 2 3 4 5 6 7 8 9 10 AP LP SP UP All
Precipitation class (mm/h or type)

# Appendix D4: Field data as a function of ambient temperature

In this appendix the field test results for the 10-minute averaged wind direction, wind speed and wind gust are presented as a function of the ambient temperature. For that purpose, the results are binned in 5°C intervals from −15°C to 35°C. The lowest and highest bin also include any cases below and above the range, respectively. All 10-minute intervals are considered where the wind variables of all 4 sensors and the ambient temperature are valid, i.e. less than 10% of the data is missing. The number of cases for each temperature interval are given in the figure below. Note that there only about 20 cases with temperatures below −10°C and in about 200 cases the temperature exceeds 30°C.

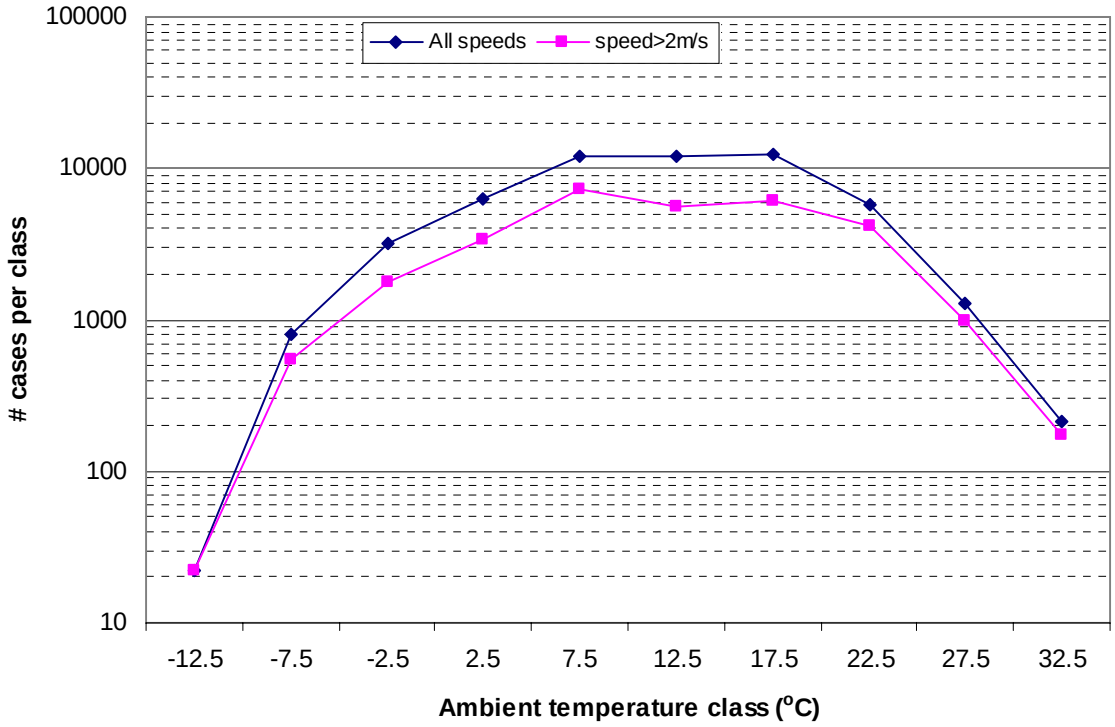


In the sections below the results for wind direction, wind speed and wind gust are reported, respectively. The differences between the sonic anemometers and the conventional wind vane and cup anemometer are presented as well as the differences between the sonics themselves. For each of the three wind parameter is shown: (i) the fraction of the cases with differences within the WMO limits; (ii) the averaged differences; (iii) the averaged absolute differences and; (iv) the standard deviation of the differences. The results are given for all wind speeds and for 10-minute averaged wind speeds of the KNMI cup anemometer above 2m/s.

## *Wind direction (all wind speeds)*

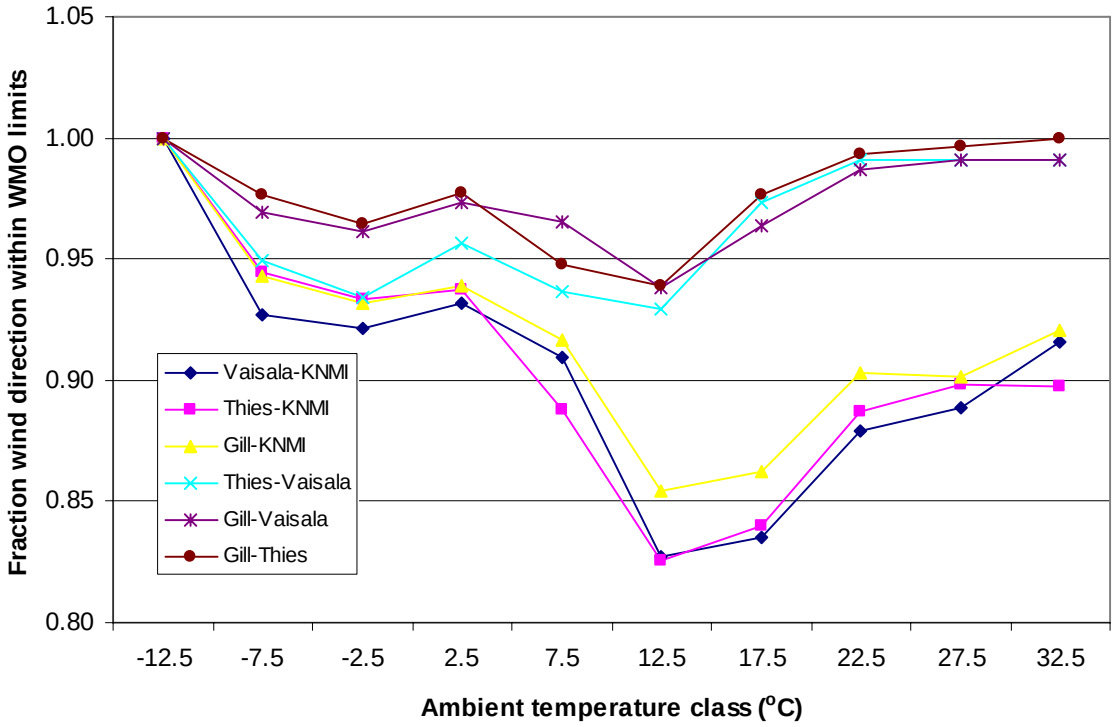


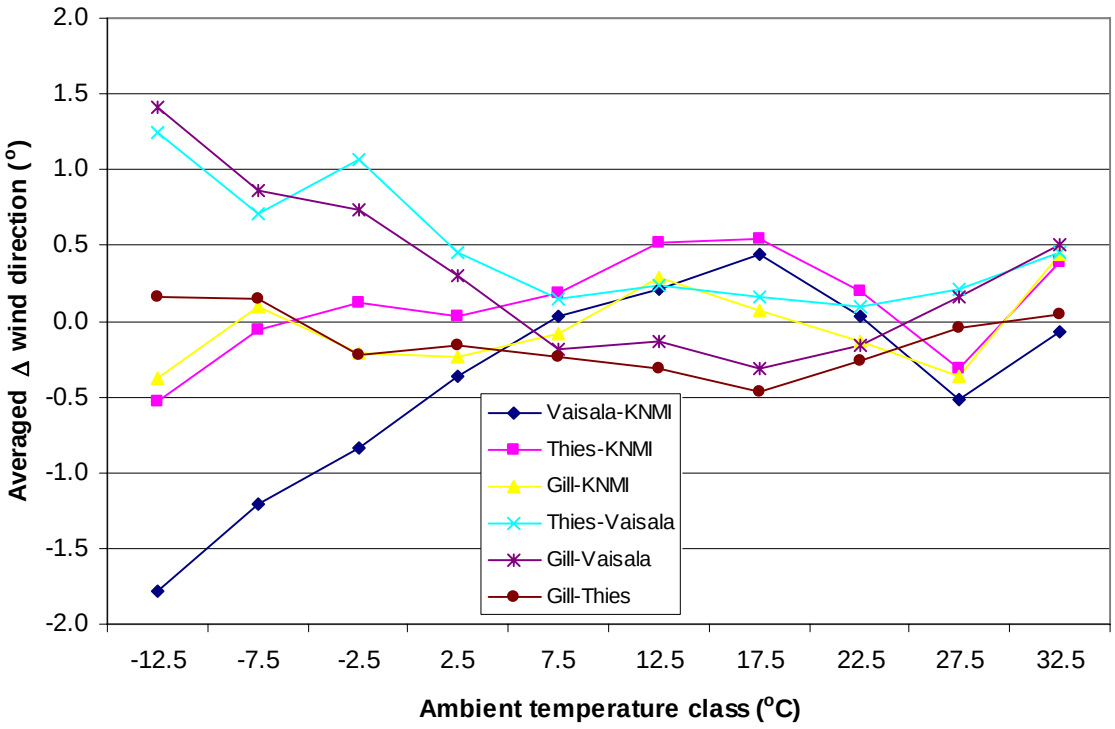

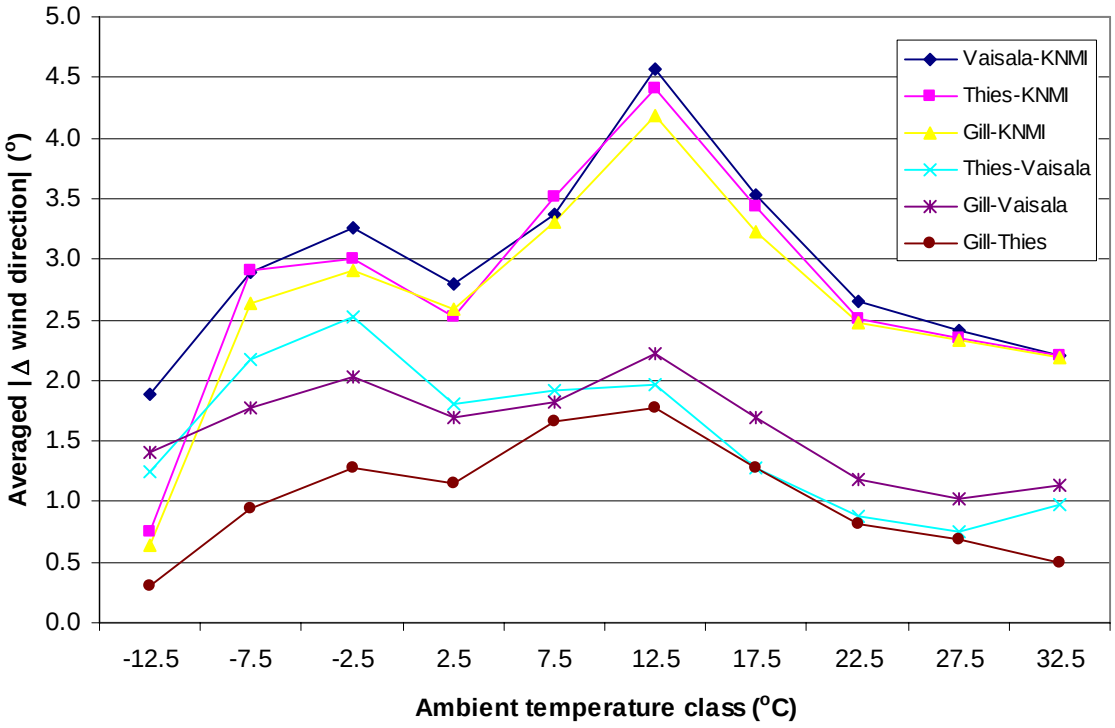
Averaged |Δ wind direction| (°)
5.0
4.5
4.0
3.5
3.0
2.5
2.0
1.5
1.0
0.5
0.0
-12.5
-7.5
-2.5
2.5
7.5
12.5
17.5
22.5
27.5
32.5
Ambient temperature class (°C)
Vaisala-KNMI
Thies-KNMI
Gill-KNMI
Thies-Vaisala
Gill-Vaisala
Gill-Thies

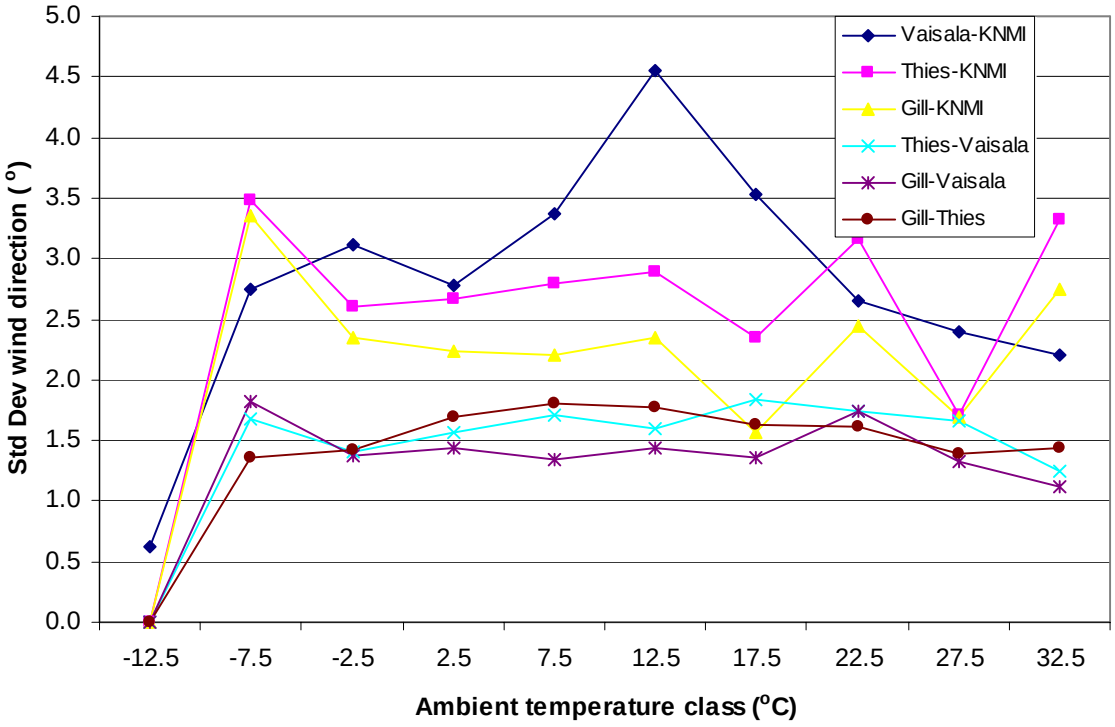
Std Dev wind direction (°)
5.0
4.5
4.0
3.5
3.0
2.5
2.0
1.5
1.0
0.5
0.0
-12.5
-7.5
-2.5
2.5
7.5
12.5
17.5
22.5
27.5
32.5
Ambient temperature class (°C)
Vaisala-KNMI
Thies-KNMI
Gill-KNMI
Thies-Vaisala
Gill-Vaisala
Gill-Thies

## *Wind direction (wind speed>2m/s)*

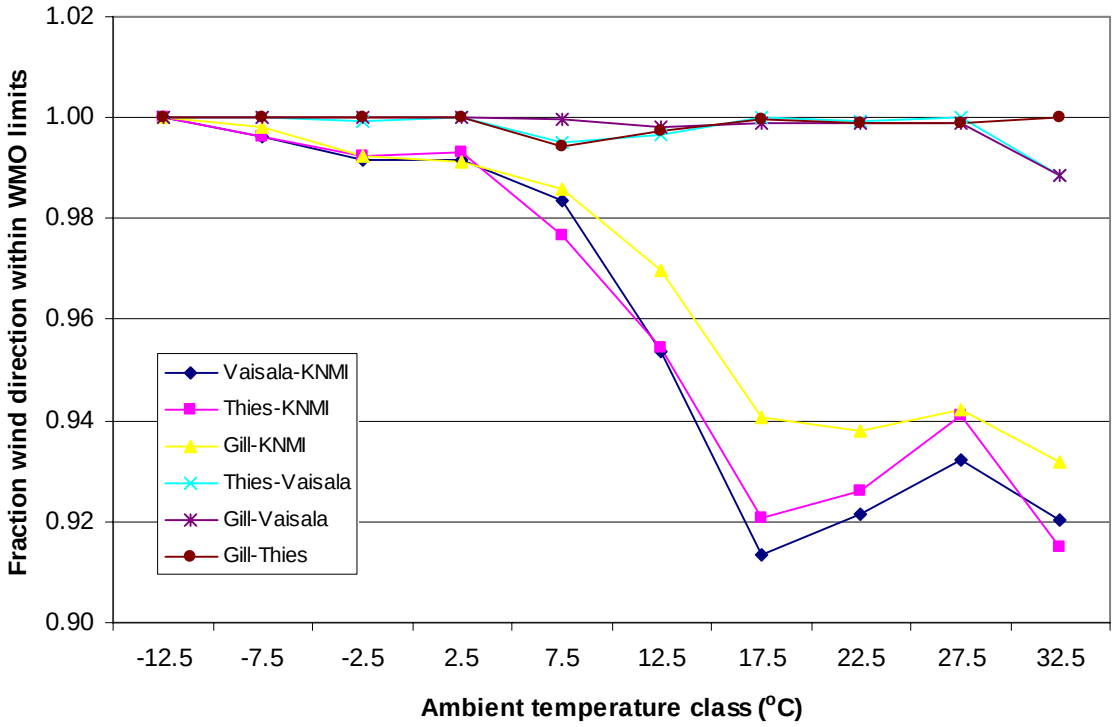


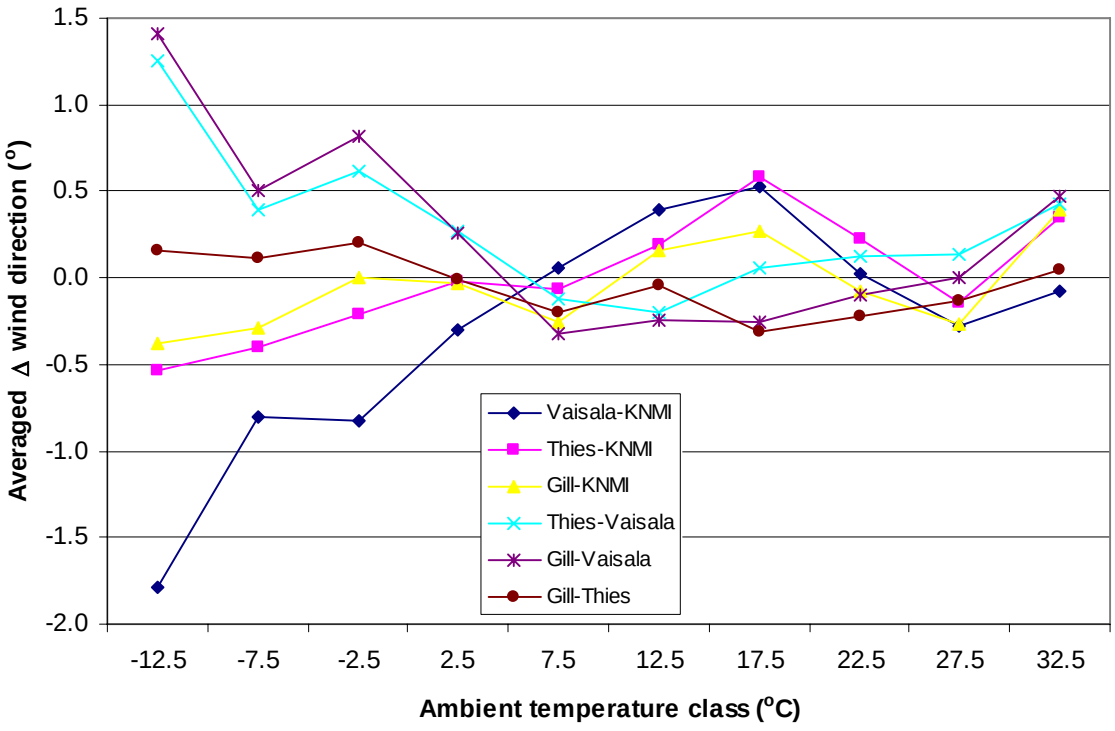

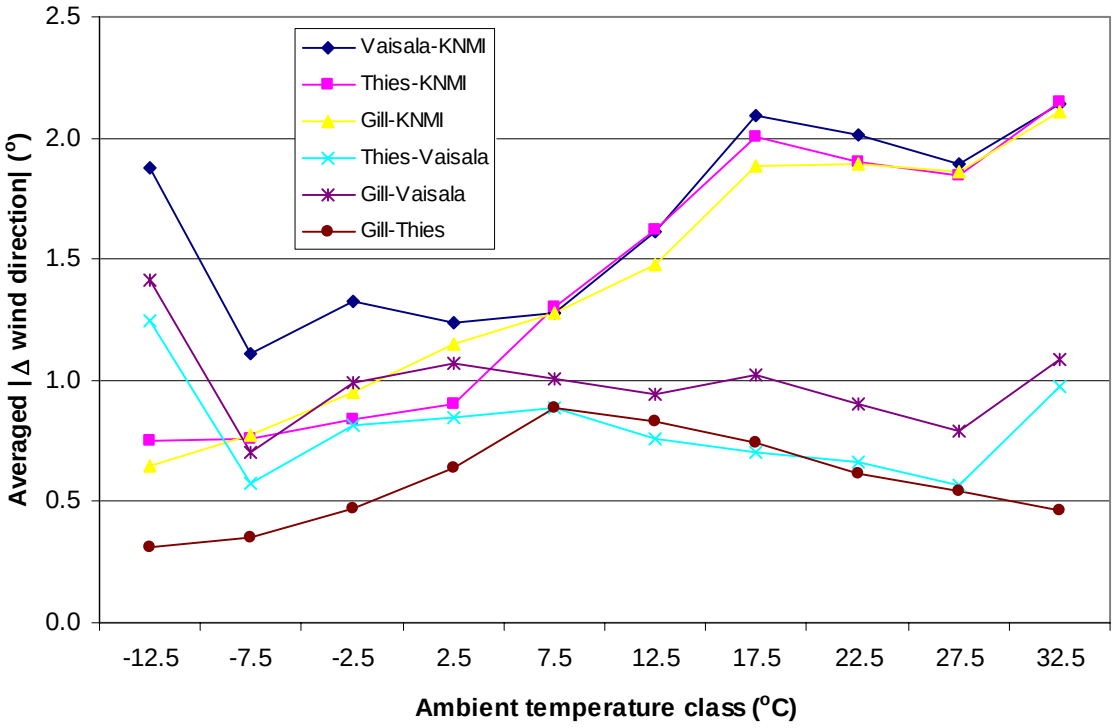
Averaged | Δ wind direction| (°)
2.5
2.0
1.5
1.0
0.5
0.0
-12.5
-7.5
-2.5
2.5
7.5
12.5
17.5
22.5
27.5
32.5
Ambient temperature class (°C)
Vaisala-KNMI
Thies-KNMI
Gill-KNMI
Thies-Vaisala
Gill-Vaisala
Gill-Thies

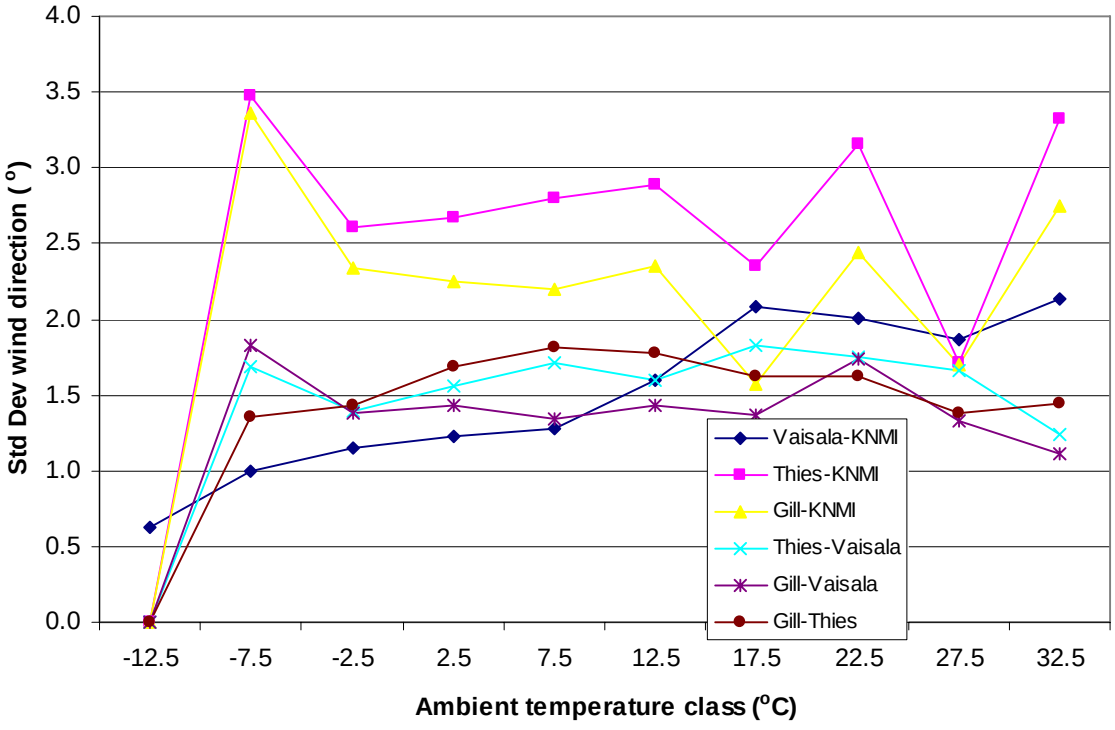
Std Dev wind direction (°)
4.0
3.5
3.0
2.5
2.0
1.5
1.0
0.5
0.0
-12.5
-7.5
-2.5
2.5
7.5
12.5
17.5
22.5
27.5
32.5
Ambient temperature class (°C)
Vaisala-KNMI
Thies-KNMI
Gill-KNMI
Thies-Vaisala
Gill-Vaisala
Gill-Thies

## *Wind speed (all wind speeds)*

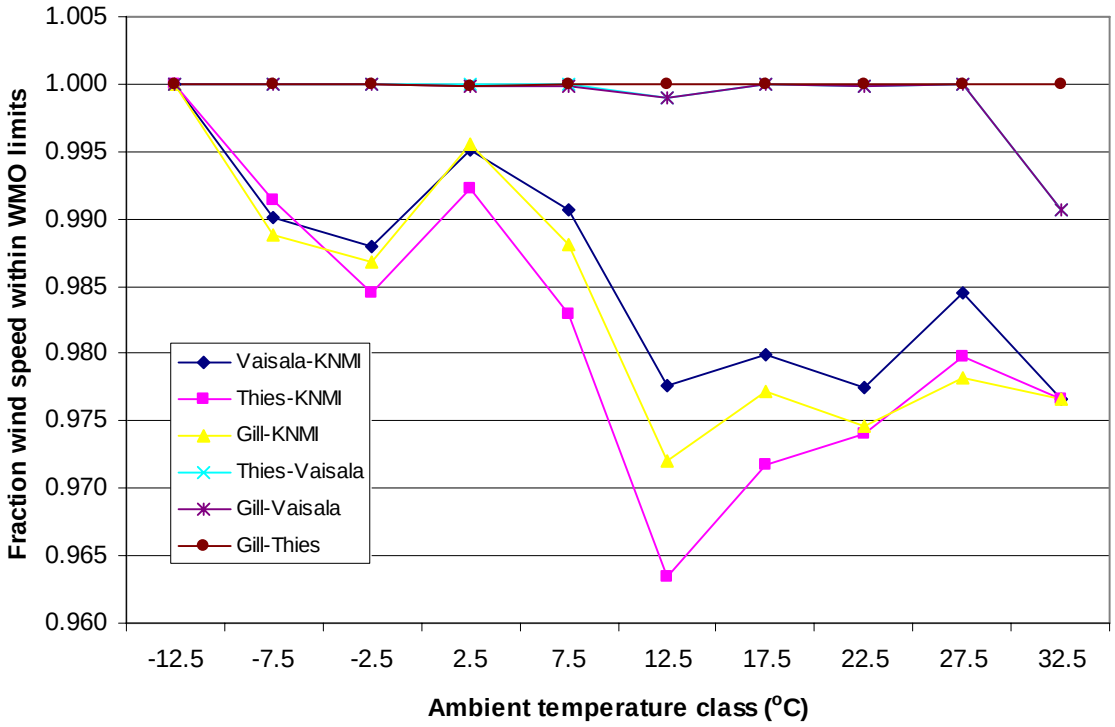


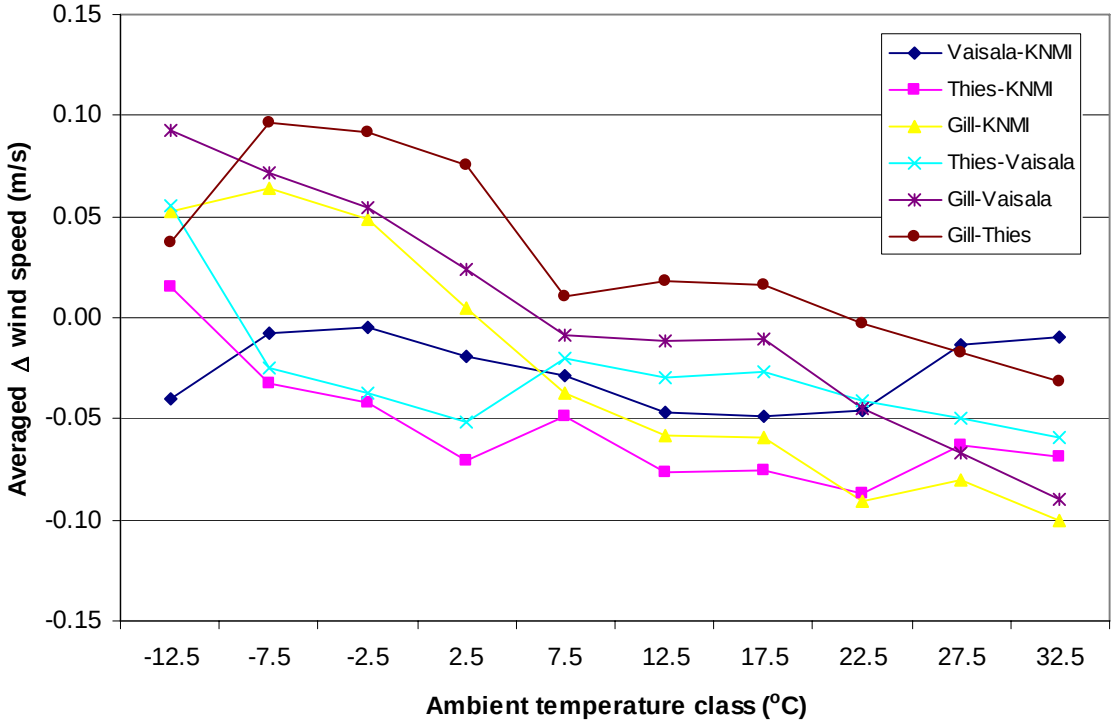

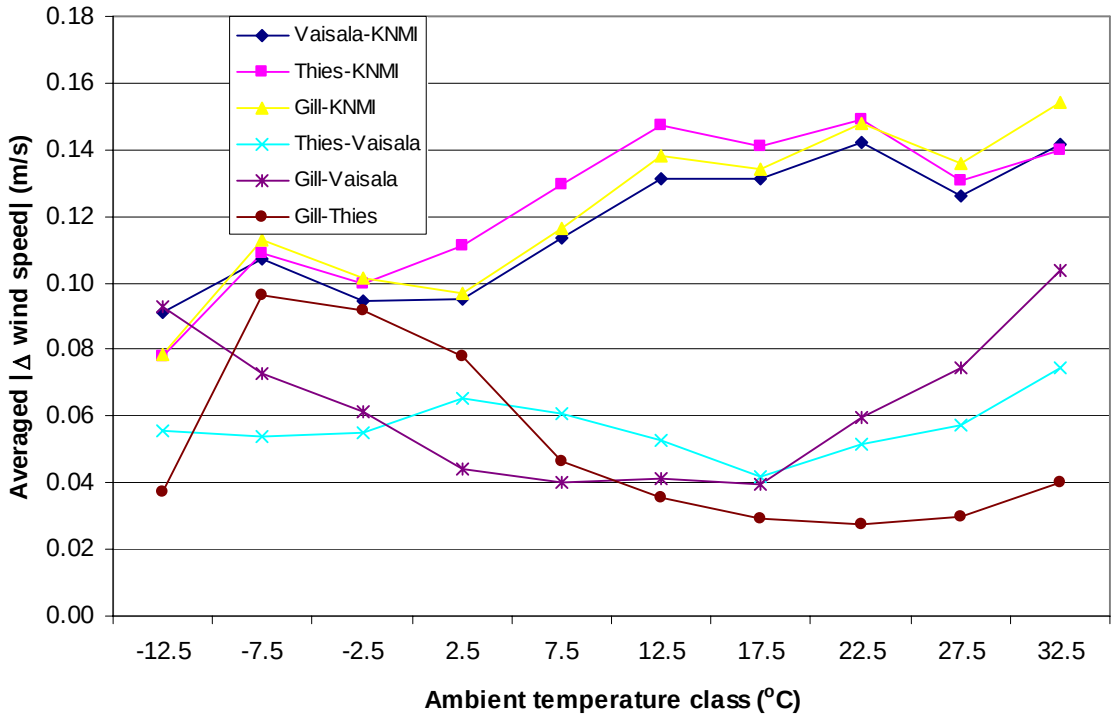
Averaged |Δ wind speed| (m/s)
0.18
0.16
0.14
0.12
0.10
0.08
0.06
0.04
0.02
0.00
Vaisala-KNMI
Thies-KNMI
Gill-KNMI
Thies-Vaisala
Gill-Vaisala
Gill-Thies
-12.5
-7.5
-2.5
2.5
7.5
12.5
17.5
22.5
27.5
32.5
Ambient temperature class (°C)

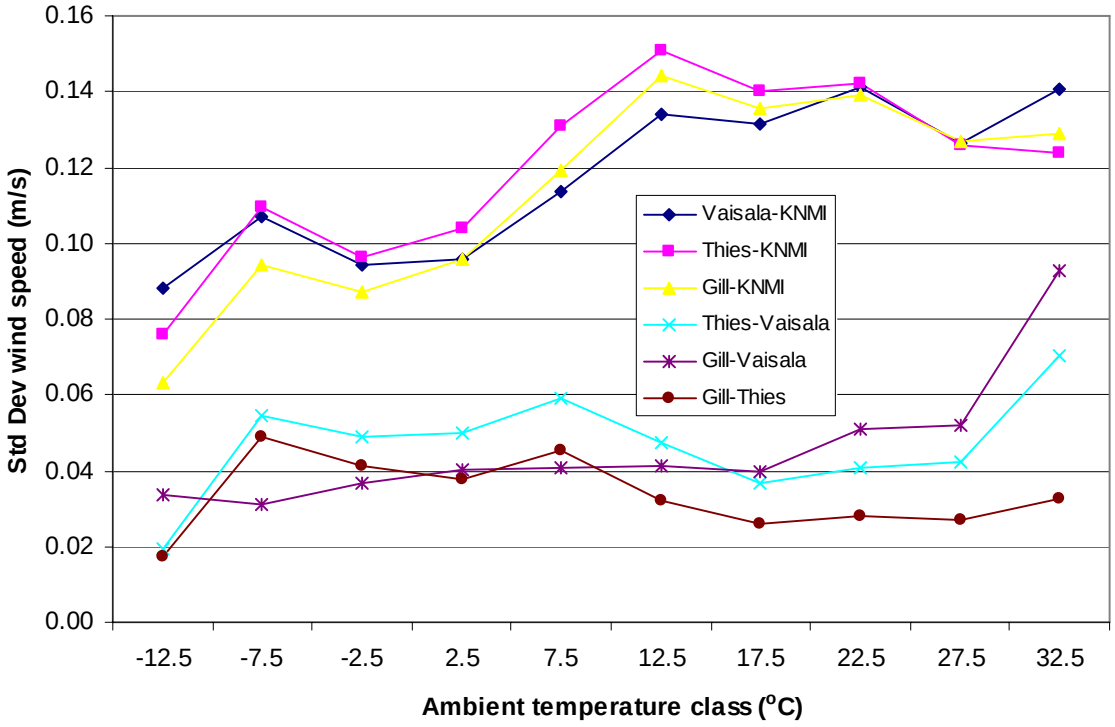
Std Dev wind speed (m/s)
0.16
0.14
0.12
0.10
0.08
0.06
0.04
0.02
0.00
Vaisala-KNMI
Thies-KNMI
Gill-KNMI
Thies-Vaisala
Gill-Vaisala
Gill-Thies
-12.5
-7.5
-2.5
2.5
7.5
12.5
17.5
22.5
27.5
32.5
Ambient temperature class (°C)

## *Wind speed (wind speed>2m/s)*

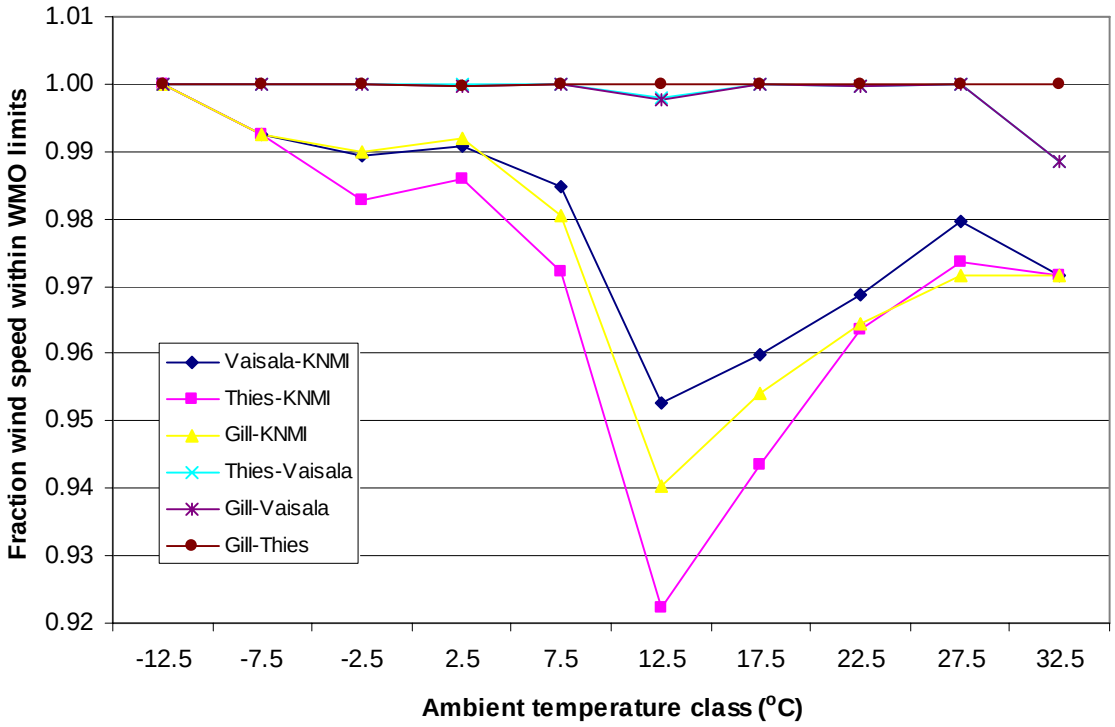


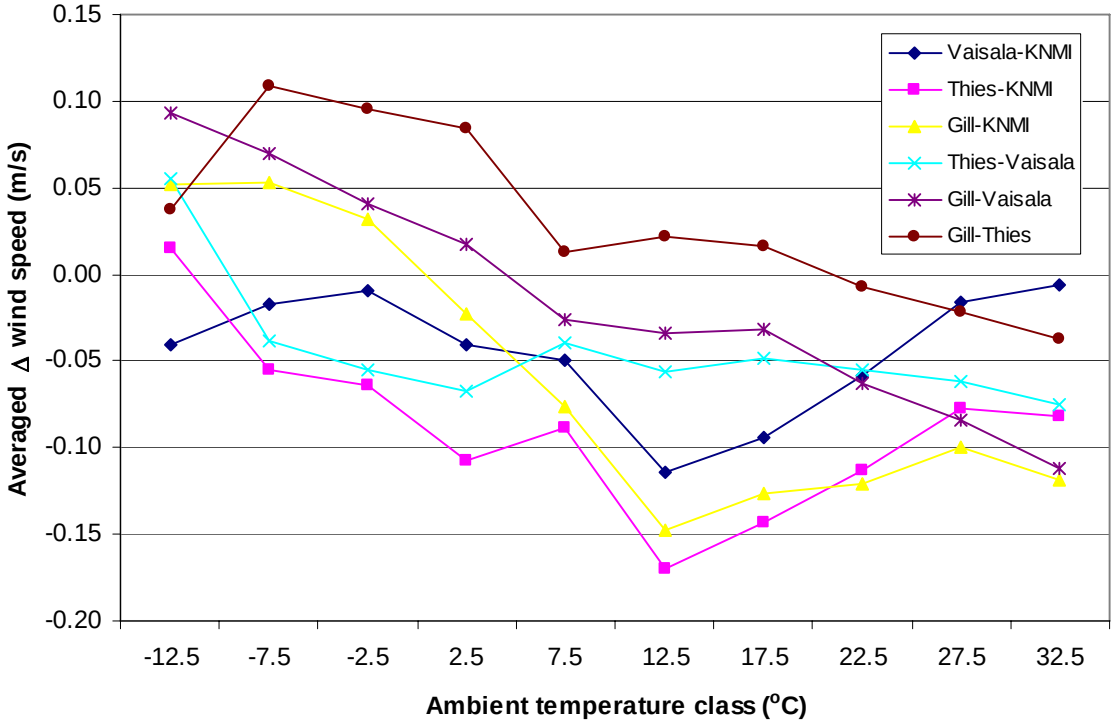

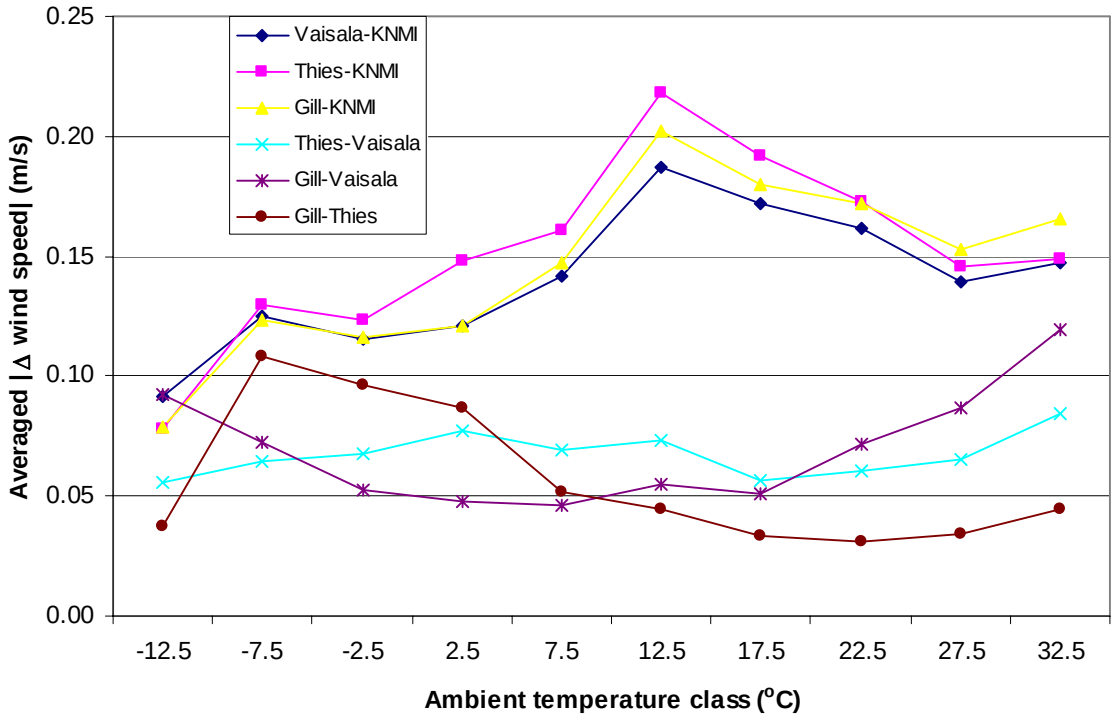
Vaisala-KNMI
Thies-KNMI
Gill-KNMI
Thies-Vaisala
Gill-Vaisala
Gill-Thies
Averaged |Δ wind speed| (m/s)
0.25
0.20
0.15
0.10
0.05
0.00
-12.5
-7.5
-2.5
2.5
7.5
12.5
17.5
22.5
27.5
32.5
Ambient temperature class (°C)

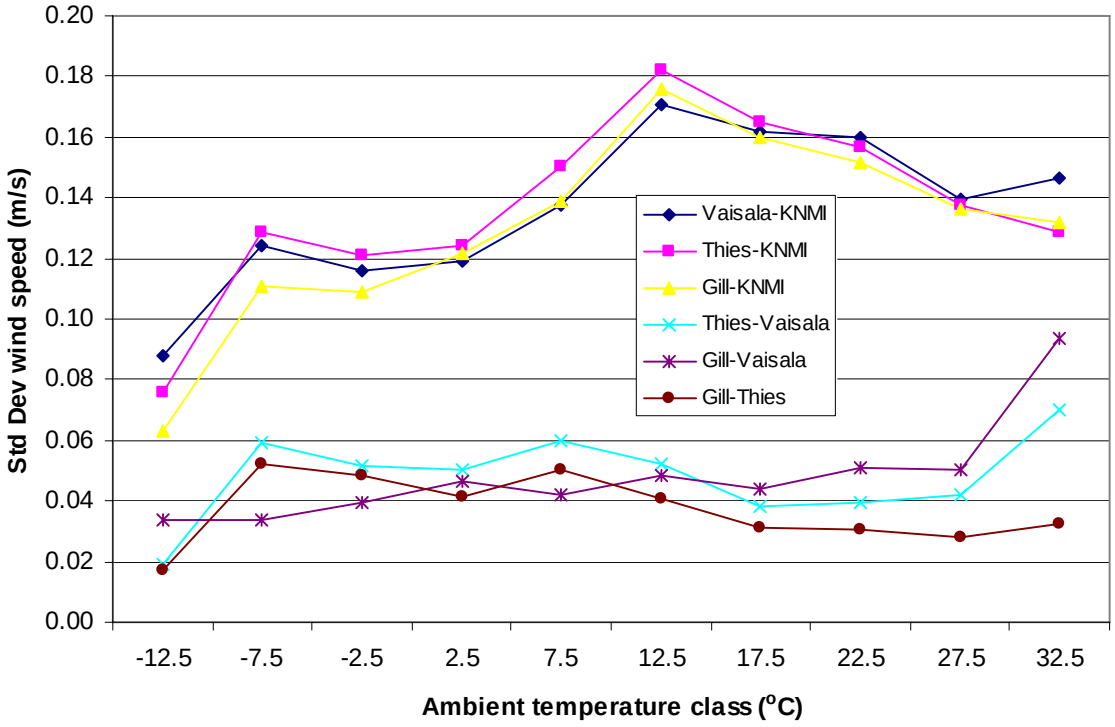
Vaisala-KNMI
Thies-KNMI
Gill-KNMI
Thies-Vaisala
Gill-Vaisala
Gill-Thies
Std Dev wind speed (m/s)
0.20
0.18
0.16
0.14
0.12
0.10
0.08
0.06
0.04
0.02
0.00
-12.5
-7.5
-2.5
2.5
7.5
12.5
17.5
22.5
27.5
32.5
Ambient temperature class (°C)

## *Wind gust (all wind speeds)*

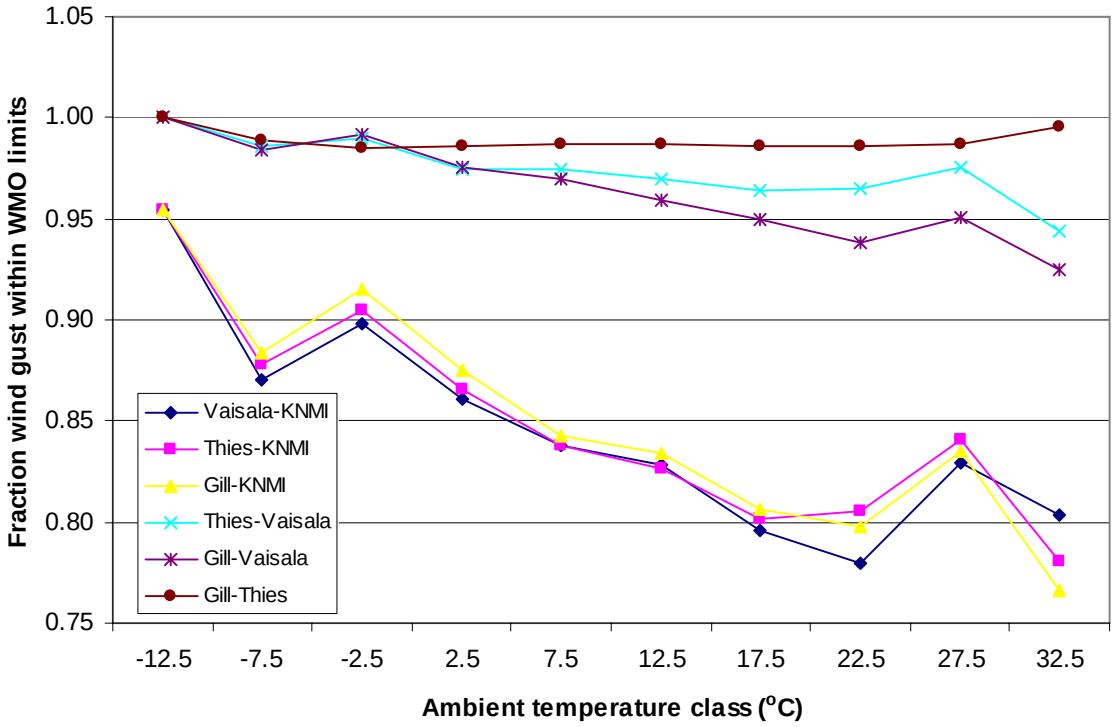


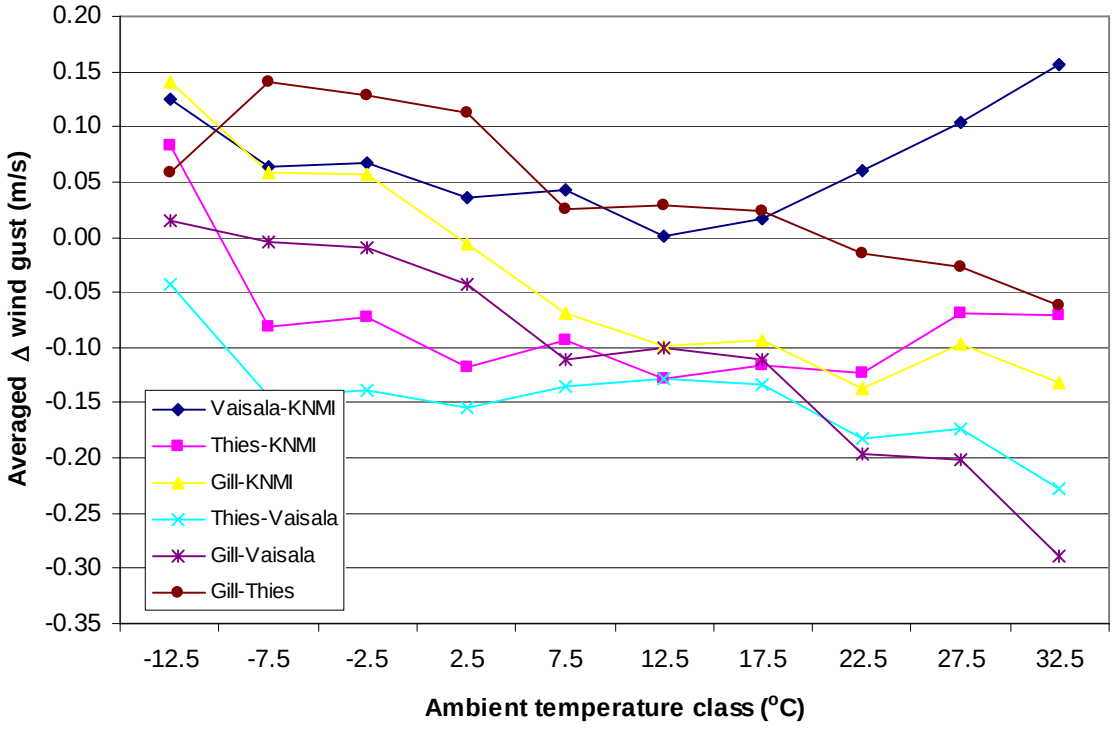

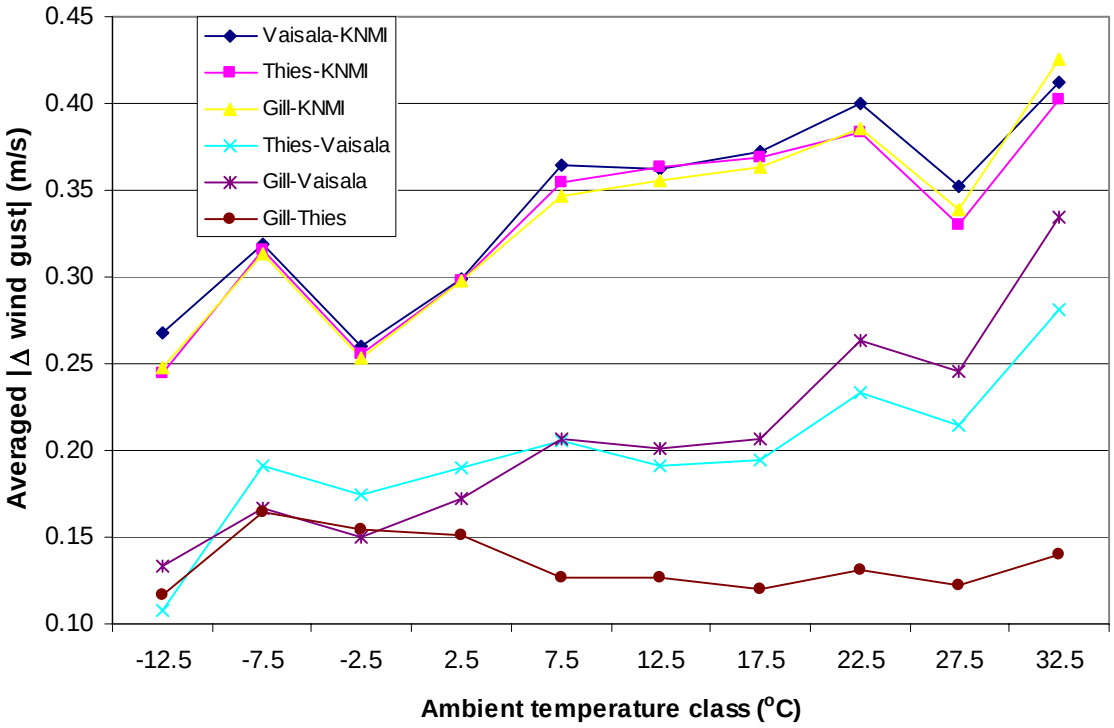
Vaisala-KNMI
Thies-KNMI
Gill-KNMI
Thies-Vaisala
Gill-Vaisala
Gill-Thies
Averaged |Δ wind gust| (m/s)
0.45
0.40
0.35
0.30
0.25
0.20
0.15
0.10
-12.5
-7.5
-2.5
2.5
7.5
12.5
17.5
22.5
27.5
32.5
Ambient temperature class (°C)

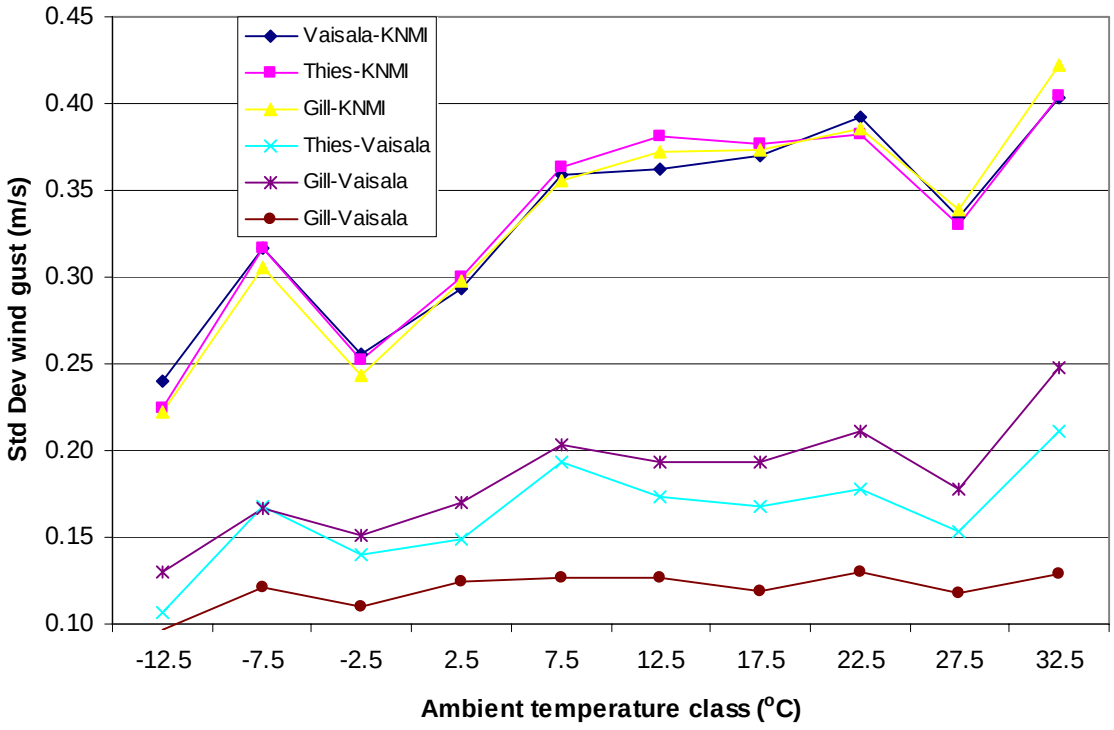
Vaisala-KNMI
Thies-KNMI
Gill-KNMI
Thies-Vaisala
Gill-Vaisala
Gill-Vaisala
Std Dev wind gust (m/s)
0.45
0.40
0.35
0.30
0.25
0.20
0.15
0.10
-12.5
-7.5
-2.5
2.5
7.5
12.5
17.5
22.5
27.5
32.5
Ambient temperature class (°C)

## *Wind gust (wind speed>2m/s)*

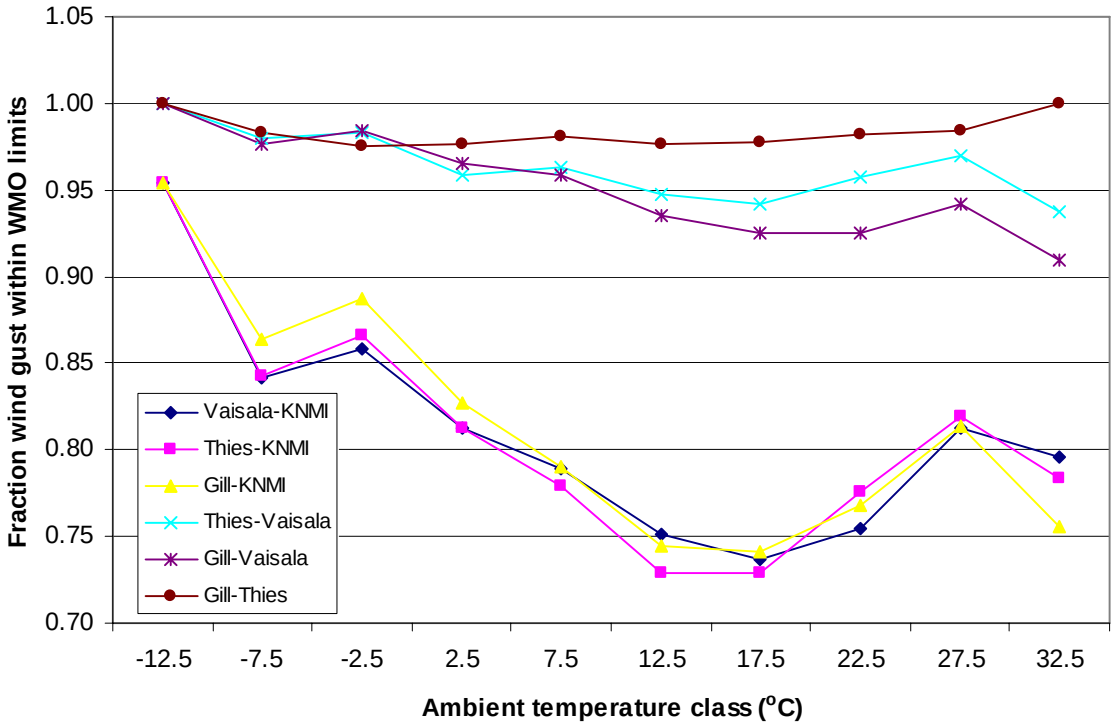


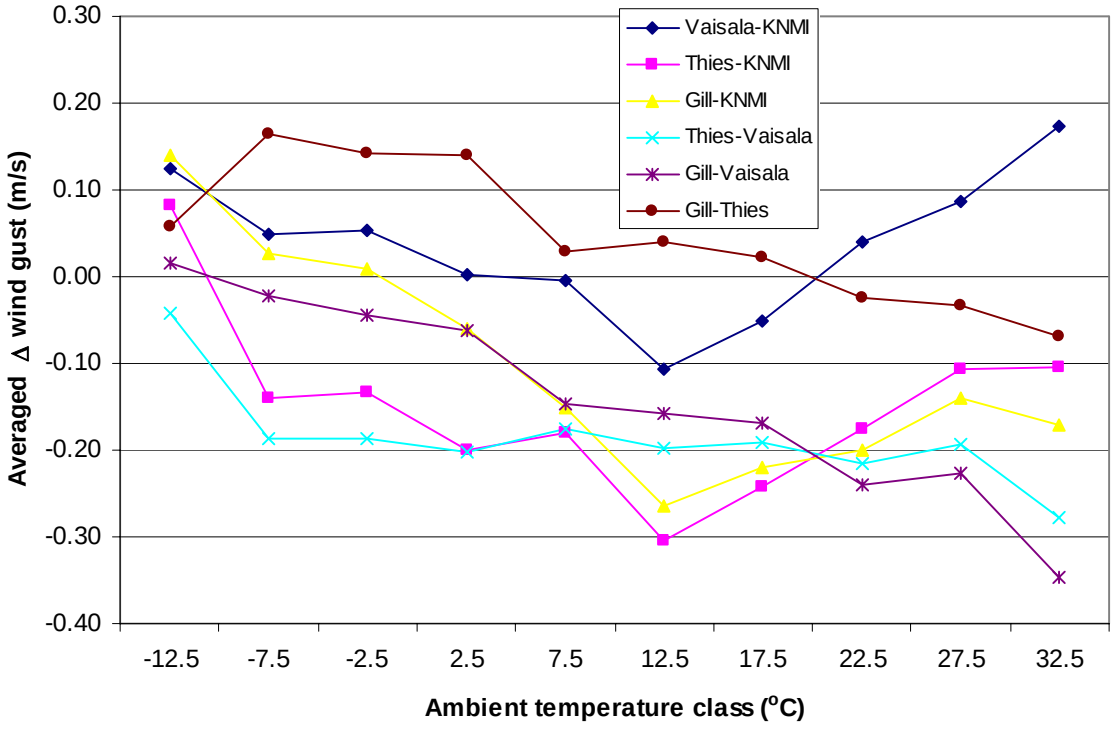

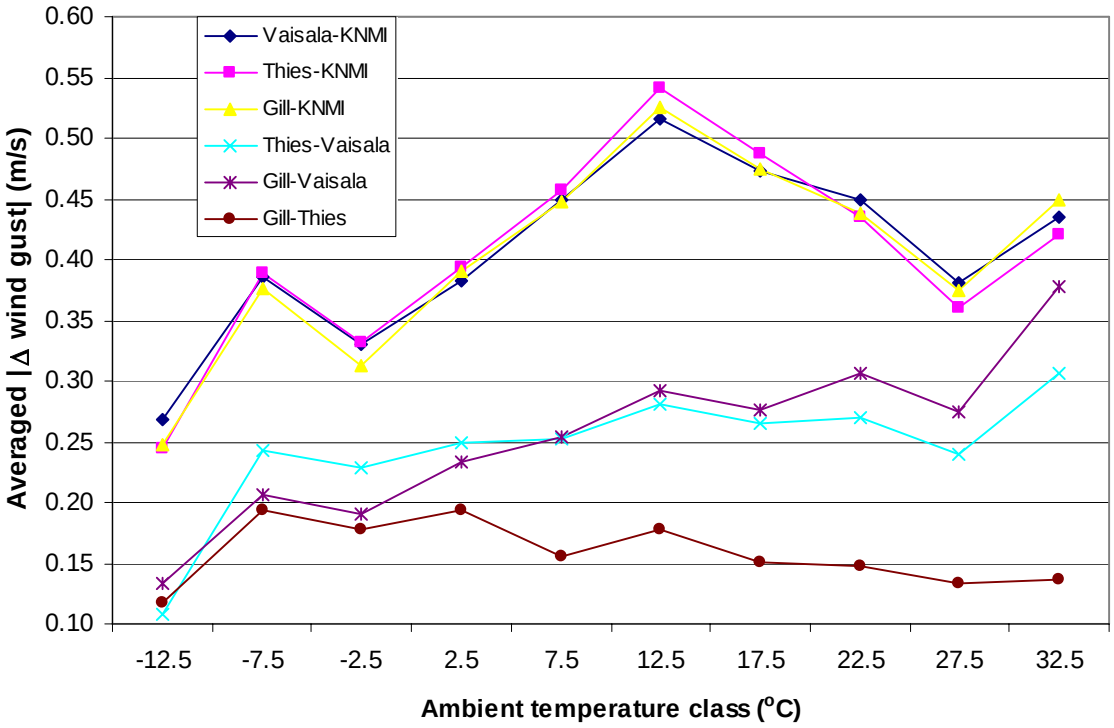
Vaisala-KNMI
Thies-KNMI
Gill-KNMI
Thies-Vaisala
Gill-Vaisala
Gill-Thies
Averaged |Δ wind gust| (m/s)
0.60
0.55
0.50
0.45
0.40
0.35
0.30
0.25
0.20
0.15
0.10
-12.5
-7.5
-2.5
2.5
7.5
12.5
17.5
22.5
27.5
32.5
Ambient temperature class (°C)

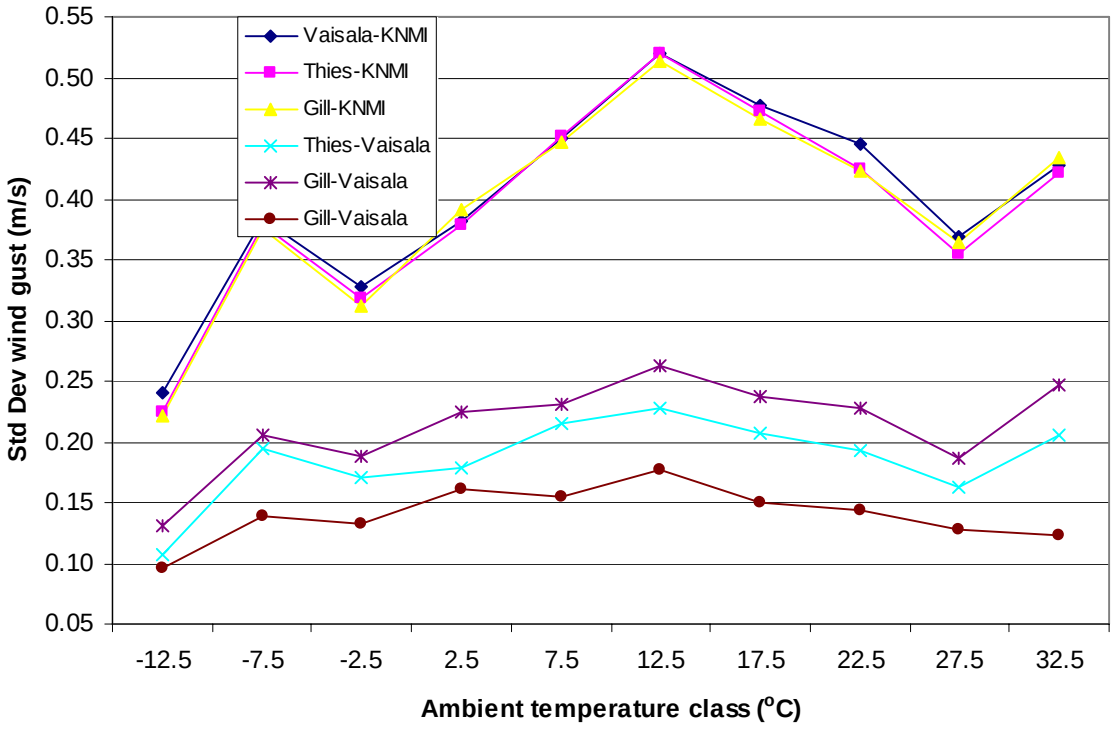
Vaisala-KNMI
Thies-KNMI
Gill-KNMI
Thies-Vaisala
Gill-Vaisala
Gill-Vaisala
Std Dev wind gust (m/s)
0.55
0.50
0.45
0.40
0.35
0.30
0.25
0.20
0.15
0.10
0.05
-12.5
-7.5
-2.5
2.5
7.5
12.5
17.5
22.5
27.5
32.5
Ambient temperature class (°C)